NOTE TO USERS

This reproduction is the best copy available.

THE MECHANISMS OF HYDROXYUREA INDUCED DEVELOPMENTAL TOXICITY IN THE ORGANOGENESIS STAGE MOUSE EMBRYO

by

Jin Yan

A thesis submitted to the Faculty of Graduate Studies and Research of McGill University in partial fuifilment of the requirements for the Degree of Doctor of Philsophy.

April, 2008

Department of Pharmacology and Therapeutics
McGill University
Montreal, Ouebec

Your file Votre référence
ISBN: 978-0-494-66685-2
Our file Notre référence
ISBN: 978-0-494-66685-2

ABSTRACT

Hydroxyurea was used as a model teratogen to investigate the role of oxidative stress and stress-response pathways in mediating developmental toxicity. When administered to pregnant mice during early organogenesis, hydroxyurea induced fetal death and growth retardation, as well as external and skeletal malformations. The malformed fetuses displayed hindlimb, vertebral column, and tail defects. Hydroxyurea treatment enhanced the production of 4-hydroxynonenal, a lipid peroxidation end product, in malformation sensitive regions of the embryo. Depletion of glutathione, a major cellular antioxidant, specifically enhanced hydroxyurea-induced malformations and elevated the region-specific production of 4--hydroxynonenal protein adducts in the embryo, without affecting the incidence or extent of hydroxyurea-induced fetal death or growth retardation. The major proteins modified by 4-hydroxynonenal were involved in energy metabolism. Thus, oxidative stress is important in the induction of malformations by hydroxyurea.

Exposure to hydroxyurea stimulated the DNA binding activity of activator protein 1 (AP-1), an early response redox-sensitive transcription factor. Activated AP-1 was composed mainly of c-Fos heterodimers. Glutathione depletion did not change the effects of hydroxyurea on AP-1/c-Fos DNA binding activities despite an augmentation of the incidence of embryo malformations. Mitogen-activated protein kinases (MAPKs) activate AP-1 in response to stress by post-transcriptional phosphorylation of AP-1 proteins. Hydroxyurea treatment dramatically enhanced the activation of stress-responsive p38 MAPKs and JNKs (c-Jun N-terminal protein kinases). Selectively blocking p38 MAPKs enhanced

the incidence of fetal death, whereas selective inhibition of JNKs specifically elevated the limb defects induced by hydroxyurea. Thus, activation of stress-response pathways impacts on the response of the embryo to a teratogenic insult.

RÉSUMÉ

L'hydroxyurée est un agent tératogène que nous avons utilisé afin de comprendre le rôle du stress oxydatif et la signalisation cellulaire induite lorsqu'il exerce une toxicité sur le développement. Nous avons montre que l'administration d'hydroxyurée à des souris femelles gestantes pendant le début de l'organogenèse peut induire la mort *in utero*, des retards de développement ainsi que des malformations externes et squelettiques. Les foetus malformés présentent des anomalies des bourgeons de membres postérieurs, de la colonne vertébrales et de la queue. Un traitement à l'hydroxyurée augmente la production du 4-hydroxynonenal, un produit de la péroxydation lipidique, dans des régions particulièrement sensibles de l'embryon. De plus, une diminution en glutathion, un des principaux antioxydants cellulaires, augmente spécifiquement les malformations induites par l'hydroxyurée et la production de protéines liées au 4-hydroxynonenal dans certaines régions de l'embryon, sans affecter l'incidence de mort fœtale ou de retard de développement induit par l'hydroxyurée. Les protéines modifiées par l'addition du 4-hydroxynonenal sont majoritairement impliquées dans le métabolisme énergétique. L'ensemble de ces données suggère que le stress oxydatif est un mécanisme important mis en jeu dans les malformations induites par l'hydroxyurée.

Nous avons ensuite montré que l'exposition à l'hydroxyurée stimule l'activité de liaison à l'ADN du complexe AP1 (activator protein 1), un facteur de transcription rapidement sensible au potentiel d'oxydoréduction. Le complexe AP1 activés par l'hydroxyurée est principalement composé d'hétérodimère contenant cFos. La

diminution de glutathion n'a pas d'effet sur l'activité de liaison de l'ADN de AP1 induite par l'hydroxyurée, malgré une augmentation de l'incidence les malformations embryonnaires. Les MAPKs (mitogen-activated protein kinases) peuvent activer AP1 en réponse à un stress, en phosphorylant les protéines du complexes AP1. Nous avons montré que le traitement à l'hydroxyurée augmente dramatiquement l'activité de p38 MAPK et JNKs (cJun N-terminal protein kinases). Le blocage sélectif de p38 augmente l'incidence de mort *in utero*, alors que l'inhibition de JNKs augmente spécifiquement les anomalies induites par l'hydroxyurée au niveau des bourgeons de membres. Ainsi, la réponse de l'embryon à un agent tératogène dépend de la voie de signalisation cellulaire induite par ce stress.

TABLE OF CONTENTS

LIST OF FIGURES

LIST OF TABLES

ABBREVIATIONS

AER	apical ectoderm ridge
ALB	albumin
ALDOA1	aldolase 1, A isoform
ANOVA	analysis of variance
AP-1	activator protein-1
ASK1	apoptosis signal-regulating kinase 1
ATF-2	activating transcription factor-2
BAD	Bcl-associated death promoter
BAX	Bcl2-associated X protein
Bcl-2	B-cell lymphoma 2
BSO	L-buthionine-S,R-sulphoximine
bZIP	basic domain and leucine zipper
CAT	Catalase
CCT8	chaperonin subunit theta
CHOP	C/EBP homologous protein
CYP	cytochrome p450
DKK1	dickkopf 1
dNDPs	deoxyribonucleoside diphosphates
EGF	epidermal growth factor
ELISA	enzyme-linked immunosorbent assay
ELK	Ets-like protein
EMSA	electrophoretic mobility shift assay
ERK	extracellular signal-regulated protein kinase
4-HNE	4-Hydroxynonenal
FGF	fibroblast growth factor
Fra-1,2	Fos-related antigens 1-2

GADD 153	DNA damage-inducible protein
GAPDH	glyceraldehyde 3-phosphate dehydrogenase
γ-GCS	gamma-glutamylcysteine synthetase
γ-GCSC	gamma-glutamylcysteine synthetase, catalytic subunit
γ-GCSM	gamma-glutamylcysteine synthetase, modulator subunit
GD	gestational day
GOT2	oxaloacetate transaminase 2
GPX	glutathione peroxidase
GR	glutathione reductase
GSH	reduced glutathione
GSSG	oxidized glutathione
GST	glutathione transferase
HNRNP A1A	heterogeneous nuclear ribonucleoprotein A1 isoform a
HSPD1	heat shock 60
HU	hydroxyurea
JDP	c-Jun dimerization protein
JNK	c-Jun N-terminal protein kinase
MAPK	mitogen-activated protein kinase
MAPKAPK	mitogen-activated protein kinase-activated protein kinase
MAK3K	mitogen-activated protein kinase kinase kinase
MAP2K	mitogen-activated protein kinase kinase
MEF-2	myocyte-specific enhancer factor 2
MKK	mitogen-activated protein kinase kinase
MLK-3	mixed lineage kinase 3
Mmp-13	matrix metalloproteinases 13
MTK1	MAP three kinase 1
NADPH	nicotinamide adenine dinucleotide phosphate
NDPs	ribonucleoside diphosphates

NFATc1	nuclear factor of activated T-cells
NF-γB	nuclear factor kappa B
PARP1	poly (ADP-ribose) polymerase famiy, member 1
Prx	Peroxiredoxin
PSM	presomitic mesoderm
PZ	progress zone
Ref-1	redox factor-1
RNR	ribonucleotide diphosphate reductase
ROS	reactive oxygen species
RT-PCR	reverse transcriptase-polymerase chain reaction
RIPA	radioimmunoprecipitation assay
RSK	ribosomal s6 kinase
SCYEI	inducible small cytokine subfamily E member 1
S.E.M	standard error of the mean
TAK1	transforming growth factor-β-activated kinase-1
TAO	thousand-and-one amino acids
TPL-2	tumor progression locus 2
TR	thioredoxin reductase
Trx	thioredoxin
Wnt	wingless/Int (mouse mammary tumor virus integration site)
ZPA	zone of polarizing activity

ACKNOWLEDGEMENTS

Firstly, and foremost, I thank my Supervisor, Dr. Barbara Hales for her invaluable guidance, unending support, constructive criticism, and endless patience throughout my research and the writing up this thesis. I really could not have imagined having a better mentor for my PhD.

I am truly grateful to Dr. Bernard Robaire for his constructive criticism during these years.

I would like to thank Dr. Alfredo Ribeiro-da-Silva, my research advisor, for his encouragement and advice.

A special thank you to Dr. Chunwei Huang, whose technical support made my lab work much easier; her invaluable friendship is a highlight of my life.

I am especially grateful to Dr. Geraldine Delbes for translating the abstract of this thesis into French.

Many thanks to my thesis proposal and progress report committee members, Dr. Ante Padjen and Dr. Jacquetta Trasler, for their advice and discussions.

I would like to thank Andrea Witkowski for conducting the GSH measurements in Chapter Three.

I would like to thank Leonid Kriazhev from Genoquebec for conducting two-dimensional electrophoresis and mass spec analysis.

I shoud also thank Michelle Carroll for always helping me and bringing happiness to the lab during these years.

I am grateful to Eugene Galdones, a computer expert, a professional photographer, and an excellent chef, for everything that he has done to make the lab time and social lives so pleasant and "delicious".

Many thanks to my labmates, Sarah E. Ali-Khan, Naveen Gnanabakthan, Genevieve Larouche, Lisanne Grenier, Mahsa Hamzeh, and Liga Bennetts, for creating a friendly working and social environment.

Finally, a deep gratitude goes to my parents. Their unlimited love gives me the real strength to overcome any obstacles in my life.

PREFACE

Format of the Thesis

This is a manuscript-based thesis, which conforms to the "Thesis Preparation and Submission Guideline" of the Faculty of Graduate Studies and Research at McGill University. This thesis consists of six chapters. Chapter One, the Introduction, provides the rationale for the studies presented in this dissertation. The model teratogen, hydroxyurea, and oxidative stress are briefly reviewed. A major cellular antioxidant, glutathione, a lipid peroxidation product, 4-hydroxynonenal (4-HNE), and the stress responsive pathways, including activator protein-1 (AP-1), and mitogen-activated protein kinases (MAPK), are also reviewed. The hypothesis and the research objectives are presented in Chapter One as well.

Four data chapters, Chapter Two, Chapter Three, Chapter Four, and Chapter Five, are included in this thesis. Chapter Two is published in Toxicological Sciences (85, 1013-1023, 2005). Chapter Three is published in the Journal of Pharmacology and Experimental Therapeutics (319: 613-621, 2006). Chapter Four and Chapter Five are manuscripts in preparation.

Chapter Six, the Final Conclusions, provides a general discussion of the results, future studies, and a list of Original Contributions. References are provided at the end of the thesis.

Contribution of Authors

All the experiments presented in this thesis were performed by the candidate with the exception of the GSH measurements described in Chapter Three, which were done by Andrea Witkowski and the two-dimensional electrophoresis and mass spec analysis described in Chapter Five, which were done by Leonid Kriazhev.

CHAPTER ONE

INTRODUCTION

1.1 Statement of the problem and purpose of the investigation

More than 6% of all of the children that are live born every year worldwide have a major developmental defect; most of these children need medical care (March of Dimes 2006). Morphologic abnormalities are the primary developmental defects identified at birth. Other manifestations of developmental defects include low birth weight as well as functional deficits, such as mental retardation, that are recognized later in infants or during childhood. Every year, it is estimated that in the world 3.3 million children less than five years old die due to serious congenital abnormalities; about 3.2 million of those who survive may be physically or mentally disabled for life (March of Dimes 2006). In addition to this impact on the live born, developmental defects are responsible for 20-30% of all early pregnancy losses (Wilcox et al., 1999), 10-20% of spontaneous abortions (Hatasaka, 1994;Zinaman et al., 1996), and 1-4% of late fetal deaths and still births (Fretts, 2005). It is impossible to calculate the emotional and mental costs for developmental defects. The annual dollar costs for one major developmental defect (spinal bifida) alone is estimated at $200 million in the United States (Sever et al., 1993).

Despite being a significant human health problem, the causes of most developmental defects are presently unknown. Since the thalidomide tragedy in the early 1960s, the study of developmental toxicology has greatly advanced. We know now that *in utero* exposure to a developmental toxicant during critical periods can disrupt normal development, resulting in congenital abnormalities. It is generally agreed that about 3% of all developmental defects are attributable to exposure to a developmental toxicant, and about 25% are induced by exposure

of a genetically predisposed individual to developmental toxicants (Nelson and Holmes, 1989;Holmes, 1997). Based on animal studies, approximately 2,500 chemicals, in addition to a few physical agents and conditions, have been identified as suspected developmental toxicants in humans (Hansen, 2006). Despite belonging to diverse groups, strikingly, many of these developmental toxicants are capable of inducing oxidative stress; these include thalidomide, phenytoin, heavy metals, irradiation, alcohol, cocaine, cigarette smoke, hypoxia, hyperthermia, and hyperglycemia, which are all recognized as human developmental toxicants (Matsuzuka et al., 2005;Ornoy, 2007;Liu and Wells, 1995;Paniagua-Castro et al., 2008;Fantel and Person, 2002). Oxidative stress can damage cellular macromolecules (membrane lipids, proteins, and nucleic acids), disturb signal transduction, and alter gene expressions. This may disrupt normal developmental process. However, given the diversity of these developmental toxicants, they may initiate multiple mechanisms to influence embryo development. Thus, the question is what role does oxidative stress play in the developmental toxicity induced by exposure to toxicants.

To answer this question, we chose hydroxyurea (HU) as a model developmental toxicant. HU, a DNA synthesis inhibitor, is widely used in the treatment of cancer and sickle cell disease (Platt et al., 1984; Kennedy, 1972; Ariel, 1970). HU induces developmental toxicity in all the experimental species that have been studied. Animal studies have shown that HU inhibits DNA synthesis and may induce oxidative stress in embryos. We hypothesize that oxidative stress is critical to hydroxyurea induced developmental toxicity. CD1 mice were chosen as our animal model. Timed pregnant CD1 mice were treated

with HU during early organogenesis, the most susceptible period of embryo to developmental toxicants induced malformations. The relationship between oxidative stress and developmental toxicity induced by HU, the role of stress-responsive pathways in HU developmental toxicity, and the proteins and genes targeted by HU were investigated.

There is no way to completely avoid exposure to environmental factors during pregnancy. By understanding the role of oxidative stress in developmental toxicity, our ultimate goal is to provide strategies to prevent developmental defects.

1.2 Hydroxyurea (HU)

HU ($CH_4N_2O_2$) is a DNA synthesis inhibitor and has been widely used clinically for the treatment of sickle cell anemia (Platt et al., 1984), hematological malignancies such as myelogenous chronic leukemia (Kennedy, 1972), and solid tumors (Ariel, 1970). Recent studies have discovered its anti-HIV effect in combination with reverse transcriptase inhibitors (Biron et al., 1996). HU is a potent developmental toxicant in animal studies. Exposure to HU at doses within 1-fold of the human dose (base on mg/m^2) induced developmental toxicity in various animal models, such as mice, hamsters, cats, dogs and monkeys (FDA, 2001). Pregnant women are advised to avoid taking HU. There are no controlled developmental toxicity studies in humans. However, a clinical case report of 32 pregnancies with HU exposure described 1 spontaneous abortion and 2 *in utero* fetal deaths; among the 24 liveborn infants, 9 were premature, 3 had minor abnormalities, and 5 presented neonatal respiratory distress (Thauvin-Robinet et

al., 2001). Despite the potential confounding impact of maternal illness, this report indicates that HU is a human developmental toxicant.

1.2.1 Mechanism of action

HU inhibits the activation of ribonucleotide diphosphate reductase (RNR) by destroying a tyrosyl free radical in the catalytic center of the R2 subunit of the enzyme (Sneeden and Loeb, 2004). RNR catalyzes the reduction of ribonucleoside diphosphates (NDPs) into deoxyribonucleoside diphosphates (dNDPs); this is the rate limiting step for *de novo* synthesis of deoxyribonucleoside triphosphates (dNTPs) (Stubbe, 1990). These dNTPs are precursors for both DNA replication and repair (Thelander and Reichard, 1979). Exposure to HU prevents the expansion of dNTP pools when cells enter S phase and stalls replication forks; HU induces DNA replication stress, triggers the formation of γ-H2AX foci at the collapsed forks (Ward and Chen, 2001), and arrests the cell cycle at the G1-S boundary (Kurose et al., 2006).

HU induces rapid cell death preferentially in S-phase cells, and this may be ascribed to the inhibition of DNA synthesis. However, in an early study of developmental toxicity, a quick onset of cell death, within 2 hours, was observed in rabbit embryos after maternal exposure to HU during organogenesis, but a profound inhibition of DNA synthesis occurred around 3-5 hours, as measured by 3H-thymidine incorporation (DeSesso, 1981). Antioxidants or a free radical scavenger pretreatment delayed the onset of cell death in embryos (DeSesso, 1981; DeSesso and Goeringer, 1990; DeSesso et al., 1994). Corroborating this finding, the hydroxylamine group (-HNOH) of the HU molecule has the potential

to react with oxygen in biological fluids and generate reactive oxygen species, including hydrogen peroxide (H_2O_2) and the hydroxyl radical (OH^-); these reactions are shown below (R, organic residue).

$$R\text{-}HNOH+O2 \longrightarrow RNO+\mathbf{H_2O_2}$$

$$R\text{-}HNOH+H_2O \longrightarrow R\text{-}H_2NOH^+ + OH^-$$

$$H_2O_2+R\text{-}H_2NOH^+ \longrightarrow R\text{-}HNOH^+ + \dot{H}_2O + \mathbf{.OH}$$ (DeSesso, 1979).

The production of reactive oxygen species can induce oxidative stress, leading to cell cycle arrest and cell death. DeSesso et al., (1979) proposed the hypothesis that the reactive oxygen species induced by HU are responsible for the cell death induced in embryos.

1.2.2 Pharmacokinetics

HU is a water soluble molecule that is rapidly distributed in a volume similar to that of total body water. After intraperitoneal administration of HU to pregnant rats during organogenesis stage, the half-life of HU was found to be about 60 minutes in the maternal plasma and estimated at 2-3 hours in the embryos (Wilson et al., 1975).

1.2.3 HU developmental toxicity in experimental animal models

Studies in rodents have shown that *in utero* exposure to HU during organogenesis results in fetal lethality, fetal growth retardation (low birth weight), morphological abnormalities (malformations) (Asano and Okaniwa, 1987), and impaired lung function (Woo et al., 2005) and learning ability in live offspring (Butcher et al., 1973). The malformed mouse fetuses mainly displayed palate,

neural tube (curly tail), and skeletal defects. A high incidence of vertebral column and limb defects were reported. Cell cycle arrest in G1-S phase and cell death have been observed in rat (Ritter et al., 1973), mouse (Herken et al., 1978), and rabbit embryos (DeSesso, 1981) after exposure to HU during organogenesis. In a recent study, apoptosis has been detected in HU target tissues in mouse embryos after exposure to HU on gestational day (GD) 13 (Woo et al., 2003). Further, increased p53 immunoactivity and enhanced mRNA level of pro-apoptosis genes, p21, bax, and cyclin G, was reported in an HU target tissue (Woo et al., 2003). Pretreatment of pregnant rabbits with antioxidants (propyl gallate, ethoxyquin) or a free radical scavenger (d-mannitol) delayed the HU-induced rapid onset of cell death in the embryos and ameliorated HU-induced developmental toxicity, in particular, limb defects (DeSesso, 1981; DeSesso and Goeringer, 1990; DeSesso et al. 1994). Thus, oxidative stress may be, at least partially, involved in HU-mediated developmental toxicity. However, the underlying mechanism of oxidative stress in mediating HU-induced developmental toxicity remains elusive.

1.3 Redox status and oxidative stress

Reactive oxygen species (ROS) include oxygen ions, peroxides, and oxygen containing free radicals, such as superoxide ($.O_2^-$), hydrogen peroxide (H_2O_2), and hydroxyl radical (.OH). In addition to induction by environmental stimuli such as irradiation, ROS are inevitablely generated during cellular metabolism. ROS, due to the unpaired electron in their valence shell, are highly reactive towards surrounding biological components, including lipids, proteins

and DNA. Under normal conditions, cellular antioxidant or defense systems can balance ROS generation by detoxifying them, thus maintaining the cells in a state of redox homeostasis. However, when the production of ROS overwhelms the cellular antioxidant capacity, oxidative stress occurs. Oxidative stress can cause cell cycle arrest and induce apoptosis or necrosis, which can disturb embryo development. This section will provide a brief review of the cellular production and detoxification of ROS, the susceptibility of embryo to oxidative stress during organogenesis, cellular responses to oxidative stress, and summarize our current knowledge of the role of oxidative stress in developmental toxicity.

1.3.1 The generation of reactive oxygen species and the antioxidant defense systems

Mitochondrial respiration is the major source of ROS; the inevitable electron leak from the electron-transport chain converts about 1–2% of total respiratory oxygen into superoxide anion ($.O_2^-$) (Cadenas and Davies, 2000) (Fig. 1.1). Superoxide can subsequently be transformed to hydrogen peroxide (H_2O_2), either spontaneously or through catalysis by superoxide dismutase (SOD) (Mayeda and Bard, 1974). If unchecked, H_2O_2 can be converted into the hydroxyl radical (.OH) via the Fenton reaction or the superoxide-driven Fenton reaction (the Haber-Weiss reaction) with transition metals (mainly, Fe^{2+}) (Liochev and Fridovich, 2002;Miller et al., 1990). The hydroxyl radical is extremely reactive, with a very short half-life (10^{-9} s *in vivo)*, and may react with the first molecule encountered (Pastor et al., 2000). Therefore, hydroxyl radicals are considered to be the most toxic ROS and can cause membrane lipid peroxidation (Esterbauer

et al., 1991), protein inactivation and degradation (Davies et al., 1991), and DNA base oxidation and strand breaks (Breen and Murphy, 1995).

A number of cellular antioxidants, such as the reduced forms of glutathione (GSH), tocopherol and flavonoids, can neutralize ROS; many antioxidant enzymes can catalyze the detoxification of ROS [reviewed in (Valko et al., 2006)]. The enzyme SOD can simultaneously convert superoxide into hydrogen peroxide (H_2O_2). Hydrogen peroxide can be broken down into water and oxygen by catalase (CAT), reduced to water by glutathione peroxidases (GPX) using reduced glutathione (GSH) as substrate, or can be converted to water by peroxiredoxin (Prx), using the thioredoxin system. The oxidized glutathione (GSSG) can be reduced back to GSH by glutathione reductase (GR), using NADPH as a cofactor. The oxidized Prx can be reduced by Trx (Thioredoxin). Oxidized Trx can be reduced through TR, using NADPH as a cofactor (Fig.1.1). Together, these antioxidants and antioxidant enzymes maintain the cellular redox status.

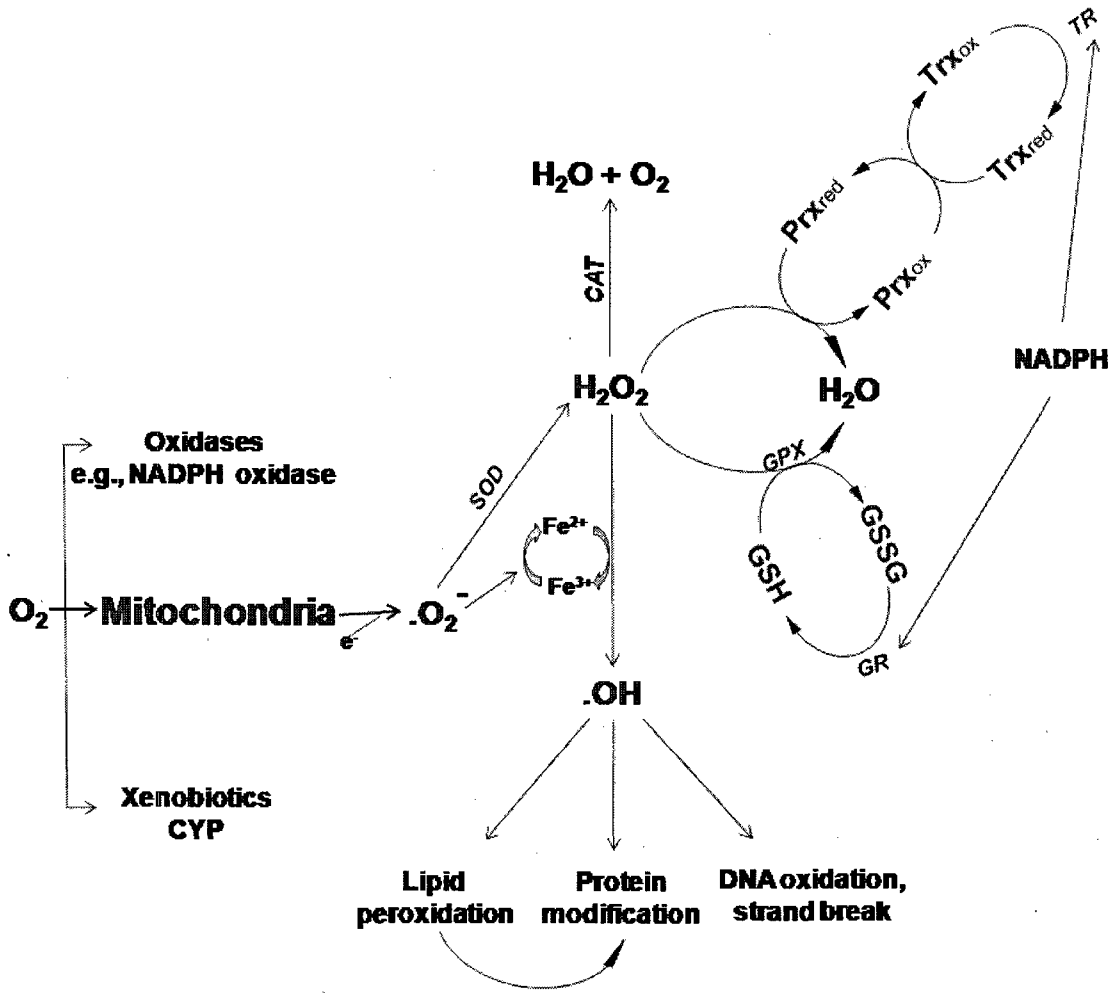

Fig. 1.1 ROS generation and detoxification. Mitochondria are the major source of superoxide anion. The activity of NADPH oxidase, during phagocytosis, and xenobiotic metabolism via CYP (cytochrome p450), can generate superoxide anion as well. NADPH oxidase, nicotinamide adenine dinucleotide phosphate-oxidase; CYP, cytochrome p450; SOD, superoxide dismutase; CAT, catalase; GPX, glutathione peroxidase; GSH, glutathione in reduced form; GSSG, glutathione in oxidized form; GR, glutathione reductase; Prx, peroxiredoxin; Trx, thioredoxin; TR, thioredoxin reductase. Modified from (Hansen, 2006).

1.3.2 The redox status in embryos during organogenesis

During early organogenesis, the embryo is most susceptible to induction of malformations by developmental toxicants because, at this stage, the basic structure of major organs is being formed via very rapid cell growth and differentiation processes. The embryo may also be particularly sensitive to ROS-mediated damage during early organogenesis. The embryo resides in a relatively hypoxic environment in the uterus until the establishment of uteroplacental circulation in early organogenesis (around GD 9 in mice and GD 10 in rats). The circulatory system brings a sudden surge of oxygen to the embryo. Concomitantly, the embryo makes a rapid transition from anaerobic to aerobic metabolism (Akazawa et al., 1994;Shepard et al., 1970;Tanimura and Shepard, 1970), and mitochondria mature with the development of cristae (Shepard et al., 1998).The drastically increased consumption of oxygen in the embryo is also reflected by the requirements for oxygen in an *in vitro* embryo culture condition. GD 9 rat embryos develop normally when the oxygen concentration is 5%, whereas, GD 10 embryos require 20% oxygen (New, 1978;Sanyal and Wiebke, 1979). Despite the possibility of an increase in the production of ROS during this transition period, the embryonic antioxidant defense system is immature compared to later stages of development. In the rat embryo, the activities of superoxide dismutase, glutathione peroxidase and glutathione reductase on GD 10 were less than 50% of that on GD 13 (Choe et al., 2001). Thus, it is not surprising that the embryo may be more sensitive to developmental toxicants that act as oxidants at this early stage of organogenesis.

1.3.3 Cellular responses to oxidative stress

Oxidative stress disrupts cellular redox status, inducing lipid peroxidation, protein oxidation, and DNA oxidation. Membrane lipids represent the primary targets of ROS. Lipid peroxidation generates highly reactive and diffusible aldehydes, such as 4-hydroxyl-2-nonenal (4-HNE), which form adducts with proteins producing protein modifications (Esterbauer et al., 1991). Protein oxidation by ROS leads, in many cases, to the generation of protein-based carbonyls, which have been used widely as a marker for protein oxidation. Interestingly, a recent study shows that the lipid peroxidation-derived aldehyde protein adducts may contribute to the major protein carbonyls that are normally detected (Yuan et al., 2007). Protein modifications may lead to changes in protein folding and function or increased susceptibility to proteolysis. Modification of functional and /or signaling proteins can impact cellular functions and disturb signal transduction. Oxidation of DNA by ROS can induce base oxidation, abasic sites and strand breaks, leading to genotoxicity (Halliwell and Aruoma, 1991;Henle and Linn, 1997).

Oxidative stress induces various cellular responses, such as growth arrest, stimulation of signal transduction pathways, gene transcription, and repair of damaged DNA. These events determine whether a cell will die by necrosis, undergo senescence or apoptosis, or will differentiate, survive and proliferate. The core event in mediating cellular responses to oxidative stress may be the changes in gene expression, possibly primarily through the activation of redox-sensitive transcription factors. Activator protein-1 (AP-1) is one of the most important early-response redox sensitive transcription factors (Gius et al., 1999).

In response to oxidative stress, AP-1 regulates the transcription of genes associated with antioxidant defence, cell cycle control (e.g., Cyclin D1), and apoptosis, either as pro-apoptotic factors (e.g., Fas) or anti-apoptotic proteins (e.g., Bcl-3) (Bakiri et al., 2000;Le-Niculescu et al., 1999;Rebollo et al., 2000). Interestingly, binding of AP-1 to DNA cannot only upregulate but also repress gene expression; for example, AP-1 activation has been reported to suppress the transcription of p53 (Schreiber et al., 1999).

Oxidative stress stimulates AP-1 activity through a variety of mechanisms. Post-translational regulation by mitogen-activated protein kinase (MAPK) is a major pathway to mediate the activation of AP-1 in response to oxidative stress (Karin, 1995). MAPK cascades are crucial for transducing signals from the cell surface into the nucleus, mediating the response of cells to a broad range of environmental stimuli. Downstream targets of MAPK include transcription factors, such as AP-1 and p53 (Lin et al., 1998), molecules involved in the detection and response to DNA damage, such as γ-H2AX (Sluss and Davis, 2006) and PARP-1 (Caldini et al., 2005), as well as a variety of pro-and anti-apoptotic factors (Noguchi et al., 2000;Donovan et al., 2002;Yamamoto et al., 1999). In addition, the AP-1 and MAPK pathways also regulate the responses of cells to physical stimuli such as growth factors, and thereby they are crucial for regulating embryo development. It is well established that the activation of AP-1 and MAPK pathways is crucial for cell fate determination upon oxidative stress; the role of these pathways in mediating the embryonic effect of developmental toxicants remains elusive.

1.3.4 Current knowledge of the role of oxidative stress in developmental toxicity

Many developmental toxicants have been found to be able to induce oxidative stress; these include thalidomide, phenytoin, hyperglycermia, ethanol, tobacco smoke, cocaine, cadmium, and irradiation (Ornoy, 2007;Paniagua-Castro et al., 2008;Fantel and Person, 2002;Ku et al., 2007; Kyriakis and Avruch, 1996;Wells et al., 1997). Treatment with N-acetylcysteine, a free radical scavenger and a glutathione precursor, or an antioxidant can prevent, partially or completely, the developmental toxicity of these developmental toxicants. Furthermore, these developmental toxicants often induce multiple malformations. In particular, neural tube and limb defects are frequently related to oxidative stress (Fantel and Person, 2002).

Thalidomide is one of the best studied developmental toxicants. Thalidomide induces cell death in limbs, resulting in limb truncation; these malformations have been related to the depletion of glutathione, DNA oxidation, activation of a redox sensitive transcription factor NF-kB, as well as activation of AP-1 (c-Jun) through MAPK (Hansen et al., 1999;Hansen and Harris, 2004;Knobloch et al., 2007). Interestingly, HU-induced limb defects may be related to oxidative stress as well, since reducing oxidative stress decreased both the incidence and severity of limb defects (DeSesso et al. 1994). Oxidative stress is capable of inducing deleterious effects in many types of cells, so how does it cause tissue-specific malformations? The fate of a cell in response to oxidative stress is determined by its antioxidant ability, damage repair capacity, and above all, the ability to sense and respond to stress. Interestingly, the antioxidant system may be not equally distributed throughout the embryo (Beck et al., 2001);

mitochondria maturation seems to be tissue-specific during the transition from anaerobic to aerobic metabolism in the embryo (Shepard et al., 1998); the stress response pathways AP-1 and MAPK may be expressed in a tissue-specific manner during embryo development. Thus, the questions are whether HU induces tissue-specific oxidative stress, and what role the activation of AP-1 and MAPK pathways might play in HU-induced developmental toxicity. The following section will clarify why glutathione, a key intracellular antioxidant, was chosen both to evaluate and manipulate oxidative stress; why the formation of 4-HNE protein adducts was used to localize oxidative stress in the embryo; why AP-1 and MAPK pathways are important; why the expression of the morphogen, Fgf8 (fibroblast growth factor 8) and DKK1 (dickkopf1), which are critical to limb and vertebral column development, were chosen as markers of the response of the embryo to HU exposure.

1.4 Glutathione

Glutathione (L-γ-glutamyl-L-cysteinylglycine), present in mammalian cells in concentrations between 1-11 mM, is the most abundant cellular non-protein thiol and plays a central role in the cellular defense against ROS. Glutathione exists in reduced (GSH) and oxidized (GSSG) forms, with GSH predominating over GSSG (Meister and Tate, 1976). GSH can donate an electron (H^+) to neutralize ROS spontaneously, or it may act as a substrate of glutathione peroxidase to reduce hydrogen peroxide, lipid peroxides and organic hydroperoxides (Gerard-Monnier and Chaudiere, 1996). During these processes, GSH itself will be oxidized to GSSG, which can either be reverted to GSH by the

action of glutathione reductase (GR) or be exported out of cells through membrane transporters (Keppler, 1999;Dickinson and Forman, 2002). The ratio of GSSG to GSH is a critical determinant of cellular redox status; and an increase in this ratio is indicative of oxidative stress.

GSH can form reversible mixed protein disulfides during oxidative stress to protect proteins from free radical attack (Coan et al., 1992), or it can conjugate with, and therefore detoxify, lipid peroxidation end products, either spontaneously or through catalysis by glutathione transferases (GSTs) (Alin et al., 1985). The *de novo* synthesis of GSH by the sequential actions of gamma-glutamylcysteine synthetase (γ-GCS) and glutathione synthetase (GS), is the primary way to restore the GSH content in most cells (Griffith and Mulcahy, 1999). The rate limiting enzyme in glutathione synthesis is γ-GCS, a heterodimeric enzyme comprised of a catalytic (γ-GCSC) and modulatory (γ-GCSM) subunit. γ-GCSC and γ-GCSM may be up-regulated in response to oxidative stress and contribute significantly to the defense against oxidative stress (Solis et al., 2002;Mulcahy and Gipp, 1995).

GSH homeostasis is essential for both normal embryo development and defense of embryo against developmental toxicants. Mice deficient in GSH die before GD 8.5 (Shi et al., 2000). Depletion of GSH by L-buthionine-S,R-sulfoximine (BSO), a selective irreversible inhibitor for γ-GCS, has been shown to disturb organogenesis and exaggerate the effects of developmental toxicants during organogenesis *in vitro* and *in vivo* (Hales and Brown, 1991;Ozolins et al., 2002). BSO has commonly been used to enhance oxidative stress in developmental toxicity studies (Harris et al., 1986).

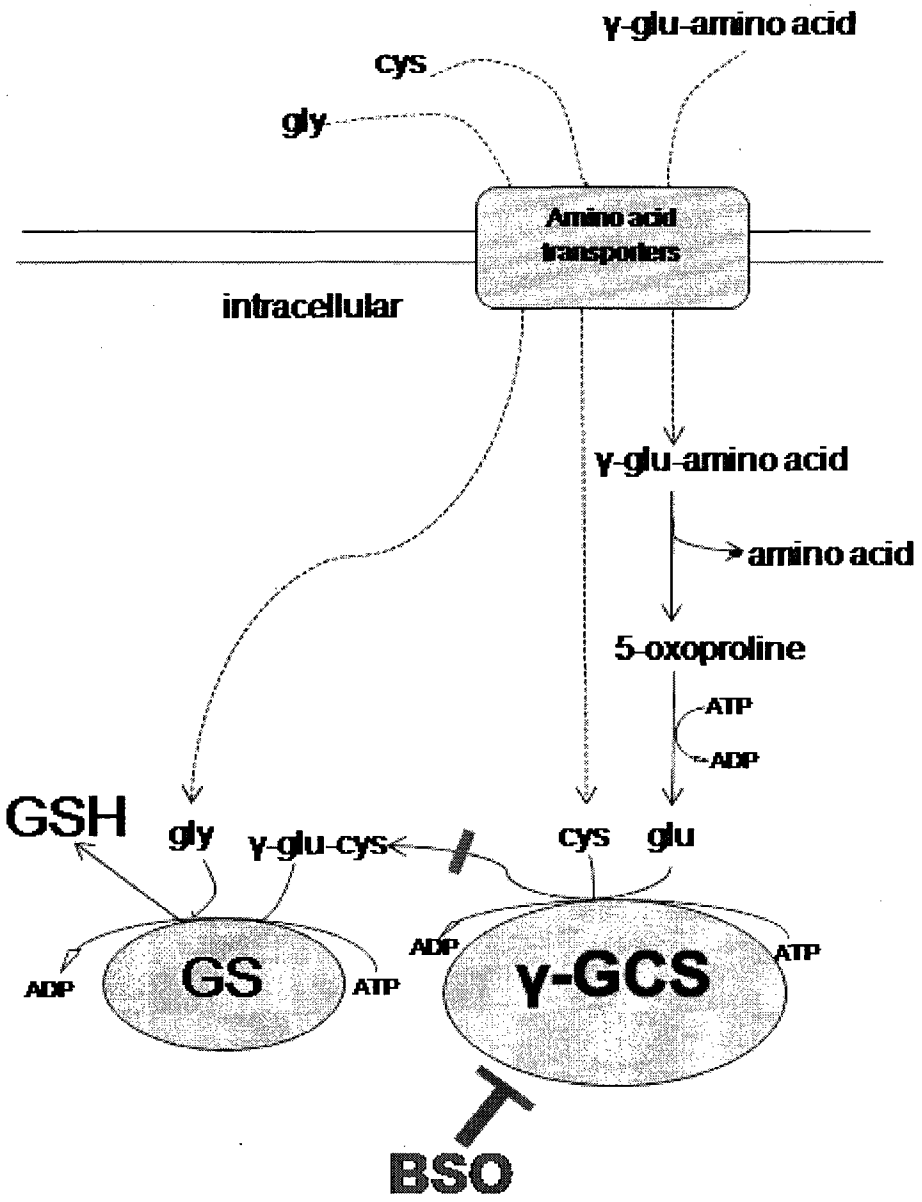

Fig. 1.2 GSH synthesis. The cysteine (cys) and glutamate (glu) transported into the cytosol directly or through a γ-glutamyl-amino acid complex, respectively, are combined by the enzyme gamma-glutamylcysteine synthetase (γ-GCS) to form γ-glutamyl cysteine, which is then combined with glycine (gly) to form GSH. γ-GCS is the rate limiting enzyme in GSH synthesis. Buthionine sulphoximine (BSO) irreversibly inhibits γ-GCS to deplete GSH. Transport pathways are indicated by dashed lines; metabolic pathways are solid lines. Obtained from (Dickinson et al., 2003).

1.5 The lipid peroxidation product 4-hydroxy-2-nonenal (4-HNE)

The polyunsaturated fatty acids in plasma membrane represent a primary target of ROS. 4-HNE is a major end product of membrane lipid peroxidation; 4-HNE can modify cellular proteins via the formation of 4-HNE-protein adducts (Esterbauer et al., 1991). It has been suggested that 4-HNE may be a second messenger of ROS (Zarkovic, 2003). The increase in 4-HNE-protein adducts can serve as a marker for oxidative stress. The development of antibodies against 4-HNE modified epitopes on proteins provides a reliable measurement tool to localize oxidative stress in the embryo after exposure to developmental toxicants, using immunohistochemistry analysis. Furthermore, immunoblotting analysis combined with mass spectrometry can identify the proteins modified by 4-HNE, supplying more information of the molecular pathway of ROS in mediating developmental toxicity. This section will provide a brief review of the formation of 4-HNE, protein modifications by 4-HNE, and the cellular responses elicited by 4-HNE-protein adducts.

1.5.1 The formation and detoxification of 4-HNE

ROS, especially hydroxyl radicals, can attack the polyunsaturated fatty acids within the plasma membrane and initiate a self-perpetuating chain-reaction, leading to the generation of lipid peroxides, which in turn break down to yield a broad array of fragments, notably aldehydes (Sevanian and Hochstein, 1985). 4-HNE is among the most abundant and cytotoxic of these aldehydes, derived from the peroxidation of the membrane n-6-polyunsaturated fatty acids, essentially linoleic and arachidonic acid (Esterbauer et al., 1991). The basal levels of 4-HNE

vary considerably in different cell types and are normally below 1 μM; however, between 10 μM to 5 mM of 4-HNE can accumulate in membranes during oxidative stress (Uchida, 2003).

Multiple enzymatic pathways can detoxify 4-HNE. The conjugation of GSH to 4-HNE catalyzed by GSTs (glutathione transferases) is the major way to prevent the interaction of 4-HNE with cellular components (Hubatsch et al., 1998;Yang et al., 2001;Gallagher et al., 2007). However, depletion of GSH leading to the disruption of redox status may also be an important biological effect of 4-HNE (Nakashima et al., 2003). Other enzymes involved in 4-HNE metabolism are the aldehyde dehydrogenases and alcohol dehydrogenases that catalyze the reduction of 4-HNE to its innocuous acid or alcohol, respectively (Hartley et al., 1995). In addition, aldose reductase and aldo-keto reductase have been reported to detoxify 4-HNE (Rittner et al., 1999;Srivastava et al., 1995).

1.5.2 Protein modifications by 4-HNE

4-HNE contains three functional groups (a C=C double bond conjugated with a C=O carbonyl, and a hydroxyl group at carbon four) which, in many cases, act synergistically. Therefore, 4-HNE is highly reactive towards thiol and amino groups in cellular macromolecules, including peptides, proteins, and nucleic acids. Quantitatively, proteins and peptides represent the most important group of 4-HNE-targeted biomolecules (Siems and Grune, 2003).

It is well established that 4-HNE can form adducts with protein side chains via Michael addition (cysteine, histidine, and lysine) or via Schiff base reaction (lysine) (Uchida, 2003). A study using synthetic polyaminoacid model compounds

has shown that the order of the molar ratio of 4-HNE/amino acid is Cysteine (0.6) > Histidine (1×10^{-3}) > Lysine (3×10^{-4}) (Poli et al., 2007). Therefore, 4-HNE is most reactive towards cysteine *in vitro*. Of note, the reaction of 4-HNE with cysteine is reversible in the presence of physiological concentrations of GSH, and this may be the only reversible 4-HNE-protein adduct (Carbone et al., 2005b). 4-HNE modified proteins are normally susceptible to proteolysis, although the protein-protein cross-linking caused by 4-HNE may influence protein turnover (Grune and Davies, 2003).

Since 4-HNE is relatively stable and highly diffusible, the proteins that have been found to be modified by 4-HNE belong to diverse groups, including its own detoxification enzyme (glutathione transferase), other related antioxidant enzymes (e.g., glutathione reductase, thioredoxin reductase), tyrosine receptors (e.g., EGFR, epidermal growth factor receptor; PDGFR platelet-derived growth factor receptor), energy metabolism enzymes (e.g., GAPDH, glyceraldehyde 3-phosphate dehydrogenase), cytoskeletal proteins (e.g., actin), chaperones (e.g. heat shock protein 90), carriers (albumin), and protein kinases [e.g., c-Jun N-terminal kinase (JNK, MAPK)] (Vindis et al., 2006;Liu et al., 1999;Aldini et al., 2006;Fang and Holmgren, 2006;Aoyama et al., 2006;Aldini et al., 2005;Carbone et al., 2005;Ishii et al., 2003;Parola et al., 1998). Adduction by 4-HNE in most case impairs the protein function, either by modification of the critical sites required for protein function or by impairment of protein folding. For instance, inactivation of antioxidant enzymes or disruption of the proper folding of heat shock proteins may further exaggerate 4-HNE-mediated damage (Carbone et al., 2004a;Aoyama et al., 2006;Fang and Holmgren, 2006). In contrast, the formation

of 4-HNE adducts may activate tyrosine receptors (e.g., EGFR) and some protein kinases, such as the JNK (Liu et al., 1999;Parola et al., 1998).

1.5.3 The cellular responses elicited by 4-HNE

Through exogenous addition of 4-HNE into the cell culture medium, experiments have shown that, at increasing concentrations, 4-HNE induces cell cycle arrest (Barrera et al., 2004;Laurora et al., 2005), differentiation (Barrera et al., 1991), and apoptosis (Sunjic et al., 2005), whereas at lower concentrations it has been found to stimulate proliferation in at least some cell types (Ruef et al., 1998). This may indicate that the regulation of intracellular concentrations of 4-HNE may be critical to cell cycle signaling. In agreement with this view, depletion of 4-HNE, by incorporation of GST isozyme (hGSTA4-4) into adherent human epithelial cell lines, caused cell transformation and indefinite proliferation (Sharma et al., 2004). The transformed cells showed an upregulated expression of growth promoters, such as, transforming growth factor β1, cyclin-dependent kinase 2, and the extracellular signal regulated kinases (ERKs), and downregulated expression of p53.

4-HNE is a potent apoptosis inducer during oxidative stress. Overexpression of GSTs in cells lead to lower steady-state levels of HNE, and these cells acquired resistance to apoptosis induced by ROS, UV, and pro-oxidant xenobiotics (Awasthi et al., 2004). Exogenous addition of 4-HNE to cell culture medium induces apoptosis in many cells of various origins (Sunjic et al., 2005;Malecki et al., 2000;Kalinich et al., 2000). 4-HNE-induced activation of the JNK/AP-1 pathway has been associated with apoptosis in different cell lines

(Kutuk and Basaga, 2007). Enhanced activation or expression of p53 has also been implicated in 4-HNE-mediated apoptosis (Cenini et al., 2007). Furthermore, induction of cytochrome C release has been suggested to contribute to 4-HNE-induced apoptosis (Raza and John, 2006). Apart from the classic apoptosis pathways, 4-HNE forms adducts with GAPDH, leading to GAPDH inactivation (Ishii et al., 2003), degradation (Tsuchiya et al., 2007), and abnormal aggregation (Uchida and Stadtman, 1993). GADPH is a classic glycolytic enzyme, however, accumulating evidence suggests that GADPH is an apoptosis executor during oxidative stress (Chuang et al., 2005).

Interestingly, while the activation of JNK by 4-HNE is often related to apoptosis, 4-HNE can induce the expression of γ-GCS, the rate-limiting enzyme of GSH biosynthesis, through the JNK pathway in a human bronchial epithelial cell line, thereby leading to a stress adaption response (Dickinson et al., 2002) . It has been suggested that the effect of 4-HNE on protein kinases is dependent on the cell type, the concentration and cellular compartmentalization of 4-HNE (Leonarduzzi et al., 2004).

1.6 Activator protein-1 (AP-1)

Cells respond to oxidative stress-induced damage primarily through changes in gene expression, which are closely regulated by transcription factors. In previous studies in our laboratory, an early response redox sensitive transcription factor, AP-1, has been found to regulate gene expression in response to oxidative stress in the rat conceptus at the organogenesis stage (Ozolins and Hales, 1997). AP-1 was one of the first mammalian transcription factors to be

identified (Angel and Karin, 1991). The major members of the AP-1 family have been demonstrated to be immediate early genes (Karin et al., 1997). AP-1 activity is induced by many physical stimuli, such as growth factors, as well as a plethora of environmental insults, that include but are not limited to, ROS, alkylating agents, UV, irradiation, heat shock, alcohol, hyperglycemia, and heavy metals; these are all known developmental toxicants (Qiang and Ticku, 2005;Luo et al., 2007;Bradbury et al., 2001;Srinivasan et al., 2004;Korashy and El-Kadi, 2008;Kolbus et al., 2000). AP-1 is not only important in mediating normal embryo development, but also crucial for regulating the cellular stress response, leading to cell survival or death. Thus, the activation of AP-1 in response to HU may indicate the response of the embryo to the insult by this developmental toxicant. Using an Enzyme-Linked ImmunoSorbent Assay (ELISA), the DNA binding activity of AP-1 can be determined readily; AP-1 DNA binding activity may provide an efficient measure to screen potential developmental toxicants.

1.6.1 The AP-1 family proteins

One major reason for the ability of AP-1 to control a broad range of biological processes is because it is not a single protein, but a mixture of dimeric complexes composed of groups of proteins that share an evolutionarily conserved bZIP (basic leucine zipper) domain (Chinenov and Kerppola, 2001). The bZIP domain of AP-1 proteins consists of a basic region directly contacting DNA, and an adjacent heptad repeat of leucine residues (leucine zipper), mediating dimer formation (Landschulz et al., 1988;Patel et al., 1990;Leonard et al., 1997). Dimerization by means of the leucine zipper domain juxtaposes the

two basic regions to form a symmetric interface that can bind to DNA. The most well documented AP-1 member belongs to the Jun (c-Jun, JunB, and JunD) and Fos (c-Fos, FosB, Fra-1, and Fra-2) families. Jun proteins form stable homo- and hetero-dimers, whereas the Fos proteins require heterodimerization to bind to DNA. Both homo- and hetero-dimers (Jun-Jun and Jun-Fos) bind with high affinity to the palindromic AP-1 recognition element (5'-TGAG/CTCA-3'), which are also known as TREs [TPA (phorbol 12-O-tetradecanoate-13-acetate)-responsive elements] (Angel and Karin, 1991).

Other AP-1 members belong to ATF (activating transcription factors, ATFa, ATF2, ATF3), JDP (Jun dimerization proteins, JDP-1 and JDP-2), and Maf protein families (Chinenov and Kerppola, 2001). ATF forms heterodimers with Jun (predominantly c-Jun-ATF2) as well as Fos proteins, which preferentially bind to the cAMP response element (CRE, 5'-TGACGTCA-3') rather than TREs (Hai and Curran, 1991). JDP proteins (especially JDP-2) may dimerize with c-Jun or ATF-2 (Aronheim et al., 1997;Jin et al., 2001), acting as a repressor of gene activation mediated by c-Jun or ATF-2, respectively. The heterodimers of Maf and Jun or Fos proteins interact with recognition sites composed of Maf (TGCtgaC) and AP-1 (TGAC) half-sites, which further expands the diversity of the AP-1 target genes (Kerppola and Curran, 1994). Furthermore, Jun proteins can interact with Maf and the structurally related Nrf2 to form antioxidant/electrophile response element (ARE/ EpRE) binding complexes, regulating the expression of antioxidant enzymes upon oxidative stress (Venugopal and Jaiswal, 1998).

Despite the high degree of structural homology, the different members of the Jun and Fos families exhibit considerable differences in DNA-binding and

transcriptional activation. In general, the binding of heterodimers of Jun-Fos to DNA is more stable than the binding of homodimers (Jun-Jun); c-Jun, c-Fos and FosB are strong transactivators, whereas JunB, JunD, Fra-1 and Fra-2 exhibit only weak transactivation potential (Hess et al., 2004). As a result, the composition of the AP-1 complex may modulate a selection of target genes. Indeed, the cellular composition of AP-1 proteins alters with the cell cycle (Kovary and Bravo, 1991a) as well as with the type of stimuli (Wisdom, 1999). Previous studies from our laboratory have found that JunD is a major component of basal AP-1 DNA binding activity, whereas c-Jun and c-Fos contribute to oxidative stress-induced AP-1 DNA binding activity in rat embryos during early organogenesis (Ozolins and Hales, 1999a).

1.6.2 AP-1 in regulation of cellular processes

AP-1 is induced rapidly in response to growth factors and tumour promoters. Studies undertaken in the past two decades have demonstrated that AP-1 controls not only cell proliferation and neoplastic transformation, but also differentiation, survival, and apoptosis (Shaulian and Karin, 2002).

AP-1 controls cell cycle progression. Microinjection of antibodies against Fos or Jun family proteins blocks the entrance of serum-stimulated quiescent mouse fibroblasts into S phase (Kovary and Bravo, 1991b). AP-1 binds to the cyclin D1 promoter and induces its transcription (Herber et al., 1994;Shen et al., 2008). Consistently, fibroblasts deficient in c-Jun show a severe proliferation defect, with decreased cyclin D1 expression (Wisdom et al., 1999). The absence of c-fos or fos B alone does not influence fibroblast proliferation; c-fos$^{-/-}$fosB$^{-/-}$

double knockout blocks the entry of cells into S-phase, and this is correlated with a specific loss of cyclin D1 induction following serum stimulation (Brusselbach et al., 1995;Brown et al., 1998). Interestingly, c-fos$^{-/-}$fosB$^{-/-}$ double knockouts are much smaller than their wildtype counterparts, presumably due to the defect in cell proliferation (Brown et al., 1998). Similarly, JunD deficient fibroblasts show growth arrest at G1- S phase; JunD knockout mice also show lower body weights than their wildtype counterparts (Thepot et al., 2000).

The role of AP-1 in the regulation of cell differentiation has been confirmed in studies of skeletal development. AP-1 (JunD/Fra2) regulates chondrocyte terminal differentiation via the induction of the transcription of Mmp-13 (matrix metalloproteinase-13, also known as collagenase-3) (Ijiri et al., 2005). AP-1 (c-Fos) is required for osteoclast differentiation, since mice deficient in c-Fos display a complete blockade of osteoclast differentiation (Grigoriadis et al., 1994). Interestingly, inserting fra-1 into the c-fos locus can totally restore osteoclast differentiation, indicating some functional equivalence between c-Fos and fra-1 (Fleischmann et al., 2000). The downstream target gene of AP-1 (c-Fos) in osteoclast differentiation has been suggested to be NFATc1 (nuclear factor of activated T cells1) (Matsuo et al., 2004).

AP-1 regulates the expression of both pro-apoptotic and anti-apoptotic genes. Consistent with this, the activation of AP-1 may either induce apoptosis or prevent cell death depending on the cell type and stimulus. AP-1 (c-Jun) regulates the expression of Dkk1, an apoptosis inducer, during limb morphogenesis and in response to oxidative stress and thalidomide treatment (Knobloch et al., 2007). AP-1 (c-Jun) may also regulate the expression of Bim, a

Bcl-2 family protein critical to neuronal apoptosis (Whitfield et al., 2001). Inhibition of c-Jun activity prevents the neuronal apoptosis induced by growth factor withdrawal and oxidative stress (Estus et al., 1994;Ham et al., 1995). Mice carrying an inactive mutant c-Jun, with serine 63 and 73 replaced by alanine ($Jun^{A63/73}$), are resistant to the kainate-induced neuronal cell death of hippocampal and cortical neurons (Behrens et al., 1999). Furthermore, mice deficient in c-Fos are resistant to light induced apoptosis in retinal photoreceptors (Hafezi et al., 1997), indicating that c-Fos may also induce apoptosis.

In contrast to this pro-apoptotic activity, AP-1 is crucial for cell survival under some circumstances. Interestingly, a study of fibroblast cells *in vitro* provides convincing evidence supporting the anti-apoptosis activity of AP-1 during oxidative stress (MacLaren et al., 2004). As noted above, fibroblast cells have been widely used for studies of the function of AP-1 in cell cycle control. Among AP-1 members, c-Jun null fibroblasts undergo the most severe growth arrest (G1/S) shortly after culture *in vitro* (Johnson et al., 1993). Strikingly, MacLaren et al., (2004) have found that these c-Jun null fibroblasts can overcome the growth arrest and proliferate successfully under low oxygen (3%) culture conditions, rather than the classic culture conditions with 21% oxygen. The growth arrest in c-Jun deficient fibroblasts was related to the enhanced DNA damage caused by exposure to 21% oxygen. Interestingly, these investigators have observed the co-localization of c-Jun with γ-H2AX foci in wildtype fibroblasts after ionizing irradiation; the impact of this co-localization is still unknown. Either the introduction of exogenous c-Jun or the deletion of p53 can completely abrogate the proliferation defect in c-Jun null fibroblasts under normal culture

conditions (21% oxygen) (Shaulian et al., 2000). Corroborating this observation, in wildtype fibroblasts, c-Jun not only represses p53 gene transcription through binding to a variant AP-1 binding site in the p53 promoter, but also inhibits the transcriptional activity of p53 via a direct interaction (Schreiber et al., 1999). Altogether, it appears that c-Jun may be a central regulator of cell cycle progression, DNA damage repair, survival, and apoptosis in response to oxidative stress in fibroblasts.

Because of the diverse combinations of AP-1 dimers, it is difficult to draw conclusions with respect to the precise function of each dimer. However, different AP-1 compositions may have different functions and AP-1 may serve as a site of the integration for both physical and chemical stress signals.

1.6.3 AP-1 in embryo development

AP-1 proteins display distinct spatial and temporal expression and activation patterns during embryo development; each AP-1 member has a distinct role in mediating embryo development, despite the existence of some functional equivalence. Mice lacking c-Jun die between GD 12.5 and GD 14.5 due to massive apoptosis of hepatocytes; these mutant mice also exhibit heart defects, probably due to cardiac stem cell dysfunction (Hilberg et al., 1993). Mice lacking Fra-1 or JunB alone die around GD 10 due to vascular defects in the extra-embryonic tissues (Schreiber et al., 2000;Schorpp-Kistner et al.,1999). Mice lacking ATF-2 die shortly after birth due to lung defects (Maekawa et al., 1999). Mice deficient in Fra-2 die within five days after birth due to a not yet identified

organ dysfunction (Eferl et al., 2007). Mice lacking FosB or JunD are viable, however, adult females display a nurturing defect and adult males have impaired spermatogenesis (Brown et al., 1996;Thepot et al., 2000). Mice deficient in c-Fos survive and are fertile but a lack of ostoclasts results in osteopetrosis (Johnson et al., 1992).

Tissue-specific knockouts have revealed more functions of AP-1 in regulating embryo development. Mice with a deletion of c-Jun in keratinocytes develop normal skin with the exception that keratinocytes in the area of the eyelids have reduced proliferation and migration, leading to open eyes at birth (Zenz and Wagner, 2006). Chondrocyte-specific inactivation of c-Jun results in a severe scoliosis phenotype; this is due to an increased apoptosis of notochordal cells (Behrens et al., 2003).

Ectopic expression of c-Fos in mice has no evident effects on most tissues, but results in the transformation of osteoblasts, leading to osteosarcomas (Grigoriadis et al., 1994). Surprisingly, mice with c-Jun overexpression have no obvious phenotype, suggestive of a loss of gene dose sensitivity to c-Jun during evolution (Grigoriadis et al., 1993).

Overall, the genetically modified mouse models indicate that AP-1 members may regulate cell proliferation, survival, differentiation, and migration during embryo development. c-Jun may also mediate apoptosis during limb and central nervous system.

1.6.4 The regulation of AP-1

Given the complexity and selectivity of action of AP-1 proteins, it is not surprising that the expression and activity of AP-1 members are tightly regulated at multiple levels. In general, enhanced AP-1 DNA binding activity can be achieved by controlling the concentration of proteins, by posttranslational phosphorylation, or by redox regulation of DNA binding activity (Angel and Karin, 1991;Abate et al., 1990). All Fos and Jun family members contain a highly conserved cysteine residue in their DNA binding domain (Abate et al., 1990). Reduction of cysteine residues enhances AP-1 DNA binding, while cysteine oxidation inhibits DNA binding. A cellular protein Ref-1(redox effector factor-1) can reduce the cysteine residues and serves as a redox regulator of AP-1 DNA binding activity (Xanthoudakis and Curran, 1992;Xanthoudakis et al., 1994).

Above all, accumulating evidence suggests that phosphorylation by MAPKs (mitogen activated protein kinases) is a major way to activate AP-1 in response to different stimuli. Firstly, upon activation, MAPKs can phosphorylate the existing DNA binding proteins to transcribe genes encoding AP-1 proteins, in particular, c-Jun and c-Fos, which are known as immediate-early genes. The expression of c-jun is regulated mainly by the binding of c-Jun-ATF2 to the CRE site in its promoter region, thereby forming a positive auto-regulation loop (Gupta et al., 1995). MAPKs also activate the ternary complex factors (ELK-1), leading to the expression of c-fos in response to different stimuli (Muller et al., 1997). It is noteworthy that although Jun and Fos mRNA levels can be rapidly induced by various stimuli, this may not be reflected at the protein levels (Angel and Karin, 1991).

Posttranscriptional phosphorylation of the pre-existing and newly-synthesized AP-1 proteins by MAPKs can enhance AP-1 transactivation potential, protein stability, and DNA-binding activity, thereby leading to the induction of transcription of their target genes (Chang and Karin, 2001). Since AP-1 members are mainly nuclear proteins, MAPK cascades have been suggested to be the major pathways transducing extracellular stimuli to AP-1. MAPK signal cascades contain three major distinct pathways, including ERKs (extracellular signal-regulated kinases), JNK (c-Jun N-terminal kinase), and p38 MAPK pathways. In general, ERKs are preferentially activated by mitogens such as growth factors, serum and phorbol esters (Troppmair et al., 1994), whereas JNK and p38 MAPK are often triggered by cytokines and stress stimuli, and thereby are known as stress-activated MAPKs (Davis, 2000;Zarubin and Han, 2005).

The phosphorylation of c-Jun by JNK is the best studied. Once activated, JNK translocates to the nucleus, where it phosphorylates c-Jun on serines 63 and 73 in the NH_2-terminal transactivation domain (Hibi et al., 1993). JNK can also phosphorylate ATF2 and JunB directly (Li et al., 1999;Morton et al., 2004) JunD does not contain a JNK docking site, thereby it can only be phosphorylated after dimerization with other Jun proteins (Kallunki et al., 1996). p38 MAPKs mainly phosphorylate ATF2 (Barancik et al., 2000). However, a recent study shows p38 MAPKs can activate c-Fos upon UV activation (Tanos et al., 2005). ERKs phosphorylate all Fos proteins (c-Fos, FosB, Fra-1, and Fra-2) in the COOH-terminal transactivation domain (Gruda et al., 1994;Chen et al., 1996;Skinner et al., 1997;Murakami et al., 1997). In addition, ERKs can

phosphorylate ATF-2 and c-Jun in response to growth factors (Ouwens et al., 2002;Leppa et al., 1998) (Fig. 1.3).

In addition to this simplified regulation, each group of MAPKs contains different isoforms important for regulating different cellular responses. Furthermore, MAPKs also activate many other substrates, which may crosstalk with AP-1 to initiate a proper cellular response upon stimuli. Thus, MAPKs will be further discussed in the next section.

1.7 Mitogen-activated protein kinases (MAPKs)

MAPK pathways have been conserved throughout evolution from yeast to humans, and they are crucial for regulating the cell response to a wide variety of environmental stresses as well as growth signals (Widmann et al., 1999). MAPK cascades typically include a three-tiered core-signaling module wherein the stress-activated MAPK kinase kinase (MAP3K) phosphorylates MAPK kinase (MAP2K) on its serine and threonine residues, which in turn phosphorylates MAPK on its threonine and tyrosine residues (Fig.1.3).

As discussed above, three groups of MAPKs have been well studied, including extracellular signal related kinase (ERK1, ERK2), Jun N-terminal kinase (JNK1, JNK2, JNK3), and p38 MAPK (p38α, p38β, p38γ, p38δ) (Widmann et al., 1999). ERK1/2 pathways are normally responsive to growth signaling, such as growth factors; whereas JNKs and p38 MAPKs are preferentially activated by inflammatory cytokines and various stress stimuli, such as ROS, UV irradiation, osmotic stress, and agents interfering with DNA and protein synthesis (Kyriakis and Avruch, 1996). The specificity of signal transmission is ensured by

interactions between the components of the MAPK cascade, either directly or via scaffold proteins (Dhanasekaran et al., 2007). Once activated, MAPKs can dually phosphorylate (serine and threonine) a large panel of substrates that include nuclear proteins (transcription factors and nuclear protein kinases) and some cytoplasmic proteins (cytoplasm protein kinases and cytoskeletal proteins) (Pearson et al., 2001). As a result, MAPK pathways control cell survival, proliferation, differentiation, and death.

Oxidative stress can stimulate MAPK cascades via apoptosis associated kinase 1 (ASK1), a member of MAP3K family initiating both JNK and p38 MAP kinase cascades (Matsukawa et al., 2004). Under normal conditions, ASK1 forms an inactive complex with reduced thioredoxin; oxidation of thioredoxin promotes the release of thioredoxin, resulting in the activation of ASK1 (Saitoh et al., 1998). Oxidative stress may also upregulate the activity of MAPKs through suppression of dual-specificity phosphatases (MAPK phosphatases) (Xu et al., 2004). Furthermore, 4-HNE may activate JNK directly, as aforementioned (Parola et al., 1998).

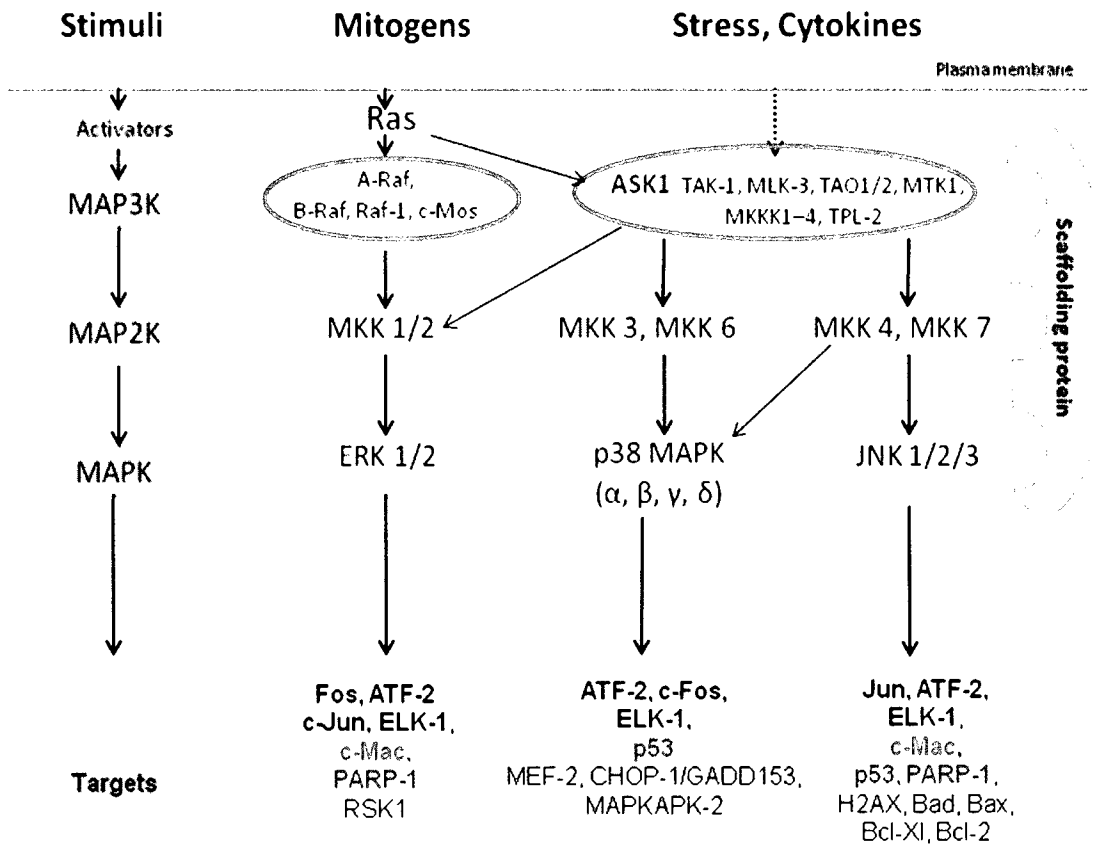

Figure 1.3 MAPK cascades. Oxidative stress can activate JNK and p38 pathways via ASK1, a MAP3K. Among the substrates of MAPKs, AP-1 members are shown in bold, as well as ELK-1, since it regulates the gene encoding c-Fos. c-Mac can be activated by ERKs and JNKs. PARP-1 can be a substrate for all three groups of MAPKs. p53 is activated by JNK and p38. PARP-1, poly (ADP-ribose) polymerase; RSK1, p90 ribosomal S6 kinase; CHOP-1/GADD153, C/EBP-homologous protein/growth arrest and DNA damage; MEF-2, myocyte-specific enhancer factor 2. Modified from (Junttila et al., 2007)

1.7.1 ERK1/2 (extracellular signal-regulated kinase 1/2)

ERK1 and ERK2 are detected at 41 kDa and 43 kDa, respectively (Hoshino et al., 1999). ERK1/2 activation is mainly responsive to growth factors and mitogens and, therefore, the activation of ERK1/2 is often related to the stimulation of tyrosine kinase receptors, such as FGFR (fibroblast growth factor receptor) and EGFR (epithelial growth factor receptor) (Ullrich and Schlessinger, 1990). Among all the MAP3Ks, Raf and Mos may be the only ones that exclusively initiate ERK1/2 pathways (Kyriakis et al., 1992;Dent et al., 1992;Force et al., 1994). Additionally, ERK1/2 pathways may be triggered by MKKKs (1–3) and TPL-2 (Lewis et al., 1998;Errede et al., 1995;Gustin et al., 1998;Salmeron et al., 1996). The MAP2Ks that phosphorylate ERKs are MKK1 and MKK2 (Crews et al., 1992;Wu et al., 1993). Upon activation, ERK1/2 can phosphorylate several transcription factors, such as the aforementioned AP-1 components (c-Fos, c-Jun, and ATF-2), as well as Elk-1 and c-Myc (Sears and Nevins, 2002;Cruzalegui et al., 1999;Sears et al., 1999). ERKs can also phosphorylate some cytoplasmic and nuclear protein kinases, for example RSK and MAPKAP kinase-2 (Gavin and Nebreda, 1999;Zhao et al., 1996;Stokoe et al., 1992). ERK pathways have long been implicated in cell growth, proliferation, and survival (Pearson et al., 2001). For instance, in addition to AP-1, c-Myc induces the expression of a large number of genes involved in proliferation and growth (Cowling and Cole, 2006). Furthermore, activated RSK can phosphorylate, and therefore inactivate, the proapoptotic protein Bad (Bonni et al., 1999).

During embryogenesis, the activation of ERK1/2 displays a discrete and dynamic pattern; most of the domains of ERK1/2 activation correspond to the

regions of FGF signaling (Corson et al., 2003). In agreement with this, the activity of ERK1/2 has been implicated in somite segmentation and limb development as a downstream regulator of FGFs (Delfini et al., 2005;Bobick and Kulyk, 2004). Moreover, targeting inactivation of Raf-1 induces embryonic death with increased apoptosis of hepatocytes and vascular defects in the extra-embryonic tissues resembling those in mice lacking c-Jun and Fra-1 or JunB (Huser et al., 2001). Knockout MKK1 induces open eye defects, which mimic the phenotype of the mice with keratinocyte-specific deletion of c-Jun; these open eye defects may be related to the disruption of EGF signaling (Zhang et al., 2003).

1.7.2 JNKs (c-Jun N-terminal protein kinases)

In contrast to ERK1/2, JNK pathways are not strongly activated in most cells by mitogens, including EGF and FGF; however, JNK pathways are vigorously activated by a wide variety of environmental stressors, such as oxidative stress, DNA damaging agents (UV, alkylating agents), ionizing radiation, heat shock, and mechanical shear stress (Adler et al., 1995;Zanke et al., 1996;Turner et al., 1998;Li et al., 1996). All of these stimuli input their signals in the JNK pathway through several MAP3Ks that include ASK, MKKK1–4, TAK-1, MLK-3, TAO1/2, MTK1, and TPL-2 (Davis, 2000). The MAP2Ks, MKK4 and MKK7 then integrate and amplify the signals from MAP3Ks and transmit them to JNK (Davis, 2000). Interestingly, MKK4 and MKK7 preferentially phosphorylate JNK on tyrosine and threonine, respectively (Gerwins et al., 1997). As dual phosphorylation of JNK on tyrosine and threonine is required for its full activation, and both MKK4 and MKK7 are activated in response to environmental stress, it is

possible that MKK4 and MKK7 co-operate to activate JNK in response to environmental stimuli (Lisnock et al., 2000;Lawler et al., 1998).

Three genes, jnk1, jnk2, and jnk3, encoding ten isoforms, have been identified in mammals (Derijard et al., 1994;Kallunki et al., 1994;Mohit et al., 1995). JNK proteins (JNK1, JNK2 and JNK3) are detected at 46 kDa and 54 kDa (Hibi et al., 1993). While the 46-kDa proteins comprise all three JNK proteins, the 54-kDa proteins are mainly restricted to JNK2 and JNK3. JNK1 and JNK2 isoforms are ubiquitously expressed, while JNK3 is highly restricted in brain, heart, and testis in fetal and postnatal mouse (Martin et al., 1996;Yang et al., 1997). The different JNK isoforms can be differentially activated and appear to differ in their ability to bind and phosphorylate different substrate proteins (Gupta et al., 1996). Interestingly, JNK3-c-Jun/AP-1 is responsible for the stress-mediated apoptosis of neuronal cells, as this apoptosis does not occur in Jnk3 null mice (Yang et al., 1997). Strikingly, 4-HNE-elicited apoptosis may also be mediated via JNK3 (Bruckner and Estus, 2002). In contrast, JNK1 and JNK2 may be essential for regulation of region-specific apoptosis during early brain development; jnk1/jnk2 double mutant embryos die around GD 11 and display an open cranial neural tube with reduced apoptosis in the hindbrain but a dramatically increased apoptosis in the forebrain region (Kuan et al., 1999). Interestingly, this function of JNK1 and JNK2 in early brain development is independent of JNK3, as $jnk1^{-/-}jnk3^{-/-}$ or $jnk2^{-/-}jnk3^{-/-}$ double mutants survive normally (Kuan et al., 1999). Thus, different JNK isoforms may have distinct functions.

JNK can phosphorylate a broad range of protein targets. As noted above, c-Jun is the most classic substrate for JNKs; other Jun family proteins (Jun B, Jun D), and ATF-2 can be phosphorylated by JNKs as well (Hibi et al., 1993; Li et al., 1999;Morton et al., 2004; Kallunki et al., 1996). JNKs can also activate other transcription factors, including Elk-1 and p53 (Cavigelli et al., 1995;Hu et al., 1997). In addition, JNKs have many other nontranscriptional substrates (Bogoyevith and kobe, 2006). In particular, JNK phosphorylates both antiapoptotic proteins (Bcl-2, Bcl-xL) and proapoptotic proteins (Bad, Bax), and the consequence of this phosphorylation, either activation or depression, depends on the cell type and stimulus (Kim et al., 2006;Deng et al., 2001;Yu et al., 2004;Yamamoto et al., 1999;Kharbanda et al., 2000). Furthermore, JNK phosphorylates H2AX (Sluss and Davis, 2006) and PARP1 in response to DNA damage induced by UV and H_2O_2 (Zhang et al., 2007). Thus, the activation of JNK pathways is critical to the determinant of cell fate in response to stress. Interestingly, despite the fact that activation of JNK in response to stress has been mostly related to apoptosis, it has been shown that activation of JNK upregulates antioxidant defense (Dickinson et al., 2002). As noted above, different isoforms of JNK may have distinct functions. Furthermore, recent studies suggest that the consequence of JNK activation is dependent on the duration of its activation; robust and sustained activation of JNK under severe stress conditions normally results in apoptosis, whereas transient activation may be protective (Liu and Lin, 2005).

1.7.3 p38 MAPKs

Similar to JNKs, the p38 MAPKs are strongly activated by environmental stress and are inconsistently activated by growth factors (Kyriakis and Avruch, 1996). In most circumstances, the same stimulus that triggers JNK activation also triggers p38 pathways. Thus, p38 and JNK share similar MAP3K, including ASK1, MTK1, TAK1, and TAO1/2 (Hutchison et al., 1998;Ichijo et al., 1997;Yamaguchi et al., 1995;Takekawa et al., 1997;Chen and Cobb, 2001). In contrast, the MAP2Ks that phosphorylate p38, MKK3 and MKK6, show a high degree of specificity toward p38, as they do not activate ERKs or JNKs (Enslen et al., 1998). However, MKK4, the MAP2K that phosphorylates JNK, possesses some MAP2K activity toward p38, suggesting that MKK4 may represent a site of integration for the p38 and JNK pathways (Guan et al., 1998).

In vertebrates, there are four isoforms of p38 MAPKs, p38α, p38β, p38γ and p38δ, which are detected at 38 kDa (Keesler et al., 1998). While MKK6 activates all p38 isoforms, MKK3 preferentially phosphorylates the p38α, p38γ, and p38δ isoforms (Keesler et al., 1998). Furthermore, the expression of p38 MAPK isoforms is cell lineage-specific and different isoforms may respond distinctly to different stimuli (Hale et al., 1999;Conrad et al., 1999). p38γ and p38δ may even exert opposite effects on AP-1 activation (Pramanik et al., 2003).

p38 and JNK often share similar substrates, for example ATF-2, Elk-1, and p53 (Yang et al., 1998;Waas et al., 2001;Kwon et al., 2002). However, some targets may be preferentially activated by p38, such as MEF-2, CHOP-1/GADD153, and protein kinases MAPKAPK-3 (Keren et al., 2006;Wang and Ron, 1996;Platanias, 2003). During embryo development, the p38 MAPK

pathway is essential for chondrogenesis in limb mesenchyme (Oh et al., 2000) , whereas, JNK may act downstream of the Wnt-3a signal to inhibit the differentiation of mesenchyme to chondrocytes (Hwang et al., 2005). As p38 activates MEF-2 (myocyte-specific enhancer factor 2), p38 also promotes myogenesis during embryo development (Keren et al., 2006). In response to stress, both p38 and JNK may be activated, however, they may show distinct and sometimes antagonistic effects (Engelbrecht et al., 2004).

Given that ERK1/2, JNKs and p38 MAPKs share many substrates and that cross-talk is exhibited amongst these substrates, how MAPKs initiate a proper response to diverse stimuli is not evident. In a recent review, Cuevas et al. (2007) has proposed that MAP3Ks can serve as "signal hubs" to regulate the specificity of MAPK activation. Interestingly, ASK1, the oxidative stress sensitive MAP3K, displays a dynamic and region-specific expression during organogenesis (Ferrer-Vaquer et al., 2007). Recent studies suggest that, while persistent activation of ASK1 often induces cell death, moderate or transient activation of ASK1 promotes cell survival and differentiation (Matsuzawa and Ichijo, 2008).

1.8 The potential morphogens influenced by HU

Organogenesis is a tightly regulated process controlled by the temporary and spatial expression of morphogens. HU-induced limb defects may be related to oxidative stress. HU also induces a high incidence of vertebral defects. Fgf8 (fibroblast growth factor 8) and Dkk1 (dickkopf1) are morphogens that are important for both limb and vertebral column development. Fgf8 regulates limb and vertebral development through ERK signals (Delfini et al., 2005;Bobick and

Kulyk,2004). The expression of Dkk1 in limb may be regulated by JNK (Grotewold and Ruther, 2002b). Therefore, these two genes were chosen for evaluation

1.8.1 Fgf8 (fibroblast growth factor 8)

The vertebrate limb is derived from a limb primordium, the limb bud, which consists of a core of mesenchymal mesoderm covered by an epithelial ectodermal layer. The apical ectoderm ridge (AER) at the distal tip of the limb bud is essential for limb development (Summerbell, 1974). Expression of Fgf8 in the AER is the earliest step of limb bud initiation; this Fgf8 expression in the AER is induced by FGF10 in the adjacent mesenchymal mesoderm through Wnt3 /β-catenin signaling (Martin, 2001). During limb development, Fgf8 is expressed exclusively in the AER and provides signals to maintain the proliferation of mesoderm cells in the progress zone (PZ) adjacent to the AER, thereby driving the limb growth along the proximal to distal axis (Capdevila and Izpisua Belmonte, 2001). The Fgf8 signal from the AER also induces the establishment of the zone of polarizing activity (ZPA) in the posterior mesoderm; the signal interaction between the ZPA and the AER regulates anterior to posterior (A-P) polarity of the limb bud (Capdevila and Izpisua Belmonte, 2001). Removal of the AER from the limb bud at the limb initiation stage induces complete loss of the limb; removal of the AER at later stages of limb development leads to the truncation of the distal part of the limb (Summerbell, 1974). The formation of the distal anterior part of the limb structure, especially the first digit, is highly sensitive to decreased levels of Fgf8. Conditional knockout of Fgf8 in forelimb buds

induces loss of the AER and mesoderm in the anterior of the forelimb bud, resulting in hypoplasia of the distal preaxial skeletal elements; the mutant mice with lower expression of Fgf8 in hindlimb exhibit an absence of the first digit of the hindlimbs (Moon and Capecchi, 2000). Reduction of Fgf8 was suggested to be related to the digit-loss induced by the developmental toxicant, cadmium chloride (Elsaid et al., 2007).

Fgf8 is also critical to vertebral column development. Vertebrae are derived from somites, which are formed in a periodic manner by budding from the presomitic mesoderm (PSM), sequentially from the head to tail, accompanying the progressive formation of the body axis (Baker et al., 2006). Somite segmentation is under the control of a "segmentation clock" that drives oscillating expression of cyclic genes in the PSM. This "segmentation clock" is established by signals from the caudal end of the tail. Fgf8 is a major signal secreted in the caudal end of the tail and it can form a gradient in the PSM, driving the somite segmentation and posterior elongation of the embryo (Dubrulle and Pourquie, 2004). Disruption of Fgf8 signals disturbed somite formation, resulting in vertebral column defects (Dubrulle et al., 2001).

1.8.2 Dkk1 (dickkopf1)

Dkk1 is a secreted protein that specifically antagonizes Wnt/β-catenin signaling (Zorn, 2001). Dkk1 was originally identified as a head inducer (Glinka et al., 1998); Dkk1 knockout mice show complete loss of the front part of the head (Mukhopadhyay et al., 2001). However, a closer look at the mutant mice without

or with lower expression of Dkk1 revealed that limb and vertebral defects were found (MacDonald et al., 2004;Mukhopadhyay et al., 2001)

Wnt 3a/β-catenin signaling is required for the induction of Fgf8 in the AER (Barrow et al., 2003). Overactivation of Wnt signaling results in expansion of the AER (Soshnikova et al., 2003). Dkk1 is expressed in AER at the time of limb bud initiation to restrain the Wnt 3a signal. Lack of Dkk1 activity in the AER caused a pronounced expansion of the AER domain and resulted in extra digits, whereas ectopic expression of Dkk1 in limb regions resulted in truncation of the distal part of the limb skeletons (Mukhopadhyay et al., 2001). Consistently, both Dkk1 null and hypomorphic Dkk1 mutants display postaxial polysyndactyly in limbs (Mukhopadhyay et al., 2001;MacDonald et al., 2004).

During limb development, programmed cell death has to occur in well-defined domains to eliminate the cells located between the differentiating cartilaginous anlagen, sculpting the shape of the limb (Chen and Zhao, 1998;Hurle et al., 1996). In the early stages of limb development (GD 10.5 to GD 12 in the mouse embryo), programmed cell death eliminates the mesodermal cells located anterior and posterior to the region of formation of the proximal skeletal components of the limb. At more advanced stages of development (GD 13 to GD 14.5 in the mouse), cell death occurs in the interdigital areas, eliminating the mesodermal cells located between the developing digits, and thus separating the digits. Interestingly, during limb development, the Dkk1 expression domain overlaps with all of these programmed cell death domains but is excluded from the areas of chondrogenesis (Mukhopadhyay et al., 2001). It has been suggested that JNK-c-Jun may function upstream of Dkk1 in inducing apoptosis

in the limb. H_2O_2 and UV irradiation enhance apoptosis in limbs via c-Jun-Dkk1 (Grotewold and Ruther, 2002b). Thalidomide-induced limb truncation has been related to the upregulation of c-Jun-Dkk1 signaling (Knobloch et al., 2007).

Wnt 3a is secreted in the caudal end of the tail and has been found to be another major signal, along with Fgf8, regulating the somite segmentation clock (Aulehla et al., 2003). Interestingly, Dkk1 is also expressed in the PSM overlapping with the Wnt-3a domain (Grotewold et al., 1999). In the mutant mice with hypomorphic expression of Dkk1, kinked tails and fused vertebrae are observed (MacDonald et al., 2004). It has been suggested that Dkk1 may be a negative feedback regulator in the segmentation clock (Niehrs, 2006).

1.9 Hypothesis

Oxidative stress is involved in HU-induced developmental toxicity; the activation of AP-1 and MAPK pathways determines the response of the embryo to HU exposure during organogenesis.

To address this hypothesis, we chose CD1 mice as our animal model. CD1 mice are easy to breed, and have large litter size and a low spontaneous malformation rate. HU was administered to timed pregnant mice on GD 9 by intraperitoneal injection. The embryo is highly susceptible to oxidative stress and HU developmental toxicity on GD 9.

Studies were done to address the following specific objectives:

Objective 1: To determine the ability of teratogenic doses of HU to induce oxidative stress and AP-1 DNA binding activity in the conceptus during early organogenesis.

Objective 2. To elucidate the relationship between oxidative stress and AP-1 activation, and between oxidative stress and the developmental toxicity induced by HU.

Objective 3: To elucidate the role of MAPK pathways in the developmental toxicity induced by HU.

Objective 4: To investigate the expression of morphogens (Fgf8 and Dkk1) and identify the proteins conjugated with 4-HNE after HU exposure.

CHAPTER TWO

Activator protein-1 (AP-1) DNA Binding Activity is Induced by Hydroxyurea (HU) in the Organogenesis Stage Mouse Embryos.

Toxicol Sci. 85(2):1013-232005 (2005)

Jin Yan and Barbara F. Hales

ABSTRACT

Hydroxyurea is a potent teratogen; free radical scavengers or antioxidants reduce its teratogenicity. Activator Protein-1 (AP-1) and NF-κB are redox sensitive transcription factors with important roles in normal development and the stress response. This study was designed to determine if exposure to teratogenic doses of hydroxyurea induces oxidative stress and alters gene expression by activating these transcription factors. Pregnant mice were treated with saline or hydroxyurea (400, 500, or 600 mg/kg) on gestational day 9 (GD 9) and killed either on GD 9, 0.5, 3 or 6 h after treatment, to assess oxidative stress and transcription factor activities, or on GD 18, to assess fetal development. Exposure to 400 mg/kg hydroxyurea did not affect the progeny, whereas exposure to 500 or 600 mg/kg resulted in dose-dependent increases in fetal resorptions and malformations, including curly tails, abnormal limbs (oligodacytyly, hemimelia, and amelia), and short ribs. Hydroxyurea did not induce oxidative stress, as assessed by the ratio of oxidized to reduced glutathione, nor did it alter NF-κB DNA binding activity in the GD 9 conceptus. In contrast, exposure to hydroxyurea at any dose increased AP-1 DNA binding activity in embryos and yolk sacs 0.5 or 3 h after treatment. Hydroxyurea-induced c-fos heterodimer activity in the embryo peaked 3-4 fold above control at 3 h and remained elevated by 6 h; in contrast, the activity of c-jun dimers was not altered by drug exposure. A dramatic and region-specific increase in c-fos immunoreactivity was found in hydroxyurea-treated embryos. The induction of

AP-1 DNA binding activity by hydroxyurea represents an early, sensitive marker of the embryonic response to insult.

INTRODUCTION

Hydroxyurea is a potent teratogen, inducing growth retardation, mortality and malformations in many experimental species (Aliverti et al., 1980;Chaube and Murphy, 1966;Wilson et al., 1975). Maternal treatment with hydroxyurea blocks DNA synthesis and induces cell death in the embryo (Herken et al., 1978;Scott et al., 1971a). Hydroxyurea inhibits ribonucleotide diphosphatase reductase, the enzyme that catalyzes the reduction of ribonucleotides to the corresponding deoxyribonucleotides that are required for *de novo* DNA synthesis. However, inhibition of DNA synthesis cannot explain the rapid cell death that is induced by hydroxyurea. The hydroxylamine (-NHOH) group in the hydroxyurea molecule is able to react with oxygen, producing hydrogen peroxide (H_2O_2) that is, in turn, converted to the hydroxyl radical (.OH) (Freese et al., 1967). Pretreatment of rabbits with antioxidants (propyl gallate, ethoxyquin, nordihydroguaiaretic acid) or a free radical scavenger (d-mannitol) delays the onset of embryonic cell death and lowers the incidence of malformations caused by hydroxyurea (DeSesso, 1981; DeSesso & Goeringer, 1990; DeSesso *et al.*, 1994), thus suggesting that the oxidative stress induced by reactive oxygen species (H_2O_2, .OH) contributes to the developmental toxicity of hydroxyurea.

Oxidative damage to embryonic macromolecules has been observed after maternal exposure to various embryotoxic chemicals (Wells et al., 1997). Oxidative stress disturbs the cellular redox status, inducing oxidative damage to cellular macromolecules (DNA, lipid and protein) and altering gene expression, possibly primarily by post-transcriptional modification of redox-sensitive transcription factors. Activator Protein-1 (AP-1) is a redox-sensitive early

response transcription factor composed of jun (c-jun, junB and junD) and fos (c-fos, fosB, fra-1 and fra2) families of nuclear proteins. The AP-1 members form hetero- (Fos-Jun) or homodimers (Jun-Jun) that recognize the DNA consensus sequence 5′-TGAG/CTCA-3′ (Angel and Karin, 1991). Oxidative stress regulates the activation of AP-1 through a variety of mechanisms, including the phosphorylation of c-Fos or c-Jun by mitogen activated protein kinase (MAPK), or oxidative/reductive modification of the cysteine residues present in the DNA binding sites of both c-Fos and c-Jun (Abate et al., 1990;Hirota et al., 1997). Increased AP-1 DNA binding activity in response to oxidative stress regulates the transcription of genes associated with antioxidant defense, cell cycle control and apoptosis, all processes that are important in protecting embryos from oxidative damage or disrupting normal development. Previous *in vitro* studies with organogenesis stage whole embryos reported that culture induced an increase in the ratio of oxidized to reduced glutathione (GSSG:GSH) and AP-1 DNA-binding activity (Ozolins and Hales, 1997;Ozolins and Hales, 1999b); depletion of GSH with L-buthionine-S,R-sulfoximine induced embryotoxicity and prolonged AP-1-binding activity (Ozolins et al., 2002).

NF-κB, also a redox-sensitive transcription factor, is involved in development, positional signalling, and programmed cell death. NF-κB is a ubiquitous, pleiotropic, multisubunit transcription factor, made up of five subunits (p50, p52, p65 or RelA, c-Rel, and Rel-B) that form homo- and hetero dimers (Verma et al., 1995). The predominant forms, p50 and p65 (RelA), are sequestered in the cytoplasm by association with I-κB; dissociation of the NF-κB:I-κB complexes followed by translocation of the released NF-κB into the

nucleus activates NF-κB post-translationally. Exposures that induce oxidative stress, such as H_2O_2, tumor necrosis factor, phorbol esters, glutathione depletion, and UV or ionizing radiation, induce NF-κB DNA binding activity (Gius et al., 1999;Haddad et al., 2000;Li and Karin, 1998;Marshall et al., 2000;Li and Karin, 1999). The regulation of NF-κB is particularly important during development. NF-κB may act in the developing limb to disturb fibroblast growth factor (FGF) signals between the apical ectodermal ridge and the underlying mesenchyme (Bushdid et al., 1998;Kanegae et al., 1998). Inhibition of NF-κB/Rel activity results in a dysmorphic apical ectodermal ridge, loss of digit formation, and reversal of the direction of limb outgrowth. Interestingly, there is evidence that NF-κB may be involved in the teratogenesis of thalidomide (Hansen et al., 2004) and phenytoin (Kennedy et al., 2004).

Glutathione, the major intracellular nonprotein thiol, exists mainly in the reduced form (GSH). Upon oxidative stress, GSH is oxidized to GSSG, protecting cellular macromolecules; GSSG can be reduced to GSH in the presence of glutathione reductase and NADPH. The GSSG:GSH ratio is tightly regulated, maintaining cellular redox status; this ratio has been used as a marker of oxidative stress (Bajt et al., 2004;Lauterburg et al., 1984;Ozolins and Hales, 1997;Suliman et al., 2004).

The goal of this study was to elucidate the impact of an exposure to hydroxyurea that is teratogenic during early organogenesis on oxidative stress and the activation of redox-sensitive transcription factors in the conceptus. Pregnant mice were treated with hydroxyurea on gestational day 9, during early

organogenesis, the period of the development most susceptible to oxidative stress and teratogenic insult.

MATERIALS AND METHODS

Animals and treatments.

Timed-pregnant CD1 mice (20-25g) were purchased from Charles River Canada Ltd. (St. Constant, QC, Canada) and housed in the McIntyre Animal Resource Centre (McGill University, Montreal, Canada). All animal protocols were conducted in accordance with the guidelines outlined in the Guide to the Care and Use of Experimental Animals, prepared by the Canadian Council on Animal Care. Female mice, mated between 8:00 am and 10:00 am (gestational day 0, GD 0), were treated with vehicle (saline) or hydroxyurea (Aldrich Chem. Co., WI, USA) at 400, 500 or 600 mg/kg by intraperitoneal injection at 9:00 am on GD 9. Dams were killed on GD 9 (0.5, 3 or 6 h after treatment; 7-10 litters/treatment group) or GD 18 (8-10 litters/treatment group) by cervical dislocation. On GD 9, the maternal liver was excised; the uterus was removed and embryos and yolk sacs were dissected out in Hanks' balanced salt solution (Gibco Laboratories, ON, Canada) for subsequent assessment of transcription factor activity or oxidative stress. On GD 18, the uteri were removed, and the numbers of implantations, resorption sites, and live and dead fetuses were recorded. All the live fetuses were inspected for external malformations. Two malformed and two normal (without obvious external malformations) fetuses were randomly chosen from each litter for skeletal double staining and evaluation.

Double staining for fetal skeletal analysis.

Ethanol-fixed fetuses were immersed in a water bath (70°C) for 7 s. The fetuses were skinned, eviscerated and placed in 95% ethanol overnight. The

ethanol was decanted and replaced with alcian blue solution (15 mg alcian blue; 80 ml 95% ethanol; 20 ml glacial acetic acid) for 24 h. The solution was then replaced with 95% ethanol. After 24 h, the ethanol was substituted with alizarin red S solution (25 mg/l alizarin red S in 1% potassium hydroxide) for 48 h. The dye was drained and replaced with 0.5% potassium hydroxide for 24 h. The skeletons were placed in a 2:2:1 solution (2 parts 70% ethanol: 2 parts glycerin: 1 part benzyl alcohol). After 24 h, stained skeletons were placed in 1:1 solution (1 part 70% ethanol:1 part glycerin) for subsequent evaluation and storage.

Glutathione determinations.

At the time of collection, the embryos and yolk sacs from each litter were placed in 60 µl of RIPA buffer (150 mM NaCl; 1% NP-40; 0.5% deoxycholate; 0.1 % SDS; 50 mM Tris, pH 7.5) containing10 µl/ml protease inhibitor cocktail (Active Motif, CA, USA). The samples were homogenized with an ultrasonicator (Sonics & Materials Inc., Newtown, CT) and centrifuged at 10,000 x g for 10 min at 4°C. From each sample, 30 µl of supernatant was removed, added to 90 µl of 5% 5-sulfosalicylic acid, and centrifuged at 10,000 x g for 10 min at 4°C. Total glutathione (GSSG + GSH) and GSSG were measured spectrophotometrically, using an enzymatic recycling assay, as previously described (Ozolins and Hales, 1997). The remaining supernatant from each sample (prior to the addition of 5-sulfosalicylic acid) was aliquoted, flash frozen in liquid nitrogen and stored at -80°C for protein assays (Bradford, 1976) (Bio-Rad Laboratories, ON, Canada) and the ELISA tests.

Electrophoretic mobility shift assays (EMSA).

To prepare nuclear extracts, tissues were placed in 3 ml/g ice-cold complete hypotonic buffer (20 mM Hepes, pH 7.5; 5 mM NaF; 10 µM Na_2MoO_4; 0.1 mM EDTA; 1 µl/ml 1M DTT; 1 µl/ml detergent) and homogenized on ice with a pellet pestle (Kontes, Vineland, NJ). After 15 min incubation on ice, the samples were centrifuged at 4°C for 10 min at 850 *g*. The pellet was resuspended in 100 µl hypotonic buffer and incubated on ice for 15 min. After the addition of 5 µl of detergent, the samples were vortexed for 10 s at the highest setting. After centrifugation at 14,000 x *g* for 30 s, 5 µl complete lysis buffer was added to the pellet, which was then sonicated for a few seconds and rocked on ice for 15 min. The supernatant was obtained by centrifugation at 14,000 x *g* for 10 min. After determination of the protein content (Bradford, 1976; Bio-Rad Laboratories, ON, Canada), the extracts were adjusted to the same protein concentration by the addition of complete lysis buffer, flash frozen in liquid nitrogen, and stored at −80°. Hypotonic buffer, lysis buffer, dithiothreitol, protease inhibitor cocktail, and detergent were supplied in a Nuclear Extract Kit (Active Motif).

DNA fragments containing the AP-1 DNA binding site (5'-CGCTTGATGAGTCAGCCGGAA-3') were end–labeled with ^{32}P-ATP by T4 polynucleotide kinase (Promega Corporation, WI, USA) and purified by chromatography on a MicroSpin G-25 column (Amersham Biosciences UK Limited, Little Chalfont, UK). Nuclear extracts (9 µg protein) were incubated for 20 min at 4°C with 4 µl binding buffer supplied in a GelShift kit (Active Motif). Samples were then reacted with 1 µl labeled AP-1 probe (about 200,000 cpm) for

20 min at 4°C and electrophoresed on 5% polyacrylamide gels in 1X TGE buffer at 200 V. Gels were dried, and radioactivity was detected by autoradiography at -80°C. To confirm the specificity of binding, a 50 fold excess of the unlabeled oligonucleotide probes or mutated AP-1 oligonucleotides (5'-CGCTTGAGGAGTCGGCCGGAA-3') was preincubated with the sample for 20 min at 4°C.

Enzyme-Linked Immunosorbent Assays (ELISA).

Embryo and yolk sac extracts were prepared as described above for glutathione determinations. The DNA binding activity of the c-Fos heterodimer complex or the c-Jun homo/heterodimers was detected using ELISA transcription factor assay kits (Active Motif). Briefly, a 96-well plate was coated with oligonucleotide containing the AP-1 consensus site, 5'-TGAGTCA - 3'. Complete binding buffer (30 µl) (10 mM Hepes, pH 7.5; 8 mM NaCl; 12% glycerol; 0.2 mM EDTA; 0.1% BSA; 0.88 mM DTT; 0.17 mg/µl poly [d(1-C)]) was added to each well. To confirm the specificity of binding, 20 pmol AP-1 wild-type oligonucleotide or 20 pmol mutated oligonucleotide was added to two wells, respectively. As a positive standard, K562 cell nuclear extract (2.5 µg) in 20 µl complete lysis buffer (20 mM Hepes, pH 7.5; 400 mM NaCl; 20% glycerol; 0.1 mM EDTA; 10 mM NaF; 10 µM Na_2MoO_4; 1 mM $NaVO_3$; 10 mM PNPP; 10 mM β-glycerophosphate; 0.89 mM DTT; 0.01% protease inhibitor cocktail) was added to two wells containing complete binding buffer. Embryo or yolk sac extracts were diluted with complete lysis buffer to 20 µl and then added to the remaining wells; embryo or yolk sac extracts containing 20 µg protein were used for the examination of c-Jun dimer

binding activity and 40 µg protein for the c-Fos dimer assays. The plates were incubated for 1 h and washed with washing buffer (10 mM phosphate buffer, pH 7.5; 50 mM NaCl; 0.1% Tween 20; 2.7 mM KCl). One hour after the addition of the phospho-c-Jun or c-Fos antibody, the plates were washed with washing buffer. HRP-conjugated secondary antibody was added and incubated for 1 h. After washing, the plates were developed with developing solution (TMB substrate solution in 1% DMSO) for 5-10 minutes; the reaction was terminated by the addition of the stop solution (0.5 M H_2SO_4). The plates were read on a spectrophotometer (SPECTRAmax Plus 384, Molecular Devices Corporation, Sunnyvale, CA) at 450 nm with correction at 655 nm. The binding activity of samples was normalized by the relative absorbance of the positive standard and then divided by the protein content in the samples. Protein content was determined in triplicate (Bradford, 1976) (Bio-Rad Laboratories, ON, Canada)

The NF-κB p65 or p50 dimer DNA-binding activities were detected separately using the p65 or p50 transcription factor assay kits (Active Motif). The experiments were done as described above for AP-1 assays except that the oligonucleotide containing the NF-κB consensus site 5'-GGGACTTTC-3' was immobilized on the 96-well plate, poly [d(1-C)] was replaced by the herring sperm DNA in the complete binding buffer, DTT was increased to 2 mM in the complete binding buffer and 5 mM in the complete lysis buffer, and Jurkat nuclear extract was used as a positive control for NF-κB p65 or p50 dimer binding activities. Embryo or yolk sac extracts containing 10 µg protein were used for the examination of p65 dimer binding activity and 40 µg protein for the p50 dimer.

Immunohistochemistry.

Embryos on GD 9 were fixed for 3 h at 4°C in Bouin's fluid. After fixation, the embryos were dehydrated in ethanol, embedded in paraffin and serially sectioned. The tissue serial sections (5 μm) were dried, deparaffinized and hydrated. The c-Fos immunohistochemistry staining was done using a rabbit ABC kit (Vector Laboratories, Inc., Burlingame, CA) as follows. The sections were incubated for 0.5 h in 0.3% H_2O_2 in PBS, followed by 2 rinses for 3 min each with PBS. The sections were then incubated in blocking serum (1.5% goat normal serum in PBS) for 0.5 h. The excess diluent solution was removed from the slides and the sections were incubated at 4°C overnight with a rabbit polyclonal anti-c-Fos IgG (sc-52, Santa Cruz Biotechnology, Inc., Santa Cruz, CA) diluted 1:100 in blocking serum. After 2 rinses for 5 min each with PBS, the biotinylated anti-rabbit IgG diluted in blocking serum was applied to the sections for 30 min. After washing 5 min in PBS, the sections were stained with a 3, 3'-diaminobenzidine solution, and counterstained with methyl blue. As a negative control for c-Fos staining, the primary antibody was omitted.

Statistical analysis.

Statistical analyses were done by two-way analysis of variance (ANOVA), one-way ANOVA, or one-way ANOVA on rank's, as appropriate, using the SigmaStat computer program, followed by a post hoc Holm Sidak TEST. The *a priori* level of significance was $P < 0.05$.

RESULTS

Developmental toxicity induced by hydroxyurea.

To assess the embryotoxicity of hydroxyurea during early organogenesis, pregnant mice on GD 9 were treated with varying doses of hydroxyurea (400, 500 or 600 mg/kg) or vehicle and were killed on GD 18. The developmental toxicity induced by hydroxyurea is illustrated in Figure 2.1. The dead fetuses were observed as resorptions. The vehicle control group had a low rate of fetal deaths (Fig. 2.1A). Exposure to 400 mg/kg hydroxyurea did not alter the incidence of fetal deaths per litter. In contrast, a dramatic increase in fetal death rate was observed in both the 500 mg/kg and the 600 mg/kg hydroxyurea treatment groups; in the high-dose treatment group, more than half of the implantations per litter were resorbed (Fig. 2.1A).

There were no obvious external abnormalities in the control group, with the exception of one fetus with exencephaly. A few fetuses with curly tails were found in the litters exposed to 400 mg/kg hydroxyurea, but the rate of malformations per litter was not significantly different from control (Fig. 2.1B). However, exposure to 500 or 600 mg/kg of hydroxyurea induced a dose-dependent increase in malformations. In the 500 mg/kg treatment group, the mean number of malformed fetuses per litter was 22.2%, while in the high-dose treatment group, 87.7% of the surviving fetuses were malformed. Both curly tail and limb malformations were observed; hindlimb malformations predominated but some fetuses had forelimb abnormalities as well. The hindlimb malformations were characterized by oligodactyly (missing digits), hemimelia (total or partial

absence of the distal half of a limb), and amelia (absence of a limb); interestingly, malformed limbs were usually found on only one side (either left or right), although there were fetuses in which the development of both hindlimbs was abnormal.

Double stained skeletons of representative fetuses from each treatment group are shown in Figure 2.1D. The cartilage is stained blue and the bone is red. No skeletal abnormalities were apparent in the control and 400 mg/kg hydroxyurea treatment groups. In contrast, one third of the surviving fetuses in the 500 mg/kg treatment group had skeletal abnormalities; the rate of skeletal malformations reached 90.2% after exposure to 600 mg/kg hydroxyurea (Fig. 2.1C). The skeletal malformations observed included limb malformations (missing digits, hemimelia, amelia), curly tails, and short ribs (Fig. 2.1D).

The effects of hydroxyurea exposure on AP-1 DNA binding activity.

Electrophoretic mobility shift assays (EMSA) were done to test the hypothesis that teratogenic exposures of hydroxyurea induce AP-1 DNA binding activity (Fig. 2.2). In the absence of nuclear extract (free probe), the migration of the oligonucleotide was not impeded; addition of nuclear extract retarded the migration of the probe, indicated as the AP-1 DNA binding band. The addition of excess unlabeled wild type oligonucleotide inhibited this binding, but excess mutated sequence did not influence the binding (Fig. 2.2A). An increase in AP-1 DNA binding activity (relative to control) was detected in the nuclear extracts prepared from the hydroxyurea-treated embryos and yolk sacs collected 3 h after treatment on GD 9 (Fig. 2.2, B and C). DNA binding activity increased in a dose

dependent manner with hydroxyurea dose (Fig. 2.2B).

Multiple AP-1 family members may contribute to AP-1 DNA binding activity; various combinations of AP-1 dimers may regulate specific sets of genes, influencing different cellular functions. The contributions of two of the principal AP-1 members, c-Jun (c-Jun homodimers or heterodimers) and c-Fos (heterodimers), to the AP-1 DNA binding activity were detected by ELISA and are reported in Figure 2.3. AP-1 c-Jun DNA binding activity was not influenced in either embryos or yolk sacs by hydroxyurea exposure at any dose (400, 500, or 600 mg/kg) or time (0.5, 3, or 6 h) after treatment (Fig. 2.3, A and B). At 30 min after hydroxyurea treatment, there was also no effect on AP-1 c-Fos DNA binding activity in embryos (Fig. 2.3C) or yolk sacs (Fig. 2.3D). In contrast, AP-1 c-Fos DNA binding activity was significantly increased in embryos 3 h after exposure to any dose of hydroxyurea (Fig. 2.3C). A threefold increase in c-Fos binding activity was observed in embryos exposed to 400 mg/kg hydroxyurea; a fourfold induction of c-Fos activity was seen in embryos exposed to 500 or 600 mg/kg of hydroxyurea (Fig. 2.3C). By 6 h, c-Fos activity in embryos exposed to 400 mg/kg hydroxyurea did not differ from control, but activity remained elevated in embryos exposed to 500 or 600 mg/kg hydroxyurea. A similar trend was observed in AP-1 c-Fos binding activity in the yolk sac after 3 h or 6 h exposure to hydroxyurea but these increases were not statistically significant (Fig. 2.3D).

The effects of hydroxyurea exposure on NF-κB DNA binding activity.

NF-κB DNA binding activity consists of homo- or heterodimeric complexes of members of NF-κB families; of these, the p50/p65 heterodimers and p50

homodimers are major components. Thus, to determine if hydroxyurea exposure altered NF-κB DNA binding activity, we examined the binding activities of NF-κB p65 and p50 dimers by ELISA (Fig. 2.4). The binding activity of NF-κB p65 dimers in the embryo (Fig. 2.4A) was approximately half of that in the yolk sac (Fig. 2.4B). Interestingly, NF-κB p50 binding activity was lower in embryos (Fig. 2.4C) on GD 9 at 3 h and 6 h post-injection than at 0.5 h; a similar trend was observed in yolk sacs (Fig. 2.4D) but the differences were not statistically significant in this tissue. However, hydroxyurea exposure had no effect on NF-κB p65 or p50 dimer activities in either the embryo or the yolk sac at any time after treatment (Fig. 2.4). Thus, hydroxyurea exposure did not "non-discriminately" induce the activity of all redox sensitive transcription factors.

The effects of hydroxyurea exposure on c-Fos immunoreactivity.

To further explore the impact of hydroxyurea exposure on c-Fos in the embryo, c-Fos immunoreactivity was localized in embryos 3 h after treatment with vehicle or hydroxyurea (Fig. 2.5), the time point at which c-Fos heterodimer DNA binding was maximal after drug exposure. C-Fos immunoreactivity was observed in the control embryo around the circumferences of the forebrain and hind brain, in the facial-acoustic neural crest complex, in somites, in the neural tube, and in the heart (Fig. 2.5B). The expression of c-Fos in mice exposed to 400 mg/kg hydroxyurea (Fig. 2.5C) was similar to control. However, exposure to 600 mg/kg hydroxyurea dramatically increased the amount of c-Fos immunoreactivity in all the areas in which c-Fos activity was displayed in the control embryos (Fig. 2.5D). In the brain region, c-Fos immunoreactivity was clearly shown around the

edge of the hindbrain in the control embryo (Fig. 2.5E); in the 600 mg/kg hydroxyurea treated embryos, immunoreactivity was intense throughout the whole hindbrain region (Fig. 2.5H). In the caudal region of the tail of 600 mg/kg hydroxyurea exposed embryos, c-Fos staining was dramatically increased in the neural tube and the area around the dorsal aorta (Fig. 2.5I), compared to control embryos (Fig. 2.5F). A dramatic increase in c-Fos immunoreactivity in hydroxyurea-treated embryos was also found in the areas around the blood cells, in the branchial arch (Fig. 2.5D), and the atrial and ventricular walls of the heart (Fig. 2.5J).

The Effects of Hydroxyurea on Glutathione Homeostasis

To estimate the oxidative stress induced by hydroxyurea, the GSH concentrations and the ratios of GSSG:GSH were determined in the maternal liver, embryos and yolk sacs 0.5, 3, or 6 h after hydroxyurea treatment (400, 500, or 600 mg/kg). The concentrations in the maternal liver were approximately twofold higher than those in the embryo or yolk sac (Table 2.1); this is consistent with a previous report that GSH content is relatively low in the conceptus (Serafini et al., 1991). Exposure to hydroxyurea did not change the GSH content in the maternal liver, embryo or yolk sac at any one time point (0.5, 3, or 6 h). However, there was a decrease in GSH content with time in the maternal liver and embryo after exposure to either 500 or 600 mg/kg hydroxyurea ($P \leq 0.05$, two-way ANOVA). The GSH concentrations were lower at 6 h than at 0.5 or 3 h in maternal liver after exposure to 600 mg/kg hydroxyurea (Table 2.1). In the embryo, exposure to 500 mg/kg hydroxyurea resulted in lower GSH

concentrations at 3 h than at 0.5 h, whereas exposure to 600 hydroxyurea resulted in a decrease in GSH content at both 3 and 6 h compared to 0.5 h (Table 2.1). Interestingly, the ratios of GSSG:GSH were about twofold higher in the maternal liver and yolk sac than in the embryos; variation was high in the yolk sac. However, GSSG:GSH ratios were not influenced by hydroxyurea exposure (400, 500, or 600 mg/kg) in the maternal liver, embryo, or yolk sac at any time (0.5, 3, or 6 h) after hydroxyurea treatment (Table 2.1). Thus, exposure to hydroxyurea did not induce oxidative stress, as assessed by the ratio of oxidized to reduced glutathione.

DISCUSSION

The goal of this study was to determine the relationship between hydroxyurea teratogenesis during early organogenesis, oxidative stress, and alterations in gene expression as a consequence of the activation of redox-sensitive transcription factors, AP-1 and NF-κB. The GSH concentrations measured in the embryo and yolk sac were less than half those in the maternal liver, suggesting that tissues in the conceptus may be less protected from oxidative stress compared to maternal organs. Exposure to teratogenic doses of hydroxyurea did not alter the GSH content of the maternal livers, embryos or yolk sacs within any one time point assessed; however, a significant decrease in GSH content was found from 0.5 h to 3 or 6 h in maternal livers and embryos exposed to high-doses of hydroxyurea. These data suggest that there may be an interaction between hydroxyurea and time post-treatment. The times post-treatment when this interaction occurred correspond to 12 noon (3 h after hydroxyurea administration at 9 AM) and 1500 h (6 h after hydroxyurea exposure). Hepatic reduced GSH concentrations have been reported to be at a nadir in mice under a normal lighting schedule at 1400 h (White et al., 1987). Decreased GSH content may be a consequence of either GSH depletion or a decrease in GSH synthesis. It is interesting that GSH content was not depleted in the yolk sac after exposure to high-dose hydroxyurea. One explanation for this finding may be that the yolk sac has a higher GSH synthesis capacity than the embryo (Hansen et al., 2004); indeed, GSH synthesis is differentially regulated in the embryo and yolk sac in response to insult. Alternatively, the high variability in

GSH content measurements in this tissue may contribute to this tissue difference in response.

As the major cellular thiol-disulfide redox buffer, GSH is important in maintaining the cellular redox status. Changes in the intracellular thiol/disulfide status trigger signal transduction pathways which increase antioxidant defences to maintain redox homeostasis, but at same time, influence normal cellular function, such as cell proliferation, differentiation, adhesion, or death. In the embryo, the ratio of GSSG/GSH was about 2-fold lower than in the yolk sac or maternal liver, suggesting that redox homeostasis in the embryo may be different than that in the maternal liver or yolk sac. Interestingly, after exposure of whole embryos in culture to diamide, more extensive S-thiolation of protein sulfhydryls by GSH was observed in the yolk sac compared to embryos proper; thus, protein sulfhydryls in the yolk sac were more sensitive or accessible to oxidation (Hiranruengchok and Harris, 1995).

Exposure to teratogenic doses of hydroxyurea did not significantly induce oxidative stress in the maternal liver, embryo or yolk sac, as assessed by the ratio of GSSG/GSH. Previous studies reported that antioxidants or a free radical scavenger delayed the cell death and partially rescued the developmental toxicity induced by hydroxyurea (Desesso, 1981;DeSesso and Goeringer, 1990; DeSesso et al., 1994) suggesting that oxidative stress was involved in the teratogenesis of hydroxyurea. Although hydroxyurea exposure did not alter the ratio of oxidized to reduced glutathione in the whole conceptus, it remains possible that hydroxyurea may induce a localized oxidative stress in specific regions of the embryo. The antioxidant defense system is not equally distributed

throughout the embryo; interestingly, limbs and the neural tube may have lower antioxidant defenses than do other regions (Mackler et al., 1998).

Significantly, AP-1 DNA binding activity was dramatically increased, even after exposure to a dose of hydroxyurea (400 mg/kg) which did not induce developmental toxicity. Higher doses of hydroxyurea (500 and 600 mg/kg), which were teratogenic, further elevated AP-1 DNA binding activity. If, as seems likely, there are a number of components that contribute to hydroxyurea teratogenicity, the risk of having a malformation may be a continuous variable, with a threshold value (Fraser, 1976). Thus, it is possible that exposure to 400 mg/kg hydroxyurea induces AP-1 activity but is below the "threshold" for malformations. AP-1 regulates the transcription of genes that are important in cell differentiation, proliferation, and apoptosis, all basic processes during embryo development. AP-1 activity may be induced by various noxious stimuli, such as heat shock (Andrews et al., 1987), heavy metals (Jin and Ringertz, 1990;Ramesh et al., 1999), and alkylating chemicals (Futscher and Erickson, 1990), all of which can be teratogenic. Interestingly, c-Fos expression was elevated in the deciduas of embryos 6 h after exposure to ethanol on GD 8 (Poggi et al., 2003). Stable overexpression of Bcl-2, a gene that protects against cell death by apoptosis, enhanced AP-1 DNA binding activity in cell lines (Feng et al., 2004). In the presence of different stimuli and in various cell types, the activation of AP-1 may have different consequences, from protecting the cell to triggering cell death. It is not clear whether hydroxyurea induced activation of AP-1 indicates a role for AP-1 in protecting the embryo from the potential teratogenic insult or in disrupting normal embryonic development.

We have shown that c-Fos heterodimers contribute to the AP-1 DNA binding activity increase induced by hydroxyurea and that c-Jun homo-/hetero dimers do not. Different AP-1 members display multiple roles in regulating embryonic development. The targeting of individual AP-1 members in transgenic null mouse experiments has demonstrated that c-Jun, JunB, or Fra-1 are essential for embryo development, however, mice lacking c-Fos, JunD, and FosB are viable but have a variety of birth defects. C-Jun null mice died during the fetal period due to cardiac defects (Eferl et al., 1999); the knockout of Fra-I or JunB induced embryo lethality as a consequence of defects in the extra-embryonic tissues (Schreiber et al., 2000;Schorpp-Kistner et al., 1999). Mice lacking FosB or JunD had a nurturing defect, or male sterility, respectively (Gruda et al., 1996;Thepot et al., 2000). Knockout c-Fos mice were viable and fertile but lacked osteoclasts, and they produce progeny with osteopetrosis (Johnson et al., 1992;Wang et al., 1992). Overexpression of c-Fos induced the transformation of osteoblasts leading to osteosarcomas (Wang et al., 1995).

The developmental toxicity of hydroxyurea was characterized by skeletal malformations, including curly tails, abnormal limbs and short ribs. The evidence that c-Fos is involved in osteogenesis (Closs et al., 1990;Sakano et al., 1997) leads us to suggest that the effects of hydroxyurea on skeletal morphogenesis may be a consequence of disturbances in the regulation of c-Fos expression and activity. The relationship between where increased c-Fos immunostaining was found in the embryos exposed to hydroxyurea and the subsequent malformations is interesting. Increased c-Fos immunostaining was found in the somites of the hydroxyurea-exposed embryos, many of which are likely to develop shortened

ribs. After exposure to 600 mg/kg hydroxyurea, c-Fos expression increased dramatically in the caudal region of the neural tube; neural tube defects at the caudal region of the tail result in curly tail malformations. Although we did not observe craniofacial defects in this study, hydroxyurea has been reported to induce craniofacial defects and cardiovascular anomalies in rats (Aliverti et al., 1980). *In utero* exposure of rabbits to hydroxyurea altered the embryonic cardiovascular system as early as 2 min post-treatment, followed by petechial hemorrhages and hematomas in the forebrain, postocular region, mandibular and nasal processes, and apparent collapse of the vasculature in the forelimb bud (Millicovsky and DeSesso, 1980). Our data show that exposure to doses of hydroxyurea that are teratogenic dramatically increased the immunoreactivity of c-Fos in the brain regions and in areas around the blood vessels. It is possible that the absence of cardiac and craniofacial defects among the fetuses in this study may be due to the protective effects of c-Fos in this regions or, alternatively, that the insult in these regions leads to an increase in embryolethality that is manifested in embryo resorptions. Elucidation of the different combinations of the c-Fos heterodimers activated by hydroxyurea in various regions of the embryo may help to explain specificity of the response to insult.

In contrast to the effect on AP-1 DNA binding activity, NF-κB DNA binding activity was not influenced by hydroxyurea treatment, although both NF-κB and AP-1 are redox-sensitive transcription factors, and NF-κB is important in limb development. This may be due to a difference in the sensitivity of these two transcription factors to insult. These data indicate that different mechanisms are

involved in regulating the response of embryonic AP-1 and NF-κB DNA binding activity to stress.

AP-1 DNA binding activity may be triggered by genotoxicity or by oxidative stress. Hydroxyurea inhibits ribonucleotide reductase, resulting in inhibition of DNA synthesis, affecting the cell cycle at G_0 to S phase. AP-1 family members are involved in promoting cell cycle progression; specifically, AP-1 has been linked to the transcriptional regulation of cyclin D1. Stress induces a complex program of c-Fos and Fra-1 chromatin trafficking that is required for cyclin D1 expression during cell cycle reentry (Burch et al., 2004). The induction of AP-1 DNA binding activity in the conceptus by hydroxyurea may disturb cell cycle recovery in the conceptus. Whether increased AP-1 DNA binding activity mediates the response of the conceptus to insult or represents a failed attempt at self protection, it is evident that it represents a sensitive and early indicator of insult.

Fig. 2.1 Effects of hydroxyurea exposure on embryo development. Female mice received saline (Control, □) or hydroxyurea (400 mg/kg, ▨ ; 500 mg/kg, ▩; 600 mg/kg, ■) on GD 9 and were killed on GD 18. The fetal death rate is expressed as the percent of total implantations that were dead (mean per litter ± SEM; n=8-10 litters) (A). The external (B) and skeletal (C) malformation rates are expressed as the percent of the live fetuses that were malformed (mean per litter ± SEM; n=6-8 litters). Asterisks denote a significant difference from control (*, $p<0.05$; **, $p<0.01$; one-way ANOVA followed by a *post hoc* Holm Sidak test). Double stained skeletons are shown in D. The red color represents bone stained by alizarin red S and the blue depicts cartilage dyed by alcian blue. Arrows indicate short ribs (SR), curly tail (CT), oligodactyly (Ol), hemimelia (HM), and amelia (AM).

Fig. 2.1

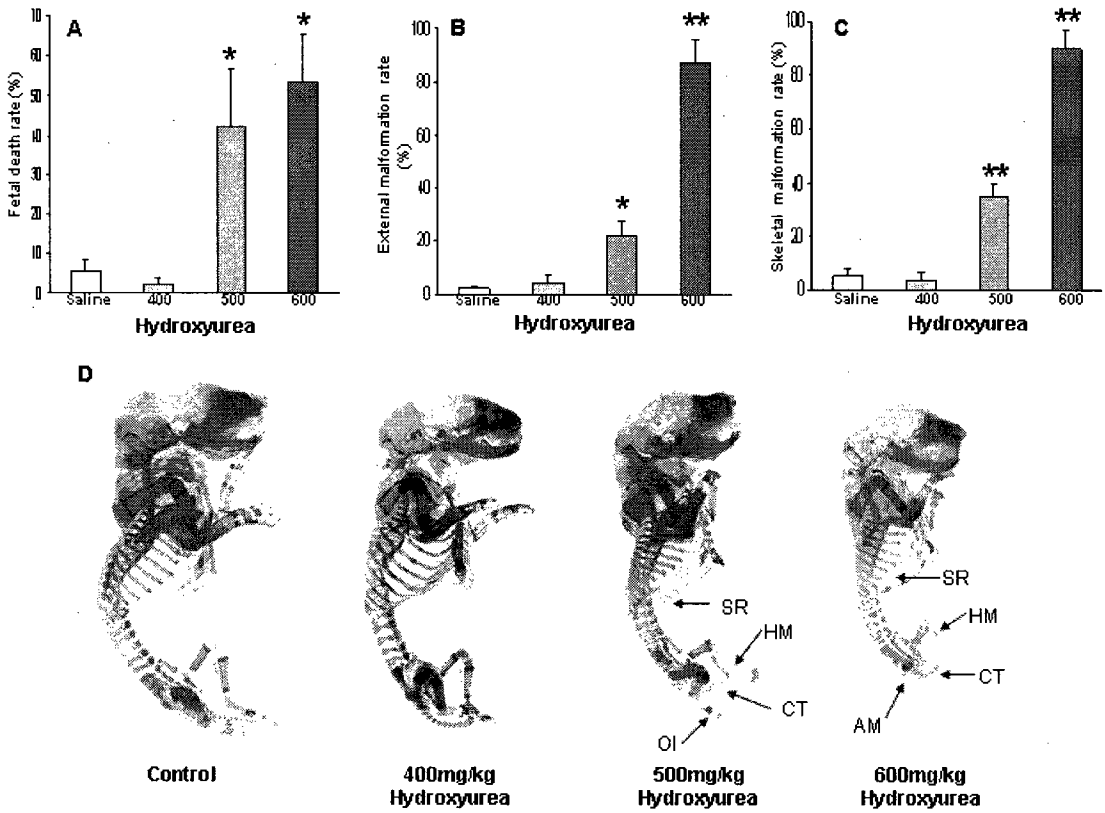
A
Fetal death rate (%)
Saline
400
500
600
Hydroxyurea
B
External malformation rate (%)
Saline
400
500
600
Hydroxyurea
C
Skeletal malformation rate (%)
Saline
400
500
600
Hydroxyurea
D
SR
HM
CT
OI
SR
HM
CT
AM
Control
400mg/kg Hydroxyurea
500mg/kg Hydroxyurea
600mg/kg Hydroxyurea

Fig.2.2 Representative EMSA of the AP-1 DNA binding activity in embryo and yolk sac samples. Nuclear extracts (9 μg) were obtained from embryos (panel B) or yolk sacs (panel C) of pregnant mice exposed to vehicle (C) or hydroxyurea (L, 400 mg/kg; M, 500 mg/kg; H, 600 mg/kg) on GD 9 (B, C). Binding controls are shown in panel A. HeLa nuclear extract served as a positive control. No binding was found in the absence of nuclear extract (Free). In the presence of HeLa nuclear extract (HeLa), or embryo nuclear extracts (Ex, obtained from control embryo), a single AP-1 DNA-binding complex was displayed; addition of 50-fold excess of unlabeled oligonucleotide probe (Wt) reduced the AP-1 binding complex, however, addition of 50-fold excess of mutated AP-1 oligonucleotides (Mu) did not influence the binding.

Fig. 2.2

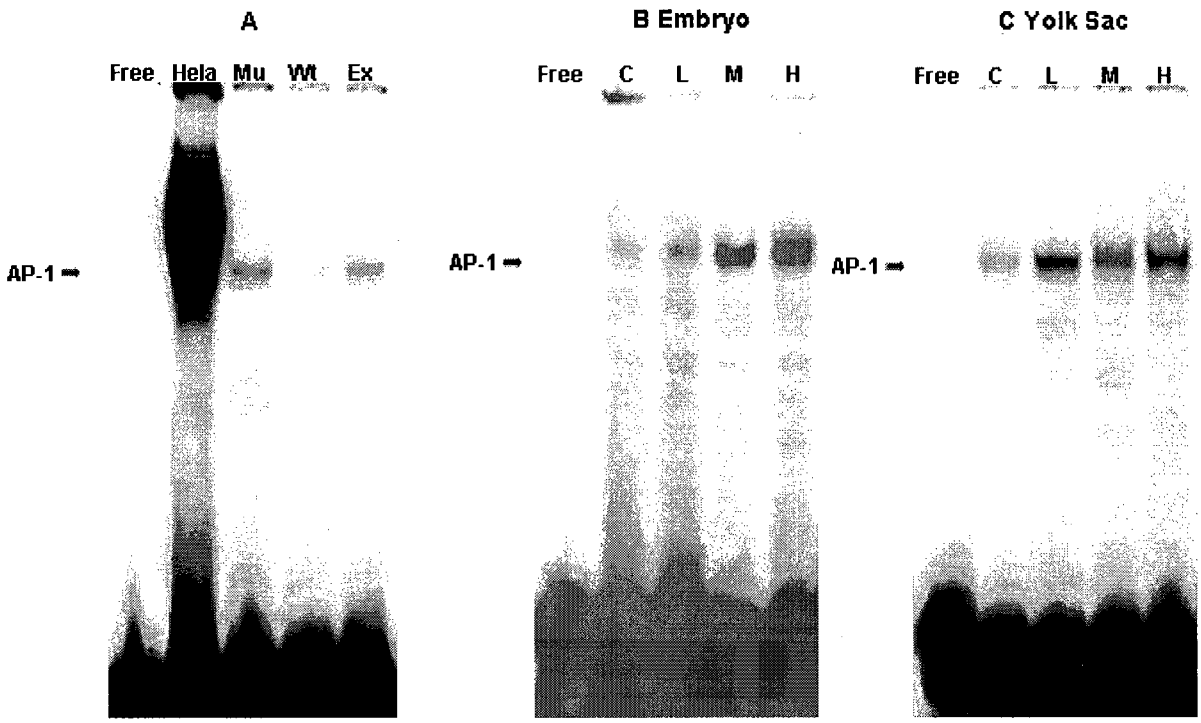
A
Free
Hela
Mu
Wt
Ex
AP-1
B Embryo
Free
C
L
M
H
AP-1
C Yolk Sac
Free
C
L
M
H
AP-1

Fig. 2.3. The effects of hydroxyurea exposure on c-Jun homo-/hetero-dimer DNA binding activity in embryos (A) or in yolk sacs (B) or on AP-1 c-Fos heterodimer DNA binding activity in embryos (C) or yolk sacs (D). Female mice received saline (Control, □) or hydroxyurea (400 mg/kg, □ ; 500 mg/kg, ▩ ; 600 mg/kg, ■) on GD 9 and were killed 0.5, 3, or 6 h after treatment. The conceptuses were removed and separated into embryo and yolk sac. The activities of AP-1 dimers containing c-Jun or c-Fos proteins were separately detected by the ELISA, as described. The data are expressed as means ± SEM (μg nuclear extract stand/μg sample protein); N=7-10 litters. Asterisks denote a significant difference from control at the same time point (*, $p<0.05$; one-way ANOVA, followed by a *post hoc* Holm Sidak test).

Fig. 2.3

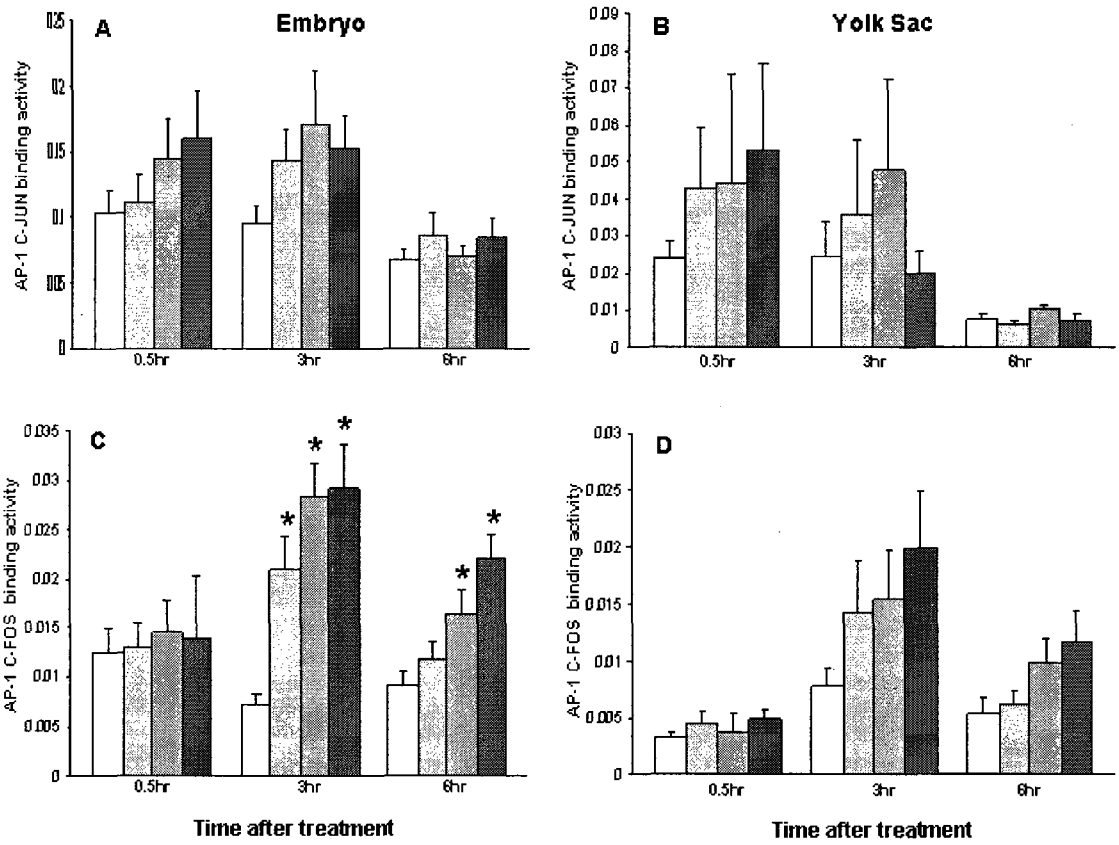
A
Embryo
AP-1 C-JUN binding activity
0.5hr
3hr
6hr
B
Yolk Sac
AP-1 C-JUN binding activity
C
AP-1 C-FOS binding activity
Time after treatment
D
AP-1 C-FOS binding activity
Time after treatment

Fig. 2.4. The effects of hydroxyurea exposure on NF-κB DNA binding activity in embryos (A, C) or in yolk sacs (B, D). Female mice received saline (Control, □) or hydroxyurea (400mg/kg, ▨; 500mg/kg, ▩ ; 600mg/kg, ■) on GD 9 and were killed 0.5, 3, or 6 h after treatment. The DNA binding activity of NF-κB p65 dimers was detected in embryos (A) or in yolk sacs (B); NF-κB p50 dimer DNA binding activity was estimated in embryos (C) or in yolk sacs (D) by ELISA. The data are expressed as means ± SEM (μg nuclear extract stand/μg sample protein); N=7-10 litters. The asterisks denote a significant difference from the same treatment group at 0.5hr. (p<0.05, one-way ANOVA followed by a *post hoc* Holm Sidak test).

Fig. 2.4

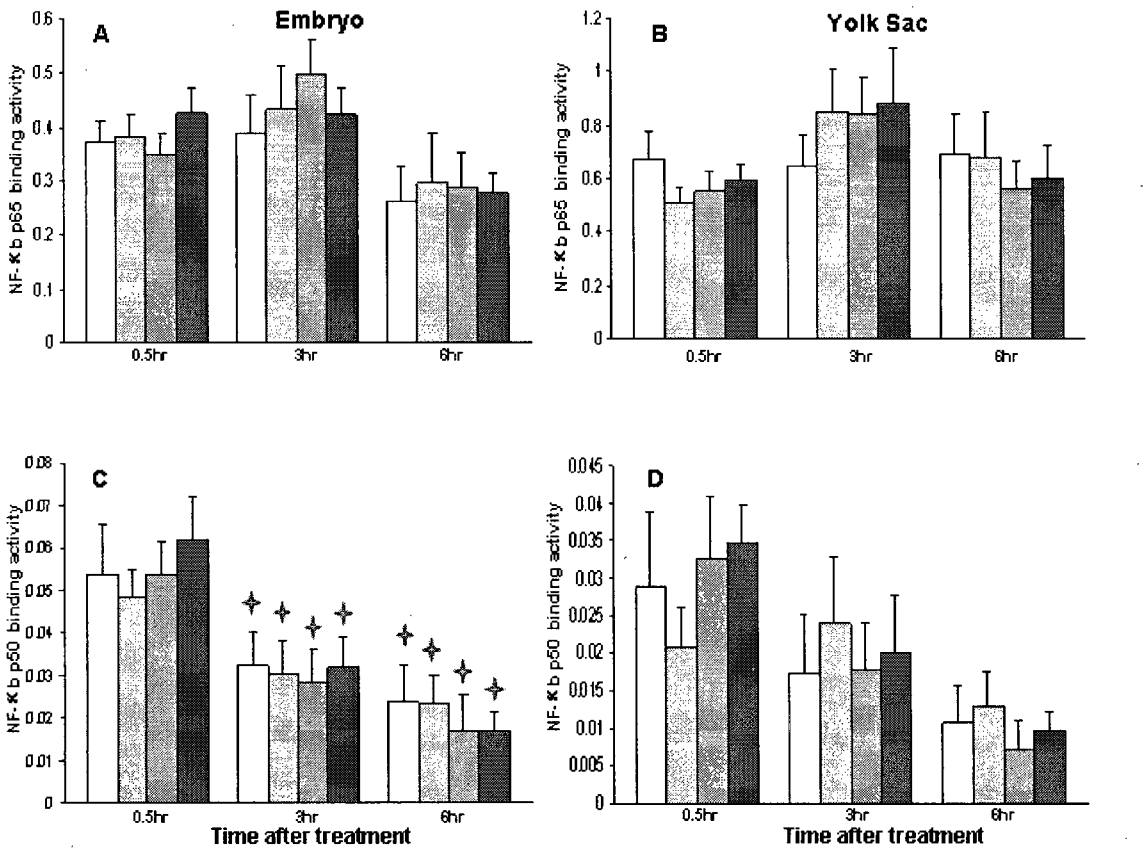
A
Embryo
B
Yolk Sac
C
D
NF-Kb p65 binding activity
NF-Kb p50 binding activity
0.5hr
3hr
6hr
Time after treatment

Fig.2.5. Effects of hydroxyurea exposure on c-Fos immunoreactivity. Timed pregnant female mice received saline, or hydroxyurea, 400 or 600 mg/kg, on GD 9 and were killed 3 h later. The embryos were fixed and sectioned. Immunoreactive c-Fos in the embryos was detected by immunohistochemistry with an anti-c-Fos antibody; sections were counterstained with methyl blue. In the negative control the primary antibody was omitted (A). c-Fos immunoreactivity in the control embryo was seen in the forebrain (FB), hindbrain (HB), facial-acoustic neural crest complex (FNC), neural tube (NT), somites (S), caudal region of the tail (CT), and heart (H). (B) Exposure to 400 mg/kg hydroxyurea for 3 h did not influence the distribution of c-Fos immunoreactivity. (C) Exposure to 600 mg/kg hydroxyurea dramatically increased c-Fos immunostaining in the forebrain (FB), midbrain (MB), hindbrain (HB), bronchial arch (BA), somites (S), neural tube (NT), caudal region of the tail (CT), and heart (H). (D) Higher magnification views of the control and 600 mg/kg hydroxyurea treated embryos in the hindbrain area (E, H), caudal region of the tail (F, I), in which the dorsal aorta (DA) and neural tube (NT) are indicated, and the heart (G, J) are provided.

Fig. 2.5

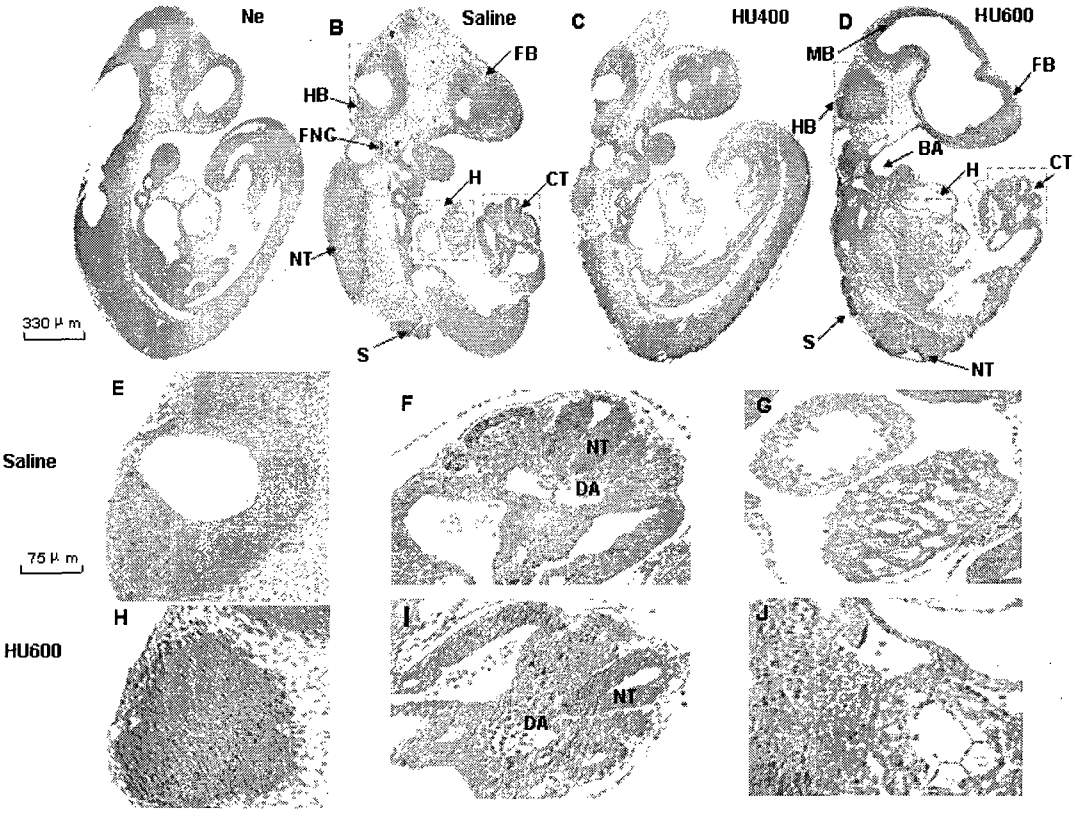
Ne
B
Saline
C
HU400
D
HU600
FB
HB
FNC
H
CT
NT
S
MB
BA
330 μ m
E
Saline
75 μ m
F
G
DA
H
HU600
I
J

Table 2.1 The effects of hydroxyurea (HU) on glutathione homeostasis

HU (mg/kg)	Maternal liver			Embryo			Yolk sac		
	0.5 h	3 h	6 h	0.5 h	3 h	6 h	0.5 h	3 h	6 h
	GSH content (nmoles/mg protein)								
0	238.8±11.8	203.3±9.7	172.1±12.3	96.9±4.8	86.3±13.9	82.5±7.8	86.9±4.7	83.3±18.0	79.9±15.1
400	220.9±10.2	183.9±9.9	180.4±8.6	86.7±7.1	81.2±16.0	92.6±9.2	66.9±6.5	82.1±30.4	69.9±5.7
500	225.3±8.0	226.2±22.0	190.1±12.5	112.4±7.0	81.4±9.4*	94.3±5.3	82.1±10.0	77.2±13.3	79.1±9.1
600	259.6±24.4	242.8±14.4	190.3±14.0*	110.0±8.0	72.0±13.1*	72.8±6.8*	73.6±7.8	99.2±27.4	64.3±5.5
	Ratios of oxidized (GSSG) to reduced (GSH) glutathione								
0	0.024±0.00	0.021±0.00	0.024±0.002	0.010±0.00	0.011±0.00	0.008±0.00	0.022±0.00	0.022±0.00	0.028±0.004
400	0.024±0.00	0.025±0.00	0.024±0002	0.013±0.00	0.014±0.00	0.011±0.00	0.040±0.00	0.031±0.00	0.034±0.004
500	0.022±0.00	0.019±0.00	0.024±0.002	0.011±0.00	0.008±0.00	0.009±0.00	0.028±0.00	0.026±0.00	0.025±0.005
600	0.021±0.00	0.018±0.00	0.022±0.002	0.012±0.00	0.010±0.00	0.011±0.00	0.032±0.00	0.022±0.00	0.028±0.004

HU is hydroxyurea. Data are means ± SEM; N= 6 – 9 litters in each treatment group.

Asterisks denote a significant difference from the hydroxyurea treated group at the same dose in the 0.5 h post-treatment group (*, $p<0.05$; two-way ANOVA followed by a *post hoc* Holm Sidak test).

CONNECTING TEXT

In Chapter Two, we found that HU treatment increased the incidence of fetal death and malformations, and enhanced the DNA binding activity of AP-1 c-Fos heterodimers in the embryo. Surprisingly, HU treatment did not influence the overall GSH content and the GSSG/GSH ratio in maternal livers, embryos and yolk sacs. HU treatment induced tissue-specific malformations; c-Fos immunoreactivity was detected in specific regions in the embryo. To further elucidate the role of oxidative stress in HU developmental toxicity and AP-1 c-Fos heterodimer DNA binding activity, in the following chapter, BSO was given to mice before HU exposure to enhance oxidative stress. The localization of oxidative stress in the embryo was detected by 4-HNE immunostaining; the impact of BSO pretreatment on HU developmental toxicity and AP-1/c-Fos DNA binding activity was evaluated.

CHAPTER THREE

Depletion of Glutathione Induces 4-Hydroxynonenal Protein Adducts and Hydroxyurea Teratogenicity in the Organogenesis Stage Mouse Embryo

J. Pharmacol. Exp.Ther. 319:613-621 (2006)

Jin Yan and Barbara F. Hales

ABSTRACT

Glutathione (GSH) homeostasis is important during organogenesis. To elucidate the impact of GSH depletion in organogenesis stage embryos on oxidative stress and drug teratogenicity, L-buthionine-S,R-sulfoximine (BSO) was given to timed pregnant CD-1 mice 4 h prior to exposure to a model teratogen, hydroxyurea [(400 mg/kg (HU-400) or 600 mg/kg (HU-600)]. Treatment with BSO or HU alone, or with BSO plus HU-400, did not alter the ratios of GSSG/GSH in the embryo; in contrast, the combination of BSO plus HU-600 did increase this ratio at both 0.5 and 3h post-HU, indicating the induction of oxidative stress in the embryos. Immunoreactivity to a product of lipid peroxidation, 4-hydroxynonenal (4-HNE) protein adducts, was detected in saline treated embryos; the intensity and nuclear localization of 4-HNE protein adduct immunoreactivity in specific regions in the embryo was significantly increased by exposure to BSO alone or BSO and either dose of HU. BSO pretreatment increased the spectrum and incidence of external and skeletal malformations (curly tail, hindlimb malformations, hydrocephaly, exencephaly, open eye, spinal bifida, and gastroschisis) induced by HU-400 and HU-600; BSO exposure did not alter the effects of HU on fetal mortality or fetal weights, or HU induction of c-Fos heterodimer dependent activator protein 1 DNA binding activity. The formation of 4-HNE protein adducts in teratogen-exposed embryos was localized to regions of the embryo that were highly susceptible to insult, namely the somites and caudal neural tube, correlating the presence of 4-HNE adducts with the disruption of pattern formation during organogenesis.

INTRODUCTION

Glutathione (γ-glutamylcysteinylglycine, GSH), synthesized *de novo* by the sequential actions of γ-glutamylcysteine synthetase (γ-GCS) and glutathione synthetase, is the principal non-protein sulphydryl in mammalian cells. GSH serves mainly as a thiol substrate for enzymes to reduce free radicals and hydroperoxides and regulate protein functions. Disturbances in GSH homeostasis may cause oxidative stress, inducing damage to cellular macromolecules (lipids, proteins, and DNA).

GSH homeostasis is critical to maintain cellular redox status and essential for normal embryo development. Targeted disruption of the catalytic subunit of γ-GCS, the rate limiting enzyme for GSH synthesis, induces embryo lethality between gestational (GD) day 7.5 and GD 8.5 (Shi et al., 2000). Depletion of GSH with L-buthionine-S,R-sulfoximine (BSO) between GD 10 and 11 in rats delays embryo growth and enhances embryonic deaths and malformations, both in vivo and *in vitro* (Slott and Hales, 1987a;Hales and Brown, 1991;Ozolins et al., 2002). Furthermore, GSH homeostasis is involved in defense of the embryo against teratogens. Thalidomide preferentially depletes GSH in thalidomide-sensitive species, but not in thalidomide-resistant species (Hansen et al., 2002). During organogenesis, the addition of GSH protects cultured rat embryos from the embryotoxicity of the aldehyde acrolein (Slott and Hales, 1987b); disruption of GSH homeostasis exaggerates the teratogenicity of many drugs, such as 5-fluorouracil and phenytoin (Naya et al., 1990;Wong et al., 1989). Although

oxidative stress has been proposed as a common mechanism of teratogen action, the underlying mechanism is not fully understood (Wells et al., 1997).

When oxidative stress occurs, the polyunsaturated fatty acids within the cellular membrane are a primary target of free radicals. 4-Hydroxynonenal (4-HNE), an α,β-unsaturated aldehyde, is a major lipid peroxidation product of n-6 polyunsaturated fatty acids. Relatively more stable than free radicals, 4-HNE passes easily among subcellular compartments to react with a variety of biomolecules bearing thiol and amino groups (Schaur, 2003). Through the formation of protein adducts, 4-HNE interferes with the activities of various signal kinases, such as protein kinase C and mitogen-activated protein kinases (MAPKs), to regulate cellular processes from proliferation to differentiation and apoptosis (Leonarduzzi et al., 2004). To the best of our knowledge, the impact of teratogen exposure on the formation of 4-HNE protein adducts in the conceptus has not been investigated previously.

Hydroxyurea (HU) is a model teratogen used to elucidate the relationship between embryotoxicity and oxidative stress (DeSesso, 1979). As a DNA synthesis inhibitor, HU destroys the free radicals in the catalytic center of ribonucleotide reductase and induces oxidative stress by generating free radicals. HU exposure induces extensive cell death in the neural tube region and limb buds (DeSesso, 1981;(Zucker et al., 1999); antioxidants delay the onset of HU-induced cell death and reduce the incidence of external abnormalities (DeSesso, 1981;DeSesso et al., 1994). We have shown previously that exposure to teratogenic doses of HU on GD 9 in CD1 mice, induces mainly hindlimb and curly

tail defects (indicative of neural tube defects), as well as a dose-dependent activation of activator protein 1 (AP-1) (Yan and Hales, 2005). AP-1 is a redox sensitive transcription factor that consists of Jun/Jun (c-Jun, JunB and JunD) or jun/fos (c-Fos, FosB, Fra-1 and Fra2) dimeric nuclear proteins (Angel and Karin, 1991). AP-1 activation is important in the embryo during organogenesis and in mediating the response to stress (Jochum et al., 2001;Wisdom, 1999).

The goal of this study was to elucidate the impact of disturbances in GSH homeostasis on HU embryotoxicity; BSO, an irreversible inhibitor of γ-GCS, was used to deplete GSH (Griffith and Meister, 1979); the formation of 4-HNE-protein adducts and AP-1 DNA binding activity was assessed as indicators of the response of the embryo to oxidative stress.

MATERIALS AND METHODS

Animals and treatments.

Timed-pregnant CD1 mice (20-25g) were purchased from Charles River Canada Ltd. (St. Constant, QC, Canada) and housed in the McIntyre Animal Resource Centre (McGill University, Montreal, Canada). All animal protocols were conducted in accordance with the guidelines outlined in the Guide to the Care and Use of Experimental Animals, prepared by the Canadian Council on Animal Care. Female mice, mated between 10:00 am and 12:00 am (GD 0), were treated with vehicle (saline) or BSO (Aldrich Chem. Co., Milwaukee, WI) at 600 mg/kg by intraperitoneal injection at 7:00 am on GD 9. After 4 h, female mice were treated with saline or HU (400 or 600 mg/kg) by intraperitoneal injection. Dams were euthanized on GD 9 (0.5 or 3 h after treatment with HU; 6-10 litters/treatment group) or GD 18 (7-10 litters/treatment group) by cervical dislocation. On GD 9, the embryos were dissected out in Hanks' balanced salt solution (Invitrogen Canada, Inc., Burlington, ON, Canada) for the subsequent assessment of GSH and GSSG concentrations, the formation of 4-HNE protein adducts, and c-Fos dependent AP-1 DNA binding activity. On GD 18, the uteri were removed, and the numbers of implantations, resorption sites, and live and dead fetuses were recorded. All the live fetuses were weighed, inspected for external malformations and then fixed in 95% ethanol for skeletal double staining and evaluation. Fetuses were skinned and double stained with alcian blue (cartilage) and alizarin red S (bone) for the analysis of skeletal malformations, as previously described (Yan and Hales, 2005).

GSH and GSSG determinations.

At the time of collection on GD 9, four embryos from each litter were fixed in paraformaldehyde (4%) for immunostaining. The remaining embryos from each litter were placed in 40 µl of modified RIPA buffer (150 mM NaCl; 1% NP-40; 0.5% deoxycholate; 0.1 % SDS; 50 mM Tris, pH 7.5) containing 10 µl/ml protease inhibitor cocktail (Active Motif Inc, Carlsbad, CA). The samples were homogenized with an ultrasonicator (Sonics & Materials Inc., Newtown, CT) and centrifuged at 10,000 x g for 10 min at 4°C. From each sample, 30 µl of supernatant were removed and prepared for the measurement of GSH and GSSG, as previously described (Yan and Hales, 2005). The remaining supernatant from each sample was aliquoted, flash frozen in liquid nitrogen and stored at -80°C for protein assays (Bradford, 1976) (Bio-Rad Canada Ltd., Mississauga, ON, Canada), enzyme-linked immunosorbent assays (ELISA) tests, and western blot analysis.

Immunofluorescence Staining.

GD 9 embryos were fixed for 5 h at 4°C in 4% paraformaldehyde. After fixation, the embryos were dehydrated in ethanol, embedded in paraffin and serially sectioned (5 µm sections). 4-HNE immunoreactivity was detected using a M.O.M immunodetection kit (Vector Laboratories, Burlingame, CA) as follows. Tissue sections were deparaffinized and hydrated. After rinsing twice for 2 min each with PBS, sections were incubated in the working solution of M.O.M. Mouse IgG Blocking Reagent for 1 h. After further rinses with PBS, two times for 2 min each, sections were incubated in the working solution of M.O.M Diluent for 5 min.

Excess Diluent solution was tipped off the slides and the sections were incubated for 30 min at room temperature with a mouse monoclonal anti-4-hydroxy-2-nonenal (4-HNE) antibody (OXIS Research, Inc., Portland, OR) at 1 µg/ml diluted in M.O.M. Diluent. After washing two times for 2 min in PBS, the sections were incubated in the working solution of M.O.M. Biotinylated Anti-Mouse IgG Reagent for 10 min, followed by washing two times for 2 min in PBS. The sections were stained with Fluorescein Avidin DCS for 5 min, washed two times for 5 min in PBS, and then mounted with propidium iodide antifade solution (Chemicon International, Temecula, CA). As a negative control for 4-HNE staining, the primary antibody was preadsorbed with 4-hydroxy-2-nonenal-diethylacetal (OXIS Research, Inc.) as described by the manufacturer.

c-Fos ELISAs.

The DNA binding activity of the c-Fos heterodimer complex was detected using ELISA transcription factor assay kits (Active Motif, CA, USA), as previously described (Yan and Hales, 2005).

Western blot analysis.

Fifteen micrograms of protein from each sample were separated with 10% SDS-polyacrylamide gel electrophoresis and then transferred onto equilibrated polyvinylidene difluoride membranes (Amersham Biosciences, Buckinghamshire, UK) by electroblotting. Membranes were blocked in 5% skim milk, and then probed with primary antibodies against 4-HNE (1:1000; OXIS Research, Inc.) or β-actin (1:500; Santa Cruz Biotechnology, Inc., Santa Cruz, CA) overnight at 4

°C. After incubation with horseradish peroxidase-conjugated secondary antibodies (1:1000), proteins were detected by enhanced chemiluminescence (Amersham Biosciences). The bands were quantified by densitometric analysis using a ChemiImager 400 Imaging system (Alpha Innotech, San Leandro, CA); the peak area represents the intensity of the band.

Statistical analysis.

Statistical analyses were done by Chi-square, or by two-way ANOVA, one-way ANOVA, or one-way ANOVA on rank's, as appropriate, using the SigmaStat computer program, followed by a *post hock* Holm-Sidak or Dunn's multiple range test. The a priori level of significance was $P < 0.05$.

RESULTS

Effects of BSO and HU on GSH homeostasis.

Whereas exposure to BSO alone did not significantly decrease GSH concentrations in the embryo by 0.5 h post-treatment, a decrease was observed at 3 h, compared to vehicle control (Fig. 3.1A). GSH concentrations in embryos exposed to HU alone (400 or 600 mg/kg) were lower at 3 h post-treatment than at 0.5 h ($p<0.05$). BSO pretreatment enhanced the GSH depletion in low-dose (400 mg/kg) HU-exposed embryos 0.5 h post-treatment, and in high-dose (600 mg/kg) HU-exposed embryos 3 h post-treatment.

The ratios of GSSG/GSH in the embryos were not altered by treatment with BSO alone or HU alone (400 or 600 mg/kg) at either 0.5 or 3 h, compared with vehicle control (Fig. 3.1B). However, BSO exposure preceding high-dose HU (600 mg/kg) dramatically increased the GSSG/GSH ratio compared with vehicle control at both 0.5 and 3 h post-treatment. Thus, although neither HU nor BSO alone induced oxidative stress, as assessed GSSG/GSH ratio, the combination did.

Localization of oxidative stress in the embryo: the formation of 4-HNE protein adducts.

The formation of 4-HNE protein adducts was assessed to elucidate the tissue specificity of the response of the embryo to BSO and HU exposure-induced oxidative stress. Embryos were examined 3 h after HU treatment, at the time when GSH homeostasis was significantly affected. In the control embryo,

low amounts of 4-HNE immunoreactivity (green color) were detected in the neural epithelium, otic pit, branchial arch, mid gut, and the caudal region of the tail (Fig. 3.2A). Exposure to HU alone (400 mg/kg) slightly increased the 4-HNE immunoreactivity in these regions (green color) (Fig. 3.2B); furthermore, 4-HNE reactivity was detected in nucleated blood cells (mainly yellow color) in these embryos (Fig. 3.2G, inset). The green fluorescence indicates that 4-HNE is localized in the cytoplasm, while the yellow suggests that the 4-HNE adducts are present in nuclei. Treatment with high-dose HU (600 mg/kg) dramatically enhanced 4-HNE reactivity in all of the regions described in control embryos (Fig. 3.2C); in addition, intense staining was observed in blood cells (Fig. 3.2H, inset), in the somites, and in the neural tube in the caudal region of the embryo (Fig. 3.2C). Most of the 4-HNE immunoreactivity in embryos exposed to 600 mg/kg HU was in the cytoplasm, but some appeared to be localized in nuclei, as shown in high magnification views of the neural tube (Fig. 3.2I, inset), and blood cells (Fig. 3.2H, inset).

Compared with vehicle control, BSO alone enhanced 4-HNE immunoreactivity in the neural tube, particularly in the neural epithelium in the midbrain region (Fig. 3.2D). Pretreatment with BSO increased the 4-HNE staining in embryos exposed to 400 mg/kg HU, specifically in the neural epithelium in the forebrain, in the mid gut, and the somites (Fig. 3.2E); this 4-HNE immunoreactivity was mainly cytoplasmic, although some nuclear localization, shown in yellow, is apparent in the forebrain neural epithelium (Fig. 3.2E). In the embryos exposed to both BSO and high-dose HU (600 mg/kg), the extent of

nuclear localization of 4-HNE immunoreactivity was dramatically increased in all the regions described above (Fig. 3.2F), as illustrated in the high magnification inset of the neural tube close to the caudal region of the tail (Inset, Fig. 3.2J). However, the integrity of the tissue in this region was affected, likely as a consequence of cytotoxicity (Fig. 3.2F).

There is little information on the nature of the 4-HNE protein adducts formed in any tissue. We used western blot analysis to elucidate the molecular weight range of the 4-HNE-protein adducts formed in embryos exposed to oxidative stress. Two high intensity bands were displayed in the molecular weight ranges of 150 and 100 kDa (Fig. 3.2K). Exposure to high-dose (600 mg/kg) HU alone increased the amounts of the 4-HNE-protein adducts found in both the high and lower molecular weight bands (Fig. 3.2 K, L, M). Pretreatment with BSO tended to increase the formation of 4-HNE-protein adducts in embryos exposed to either dose of HU.

Effects of BSO pretreatment on the AP-1 c-Fos heterodimer DNA binding activity induced by HU.

We reported previously that maternal exposure to HU (400 mg/kg or 600 mg/kg) induced c-Fos heterodimer-dependent AP-1 DNA binding activity in the embryo (Yan and Hales, 2005). Our goal here was to determine the impact of BSO pretreatment on HU-induced activation of c-Fos binding activity. The relative binding activity of c-Fos heterodimers in the embryo was enhanced by exposure to HU alone (400 or 600 mg/kg) at 3 h in a dose-dependent manner (Fig. 3.3). BSO alone did not influence c-Fos DNA binding activity. Furthermore,

pretreatment with BSO had no effect on the extent to which HU exposure induced the activation of AP-1 c-Fos dimers in embryos (Fig. 3.3).

Effects of BSO pretreatment on HU embryotoxicity.

Exposure to BSO alone on GD 9 did not affect progeny outcome, as assessed on GD 18 by fetal mortality, live fetal body weights, and external or skeletal abnormalities (Fig. 3.4, A-D). Exposure to 400 mg/kg HU alone was not embryo-lethal or teratogenic but did induce a reduction in fetal weights (Fig. 3.4B). In contrast, exposure to high-dose HU (600 mg/kg) increased the incidence of fetal deaths, external malformations, and skeletal deformities, in addition to causing growth retardation. BSO pretreatment did not affect the incidence of fetal mortality or growth retardation induced by either dose of HU (Fig. 3.4, A and B). Dead fetuses were observed as embryo resorptions, with the exception of two fetuses in the 400 mg/kg HU group and one fetus in the 600 mg/kg HU group, which appeared as late fetal deaths.

Although BSO pretreatment did not significantly increase the overall incidence of malformed fetuses per litter, a 2.4-fold increase in the percent of malformed fetuses per litter was observed after pretreatment with BSO in the low-dose HU (400 mg/kg) group and a 1.4-fold increase was observed among litters exposed to high-dose HU (600 mg/kg) (Fig. 3.4C). However, both the incidence and the spectrum of specific external malformations were enhanced significantly by BSO pretreatment of HU exposed dams (Tables 3.1 and 3.2).

No external malformations were apparent in control fetuses (Fig. 3.5A). One fetus with hydrocephaly (1 of 63) was observed among the litters exposed to BSO alone (Fig. 3.5D). Tail defects (10 of 108) were observed among the fetuses exposed to low-dose HU alone (400 mg/kg) (Table 3.1; Fig. 3.5B); the combination of BSO with this dose of HU resulted in fetuses with curly tail, hindlimb malformations (Fig. 3.5E), hydrocephaly, exencephaly, open eye, spinal bifida, and gastroschisis (Table 3.1). Tail and hindlimb abnormalities predominated in the fetuses exposed to 600 mg/kg HU either alone or with BSO pretreatment (Fig. 3.5, C and F). Low incidences of hydrocephaly, spinal bifida and open eye defects were found in the 600 mg/kg HU group; forelimb oligodactyly, spinal bifida, and gastroschisis were observed among the fetuses exposed to 600 mg/kg HU and BSO (Table 3.1). BSO pretreatment particularly enhanced the incidence of hindlimb defects induced by HU. Although no hindlimb defects were observed in the group exposed to low-dose HU alone, 11.5% were observed after exposure to 400 mg/kg HU in combination with BSO. BSO pretreatment also increased the incidence of hindlimb defects in the 600 mg/kg high-dose HU treatment group, from 31.0% to 68.9%. In addition, 3 fetuses with forelimb defects (ectrodactyly or hemimelia) (Table 3.1; Fig. 3.5, F and J) were observed uniquely in the litters exposed to BSO and 600 mg/kg HU.

Strikingly, the hindlimb defects observed occurred mainly at the first digit and included agenesis, truncation or displacement. Defects (aplasia / hypoplasia) of more than the first digit were observed at a very low frequency, in 1 fetus (1.7%) in the group treated with high-dose HU alone and 6 fetuses (9.8%) in the

group exposed to this dose of HU with BSO (Table 3.1; Fig. 3.5K). Interestingly, in the fetuses exposed to BSO in combination with 400 mg/kg HU, 3 cases of tibial polydactyly were observed as an extra digit at the great toe, in addition to the predominant aplasia or hypoplasia at the first toe (Fig. 3.5, E and I).

No apparent skeletal abnormalities were observed in vehicle controls (Fig. 3.6A). Similarly to the external malformations, BSO pretreatment exaggerated the skeletal malformations induced by HU. In the group treated with 400 mg/kg HU, the skeletal malformation rate per litter increased 2.3-fold when the dams were pretreated with BSO (Fig. 3.4D); exposure to 600 mg/kg HU in combination with BSO increased the rate of skeletal deformities in live fetuses from 78.8% to 100%. The predominant skeletal abnormalities which were observed consisted of lumbarsacral vertebral and hindlimb defects (Table 3.2). The vertebral defects were partial ossification, fusion or misalignment of centra, or misalignment of the vertebral arch; more severe deformities were found in the fetuses exposed to HU (400 or 600 mg/kg) in combination with BSO (Fig. 3.6, B, C, E, and F). The hindlimb defects were mainly at the anterior axis, displayed as ectrodactyly at the first digit and tibial aplasia or hypoplasia (Fig. 3.6); in the few instances of forelimb defects, radius agenesis occurred (Table 3.2). Low frequencies of tail malformations (aplasia/hypoplasia), sternal defects (partial ossification, misalignment), or forked ribs were also observed in the HU treated groups in the presence or absence of BSO (Table 3.2); pretreatment with BSO did not influence either the incidence or the severity of these defects.

DISCUSSION

In the organogenesis stage embryo, the inhibition of GSH synthesis with BSO induced oxidative stress as assessed by the GSSG/GSH ratio, the formation of 4-HNE protein adducts, and the activation of redox-sensitive transcription factors such as AP-1. Interestingly, BSO enhanced HU teratogenicity without affecting fetal mortality or weights. The effects of the combination of BSO and HU were region-specific in the embryo, both with respect to the malformations that resulted and the localization of 4-HNE protein adduct immunoreactivity. Interestingly, region-specific 4-HNE-protein adducts were found in early organogenesis-stage embryos even in the absence of an exposure to exogenous chemicals; these adducts were localized mainly to the neural tube, otic pit, branchial arch, mid-gut, and the caudal region of the tail. These "naturally occurring" 4-HNE protein adducts were found predominantly in the cytoplasm. Increases in the formation of 4-HNE adducts may indicate the presence of higher levels of free radicals in these regions. Alternatively, differences in the composition of membrane phospholipids may alter susceptibility to the induction of lipid peroxidation. Finally, region specific differences in the capacity of the embryo to detoxify 4-HNE by conjugating it with GSH, catalyzed by the glutathione S-transferases, may be important in detoxifying 4-HNE in target cells (Awasthi et al., 2005).

The impact of 4-HNE on the fate of the cell is dose-dependent; at low levels, 4-HNE promotes cell proliferation, while at higher concentrations, it induces cell cycle arrest, differentiation, and finally apoptosis (Awasthi et al.,

2005). Exposure to 4-HNE induces vascular smooth muscle growth, accompanied by the activation of MAPKs (extracellular signal-regulated kinase, c-Jun N-terminal kinase, and p38), the induction of c-fos and c-jun gene expression, and AP-1 DNA binding activity (Kakishita and Hattori, 2001). The generation of 4-HNE in specific regions of the embryo may suggest the involvement of 4-HNE in the regulation of proliferation, differentiation, and apoptosis during normal development.

4-HNE regulates cell signal cascades mainly due to the formation of 4-HNE-protein adducts (Leonarduzzi et al., 2004). Our western blot data show that there are two predominant 4-HNE-protein adduct bands in the 100- and 150-kDa regions. Characterization of the identities of the proteins in these bands would help to elucidate the pathways regulated by 4-HNE during normal organogenesis. In the retina, triosephosphate isomerase, α enolase, heat shock cognate 70 and βB2 crystallin were identified as proteins that were frequently modified and had the highest molar content of 4-HNE (Kapphahn et al., 2006), whereas heat shock protein 90 was found to be consistently modified by 4-HNE in the liver of alcohol treated rats (Carbone et al., 2005a). 4-HNE-protein adducts influence a variety of signal cascades, including signals for limb patterning such as the MAPKs (Kawakami et al., 2003;Zuzarte-Luis et al., 2004). Although the possibility of increased membrane leakage by oxidative damage cannot be excluded, an increase in the nuclear localization of 4-HNE with the increase in HU doses suggests that 4-HNE may transduce signals from the membrane to nuclear

compartment. Identification of the proteins conjugated with 4-HNE should help to elucidate the underlying embryopathy of limb malformations.

The tissue-specific localization of 4-HNE protein adducts, either as part of a signal pathway during normal development or as a response to oxidative stress during abnormal development, may indicate that these specific regions are more susceptible to oxidant insults. We propose that the specific external and skeletal malformations induced by exposure to HU are related to the localized increases in 4-HNE immunoreactivity that we observed in the somites (vertebral column and hindlimb defects), the caudal end of the neural tube (tail defects), and the optic vesicle (open eye). Intense 4-HNE-protein adduct immunofluorescence was also observed in nucleated blood cells, suggesting that hematopoietic cells are highly susceptible to oxidative stress during the switch from glycolysis to aerobic metabolism. Interestingly, glucose-6-phosphate dehydrogenase, important in generating the reduced NADPH needed to maintain GSH in its reduced form, is essential for the establishment of blood circulation at this stage of development (Longo et al., 2002); a deficiency in glucose-6-phosphate dehydrogenase enhances the sensitivity of organogenesis-stage embryos to oxidative stress (Nicol et al., 2000).

One of the mechanisms by which oxidative stress may have differential effects, depending on the endpoint assessed, is via the regulation of redox sensitive transcription factors such as AP-1. Oxidative stress regulates the activation of AP-1 through a variety of mechanisms (Abate et al., 1990;Hirota et al., 1997). We report that a BSO pretreatment which decreased GSH and

increased the formation of 4-HNE protein adducts did not enhance the effects of HU on c-Fos dependent AP-1 DNA binding activity in mouse embryos. This is interesting because 4-HNE has been reported to interfere with the activities of protein kinases which regulate AP-1 activity, namely MAPKs, such as c-Jun N-terminal kinases, p38, and extracellular signal-regulated kinase1/2 (Leonarduzzi et al., 2004). In studies with vascular smooth muscle cells, the effects of 4-HNE on the expression of AP-1 constituents was concentration- and AP-1 family member specific (Kakishita and Hattori, 2001). Exposure of these cells to 4-HNE concentrations ≤ 2.5 μM dramatically induced c-fos mRNA expression without influencing that of c-jun; however, exposure to 4-HNE concentrations from 2.5 to 10 μM resulted in an increase in c-jun expression and a decrease in c-fos mRNA concentrations (Kakishita and Hattori, 2001). Concomitantly, AP-1 DNA binding activity peaked after exposure to 2.5 μM 4-HNE, then declined with increases in 4-HNE concentration (Kakishita and Hattori, 2001). We have reported previously that HU induced c-Fos immunoreactivity in the GD 9 mouse embryo is localized in the brain region, branchial arch, somites, neural tube, heart and the areas around the blood cells in embryos (Yan and Hales, 2005). Here, we demonstrate that 4-HNE protein adduct immunoreactivity is detected in most of the same regions.

There is extensive interest in the development of strategies to protect the conceptus against oxidative stress-mediated insult during organogenesis. Although maternal dietary antioxidant supplementation has clearly been successful in improving fetal outcomes in animal models of experimental diabetes

(Cederberg et al., 2001) or after exposure to specific teratogens, including HU (DeSesso, 1981;Wells et al., 2005), in some instances, high-doses may be pro-oxidative and enhance adverse effects, such as tumorigenesis in p53 null mice (Chen and Wells, 2006). If 4-HNE plays an important role in mediating the toxicity of reactive oxygen species in the embryo, an alternate approach would be to enhance 4-HNE detoxification by inducing glutathione and the glutathione S-transferases; there is evidence that this approach is effective in the protection by 3H-1,2-dithiole-3-thione of cultured cardiomyocytes against 4-HNE (Li et al., 2005). If, as suggested above, 4-HNE plays a role in mediating the effects of reactive oxygen species by activating MAPKs, such as p38 MAPK, treatment with a MAPK inhibitor may protect the embryo against insult. Interestingly, inhibition of p38 MAPK rescued hematopoetic stem cells from reactive oxygen species induced defects in repopulating capacity (Ito et al., 2006).

Clearly, both the formation of 4-HNE protein adducts and the induction of c-Fos immunoreactivity represent responses of the embryo to insult. We propose that such localized stress responses play a role in determining the pattern of malformations induced by exposure of the embryo to a teratogen.

Fig. 3.1. GSH concentrations (**A**) or GSSG/2GSH ratios (**B**) in embryos exposed to HU without or with BSO pretreatment. Pregnant mice were given saline (-) or BSO at 600 mg/kg (+) 4 h before treatment with saline (-) or HU 400 mg/kg (L) or 600 mg/kg (H) on GD 9. Embryos were collected 0.5 or 3 h after HU exposure. Each bar (mean ± SEM) represents 6-10 litters. *, significant difference from vehicle control (- / -) at the same time point (*: $p<0.05$; **: $p<0.01$); †, significant difference between the HU-treated groups in the presence or absence of BSO ($p<0.05$); ‡, significant difference from the same treatment group at 0.5 h ($p<0.05$).

Fig. 3.1

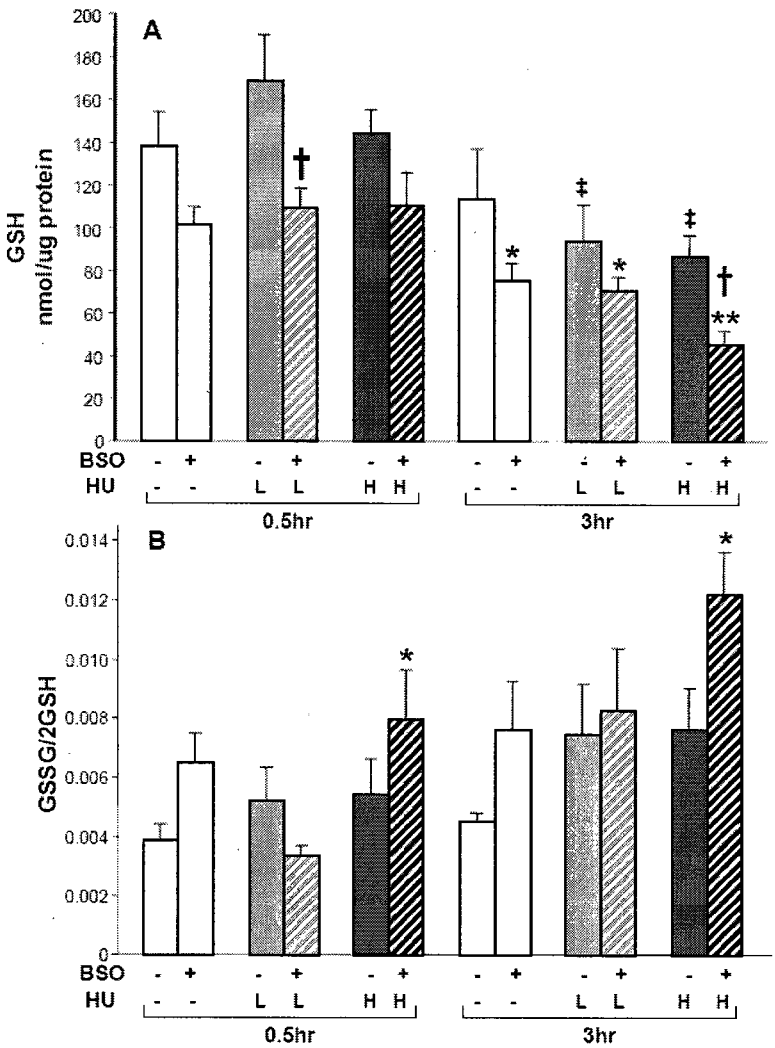
A
GSH
nmol/ug protein
200
180
160
140
120
100
80
60
40
20
0
BSO - + - + - + - + - +
HU - - L L H H - - L L H H
0.5hr
3hr
B
GSSG/2GSH
0.014
0.012
0.010
0.008
0.006
0.004
0.002
0
BSO - + - + - + - + - +
HU - - L L H H - - L L H H
0.5hr
3hr

Fig. 3.2. The localization of 4-HNE protein adducts in embryos exposed to HU without or with BSO pretreatment. Timed pregnant female mice received saline or BSO 4 h before HU treatment at 400 or 600 mg/kg on GD 9 and were euthanized 3 h after HU treatment. The embryos were fixed in 4% in paraformaldehyde and processed for immunofluorescence staining with an antibody against 4-HNE. 4-HNE adducts were detected with fluorescein (in green); embryos were 600 mg/kg; D, BSO; E, HU 400 mg/kg combined with BSO; F, HU 600 mg/kg combined with BSO. Higher magnification views of the blood cells in the embryos exposed to HU 400 mg/kg or HU 600 mg/kg are provided in G or H, respectively. Higher magnification views of the neural tube close to the caudal region of the tail in an embryo treated with HU 600mg/kg without or with BSO are provided in I or J, respectively. Arrows indicate forebrain (FB), midbrain (MB), hindbrain (HB), otic pit (OP), bronchial arch (BA), neural tube (NT), mid gut (MG), somites (S), and caudal region of the tail (CT). K, Western blot analysis of 4-HNE protein adducts in whole embryo lysates obtained at the same times as indicated above. 4-HNE protein adducts were detected mainly as two strong bands around 150 or 100 kDa. Quantification of these bands by densitometry analysis is presented in L and M, respectively. Each bar (mean ± S.E.M.) represents 5 litters. Asterisks denote a significant difference from saline control (*, $p<0.05$; ** $p<0.01$).

Fig. 3.2

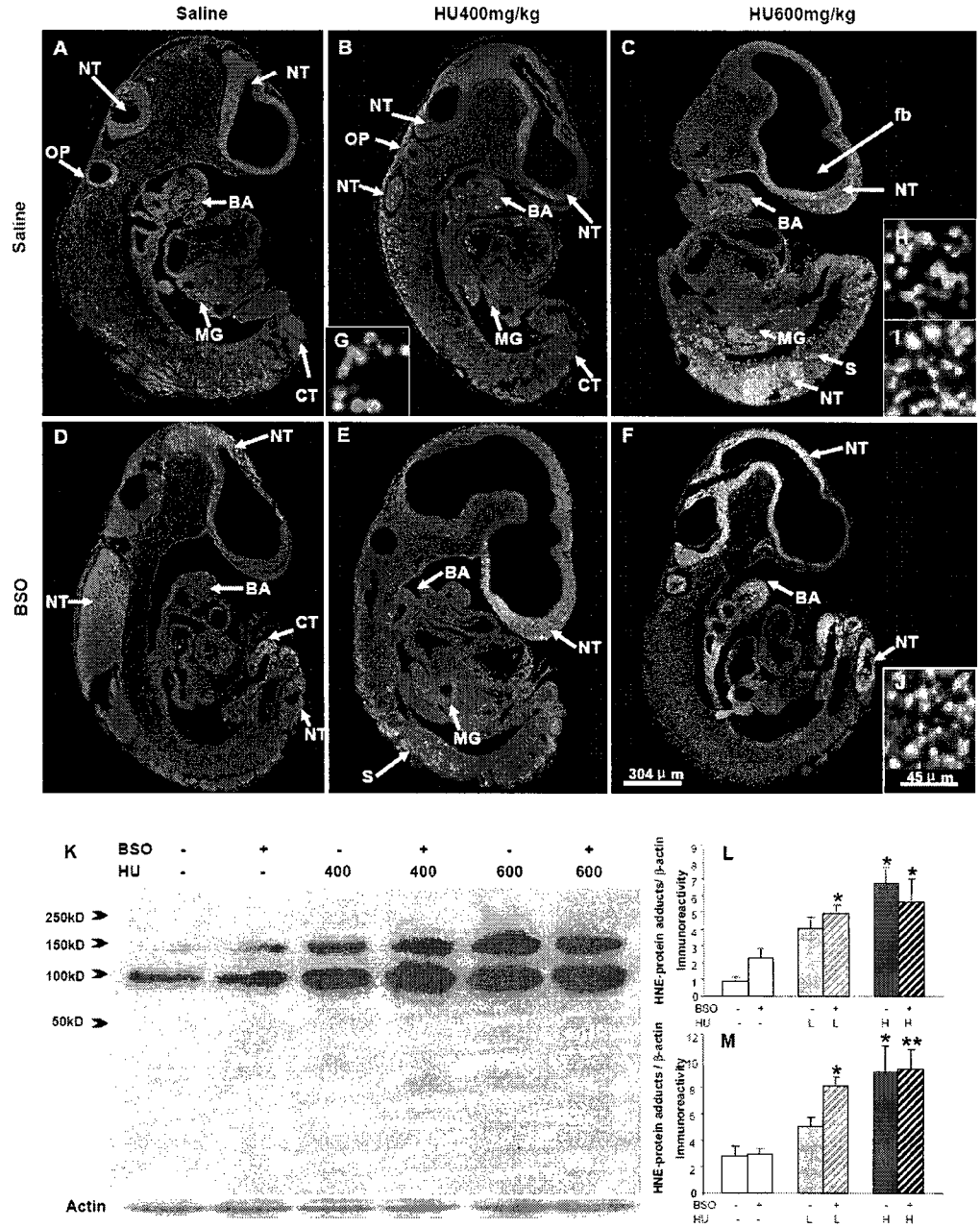
Saline
HU400mg/kg
HU600mg/kg
Saline
BSO
A
B
C
D
E
F
G
H
I
J
NT
OP
BA
MG
CT
fb
S
304 μ m
45 μ m
K
BSO
HU
400
600
250kD
150kD
100kD
50kD
Actin
L
M
HNE-protein adducts / β-actin Immunoreactivity

Fig. 3.3. AP-1 c-Fos heterodimer DNA binding activity in embryos exposed to HU without or with BSO pretreatment. Pregnant mice treated with saline (-) or BSO at 600 mg/kg (+) 4 h before saline (-) or HU 400mg/kg (L) or 600mg/kg (H) injection, were euthanized 0.5 or 3 h after HU exposure. AP-1 c-Fos heterodimer DNA binding activity was measured using an ELISA assay as described under *Materials and Methods*. The data are expressed as mean ± S.E.M. (micrograms of nuclear extract standard per microgram of sample protein); each bar (mean ± S.E.M.) represents 7 to 10 litters. *, significant difference from control (-/-) at the same time point ($P<0.05$).

Fig. 3.3

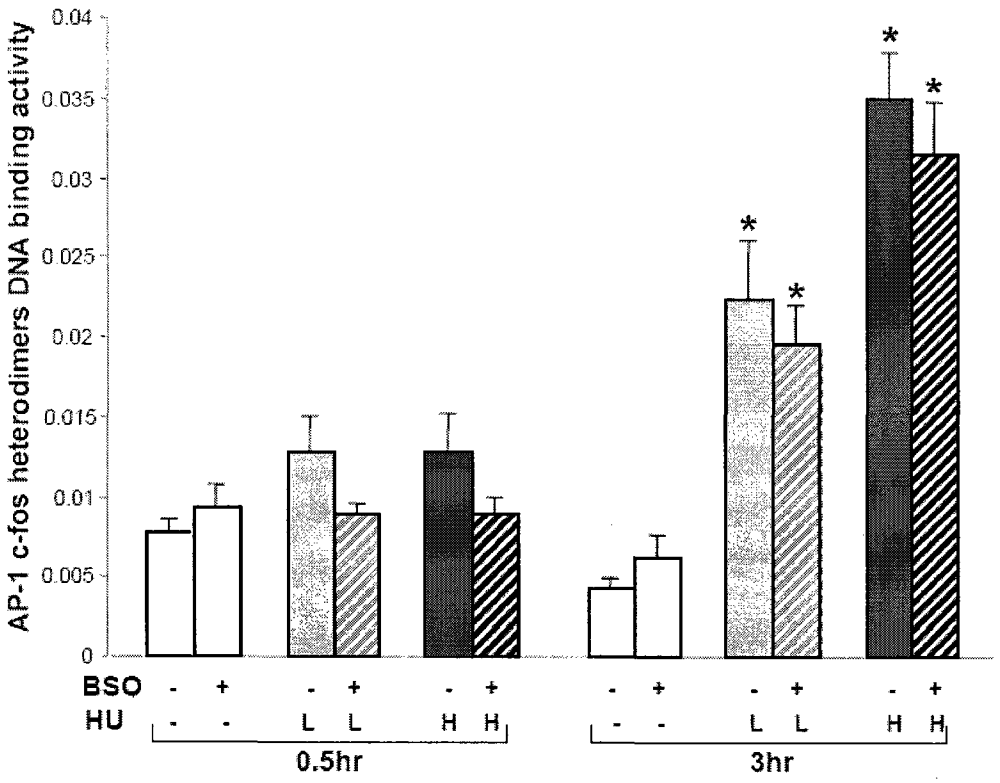
AP-1 c-fos heterodimers DNA binding activity
0.04
0.035
0.03
0.025
0.02
0.015
0.01
0.005
0
BSO - + - + - + - + - + - +
HU - - L L H H - - L L H H
0.5hr
3hr
*
*
*
*

Fig. 3.4. Effects of BSO pretreatment on HU induced fetal death rate (A), live fetal weight (B), external malformation rate in live fetuses (C), and skeletal malformation rate in live fetuses (D). Female mice received saline (-) or BSO at 600 mg/kg (+) 4 h before treatment with saline (-), HU 400mg/kg (L) or HU 600mg/kg (H) and were euthanized on GD 18. The fetal death rate is expressed as the percentage of total implantations that were dead; the live fetal weight is expressed as the mean body weights of live fetuses/litter; the external and skeletal malformation rates are expressed as the percentage of the live fetuses per litter that were malformed. Data represent means per litter ± S.E.M., with 7-10 litters per treatment group. Asterisks denote a significant difference from saline control (*, $p<0.05$; ** $p<0.01$).

Fig. 3.4

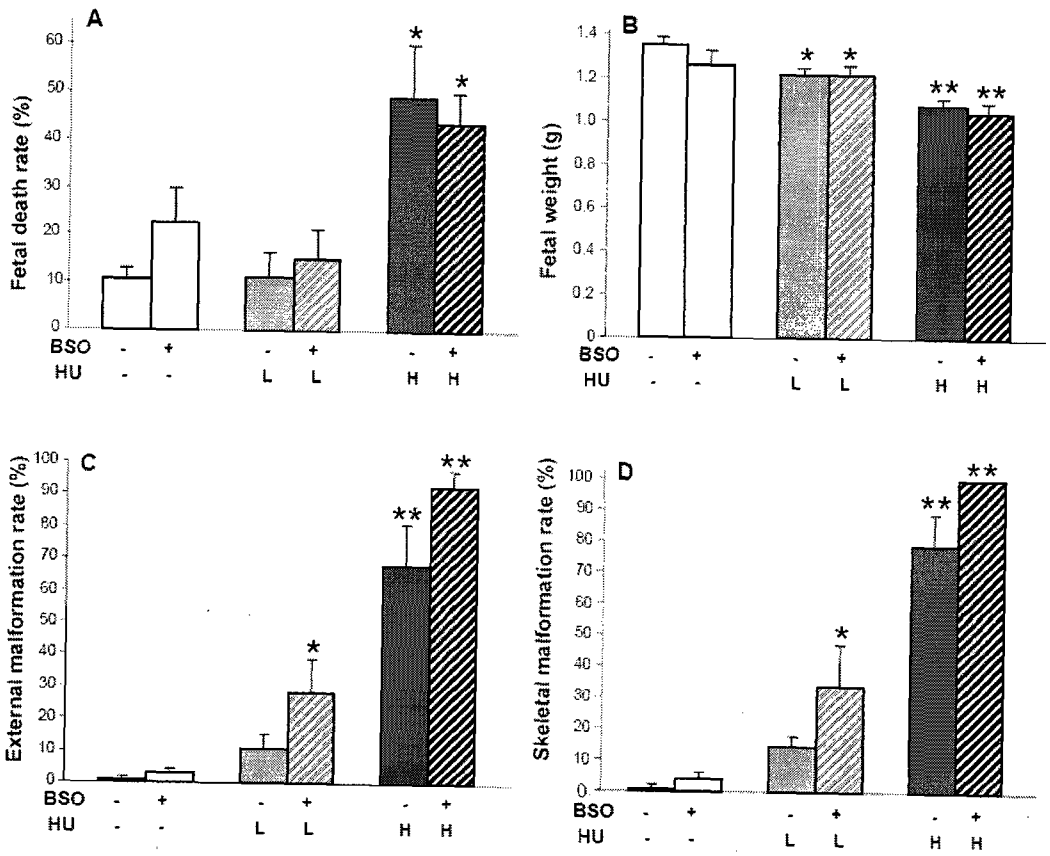
A
Fetal death rate (%)
0
10
20
30
40
50
60
BSO - + - + - +
HU - - L L H H
B
Fetal weight (g)
0
0.2
0.4
0.6
0.8
1.0
1.2
1.4
BSO - + - + - +
HU - - L L H H
C
External malformation rate (%)
0
10
20
30
40
50
60
70
80
90
100
BSO - + - + - +
HU - - L L H H
D
Skeletal malformation rate (%)
0
10
20
30
40
50
60
70
80
90
100
BSO - + - + - +
HU - - L L H H

Fig. 3.5. External malformations induced by exposure to HU without or with BSO. Limb and tail (short and/or curly) defects were predominant. A, control fetus. A higher magnification view of the right limb is provided in G; B, HU 400 mg/kg-treated fetus with curly tail (CT); C, HU 600 mg/kg-treated fetus with curly tail and hypoplasia of the first digit of the right hindlimb. A higher magnification view of the right hind limb is provided in H; D, BSO alone-treated fetus with hydrocephaly (HC); E, BSO with HU 400 mg/kg-treated fetus with curly tail and hindlimb defects. A higher magnification view of the hind limbs is provided in I: the higher limb is the right hindlimb with an extra digit at the great toe, indicated by a white arrow, and the bottom one is the left hindlimb, with first digit agenesis; F, BSO with HU 600 mg/kg treated fetus with fore- and hind-limb defects and gastroschisis (GS). A higher magnification view of the right forelimb or hindlimbs are provided in J or K, respectively. Only one digit is at the distal part of the right forelimb (J). The left hindlimb only has two digits (higher limb in K), and the right hindlimb displays agenesis of the first digit (bottom limb in K).

Fig. 3.5

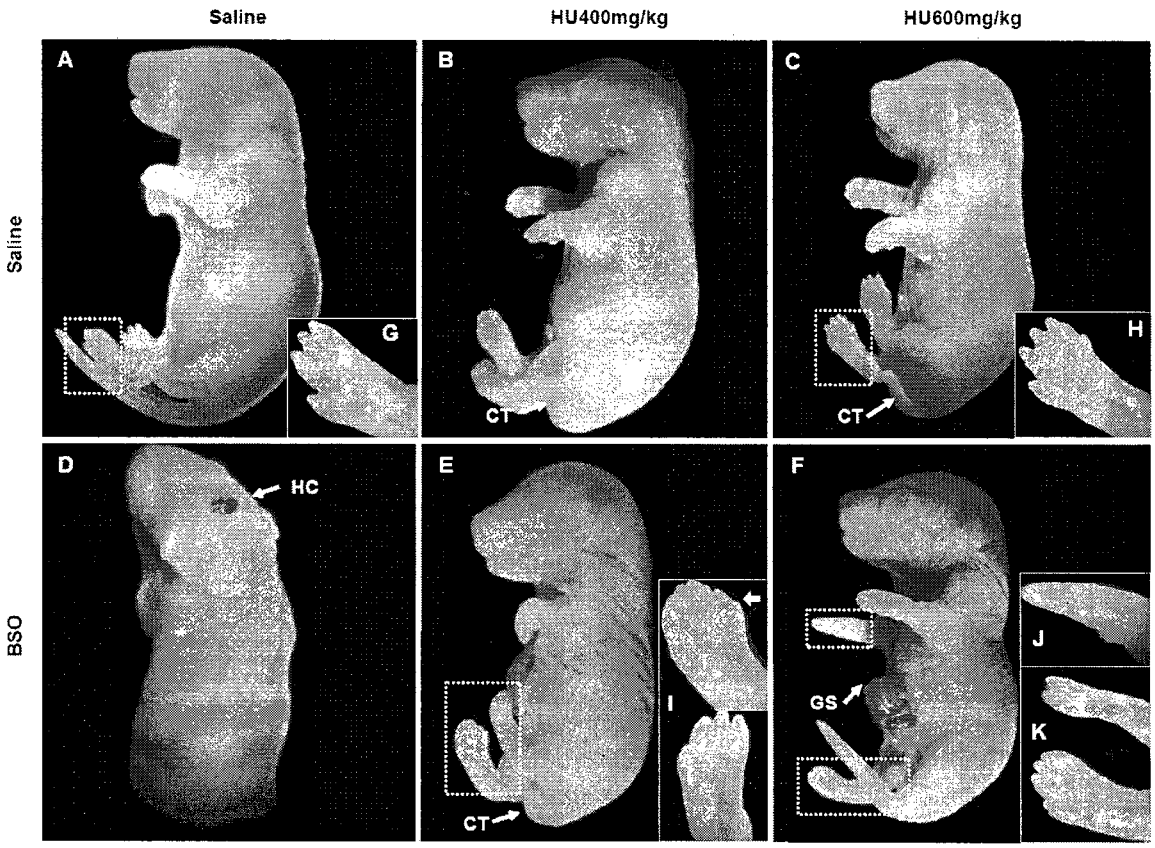
Saline
HU400mg/kg
HU600mg/kg
Saline
BSO
A
B
C
D
E
F
G
H
I
J
K
CT
CT
CT
HC
GS

Fig. 3.6. Double-stained skeletons of the fetuses exposed to HU without or with BSO. The red color represents bone stained by alizarin red S and the blue depicts cartilage dyed by alcian blue. The vertebral defects were predominantly at the lumbarsacral vertebrae and the anterior axis of hindlimbs. The lumbarsacral vertebrae are depicted in the control fetus (A), and a higher magnification view of the hindlimb of a control fetus is provided in G. Arrow heads indicate the deformities of lumbarsacral vertebrae: partial ossification of the centra in B (HU 400 mg/kg); partial ossification, fusion, and misalignment of centra in E (HU 400 mg/kg and BSO); partial ossification, fusion and misalignment of centra, and misalignment of the vertebral arch in C (HU 600 mg/kg) or F (HU 600 mg/kg plus BSO). Arrows indicate limb defects including tibia aplasia (TA), tibia hypoplasia (TH), fibula bent (FB), aplasia of the first digit (AFD), hypoplasia of the first digit (HFD), oligodactyly of more than the first digit (OL).

Fig. 3.6

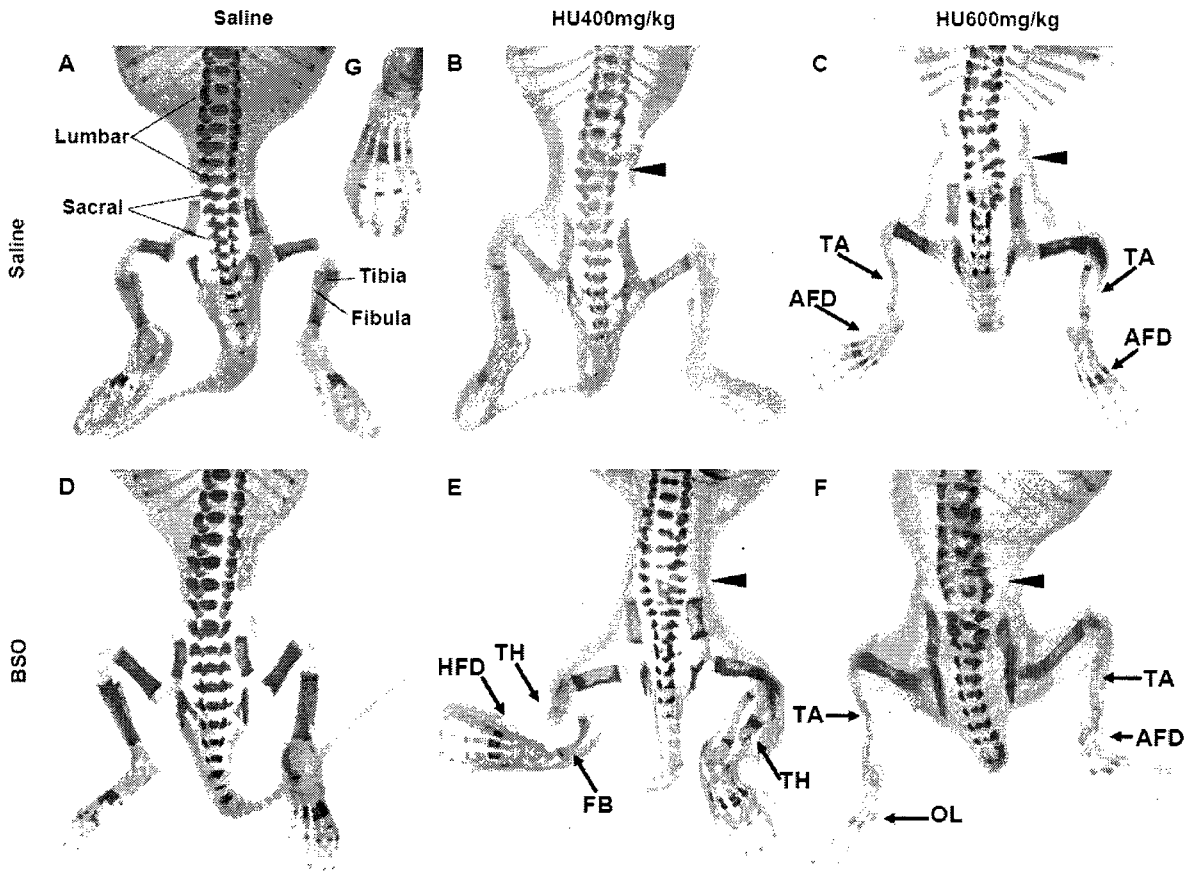
Saline
HU400mg/kg
HU600mg/kg
A
G
B
C
Lumbar
Sacral
Tibia
Fibula
TA
AFD
TA
AFD
Saline
D
E
F
BSO
HFD
TH
TA
TA
AFD
TH
FB
OL

Table 3.1 Incidence and types of external malformations in fetuses following maternal treatment with hydroxyurea (HU, 400 or 600 mg/kg) or L-buthionine-S, R- sulfoximine (BSO) plus HU.

Percentages (in parentheses) are represented as the malformed fetuses out of the fetuses examined; a single fetus may be represented more than once in listing individual defects.

	Treatment (mg/kg)					
	Saline	**BSO**	**HU (400)**	**HU (400) +BSO**	**HU (600)**	**HU (600) +BSO**
No. of litters examined	9	7	10	10	9	8
No. of fetuses examined	111	63	108	113	58	61
Abnormal hindlimb				13 (11.5%) **	18 (31.0%)	42 (68.9%) **
Aplasia / hypoplasia of the first digit				11 (9.7%)	17 (29.3%)	35 (57.4%)
Aplasia / hypoplasia of more than one digit					1 (1.7%)	6 (9.8%)
Polydactyly				3 (2.7%)		
Amelia					1 (1.7%)	1 (1.6%)
Abnormal forelimb (Ectrodactyly, hemimelia)						3 (4.9%)
Curly/hypoplastic tail			10 (9.3%)	18 (15.9%)	30 (51.7%)	35 (57.4%)
Hydrocephaly		1 (1.6%)		1 (0.9%)	3 (5.2%)	
Exencephaly				1 (0.9%)		
One open eye				3 (2.7%)	2 (3.2%)	
Spinal bifida				3 (2.7%)	1 (1.7%)	1 (1.6%)
Gastroschisis				1 (0.9%)		4 (6.6%)

** Significant difference at $p<0.001$ level between the hydroxyurea treated group with or without BSO pretreatment.

Table 3.2 Skeletal malformations in fetuses following maternal treatment with hydroxyurea (HU, 400 or 600 mg/kg) or L-buthionine-S,R-sulfoximine (BSO) plus HU.

Percentages (in parentheses) are represented as the malformed fetuses out of the fetuses examined; a single fetus may be represented more than once in listing individual defects.

	Treatment (mg/kg)					
	Saline	BSO	HU(400)	HU(400) +BSO	HU(600)	HU(600) +BSO
No. of litters examined	9	7	10	10	9	8
No. of fetuses examined	18	30	25	63	49	52
Abnormal lumbarsacral vertebrae [a]			2(8.0%)	19(30.2%)	22(44.9%)	39(75.0%)*
Abnormal thoracic vertebrae [a]						2(3.8%)
Abnormal hindlimb				14(22.2%)*	21(42.9%)	41(78.9%)**
Tibia aplasia / hypoplasia				14(22.2%)	21(42.9%)	39(75.0%)
Fibula bent				3(4.5%)	1(2.0%)	12(23.1%)
Digits aplasia / hypoplasia				10(15.9%)	16(32.7%)	32(61.5%)
Femur hypoplasia						1(1.9%)
Amelia					1(2.0%)	1(1.9%)
Abnormal forelimb						2(3.8%)
Oligodactyly						2(3.8%)
Radius aplasia						2(3.8%)
Tail aplasia/hypoplasia			3(12.0%)	11(17.4%)	16(32.7%)	19(36.5%)
Abnormal Sternebrae [b]		2(6.7%)	2(8.0%)	6(9.5%)	10(20.4%)	20(38.5%)
Forked ribs				1(1.6%)	11(22.4%)	6(11.5%)

* Significant difference at $p<0.5$ or **$p<0.001$, respectively, between the hydroxyurea-treated group with or without BSO pretreatment.

[a] Vertebral column malformations include a fused, incompletely ossified, misaligned or misshapen vertebral centra or vertebral arch.

[b] Sternebral abnormalities include misalignment, incomplete ossification, or an extra ossification site.

CONNECTING TEXT

In Chapter Three, increased immunoreactivity of 4-HNE protein adducts was detected in regions of the embryo that are highly sensitive to HU-induced malformations, including hindlimb, lumbarsacral vertebral column, and tail. GSH depletion further enhanced the production of 4-HNE protein adducts and increased the incidence and severity of HU-induced malformations at hindlimb and lumbarsacral vertebral column, without altering HU-induced fetal death and growth retardation. This indicated that oxidative stress may mainly attribute to HU-induced specific malformations. Surprisingly, the DNA binding activity of c-Fos heterodimers was not affected by GSH depletion. AP-1 is activated by MAPKs via post-translational phosphorylation in response to stress. Thus, in the following chapter, the effects of HU on the activation of MAPKs are evaluated and specific inhibitors for MAPKs were used to elucidate the role of MAPKs in HU developmental toxicity.

CHAPTER FOUR

p38 and JNK Mitogen-Activated Protein Kinase (MAPK) Signaling Pathways Play Distinct Roles in the Response of Organogenesis Stage Embryos to a Teratogen

Jin Yan and Barbara F. Hales

ABSTRACT

Mitogen-activated protein kinase (MAPK) signaling plays an important role during embryo development. We hypothesize that MAPK activation is a determinant of the fate of organogenesis-stage embryos exposed to insult. To test this hypothesis, CD1 mice were exposed to a model teratogen, hydroxyurea, on gestational day 9. Hydroxyurea exposure triggered a dramatic, transient increase in the activation of p38 MAP kinases and c-Jun N-terminal kinases (JNKs) in embryos, without activating extracellular-signal regulated kinases 1 and 2 (ERKs 1/2). Selectively blocking p38 MAP kinases with SB203580 enhanced hydroxyurea-induced fetal mortality without affecting growth retardation or the incidence of deformities among surviving fetuses. In contrast, selectively blocking JNKs with L-JNKI1 did not affect hydroxyurea-induced fetal death but doubled the incidence of hindlimb defects observed. Thus, p38 MAP kinases and JNKs play distinct roles in protecting the conceptus against insult. Pharmacological inhibition of teratogen exposure induced MAPK activation has adverse consequences on the embryo.

INTRODUCTION

Mitogen-activated protein kinases (MAPKs) are serine/threonine protein kinases that mediate signal transduction from the cell surface to the nucleus. Upstream MAP kinase kinase kinases (MAP3Ks) activate MAP kinase kinases (MAP2Ks), which in turn activate MAPKs by dual-phosphorylation on threonine and tyrosine residues (Pearson et al., 2001). Downstream MAPK substrates include transcription factors or their components, such as AP-1 and p53 (Turjanski et al., 2007), molecules involved in the detection and response to DNA damage, such as PARP-1 and γH2AX (Caldini et al., 2005;Sluss and Davis, 2006), as well as a variety of pro-and anti-apoptotic factors (Bogoyevitch and Kobe, 2006). Among the most widely studied MAPK families are extracellular-signal regulated kinases 1 and 2 (ERK1/2), p38 MAP kinases (α, β, γ, and δ), and c-Jun N-terminal kinases (JNKs1, 2 and 3) (Turjanski et al., 2007). The ERK1/2 pathways, thought to be triggered preferentially by growth factors and mitogens, play an important role during development in the regulation of cell proliferation and differentiation (Turjanski et al., 2007). Activation of the p38 and JNK MAPKs is triggered by stimuli ranging from growth factors to a variety of stress stimuli, including intracellular pH changes, ultraviolet irradiation, heat shock, DNA damaging agents, hyperglycemia, ethanol, hypoxia and oxidative stress (Kyriakis and Avruch, 1996;Ku et al., 2007). Stress response MAPKs control defense responses that determine whether cells survive, differentiate or apoptose.

MAPK pathways play crucial roles during normal embryo development. During mouse embryogenesis ERK is activated in discrete spatial and temporal domains, correlated with regions of fibroblast growth factor signaling (Corson et

al., 2003). During limb development, ERK activation may transduce proliferation and differentiation signals to regulate growth, pattern formation and skeletogenesis (Bobick et al., 2007). The p38 MAP kinase pathway is essential for cartilage formation in limb mesenchyme; inhibition of the p38 MAPK pathway leads to sustained Wnt7a signaling and inhibits precartilage condensation and chondrogenesis (Jin et al., 2006). JNK pathway signaling is of particular importance during neuronal development, as mice lacking both *Jnk1* and *2* die during mid-gastrulation with neural tube defects (Sabapathy et al., 1999). In the limb, JNK may function downstream of BMP signals to sculpt the limb bud by triggering programmed cell death through induction of *Dkk1*, an inhibitor of *Wnt* (Grotewold and Ruther, 2002b).

The extent to which disturbances in MAPK signaling pathways mediate teratogen-induced abnormal development remains to be elucidated. All three MAPK pathways were activated in organogenesis-stage mouse embryos exposed *in vitro* to heat shock, whereas exposure to cyclophosphamide or staurosporine activated only the p38 MAP kinase pathway (Mirkes et al., 2000). Induction of *Dkk1*, a downstream target of JNK-c-Jun, was associated with thalidomide induced limb truncations (Knobloch et al., 2007). Cadmium induced limb reduction defects in C57BL/6N mice were correlated with decreased activation of ERK1/2 phosphorylation, compared to the less sensitive SWV strain (Elsaid et al., 2007).

Reactive oxygen species (ROS) modulate MAPK signaling (Torres and Forman, 2003). Oxidative stress, an imbalance between the rate of formation of ROS and their detoxification by antioxidant defense systems, is induced by a

number of developmental toxicants, including heat shock, cadmium and thalidomide (Flanagan et al., 1998;Kovacic and Somanathan, 2006). Together, these findings have led us to propose that oxidative stress-induced modifications to DNA, proteins and lipids in the embryo disrupt normal development at least in part by affecting MAPK signaling. In previous studies, we found that *in utero* exposure to a model teratogen, hydroxyurea, disturbs skeletal development, depletes glutathione, increases the formation of 4-hydroxynonenal protein adducts, and induces activator protein-1 (AP-1) DNA-binding activity in embryos (Yan and Hales, 2005;Yan and Hales, 2006). AP-1 subunits, Jun, Fos and ATF proteins, are downstream targets of MAPK signaling (Turjanski et al., 2007). Furthermore, AP-1 plays a crucial role in the decision of cells to proliferate, differentiate or die; tight regulation of AP-1 activity is necessary for normal limb development (Tufan et al., 2002).

The potential use of selective MAPK signaling pathway inhibitors as drugs has generated intense interest. To test the hypothesis that MAPK signalling pathways play an important role in determining the response of organogenesis stage embryos to teratogen exposure, we investigated the impact of maternal exposure to teratogenic doses of HU on the activation of MAPKs (ERK1/2, JNK, and p38) in the embryo and evaluated the consequences of selectively blocking these MAPK pathways on the developmental toxicity of HU. Exposure of organogenesis stage embryos to a model teratogen transiently activates p38 and JNK MAP kinases; however, inhibition of this activation has adverse consequences to the embryo.

MATERIALS AND METHODS

Animals and treatments.

Timed-pregnant CD1 mice (20-25g) were purchased from Charles River Canada Ltd. (St. Constant, QC, Canada) and housed in the McIntyre Animal Resource Centre (McGill University, Montreal, Canada). All animal protocols were conducted in accordance with the guidelines outlined in the Guide to the Care and Use of Experimental Animals, prepared by the Canadian Council on Animal Care. Female mice were mated between 8:00 am and 10:00 am on gestational day 0 (GD 0). On GD 9, vehicle (saline) or HU (400 or 600mg/kg) was given to the female mice by intraperitoneal injection at 9:00 am. Dams were euthanized at 0.5, 3, or 6 h after treatment with HU. The embryos were dissected out in Hanks' balanced salt solution (Gibco Laboratories, ON, Canada) for subsequent assessment of the activation of MAP kinases and c-Jun.

SB 203580 (EMD Biosciences, Inc., La Jolla, CA), a p38 MAP kinase inhibitor (Cuenda et al., 1995), L-JNKI1 (c-Jun N-terminal Kinase Peptide Inhibitor 1, L-stereoisomer, Axxora, LLC, San Diego, CA), a JNK inhibitor (Bonny et al., 2001), or the JNK inhibitor L-TAT control peptide (Axxora LLC), was administered to the female mice before treatment with HU (400 or 600 mg/kg) on GD 9. SB 2003580 (chloride form) was dissolved in saline and given to the female mice by intraperitoneal injection 30 min before HU exposure; L-JNKI1 or the L-TAT control peptide was dissolved in PBS and administered by tail-vein injection immediately prior to HU treatment. Dams were euthanized on GD 9 at 0.5, 3, or 6 h after HU treatment or on GD 18 for the evaluation of developmental toxicity. On GD 9, the embryos were dissected out in Hanks' balanced salt solution for the subsequent

assessment of MAP kinase activation. On GD 18, the uteri were removed, and the numbers of implantations, resorption sites, and live and dead fetuses were recorded. All the live fetuses were weighed, inspected for external malformations, and then double-stained with Alician Blue (cartilage) and Alizarin red S (bone) for the analysis of skeletal malformations, as described previously (Yan and Hales, 2005).

Western blotting.

At the time of collection on GD9, embryos were pooled by litter. Whole tissue lysates were prepared for phospho-c-Jun and MAP kinase determinations. Samples were placed in 40 µl RIPA buffer (150 mM NaCl; 1% NP-40; 0.5% deoxycholate; 0.1 % SDS; 50 mM Tris, pH 7.5) containing 10 µl/ml of the protease inhibitor cocktail and 20µl/ml of the phosphatase inhibitor mix (Active Motif, Carlsbad, CA). The samples were homogenized with an ultrasonicator (Sonics & Materials Inc., Newtown, CT), and centrifuged at 10,000 g for 15 min at 4°C. The supernatants were used for immuno-blotting.

Proteins from each sample (7.5 or 15 µg, for 15 well or 10 well gels, respectively) were separated by 10% sodium dodecyl sulfate-polyacrylamide gel electrophoresis and then transferred onto equilibrated polyvinylidene difluoride membranes (Amersham Biosciences, Buckinghamshire, UK) by electroblotting. Membranes were blocked with 5% skim milk for 1 h at room temperature, and then probed overnight at 4 °C with primary antibodies against phospho-c-Jun (1:1000), phospho-JNK (1:1000), phospho-p38 (1:1000), phospho-ERK1/2 (1:1000), ERK2 (1:1000), or actin (1:5000). Rabbit polyclonal anti-phospho-c-Jun

(Ser 63), anti-phospho-JNK (Thr183/Tyr185), monoclonal anti-phospho-p38 (Thr180/Tyr182), and mouse monoclonal anti-phospho-ERK1/2 (Thr202/Tyr204) antibodies were purchased from Cell Signaling Technology (Beverly, MA). Rabbit polyclonal anti-ERK2 and goat polyclonal anti-actin (I-19) were obtained from Santa Cruz Biotechnology (Santa Cruz, CA).

After incubation with horseradish peroxidase-conjugated secondary antibodies (1:10,000) for 2 h at room temperature, proteins were detected by enhanced chemiluminescence (Amersham Biosciences, Buckinghamshire, UK). The bands were quantified by densitometric analysis using a Chemi-Imager 400 imaging system (Alpha Innotech, San Leandro, CA); the peak area represents the intensity of the band. Each experiment was replicated five times with different litters (n=5).

Statistical analysis.

Statistical analyses were done by Chi- square, or by two-way ANOVA, one-way ANOVA, or one-way ANOVA on ranks, as appropriate, using the SigmaStat computer program, followed by a *post hock* Holm-Sidak or Dunn's analysis. The a priori level of significance was $P < 0.05$.

RESULTS

Activation of MAPKs by HU treatment.

Since the maximal increase in AP-1 DNA-binding activity in embryos exposed to HU occurred 3 h post-treatment (Yan and Hales, 2005), we determined the activation of MAP kinases in embryos 0.5, 3, and 6 h post-treatment with low (L, 400 mg/kg) or high (H, 600 mg/kg) dose HU (Fig. 4.1). The phosphorylation of MAP kinases (p38, JNK, and ERK1/2) was examined by immunoblot analysis using phospho-specific MAP kinase antibodies. High-dose HU induced a transient but dramatic increase in the phosphorylation of p38 and JNK at 3 h (Fig. 4.1A). The phosphorylation of both p38 and JNK was significantly higher in the HU-600mg/kg treated groups than the control groups at 3 h post-treatment; by 6h, the phosphorylation of p38 and JNK was not statistically different from controls (Fig. 4.1 B and C). Unlike p38 and JNK, the phosphorylated form of ERK1/2 was not detected by immunoblot analysis, even after maximally loading the samples. When the same membrane was probed with an antibody against ERK2, two distinct bands of non-phosphorylated ERK1/2, at 44 kDa and 42 kDa, were revealed (Fig. 4.1A). Therefore, *in utero* exposure to a teratogenic dose of HU triggered the activation of two major stress-responsive MAPKs, p38 and JNK, but did not activate the ERK1/2 pathway. Our next objective was to determine how HU-induced activation of p38 and JNK contributes to its embryotoxicity.

Inhibition of p38 and JNK MAP kinases.

To elucidate the specific roles of p38 and JNK MAP kinases in mediating the response of the embryo to insult with HU, we selectively blocked their signaling pathways. SB203580, a pyridinylimidazole compound, is an ATP competitive inhibitor of the p38 MAPK pathway (Cuenda et al., 1995). L-JNKI1 (L-stereoisomer), a cell permeable peptide, is a substrate based peptide inhibitor of the JNK-MAPK pathway (Paliga et al., 2005); L-JNKI1 competitively blocks the interaction between JNK and its substrates, but does not influence JNK activation itself. Since, to the best of our knowledge, this is the first time that either MAPK inhibitor has been administered in an *in vivo* study to modify MAPK signaling in embryos, we determined the appropriate dosages needed to block these pathways. Timed pregnant mice were given SB203580 (0.5, 1.0, or 3.0 mg/kg) or L-JNKI1 (1.5 or 3 µl /10g) prior to treatment with HU at 600mg/kg. Embryos were obtained 3 h after HU exposure, when HU-600mg/kg activation of p38 and JNK had reached its peak.

SB203580 prevented the HU-600mg/kg triggered phosphorylation of p38 MAP kinase in a dose dependent manner; at 3.0 mg/kg, SB203580 reduced the phosphorylation of p38 to a level lower than that in saline controls (Fig. 4.2 A and F). Furthermore, 3.0 mg/kg SB203580 had no effect on the phosphorylation of JNK (Fig. 4.2B, second lane; 4.2H, second bar) or its downstream substrate, c-Jun (Fig. 4.2C, last lane; 4.2G, last bar). Based on these data, we decided to use SB 203580 at 3mg/kg dosage for our subsequent study.

L-JNKI1 was given to timed pregnant mice by tail vein injection immediately prior to treatment with HU (600mg/kg) to minimize metabolic

degradation of the peptide. As shown in Fig. 4.2C and 4.2G, L-JNKI1, at 1.5 µl/10g (about 5 µl per mouse) or 3.0 µl/10g (about 10 µl per mouse), successfully prevented HU-induced increased phosphorylation of c-Jun (Fig. 4.2, C and G); the control peptide, at 3.0 µl/10g, had no effect on c-Jun phosphorylation (Fig. 4.2C, lane 5; 4.2G, bar 5). As expected from its mechanism of action, L-JNLI1 (1.5 or 3.0 µl/10g) did not affect JNK phosphorylation (Fig. 4.2, D and H). Furthermore, L-JNKI1 did not block the p38 MAP kinase pathway (Fig. 4.2E; 4.2F, last bar). Since L-JNKI1 at 1.5 µl/10g efficiently blocked the JNK pathway, we chose this dose for further study.

Effects of p38 MAP kinase inhibition on HU-induced developmental toxicity.

HU at 600mg/kg elevated the rate of fetal deaths, reduced the body weights of live fetuses, and increased the rate of external and skeletal malformations; in contrast, the only effect of maternal exposure to 400 mg/kg was a reduction in live fetal weights (Figs. 4.4, 4.5). The major external malformations induced by HU exposure were hindlimb ectrodactyly, mainly observed as a completely or partially missing first digit (Tables 4.1-1 and 4.2-1).

A variety of skeletal malformations was observed in the high-dose HU-exposed fetuses (Fig. 4.3); among these, vertebral column defects (fused, partially ossified, or misaligned vertebrae) (Fig. 4.3C), hindlimb ectrodactyly and hemimelia (Fig. 4.3, C and D), and curly tail defects (Fig. 4.3C) were predominant; fused or mismatched sternebrae (Fig. 4.3E) and fused or forked ribs (Fig. 4.3, C and E) were observed at low incidences. The hindlimb defects observed were primarily missing or truncation of the first digit and tibia (Fig. 4.3,

C and D), and partial or complete absence of more than the first digit, with the sequence from anterior (first digit) to posterior.

Administration of the p38 inhibitor SB203580 alone did not influence progeny outcome (Fig. 4.4). Interestingly, rather than rescue the embryos exposed to HU-600 mg/kg, pretreatment with SB203580 dramatically increased (from 41.1% to 74.8%) the number of dead fetuses per litter (Fig. 4.4A). Dead fetuses appeared as embryo resorptions. Despite this striking elevation in fetal mortality, SB203580 inhibition of p38 activation did not influence other measures of developmental toxicity in the HU-exposed surviving fetuses from either the 400 or 600mg/kg treatment groups. Similar body weights were found among the fetuses exposed to HU with or without SB203580 pretreatment (Fig. 4.4B). The overall incidence of external or hindlimb malformations was not different between the groups treated with HU alone or SB203580 plus HU (Fig. 4.4, C and D). Furthermore, malformed fetuses bore similar types of external abnormalities, whether they had been pretreated with SB203580 or not. As illustrated in Table1-1, high frequencies of hindlimb and tail defects were observed among the fetuses treated with HU alone or HU plus SB203580; the incidences of forelimb abnormalities, open eye defects, and gastroschisis were very low in all groups. No significant differences in the rate of any individual malformations were found among the groups exposed to HU with or without SB203580 pretreatment. One fetus in the HU 400mg/kg treatment group had excencephaly (1.0%), while one the HU-600mg/kg group had spina bifida (1.6%); the incidence of these neural tube defect rates is too low to be considered significant. Similar results were

found when skeletal malformations were examined, as shown in Table 4.1-2. The inhibition of p38 activation did not alter either the spectrum or the frequency of the HU induced malformations observed (verterbral column, hindlimb, sternebrae, ribs and forelimb defects).

Effects of JNK inhibition on HU-induced developmental toxicity.

L-JNKI1 alone did not induce developmental toxicity, nor did it affect the susceptibility of embryos to HU-induced embryotoxicity, as assessed by the incidence of fetal mortality (Fig. 4.5A), the extent of growth retardation (Fig. 4.5B) or the overall incidence of external abnormalities (Fig. 4.5C). Nevertheless, L-JNKI1 pretreatment specifically enhanced the incidence of hindlimb malformations, both external and skeletal, in HU-600mg/kg -exposed fetuses (Fig. 4.5D, Tables 4.2-1 and 4.2-2).

In the HU-600mg/kg treated group, the frequency of hindlimb defects was dramatically increased by L-JNKI1, from 44.9% to 85.7%. In contrast to this observation, the incidences of other deformities in the HU-exposed fetuses, such as curly tail defects, forelimb defects, open eye, spina bifida and gastroschisis, were not affected significantly by L-JNKI1 pretreatment. Evaluation of the fetal skeletons (Table 4.2-2) revealed similar results: blocking the JNK pathway increased the incidence of hindlimb defects by more than 2-fold (31.1% versus 74.1%, $p<0.01$) in the 600mg/kg HU-exposed group. Again, the frequency of other skeletal abnormalities, including vertebral, sternebrae, rib and forelimb defects, in the HU-treated fetuses was not altered significantly by L-JNKI1 pretreatment. Interestingly, even though the incidence of hindlimb defects

increased dramatically in fetuses exposed to HU plus L-JNKI1, neither their pattern nor their severity was significantly affected. Whether L-JNKI1 was administered or not, HU-600mg/kg exposure affected mainly the pre-axial skeletal elements of hindlimbs, shown as ablation or truncation of the tibia (31.1% versus 72.2%) or first digit (28.9% versus 72.2%); truncation of the femur was observed rarely (2.2% versus 5.6%).

DISCUSSION

Maternal exposure to teratogenic doses of HU triggered a transitory activation of p38 and JNK MAPKs in the embryo; the ERK1/2 pathway was not activated. Although phosphorylated ERK1/2 are expressed in restricted regions in the developing embryo and have an important role in regulating chondrogenesis (Bobick et al., 2007), the ERK kinase pathway does not appear to play a role in the response of the embryo to HU exposure.

The use of pharmacological inhibitors to selectively block activation of either the p38 or JNK MAPK pathways did not rescue the embryos from HU-induced embryotoxicity; rather, inhibition of MAPK activation augmented the embryotoxicity of HU. Thus, HU-induced activation of p38 and JNK MAP kinases must have stimulated defense responses in the embryo that protected it from this teratogen. Interestingly, the consequences of inhibiting MAPK signaling activation were pathway selective: inhibition of p38 MAP kinase activation enhanced fetal mortality, whereas inhibition of JNK signaling doubled the incidence of hindlimb malformations. Indeed, distinct and sometimes antagonistic effects have been reported for these two stress signaling pathways previously (Wada et al., 2007).

The conceptal deaths induced by exposure to HU on GD 9 were observed as resorption sites. We predict that these embryo deaths occurred shortly after HU exposure since no identifiable tissues remained by GD 18. Murine embryo development becomes dependent on p38 MAP kinases at the 8-16 cell stage, when inhibition of p38 MAP kinases disrupts the assembly and functions of filamentous actin (Paliga et al., 2005). During limb development, bone morphogenetic proteins (BMPs) activate p38 MAP kinase in interdigital tissues

undergoing regression, upregulating some of the genes that mediate programmed cell death (Zuzarte-Luis et al., 2004). However, p38 MAP kinase has an opposite role in neuronal cells *in vitro*: inhibitors of p38 promote cell survival (Horstmann et al., 1998) and have been reported to protect hippocampal cells against ethanol cytotoxicity (Ku et al., 2007). The mechanism by which inhibition of p38 MAP kinase activation is detrimental in one system, or at one time during development, and plays a protective role elsewhere remains to be determined.

Transient activation of JNK appears to specifically modulate the ability of cells in the hindlimb forming region of the embryo to respond to stress. Previously, we demonstrated that depletion of glutatione elevated the incidence of hindlimb abnormalities induced by HU (Yan and Hales, 2006). This increase in hindlimb malformations was associated with an increase in immunoreactive 4-hydroxy-2-nonenal (HNE) protein adducts in hindlimb-forming regions. 4-HNE, a lipid peroxidation end product, increases the phosphorylation of JNK1 and c-Jun proteins in HBE1 cells and the levels of active phosphorylated forms of c-Jun in cultured neurons (Dickinson et al., 2002;Pugazhenthi et al., 2006). We hypothesize that HU-induced oxidative stress disrupts the redox homeostasis of the hindlimb forming region of the embryo, increasing 4-HNE protein adducts; either the glutathione depletion or the 4-HNE protein adducts trigger activation of the JNK pathway and increase AP-1 binding activity. Increased AP-1 binding activity will induce the transcription and translation of glutamate cysteine ligase, the rate limiting enzyme in glutathione synthesis, and restore the glutathione pool, thus limiting the extent of insult during this critical period of limb development.

Redox homeostasis is critical during limb development. The administration of N-acetylcysteine, a glutathione precursor, ameliorated both the oxidative stress and hindlimb defects induced by another model teratogen, 5-bromo-2-deoxyuridine (Sahambi and Hales, 2006). Furthermore, the species specificity of the teratogenicity of thalidomide has been attributed to a difference between rabbit (susceptible) and mouse (resistant) embryo limbs: rabbit limbs have a lower antioxidant capacity and enhanced susceptibility to glutathione depletion (Hansen et al., 2002).

The limb defects induced by HU appeared specifically as the loss of preaxial elements, usually the tibia and first digit; in a few fetuses, more than one digit was missing. Inhibition of stress-activated JNK signalling in the embryo dramatically increased the incidence of hindlimb malformations but did not affect the type of defects observed. This is unexpected as JNK-dependent apoptosis plays a critical role in sculpting limb pattern formation in the chick limb bud (Grotewold et al., 2002) and the Drosophila leg (Manjon et al., 2007). *In vitro* cell culture studies have shown that the JNK pathway inhibits chondrogenesis (Hwang et al., 2005). The role of stress-activated JNK may be distinct from that of JNK signaling during normal development. When they become available, isozyme-specific JNK inhibitors might help to dissect out the contributions JNKs 1, 2 and 3 to the stress response.

Although the downstream consequences of activation of the p38 and JNK MAPK pathways are clearly distinct, it is possible that they are regulated by a common upstream pathway. It has been proposed that MAP3Ks serve as "signal hubs" to regulate the specificity of MAPK activation (Cuevas et al., 2007). ASK1

is one such MAP3K, upstream of JNK and p38 kinases; furthermore, ASK1 is preferentially activated by stress stimuli, specifically by oxidative stress (Cuevas et al., 2007). A dynamic and regional specific expression of *ASK1* (apoptosis-signal regulating kinase1) was found recently in chick and mouse embryos (Ferrer-Vaquer et al., 2007), including the limb region. Mice deficient in ASK1 develop normally, but this may be due to gene redundancy (Tobiume et al., 2001). Although ASK1 was identified initially as a cell death inducer, evidence is emerging that moderate or transient activation promotes cell survival and differentiation (Takeda et al., 2000).

Selective MAPK signaling pathway inhibitors have potential as drugs for the treatment of human inflammatory diseases, prevention of acute ischemic damage, reduction of neurodegeneration, or inhibition of pancreatic β cell death. Interestingly, there are also natural products, such as resveratrol, tangeretin, and ligustilide, to which pregnant women may be exposed, that inhibit MAPK signaling *in vitro* (Malemud, 2007). In one study in which the impact of manipulation of MAPK activation on embryo development was evaluated, sorbitol-induced JNK activation mimicked the effects of hyperglycemia in inducing diabetic embryopathy (Yang et al., 2007).

It is clear that regulation of MAPK signaling in the conceptus exposed to a developmental toxicant is complex. We have demonstrated that inhibition of the transitory activation of MAPK signaling triggered by such an insult has adverse consequences to the conceptus: p38 MAP kinase and JNK signaling pathways stimulated defense responses that protected the embryo from damage. The therapeutic potential of MAPK pathway inhibitors is such that understanding the

impact of even short term exposure to these substances during pregnancy is a priority.

Fig. 4.1. HU induced the activation of MAP kinases. A, Western blot analysis of MAP kinases in embryos at 0.5, 3, and 6 h after treatment with HU at 400mg/kg (L) or 600mg/kg (H). Panel 1: phosphorylated p38 MAP kinase; panel 2: phosphorylated JNK; panel 3: phosphorylated ERK1/2; panel 4: total ERK1/2. B and C, Scan densitometry quantification of the phosphorylated p38 bands and phosphorylated JNK bands, respectively. Each bar (mean±S.E.M) represents five litters. *, significantly different from saline control at the same time point ($p<0.05$).

Fig. 4.1

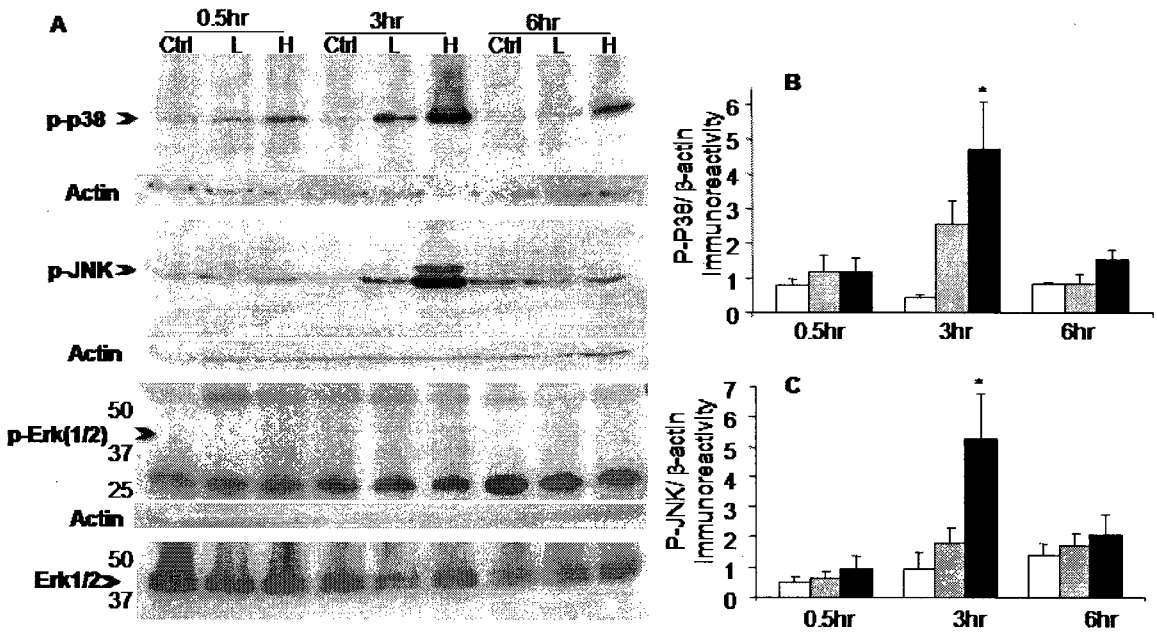
A
0.5hr
3hr
6hr
Ctrl
L
H
p-p38
Actin
p-JNK
Actin
50
p-Erk(1/2)
37
25
Actin
50
Erk1/2
37
B
P-P38/ β-actin Immunoreactivity
0.5hr
3hr
6hr
C
P-JNK/ β-actin Immunoreactivity
0.5hr
3hr
6hr

Fig. 4.2. Inhibition of p38 or JNK MAP kinases by SB203580 or L-JNKI, respectively. A, SB203580 at 0.5, 1.5, and 3 mg/kg (SB0.5, SB1.5, and SB3.0) dose-dependently reversed the phosphorylation of p38 induced by HU at 600mg/kg (HU600). B, SB203580 at 3mg/kg did not affect the phosphorylation of JNK induced by HU600. C, L-JNKI1, at 1.5 or 3µl/10g (JNKI1.5, JNKI3.0), blocked the phosphorylation of the JNK downstream substrate, c-Jun. The L-TAT control peptide at 3µl/10g (pep 3.0) and the SB203580 at 3mg/kg did not affect the phosphorylation of c-Jun. D, L-JNKI1, at 1.5 or 3µl/10g, had no effect on the phosphorylation of JNK. E, L-JNKI1, at 1.5 µl/10g, did not influence the phosphorylation of p38 induced by HU600. F, G, and H, Scan densitometry quantification of the phosphorylated p38, c-Jun, and JNK. Values were normalized against to the corresponding vehicle control and expressed as fold changes. n=2-3.

Fig. 4.2

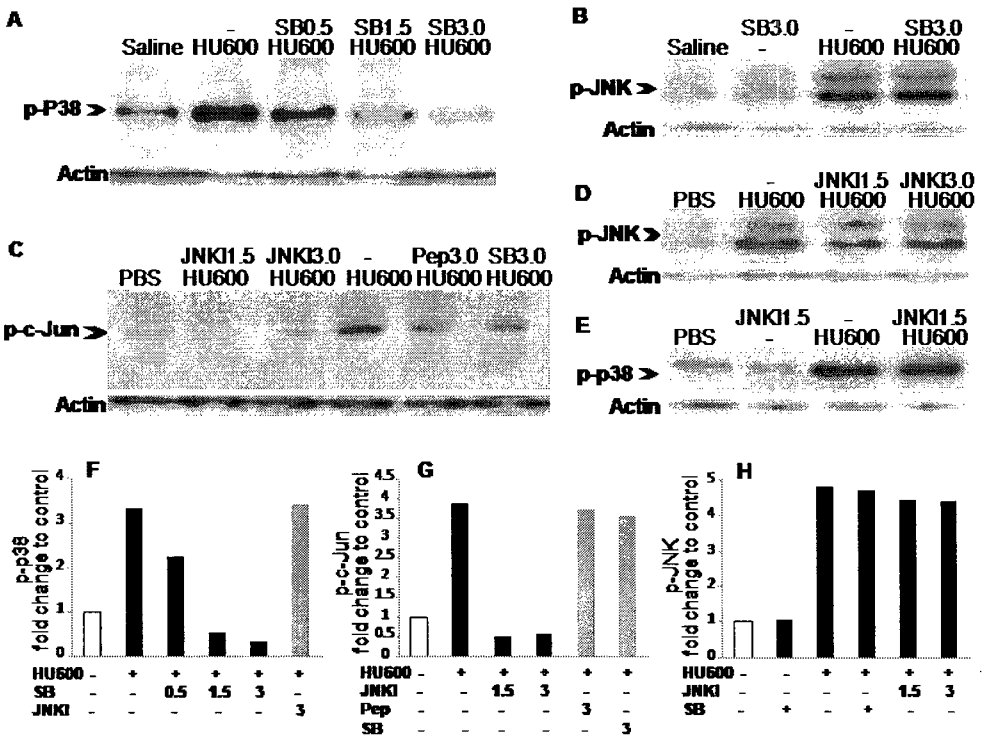
A
Saline
HU600
SB0.5 HU600
SB1.5 HU600
SB3.0 HU600
p-P38
Actin
B
Saline
SB3.0
HU600
SB3.0 HU600
p-JNK
Actin
C
PBS
JNKI1.5 HU600
JNKI3.0 HU600
HU600
Pep3.0 HU600
SB3.0 HU600
p-c-Jun
Actin
D
PBS
HU600
JNKI1.5 HU600
JNKI3.0 HU600
p-JNK
Actin
E
PBS
JNKI1.5
HU600
JNKI1.5 HU600
p-p38
Actin
F
p-p38 fold change to control
HU600
SB
JNKI
G
p-c-Jun fold change to control
HU600
JNKI
Pep
SB
H
p-JNK fold change to control
HU600
JNKI
SB

Fig. 4.3. Double stained skeletons of the fetuses exposed to saline (A, B, F) or HU-600mg/kg (C-E). Ossified portions of the fetal skeletons are stained red and cartilage portions are blue. (A) Normal vertebrae, hindlimbs, and tail of a control fetus; (F) a higher magnification view of the hindlimb of this control fetus. (B) Normal sternebrae and rib cage of a control fetus. (C) HU-600mg/kg-treated fetus; arrows indicate the deformed vertebral column (DV), short truncated tibia (tibia hypoplasia, TH), curly tail (CT), and fused ribs (FB). (D) A higher magnification image of the hindlimb of a HU-600mg/kg-exposed fetus; arrows indicate the missing tibia (tibia aplasia, TA) and missing first digit (aplasia of the first digit, AFD). (E) The fused and mismatched sternebrae and forked ribs of the HU-600mg/kg-treated fetus.

Fig. 4.3

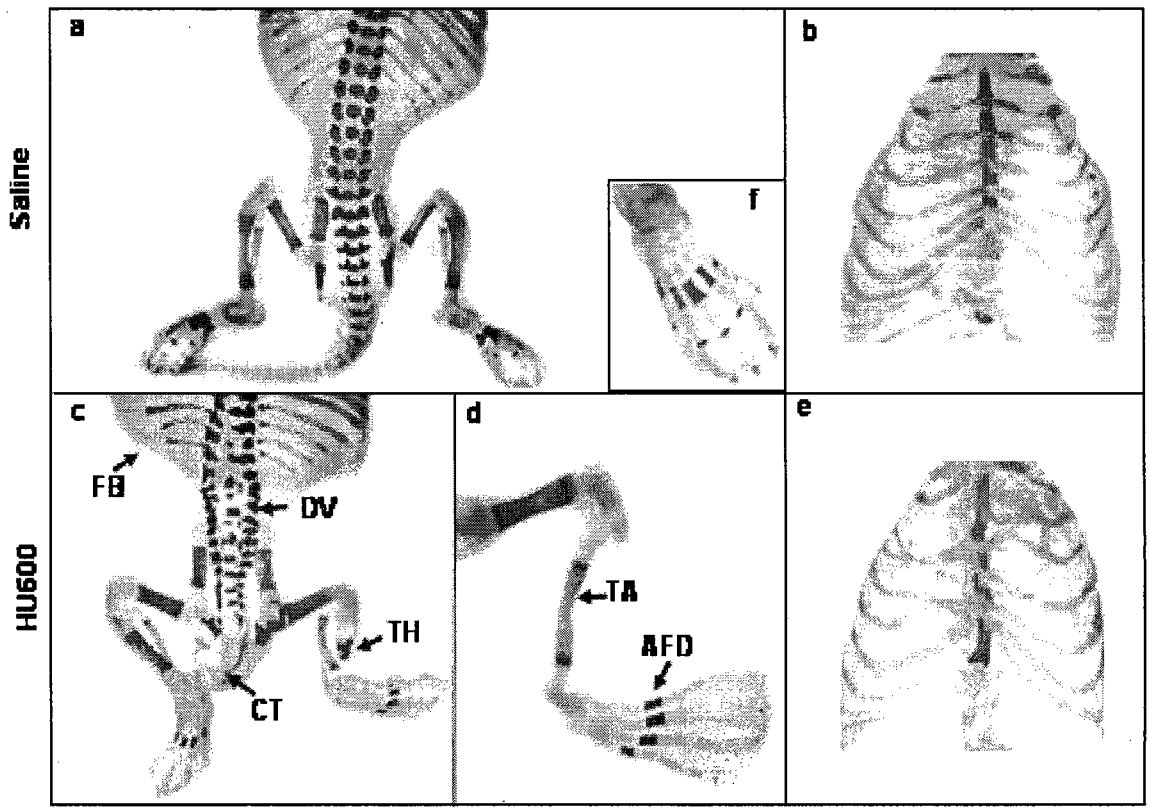

Fig.4.4. Effects of p38 MAP kinase inhibition on HU-induced developmental toxicity. A, Fetal death rates (the percentage of total implantations that were dead). B, Live fetal weights. C, External malformation rates of live fetuses. Data represent means per litter ± S.E.M., with 7 to 11 litters per treatment group. *, significantly different from vehicle control (*, $p < 0.05$; **, $p < 0.01$); †, significant difference between the HU treated group with or without SB203580 (†, $p < 0.05$); statistical analysis was done by two-way, one-way ANOVA, or one-way ANOVA on ranks, as appropriate. D, Hindlimb malformation rates, the data are expressed as the percentage of hindlimb-deformed fetuses of the total live fetuses observed. Fetuses from 7 to 11 litters per treatment group were evaluated. *, significantly different from vehicle control (*, $p < 0.5$; **, $p < 0.01$; Chi-square). SB, SB203580; (-), saline; (+), SB203580 at 3 mg/kg; L, HU400mg/kg; H, HU600mg/kg.

Fig. 4.4

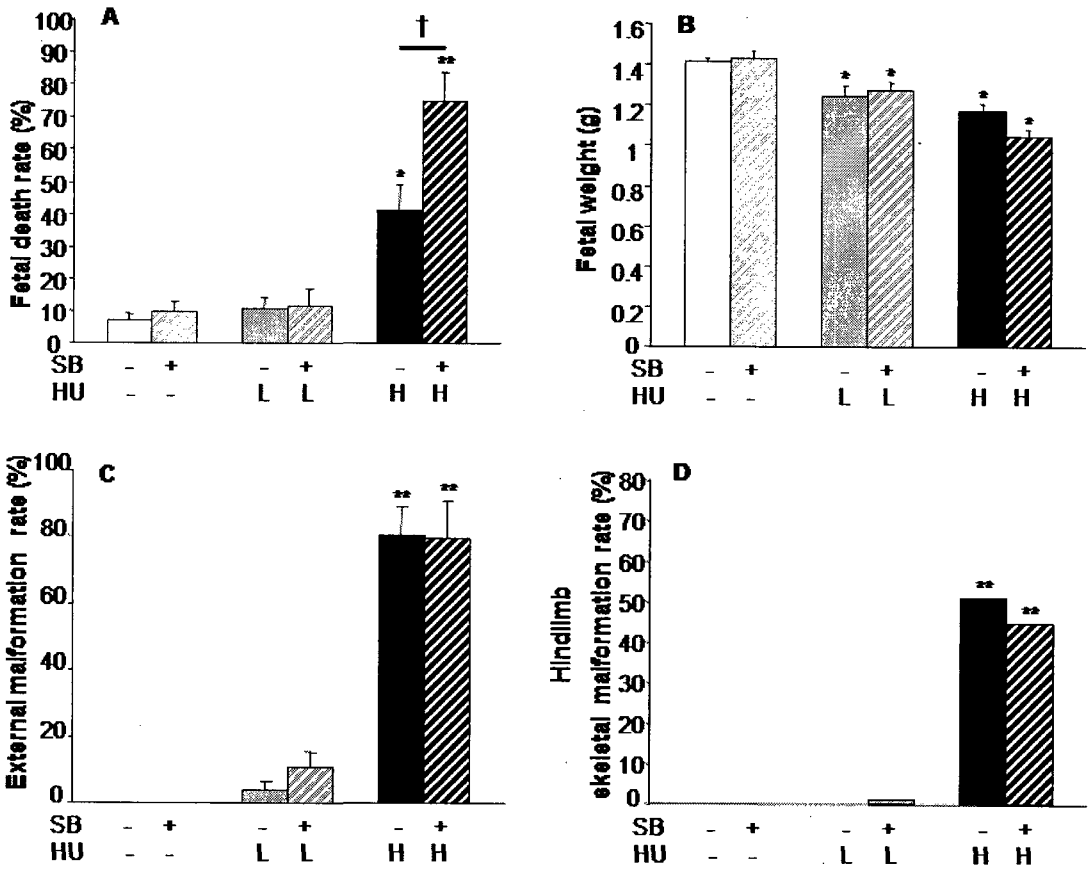
A
Fetal death rate (%)
100
90
80
70
60
50
40
30
20
10
0
†
*
**
SB - + - + - +
HU - - L L H H
B
Fetal weight (g)
1.6
1.4
1.2
1
0.8
0.6
0.4
0.2
0
*
SB - + - + - +
HU - - L L H H
C
External malformation rate (%)
100
80
60
40
20
0
**
SB - + - + - +
HU - - L L H H
D
Hindlimb skeletal malformation rate (%)
80
70
60
50
40
30
20
10
0
**
SB - + - + - +
HU - - L L H H

Fig. 4.5. Effects of JNK inhibition on HU-induced developmental toxicity. (A) Fetal death rates (the percentage of total implantations that were dead). (B) Live fetal weights. (C) External malformation rates of live fetuses. Data represent means per litter ± S.E.M., with 7 to 10 litters per treatment group. Asterisks indicate a significant difference from vehicle control (*, $p < 0.05$, **, $p < 0.01$; one-way ANOVA or one-way ANOVA on ranks, as appropriate). (D) Hindlimb malformation rates; the data are expressed as the percentage of hindlimb deformed fetuses of the total live fetuses observed. Fetuses from 7 to 10 litters per treatment group were evaluated. *, significantly different from vehicle control (**, $p < 0.01$; Chi- square); †, a significant difference between the HU treated group with or without L-JNKI1 (†, $p < 0.05$). (-), PBS; (+), L-JNKI1 at 1.5 µl/10g mg/kg; L, HU400mg/kg; H, HU600mg/kg.

Fig. 4.5

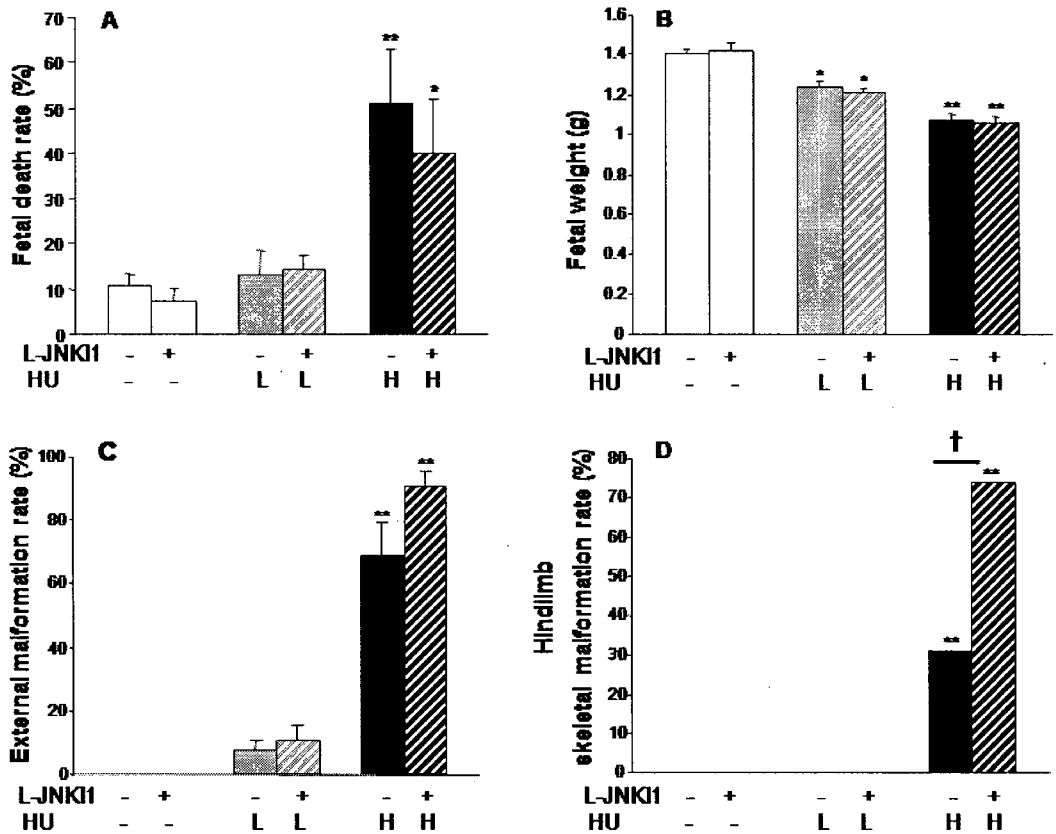
A
Fetal death rate (%)
70
60
50
40
30
20
10
0
**
*
L-JNKI1 - + - + - +
HU - - L L H H
B
Fetal weight (g)
1.6
1.4
1.2
1
0.8
0.6
0.4
0.2
0
*
*
**
**
L-JNKI1 - + - + - +
HU - - L L H H
C
External malformation rate (%)
100
80
60
40
20
0
**
**
L-JNKI1 - + - + - +
HU - - L L H H
D
Hindlimb skeletal malformation rate (%)
80
70
60
50
40
30
20
10
0
†
**
**
L-JNKI1 - + - + - +
HU - - L L H H

Table 4.1-1. Effects of inhibition of p38 activation on HU induced live fetal external malformations.

	Treatment (mg/kg)					
	Saline	SB	HU400	SB-HU400	HU600	SB-HU600
No. of litters examined	8	7	9	8	9	11
No. of fetuses examined	97	77	96	90	64	52
Abnormal hindlimb: (Ectrodactyly, hemimelia)					29 (45.3%)	21 (40.4%)
Curly/hypoplastic tail			3 (3.1%)	3 (3.3%)	26 (40.6%)	15 (28.8%)
Abnormal forelimb: (Ectrodactyly, hemimelia)					2 (3.1%)	7 (13.5%)
Open eye				1 (1.1%)	4 (6.2%)	1 (1.9%)
Spinal bifida					1 (1.6)	
Gastroschisis				1 (1.1%)	2 (3.1%)	3 (5.8%)
Excencephaly			1 (1.0%)			

• percentages are represented as the malformed fetuses out of the fetuses examined; a single fetus may be represented more than once in listing individual defects.

Table 4.1-2. Effects of inhibition of p38 activation on HU induced live fetal skeletal malformations.

	Treatment (mg/kg)					
	Saline	SB	HU400	SB-HU400	HU600	SB-HU600
No. of litters examined	8	7	8	8	9	9
No. of fetuses examined	38	62	82	89	61	47
Abnormal vertebrae [a]			4 (4.9%)	6 (6.7%)	54 (88.5%)	42 (89.4%)
Abnormal hindlimb:				1 (1.1%)	31 (50.8%)	21 (44.7%)
Tibia aplasia / hypoplasia				1 (1.1%)	29 (47.5%)	20 (42.6%)
Digits aplasia / hypoplasia					30 (49.2%)	19 (40.4%)
Polydactyly					1 (1.6%)	
Abnormal Sternebrae [b]	1 (2.6%)		8 (9.7%)	8 (8.9%)	8 (13.1%)	8 (17.0%)
Forked/fused ribs				1 (1.1%)	9 (14.8%)	8 (17.0%)
Abnormal forelimb [c]					2 (3.3%)	3 (6.4%)

• percentages are represented as the malformed fetuses out of the fetuses examined; a single fetus may be represented more than once in listing individual defects.
[a]: vertebral column malformations include fused, incomplete ossification, misaligned or misshapen of the vertebral centra or vertebral arch.
[b]: sternabral abnormalities include misaligned, fused or incomplete ossification site.
[c]: Forelimb malformations include ectrodactyly or hemimelia.

Table 4.2-1. Effects of inhibition of JNK activation on HU induced live fetal external malformations.

	Treatment (mg/kg)					
	Saline	L-JNKI1	HU400	L-JNKI1-HU400	HU600	L-JNKI1-HU600
No. of litters examined	9	7	10	9	8	7
No. of fetuses examined	93	87	112	113	49	56
Abnormal hindlimb: (Ectrodactyly, hemimelia)					22 (44.9%)	48 (85.7%) **
Curly/hypoplastic tail			4 (3.6%)	7 (6.2%)	10 (20.4%)	18 (32.1%)
Abnormal forelimb: (Ectrodactyly, hemimelia)					2 (4.1%)	
Open eye			4 (3.6%)	5 (4.4%)		7 (12.5%)
Spinal bifida						4 (6.6%)
Gastroschisis			1 (0.9%)			4 (6.6%)

- percentages are represented as the malformed fetuses out of the fetuses examined; a single fetus may be represented more than once in listing individual defects.
- ** Significant difference at $p<0.001$ level between the hydroxyurea treated group with or without L-JNKI1 pretreatment

Table 4.2-2. Effects of inhibition of JNK activation on HU induced live fetal skeletal malformations.

	Treatment (mg/kg)					
	Saline	L-JNKI1	HU400	L-JNKI1-HU400	HU600	L-JNKI1-HU600
No. of litters examined	9	7	10	9	8	7
No. of fetuses examined	51	56	111	97	45	54
Abnormal vertebrae [a]			4 (3.6%)	18 (18.6%)	43 (95.6%)	54 (100.0%)
Abnormal hindlimb:					14 (31.1%)	40 (74.1%) **
Tibia aplasia / hypoplasia					14 (31.1%)	39 (72.2%) **
Digits aplasia / hypoplasia					13 (28.9%)	39 (72.2%) **
Femur hypoplasia					1 (2.2%)	3 (5.6%)
Abnormal Sternebrae [b]			8 (7.2%)	11 (11.3%)	7 (15.6%)	8 (14.8%)
Forked/fused ribs				2 (2.1%)	5 (11.1%)	2 (3.7%)
Abnormal forelimb [c]					2 (4.4%)	

- percentages are represented as the malformed fetuses out of the fetuses examined; a single fetus may be represented more than once in listing individual defects.

** Significant difference at $p<0.001$ level between the hydroxyurea treated group with or without L-JNKI-1 pretreatment

[a]: vertebral column malformations include fused, incomplete ossification, misaligned or misshapen of the vertebral centra or vertebral arch.

[b]: sternabral abnormalities include misaligned, fused or incomplete ossification site.

[c]: Forelimb malformations include ectrodactyly or hemimelia.

CONNECTING TEXT

In the previous chapters, we found that the caudal tissues of the embryo are specifically susceptible to HU-induced malformations; oxidative stress may disturb the development of the hindlimb and lumbarsacral vertebral column. Interestingly, inhibition of JNK pathways specifically enhanced the hindlimb defects. To further elucidate the mechanism of oxidative stress in disrupting the formation of hindlimb and vertebral column, in the following chapter, we dissected the embryo into head, body, and caudal part (malformation sensitive region); the distribution of 4-HNE protein adducts in different part of the embryo was evaluated by Western blot analysis and the proteins conjugated to 4-HNE in the caudal region of the embryo were identified. Furthermore, the expression of genes involved in defense against oxidative stress, and limb and vertebral column development was evaluated.

CHAPTER FIVE

Hydroxyurea, A Model Teratogen, Alters Oxidative Stress Responsive Signaling Pathways and Induces 4-Hydroxynonenal (4-HNE) Protein Adducts In The Tail Region of Mouse Embryos.

Jin Yan and Barbara F. Hales

ABSTRACT

In utero exposure to hydroxyurea, a model teratogen, induces hindlimb, lumbosacral vertebral, and tail defects. This disruption in the pattern formation of caudal structures is enhanced by inhibition of glutathione synthesis, suggesting that hydroxyurea-induces oxidative stress in this region. To elucidate the basis for the sensitivity of this region to insult with hydroxyurea, we determined the effects of treating timed pregnant CD1 mice on GD 9 on the expression of genes that mediate the response to oxidative stress and play a role in establishing caudal structures. The expression of Dickkopf-1 (Dkk1), a secreted Wnt/beta-catenin signaling inhibitor, was higher in the tail than in the head or body; exposure to hydroxyurea decreased the expression of both Dkk1 and fibroblast growth factor, Fgf8 in the tail. Reactive oxygen species (ROS) react with polyunsaturated fatty lipids to generate 4-hydroxynonenal (4-HNE), an α,β-unsaturated small aldehyde. The formation of 4-HNE protein adducts was elevated in the caudal region of control embryos; hydroxyurea-exposure further elevated 4-HNE-protein adduct formation in this area. 4-HNE-protein adducts in the tail regions of control and hydroxyurea-exposed embryos indicate the presence of excess ROS. Proteins modified by 4-HNE in the tail region were identified by 2D gel electrophoresis and mass spectrometric analysis. Interestingly, three of these proteins, glyceraldehyde-3-phosphate dehydrogenase (GAPDH), glutamate oxaloacetate transaminase 2 (GOT2), and aldolase 1, A isoform (ALDOA1), are involved in energy metabolism. Strikingly, hydroxyurea treatment decreased the amount of 4-HNE-conjugated GAPDH and

altered its electrophoretic mobility, indicating a conformational change. We propose that GAPDH represents a sensitive target for teratogen-induced oxidative stress during organogenesis.

INTRODUCTION

A number of diverse teratogens induce oxidative stress, yet there is little information with respect to how this oxidative stress disrupts embryo development (Hansen, 2006). Hydroxyurea (HU) has been studied as a model teratogen to investigate the role of oxidative stress in chemical teratogenesis (Yan and Hales, 2005;Yan and Hales, 2006). *In utero* exposure of CD1 murine embryos to HU during organogenesis induces malformations primarily in caudal tissues, resulting in a high incidence of hindlimb, vertebral column and curly tail defects (Yan and Hales 2005;Yan and Hales 2006). The hindlimb defects observed were mainly missing or truncated distal pre-axial skeletal elements, including the tibia and first digit; the vertebral column defects were most severe at the lumbarsacral level and included partial ossification, fusion, and misalignment of vertebrae. Inhibition of the synthesis of glutathione with buthionine sulfoximine increased the incidence of both hindlimb and vertebral defects in HU-exposed fetuses (Yan and Hales 2006). Thus, HU-induced oxidative stress disrupts the growth and patterning of caudal structures. The basis for the enhanced sensitivity of this region to insult and the molecular pathways that are involved in mediating this response remain to be identified.

Candidate pathways that are important in limb development include Dickkopf-1 (Dkk1), a secreted Wnt/beta-catenin signaling inhibitor, and the fibroblast growth factors Fgf8 or Fgf10. During organogenesis, Dkk1 expression is observed in the ventral diencephalon, branchial arch, presomitic mesoderm, heart, limb buds, and tail bud (Grotewold et al., 1999). Mice deficient in Dkk1

have severe truncation of the head structures anterior to the midbrain, in addition to extra pre- or postaxial digits and digit fusion (Mukhopadhyay et al., 2001). The expression of Dkk1 during limb development overlaps with sites of programmed cell death (PCD) in the anterior and posterior necrotic zones (ANZ and PNZ) and the apical ectodermal ridge (AER); Dkk1 is excluded from regions of chondrogenesis. Ectopic expression of Dkk1 in limb regions results in truncation of the distal part of the limb skeleton, coupled with extensive apoptosis. It has been suggested that the induction of c-Jun-Dkk1 by oxidative stress is responsible for thalidomide induced limb reductions (Knobloch et al., 2007).

Fibroblast growth factors, Fgf8 and Fgf10, are also crucial for limb growth and patterning. Fgf8 is expressed in the limb AER (Mahmood et al., 1995), whereas Fgf10 is expressed in the mesenchyme underneath the AER (Ohuchi et al., 1997). Fgf10 induces the expression of Fgf8 in the AER, which in turn maintains the expression of Fgf10. In contrast to Dkk1, Fgf8 and Fgf10 function mainly as "proliferation and differentiation factors", regulating limb initiation, outgrowth, and chondrogenesis (Capdevila and Izpisua Belmonte, 2001). Mice lacking Fgf10 show complete truncation of both fore- and hindlimbs (Sekine et al., 1999). A conditional knockout of Fgf8 in limbs results in hypoplasia of distal pre-axial skeletal elements (Lewandoski et al., 2000;Moon and Capecchi, 2000). Interestingly, Wnt signaling is upstream of the Fgfs and involved in the positive feedback loop between Fgf8 and Fgf10 (Martin, 2001). Lack of Dkk1 activity in the AER causes a pronounced expansion of the Fgf8 domain (Mukhopadhyay et al., 2001). Reduction of Fgf8 may be related to the digit-loss induced by cadmium chloride, another teratogen that triggers oxidative stress (Elsaid et al., 2007). In

addition to regulating limb development, Fgf8 mRNA secreted from the tail bud forms a gradient in the presomite regions that is critical to somite segmentation and posterior elongation of the embryo (Dubrulle and Pourquie, 2004). Disruption of somitogenesis disturbs vertebral column development (Shifley and Cole, 2007). We hypothesize that exposure to HU may disturb the expression of Dkk1, Fgf8 or Fgf10 in the organogenesis stage embryo.

Inhibition of glutathione synthesis enhances the teratogenicity of HU and increases the presence of a product of lipid peroxidation, 4-hydroxy-2-nonenal (4-HNE) in embryos (Yan and Hales, 2006). 4-HNE, an α,β-unsaturated small aldehyde, is produced when reactive oxygen species (ROS) react with n-6 polyunsaturated fatty lipids in cell membranes. 4-HNE, a relatively stable and highly diffusible electrophile, forms adducts with cellular nucleophiles (Esterbauer et al., 1991); in particular, 4-HNE undergoes Michael addition reactions with cysteine, lysine, and histidine residues, as well as Schiff-based addition with lysine residues on proteins (Uchida, 2003). Conjugation with 4-HNE may modify protein folding and function, cause cross-links, or trigger protein degradation (Friguet et al., 1994;Carbone et al., 2004a;Carbone et al., 2004b). The proteins that are conjugated to 4-HNE belong to diverse functional groups, including energy metabolism (Humphries and Szweda, 1998;Musatov et al., 2002), chaperone function (Kapphahn et al., 2006), cytoskeletal components (Aldini et al., 2005), protein kinases (Sampey et al., 2007;Parola et al., 1998), and receptors (Vindis et al., 2007). It has been suggested that 4-HNE mediates signals critical to the regulation of cell proliferation, differentiation and apoptosis under stress (Uchida et al., 1999;Marinari et al., 2003;Kutuk and Basaga, 2007).

To date, the role of 4-HNE in oxidative stress induced teratogenicity has not been investigated. The goal of the current study is to determine if HU exposure generates region specific 4-HNE protein adducts in the embryo and to identify the proteins targeted.

MATERIALS AND METHODS

Animals and treatments.

Timed-pregnant CD1 mice (20-25g) were purchased from Charles River Canada Ltd. (St. Constant, QC, Canada) and housed in the McIntyre Animal Resource Centre (McGill University, Montreal, Canada). All animal protocols were conducted in accordance with the guidelines outlined in the Guide to the Care and Use of Experimental Animals, prepared by the Canadian Council on Animal Care. Female mice were mated between 8:00 am and 10:00 am on gestational day 0 (GD 0). On GD 9, vehicle (saline) or HU (400 or 600mg/kg) were given to the female mice by intraperitoneal injection at 9:00 am. Dams were euthanized 3 h after treatment with HU. The embryos were dissected out in Hanks' balanced salt solution (Gibco Laboratories, ON, Canada), and cut into three parts (head, body and tail) along the cranial-caudal axis as indicated in Figure 1A. The head, body, and tail parts from two embryos per litter were put in RNAlater RNA Stabilization Reagent (Qiagen, Mississauga, ON, Canada), flash frozen with liquid nitrogen, and stored at –80°C for subsequent assessment of gene expression by real-time PCR. Protein extracts were obtained immediately from the parts of the remaining embryos for each litter for subsequent assessment of 4-HNE-protein adducts by western blot analysis. For two-dimensional gel electrophoresis, the tail parts from four litters of embryos exposed to vehicle or HU600 were pooled and subjected to protein extraction immediately.

Real time qRT-PCR.

Total RNA was extracted with the RNeasy Micro Kit (Qiagen, Mississauga, ON, Canada) following the manufacturer's guidelines. The extracted total RNAs were quantified by spectrophotometric ultraviolet absorbance at 260 nm. Omniscript reverse transcriptase kits (QIAGEN) were used following the manufacturer's guidelines to synthesize cDNAs from the RNA samples (250ng/sample). One microliter of the 25-times diluted reverse transcription final reaction was used as template cDNA, and Quantitect two-Step SYBR® Green RT-PCR (Qiagen) was completed using the Roche LightCycler® (Roche Diagnostics, Laval, Canada), according to the manufacturer's instructions. PCR thermal cycling parameters were: 94°C for 15 sec, 55°C for 30 sec and 72°C for 20 sec (for 40-55 cycles, depending on the primers). The cDNA from whole embryos was diluted to 1, 25, 50 and 100 ng/µl for standard curves for quantification. Transcripts for: *Dkk1* (Dickkopf-1), *fgf8* or *fgf10* (fibroblast growth factor 8 or 10), *Gclc* (glutamate-cyste*ine ligase catalytic subunit), Gclm* (glutamate-cysteine ligase modifier subunit), and *Gsta4* (glutathione S-transferase, alpha 4) were analyzed; gene expression was normalized against 18S rRNA. The forward (F) and reverse (R) primer sequences used for RT-PCR were as follows: *Dkk1*: F (5'-ctgaccacagccattttcct-3') and R (5'-cggagccttcttgtccttt-3'); *fgf10*: F (5'-ttcctcctcgtccttctcct-3') and R (5'-ctgaccttgccgttcttctc-3'); *fgf8*: F (5'-ctcattgtggagaccgatactt-3') and R (5'-atacgcagtccttgcctttg-3'); *Gclc*: F (5'-catctaccacgcagtcaagg-3') and R (5'-tcgcctccattcagtaacaa-3'); *Gclm*: F (5'-cacaatgacccgaaagaactg-3') and R (5'-gacttgatgattcccctgct-3'); *Gsta4*: F (5'-tggagtggagtttgaggaaga-3') and R (5'-

cctggtctgtgtcagcatca-3'); 18S rRNA: F (5'-aaacggctaccacatccaag-3') and R (5'-cctccaatggatcctcgtta-3').

Protein extraction.

Samples were placed in 10-25 µl RIPA buffer (150 mM NaCl; 1% NP-40; 0.5% deoxycholate; 0.1 % SDS; 50 mM Tris, pH 7.5) containing 10 µl/ml protease inhibitor cocktail and 20 µl/ml phosphates inhibitor (Active Motif, Carlsbad, CA). The samples were homogenized with an ultrasonicator (Sonics & Materials Inc., Newtown, CT), and centrifuged at 10,000 g for 15 min at 4°C. The supernatants were collected and stored at -20°C.

Western blot analysis of 4-HNE-protein adducts.

Protein concentrations were determined using the Bio-Rad Bradford protein assay (Bio-Rad Laboratories, ON, Canada). The amount of 7.5 µg of protein from each sample was separated by 10% sodium dodecyl sulfate-polyacrylamide gel electrophoresis (15 wells) and then transferred onto equilibrated polyvinylidene difluoride membranes (Amersham Biosciences, Buckinghamshire, UK) by electroblotting. Membranes were blocked with 5% skim milk for 1 h at room temperature, and then probed by primary antibody against 4-HNE-protein adducts (1:500) or actin (1:5000) overnight at 4 °C. After incubation with horseradish peroxidase-conjugated secondary antibody (1:10,000) for 2 h at room temperature, proteins were detected by enhanced chemiluminescence (Amersham Biosciences, Buckinghamshire, UK). The intensities of the protein bands were scanned and quantified with a Chemi-Imager 400 imaging system

(Alpha Innotech, San Leandro, CA); the peak height represents the intensity of the band.

Mouse monoclonal antibody against 4-HNE-modifided proteins was purchased from OXIS International Inc., CA and reconstituted with 1 ml of distilled water to final concentration as 100 µg/ml antibody. Goat polyclonal anti-actin (I-19) was purchased from Santa Cruz Biotechnology, CA.

Two-dimensional (2D) gel electrophoresis and western blot analysis of 4-HNE-protein adducts.

Protein determination, separation and mass spectrometry were conducted by the Genome Quebec Innovation Centre (Montreal, QC, Canada). Protein concentration was determined with use of 2D Quant Kit (Amersham, Baie D'Urfe, QC, Canada). Fifty micrograms of protein in 155 µl of Destreak rehydration buffer supplemented with 1% IPG Buffer (3-10NL, Amersham) were placed in each of four chambers of ZOOM IPGRunner Cassette (Invitrogen, Burlington, ON, Canada). ZOOM Dry Strips (7 cm, pH range 3-10NL, Invitrogen) were placed in the chambers that were then sealed and left for rehydration for 16 hrs. The cassette was inserted in ZOOM IPGRunner (Invitrogen) and voltage gradient (200V-2000V) was applied as recommended by the manufacturer. A total of 2000 vhrs was applied. After isoelectrophocusing (IEF) was completed, strips were equilibrated with SDS using NuPAGE LDS Sample Buffer (1X, Invitrogen), reduced with 2% dithiothreitol (DTT, Amersham), and alkylated with iodacetamide (IAA, Sigma). Both steps (DTT and IAA) were done at room temperature for 15 min. Electrophoresis in the second dimension (SDS-PAGE) was done on gradient

4-12% BisTris precast minigels (Invitrogen) immobilized with 1% agarose in XCell SureLock (Invitrogen). The upper and lower chambers were filled with MOPS Running Buffer (Invitrogen); molecular weight standards (Broad Range Protein Molecular Weight Markers, Amersham, 0.9 µg/gel) were placed in the marker wells and 200V were applied for 50 min. After completion of the run, one of every pair of gels was fixed overnight in 50% methanol/10% acetic acid fixation solution and stained with silver nitrate by modified Shevchenko's protocol (Yan et al., 2000). Gel images were acquired on an ImageScanner (Amersham) in TIF format.

Immediately after SDS-PAGE, the second gel was covered with a nitrocellulose membrane, placed between two sheets of Whatman paper and two sponges, and inserted into an XCell II Blot Module (Invitrogen). The module was then placed in XCell SureLock. Transfer Buffer (Invitrogen) supplemented with 10% methanol was added in the module, and protein transfer was carried out at 30V for 1 hr. The quality of the protein transfer was controlled by staining with Ponceau S. The membranes were blocked with 5% skim milk for 1 h at room temperature after washing off the Ponceau S stain, and then probed with primary antibodies against 4-HNE-modifided proteins (1:500, OXIS International, Inc.) overnight at 4 °C. After incubation with horseradish peroxidase-conjugated secondary antibodies (1:10,000) for 2 h at room temperature, proteins were detected by enhanced chemiluminescence (Amersham Biosciences, Buckinghamshire, UK).

Mass spectrometry.

Protein spots on the silver-stained 2D gels that correspond to those detected by immunoblotting of 4-HNE-modified proteins were excised from the gel and subjected to trypsin digestion. Sample injection and HPLC separation were done using an Agilent 1100 series system (Agilent Technologies, Mississauga, ON, Canada). Twenty microlitters of digest solution was loaded on to a Zorbax 300SB-C18 5X0.3mm trapping column and washed for 5 min at 15 µl/min with 3% Acetonitrile (ACN): 0.1% formic acid (FA). Nano-HPLC peptide separation was done using a New Objective (Woburn, MA) Biobasic C18 10X0.075mm picofrit analytical column. The gradient was 10% ACN: 0.1% FA to 95% ACN: 0.1% FA in 15 min at 200 nl / min.

Mass spectrometry was done with a QTRAP 4000 from Sciex-Applied Biosystems (Concord, ON). Information-dependent ms/ms analysis was done on the 3 most intense ions selected from each full scan MS with dynamic exclusion for 90 sec. The survey scan used was an enhanced MS scan from 3500 to 1600 m/z at 4000 amu/sec using Dynamic Fill time. MSMS data was acquired for three scans from 70 to 1700 m/z using a fixed 25 ms trap fill time and with Q0 trapping activated. Peaklists were generated with Mascot Distiller 1.1 from Matrixscience (Boston, MA). Searches of sequences from NCBInr database using a rodent taxonomy filter (157986 sequences) were done with Mascot 1.9 using Trypsin as digestion enzyme, and carboxyamidomethylation of cysteines as fixed modification, methionine oxidation as variable modification and 1.5 Da precursor and 0.8 fragment search tolerances.

2D Western blot analysis of GAPDH.

Membranes obtained from 2D Western blot of 4-HNE-modified proteins were stripped once with stripping buffer (2% SDS; 62.5mM Tris, pH6.7; 100mM β-mercaptoethanol). After washing 3 times with TBST (0.1% Tween-20) for 10 min each, membranes were blocked with 5% skim milk for 1 h at room temperature, probed with a primary antibody against GAPDH (1:2000, rabbit polyclonal IgG, Abcam Inc., MA) at 4°C overnight, and incubated with horseradish peroxidase-conjugated secondary antibody (1:10000) for 2 h at room temperature. Proteins were detected by enhanced chemiluminescence (Amersham Biosciences, Buckinghamshire, UK). The intensities of the protein spots were quantified with a Chemi-Imager 400 imaging system (Alpha Innotech, San Leandro, CA).

Statistical analysis.

Statistical analyses were done by two-way ANOVA or one-way ANOVA on ranks, as appropriate, using the SigmaStat computer program, followed by a *post- hock* Holm-Sidak or Dunn's analysis. The a priori level of significance was $P < 0.05$.

RESULTS

HU-induced changes in gene expression are region specific.

Our first goal was to determine the region specificity of the effects of HU exposure on the expression of candidate genes in embryos. As indicated in Fig. 5.1A, each embryo was cut at two sites, the caudal end of the first branchial arch (the head) and the cranial end of the third somite from the caudal end of the embryo (about the 20th somite) (separating the body and the tail). The head part will form mainly the cranial-facial structures; the body part will form forelimbs, thoracic and most abdominal organs, the rib cage, and the thoracic and upper cervical vertebrae; the tail part will form hindlimbs, lower cervical and lumbarsacral vertebrae, and the tail. Hindlimbs outgrow at the level of the 23rd-28th somite; embryos were sectioned near the 20^{th} somite to ensure that hindlimb outgrowth tissues were found in the tail sections. The cranial and body sections of embryos are considered to be relatively less sensitive to HU-teratogenesis after treatment on GD 9, whereas the tail or caudal region is highly sensitive (Yan and Hales, 2006).

The expression of three genes crucial for limb growth and patterning, Dkk1, Fgf8 and Fgf10, was analyzed by real-time qRT-PCR (Fig. 5.1B). The expression of Dkk1 was higher in the tail than in the head or body of control embryos. Interestingly, treatment with HU-600mg/kg significantly reduced Dkk1 expression in both the head and tail sections (Fig. 5.1B). Fgf8 expression was lower in the body of control embryos than in the tail; this pattern of gene expression appeared to be reversed for Fgf10, with lower expression in the head

and tail than the body (Fig. 5.1, C and D). Exposure to HU-600mg/kg significantly decreased the expression of Fgf8 in all three embryo sections. In contrast, Fgf10 expression was significantly reduced only in the body. Thus, both Dkk1 and Fgf8 were highly expressed in the tail region; furthermore, HU-exposure downregulated the expression of both of these genes in this malformation-sensitive area. To explore the basis for the sensitivity of this tissue to insult, we determined the regional distribution of 4-HNE proteins adducts as an indicator of oxidative stress.

The distribution of 4-HNE-protein adducts in mouse embryos.

Proteins extracted from the head, body and tail of control and HU-exposed embryos were analyzed by Western blot analysis to determine the relative distribution of 4-HNE-protein adducts (Fig. 5.1A). Interestingly, a major 4-HNE immunoreactive band was observed in the 65 kDa molecular weight range. A remarkably higher content of these 65 kDa 4-HNE-protein adducts was found in the tail than in the body and head parts of the embryos treated with HU (400 or 600 mg/kg) (Fig. 5.2A). Multiple low-intensive bands of 4-HNE-protein adducts were detected below 50 kDa, but none of these adducts showed obvious different allocations in three parts of the embryo after treatment with either saline or HU (Fig. 5.2A). Quantification of the 4-HNE-protein adducts revealed that, indeed, the concentration of adducts was significantly elevated in the tails in all treatment groups (Fig. 5.2B). HU exposure further increased 4-HNE protein adducts in these tail regions.

Since 4-HNE can be detoxified by conjugation to glutathione, we asked whether the high 4-HNE adduct formation in the tail region was due to relatively lower expression of γ-Gcsc and γ-Gcsm, subunits of γ-glutamylcysteine synthetase, the rate limiting enzyme for glutathione synthesis. Although the expression of γ-Gcsc showed a trend to decrease from the head to the tail in control embryos (Fig. 5.2C), this was not statistically significant. HU exposure did decrease the expression of Gcsc in the body (Fig. 5.2C) and Gcsm in the head (Fig. 5.2D); neither of these effects explains the elevation in tail region 4-HNE protein adducts. The conjugation of 4-HNE with glutathione is catalyzed by GSTA4 (glutathione-S-transferase A4) (Yang et al., 2001). No region specificity in the distribution of Gsta4 was observed (Fig. 5.2E); HU treatment significantly decreased the expression of Gsta4 only in the body.

The identification of 4-HNE-conjugated proteins.

Our next goal was to identify the 4-HNE-protein conjugates that were enriched in the embryonic tail. The tail parts from embryos treated with saline or HU600 were collected and subjected to 2D gel electrophoresis (Fig. 5.3, A and B). Immunoblot analysis with the antibody against 4-HNE-modified proteins revealed eight protein spots in both control and HU treated embryos, as shown in Fig. 5.3C and 5.3B. According to the molecular weight range, spots 7 and 8 may be the 4-HNE-protein adducts specifically highly concentrated in the tail part, while spots 1-6 may be more evenly distributed throughout the three embryo regions.

Using MS, identifications were assigned to seven spots (2-8), as summarized in Table 5.1. The tail-localized 4-HNE-modified proteins were identified as albumin (ALB, spot 8), chaperonin subunit theta (CCT8) and possibly heat shock 60 (HSPD1, spot 7). 2D Western blots (n=2) did not detect a consistent change in the intensity of these three protein adducts when control embryos were compared to HU-exposed embryos. Interestingly, among the lower molecular weight protein adducts (perhaps not tail specific), three of the identified proteins are involved in energy metabolism. These include: glutamate oxaloacetatetransaminase 2 (GOT2, spot 2); aldolase 1, A isoform (ALDOA1, spot 3); and glyceraldehyde-3-phosphate dehydrogenase (GAPDH, spot 5). HU exposure resulted in increases in 4-HNE-conjugated GOT2 (1.6-fold), AIDO1A (1.6-fold), and GAPDH (1.8-fold) compared to controls. The two remaining 4-HNR modified proteins that were identified are inducible small cytokine subfamily E member 1 (SCYEI, spot 4) and heterogeneous nuclear ribonucleoprotein A1 isoform a (HNRNP A1A, spot 6). HU exposure increased the amounts of both SCYEI (1.8-fold) and HNRNP A1A (2.1-fold) compared to control.

GAPDH modifications.

Since we identified GAPDH as a 4-HNE target protein in the malformation sensitive tail region of HU exposed embryos and glycolysis is critical at this stage of organogenesis, we probed the membranes obtained from 2D gel electrophoresis with antibody to GAPDH (Fig. 5.4). The GAPDH immunoreactive spot matched the spot on the corresponding silver-stained gel identified by MS (Fig. 5.4, A-D). Interestingly, HU treatment not only increased the conjugation of

4-HNE to GAPDH, but also decreased the amount of GAPDH detected and altered the protein conformation of GAPDH, as reflected by a shortened protein migration trail towards the lower isoelectric point (Fig. 5.4, C and D).

DISCUSSION

A markedly higher content of 4-HNE-protein adducts was observed in the tail, compared to the head or body regions, of both control and HU-exposed embryos, indicating either that more ROS are generated here or that this area is less able to detoxify ROS. This enhanced oxidative stress in the caudal area may be the basis for the susceptibility of this part of the embryo to HU-induced teratogenesis.

HU exposure decreased the expression of two oxidative stress responsive genes involved in the development of caudal structures, Dkk1 and Fgf8. Even in control embryos the expression of Dkk1 was higher in the tail than in the head or body. It is not likely that the caudal malformations induced by HU are associated with this downregulation of Dkk1 expression, as previous studies have shown that teratogens, such as thalidomide, and oxidative stress itself upregulate Dkk1 expression (Knobloch et al., 2007;Grotewold and Ruther, 2002 a, b). Indeed, increased expression of Dkk1 is associated with increased apoptosis (Grotewold and Ruther, 2002 a, b). However, the decrease in Fgf8 in the tail region is consistent with the types of limb malformations induced by HU exposure, i.e. limbs with distal truncations and missing first digits (Moon and Capecchi, 2000). Furthermore, the decrease in Dkk1 expression may be a consequence of the reduction in Fgf8 expression, as Fgf8 signaling in the AER may be required for the expression of Dkk1 in the underlying mesoderm (Grotewold and Ruther, 2002a). The expression of Fgf8 in limb and tail buds is mediated by Wnt signaling (Aulehla and Herrmann, 2004) and, in a number of experimental

systems, oxidative stress antagonizes Wnt signaling (Shin et al., 2004;Almeida et al., 2007).

Interestingly, three proteins that are important in energy metabolism, GAPDH, GOT2, and ALD1A, were identified as 4-HNE modified proteins in the tail region; the amounts of these modified proteins were increased in HU exposed embryos. This finding suggests that HU induced oxidative stress may inhibit energy metabolism in the caudal regions of exposed embryos. The increase in the binding of 4-HNE to GAPDH after HU treatment changed both the amounts of GAPDH detected in Western blots and the protein conformation. 4-HNE modifications may trigger GAPDH degradation, decrease glycolytic activity, and induce apoptosis (Ishii et al., 2003;Botzen and Grune, 2007). This would be consistent with the suggestion that GAPDH serves as an oxidative stress sensor, acting as a pro-apoptosis factor (Chuang et al., 2005). HU also enhanced the conjugation of 4-HNE with SCYE1, a tRNA binding protein that facilitates apoptosis (van et al., 2006). Previous studies have reported that HU induced acute cell death in embryos, including in the limb bud region (DeSesso et al., 1994). Ectopic cell death in the AER decreased the expression of Fgf8 and Dkk1(Grotewold and Ruther, 2002b).

Additional proteins that were specifically modified by 4-HNE in the tail were albumin, CCT theta, and possibly HSPD1. The 4-HNE-albumin adduct has been suggested to be an *in vivo* marker of oxidative stress (Szapacs et al., 2006). CCT, a cytosolic chaperonin containing 8 subunits, is important in folding cytoskeleton proteins (Valpuesta et al., 2002). CCT interacts with its substrates through a particular combination of the 8 subunits that are critical to the

conformational change of CCT and consequent protein folding activity; the theta subunit participates in the folding of actin and tubulin (Valpuesta et al., 2002), both essential in the developing embryo. HSPD1, mainly localized in mitochondria, is also a chaperonin that is important in the folding or refolding of mitochondrial proteins, as well as in facilitating the degradation of misfolded or denatured proteins (Garrido et al., 2001). In addition, HSPD1 has been suggested to be a pro-apoptotic chaperone (Garrido et al., 2001). If the high amounts of 4-HNE-albummin, CCT8, and HSPD1 conjugates in the tail regions of embryos impact on the function of these proteins, it is likely that the trafficking and functions of other proteins are also disturbed. RNA processing may also be affected as HNRNP A1, another 4-HNE target, is involved in this function (Burd and Dreyfuss, 1994).

Together, these data indicate that the caudal region of the embryo is highly susceptible to oxidative stress in response to teratogen exposure. We propose that the protein modifications induced by this oxidative stress may affect glycolysis, alter protein trafficking, increase apoptosis, and downregulate the expression of pattern formation genes.

FIG. 5.1. (A) Illustrated the separation of the mouse embryo. Head part (*h*), from the cranial end (top) of the embryo to the caudal end of the first branchial archl; body part (*b*), the region between the head and tail part; tail part (*t*), from the cranial border of the third somites (counted from the caudal end) to the caudal end of the embryo. (B-D) Real-time qRT-PCR analyzed the expression of Dkk1, Fgf8, and Fgf10 in three parts of the embryo treated with control (saline) or HU-600mg/kg (HU600). Values for each gene were normalized to 18S rRNA levels. Each bar (mean ± SEM) represents 5 litters. *, denotes a significant difference from saline control (*, $p<0.05$; ** $p<0.01$); †, denotes a significant difference between different part of the embryo within the same treatment group (†, $p<0.05$; ††, $p<0.01$).

Fig. 5.1

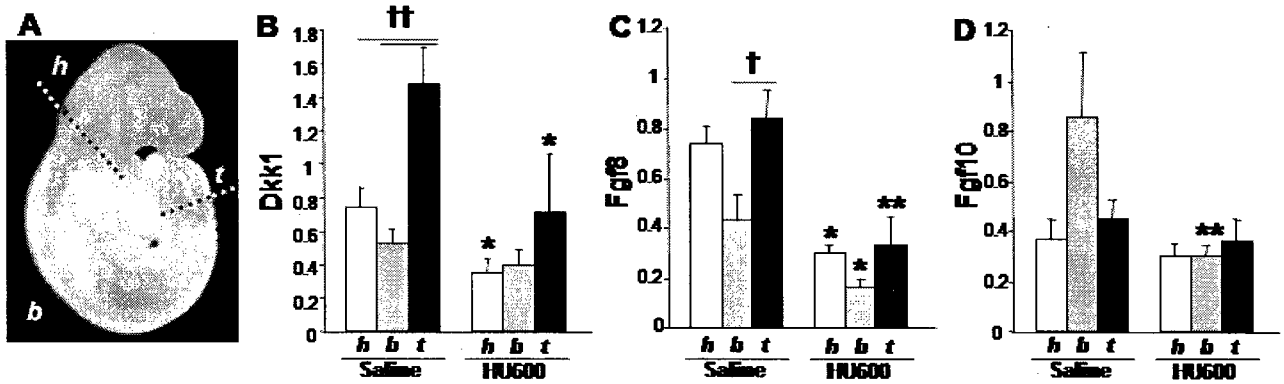

FIG. 5.2. (A) Western blot analysis of 4-HNE-protein adducts in the three parts of embryos exposed to vehicle (saline), or hydroxyurea (HU400: 400mg/kg, or HU600, 600mg/kg). All 4-HNE protein adducts were quantified by scan densitometric analysis, as indicated in (B). Each bar (mean ± SEM) represents 3 litters. Asterisks denote a significant difference (*, $p<0.05$; ** $p<0.01$). (C-E) Real-time qRT-PCR analysis of the expression of *Gclc*, *Gclm*, and *Gsta4*. Values for each gene were normalized to 18S rRNA levels. Each bar (mean ± SEM) represents 5 litters. "*", denotes a significant difference from saline control (*, $p<0.05$); "†", denotes a significant difference between different parts of the embryo within the same treatment group (†, $p<0.05$).

Fig. 5.2

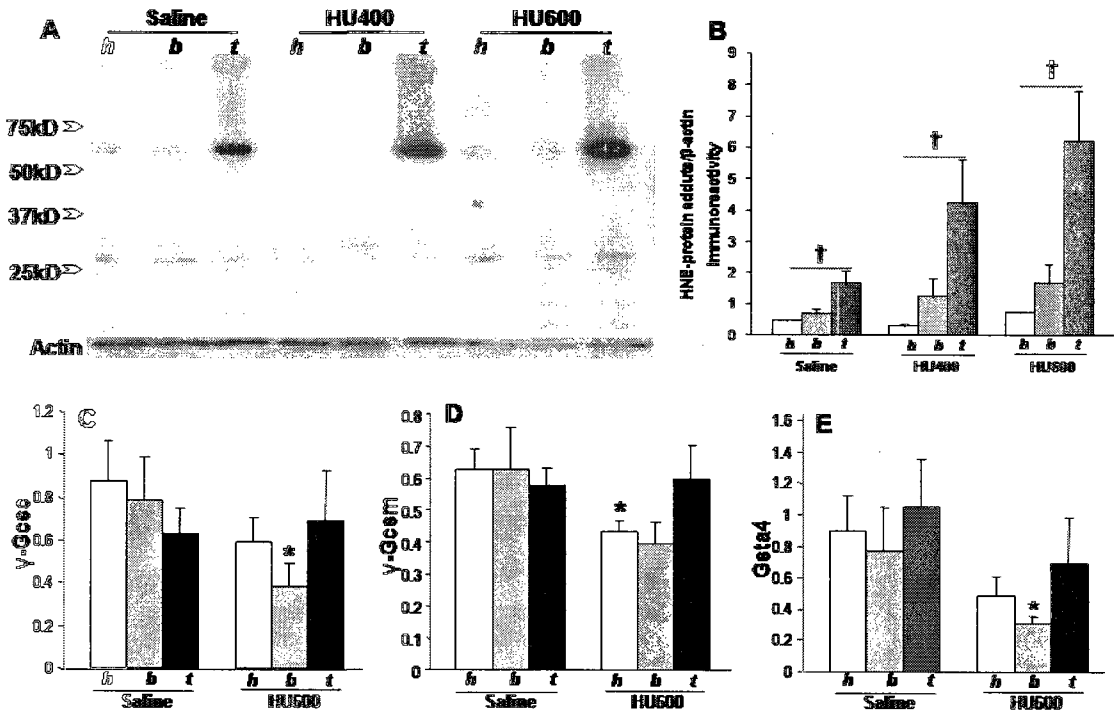
A
Saline
HU400
HU600
h b t
75kD
50kD
37kD
25kD
Actin
B
HNE-protein adduct/β-actin immunoreactivity
Saline
HU400
HU600
C
γ-Gcsc
D
γ-Gcsm
E
Gstα4

FIG. 5.3. 2D gel electrophoresis of the tail samples obtained from embryos treated with saline (controls, A) or HU (600mg/kg, B), and the corresponding 2D Western blots illustrating immunoreactive 4-HNE-protein adducts (C, control; D, HU-600mg/kg-treated). Spots 1–8 were analyzed by MS (see Table 1). (n=2)

Fig. 5.3

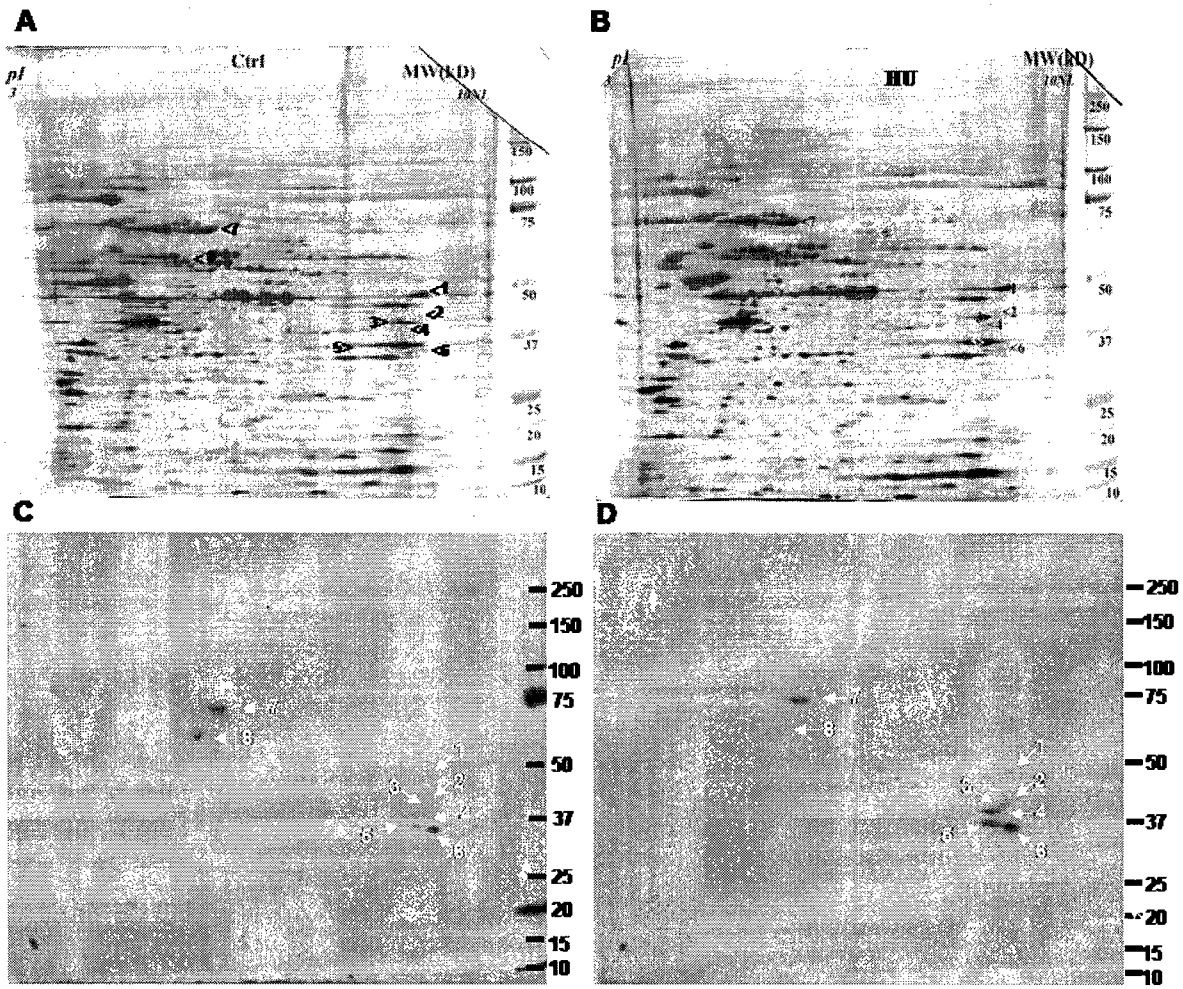

FIG. 5.4. 2D gel electrophoresis of the tail samples obtained from embryos treated with saline (control, A) or HU (600mg/kg, HU600) (B) and the corresponding 2D Western blots illustrating GAPDH immunoreactive protein spots (Control, C; HU600, D). (n=2).

Fig. 5.4

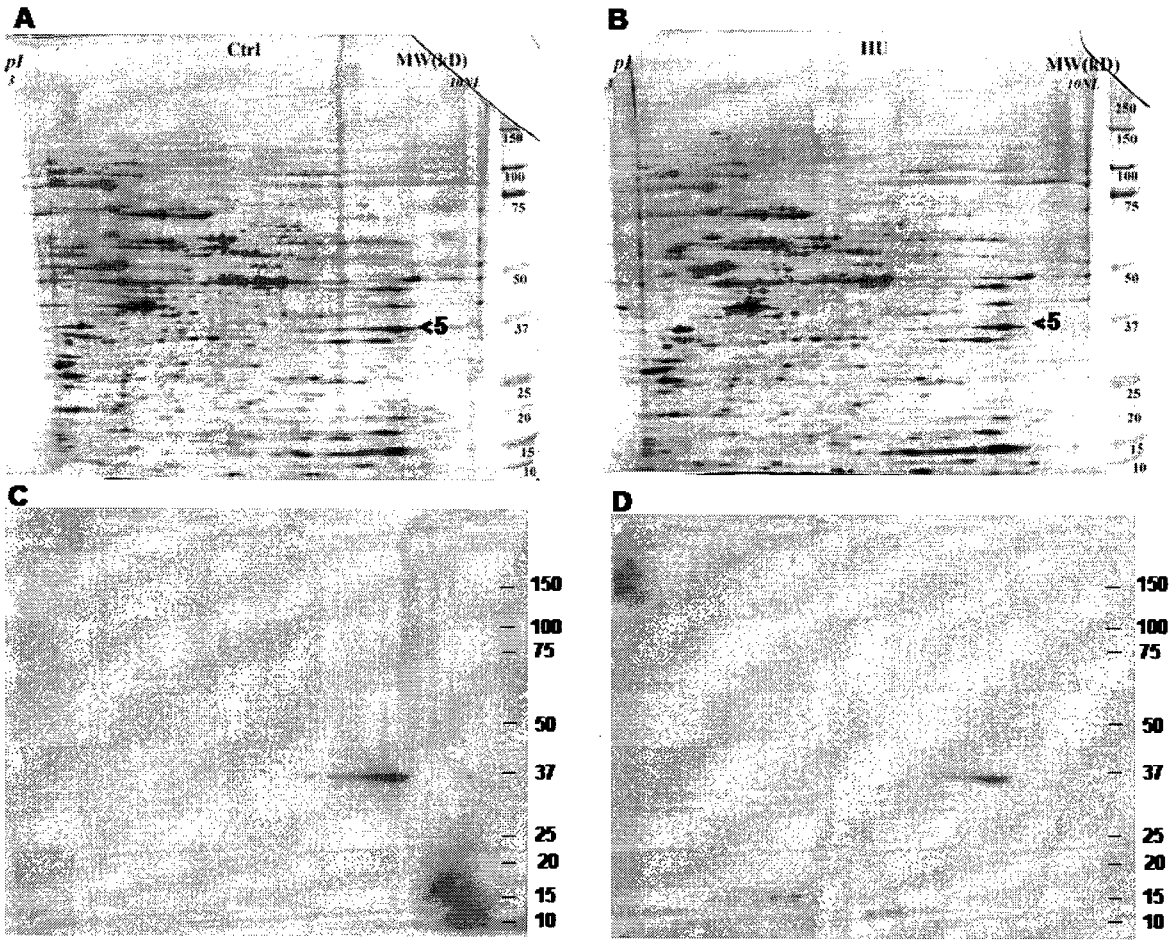
A
Ctrl
MW(KD)
pI
3
10NI
150
100
75
50
37
25
20
15
10
<5
B
HU
MW(KD)
pI
3
10NI
150
100
75
50
37
25
20
15
10
<5
C
150
100
75
50
37
25
20
15
10
D
150
100
75
50
37
25
20
15
10

Table 5.1. The identification of proteins conjugated with 4-HNE in the tail regions of embryos.

Spot No.	Protein name	Function	MW	pI	Sequence Coverage (%)
#1	Unnamed protein	-	50.4	9.1	24
#2	GOT2	Amino acid metabolism, Kreb's cycle	47.8	9.13	28
#3	ALDOA	Glycolysis	39.8	8.31	49
#4	SCYE1	Protein translation, apoptosis	35.5	8.75	40
#5	GAPDH	Glycolysis	36.1	8.44	44
#6	HNRNPA1A	RNA processing	34.3	9.27	23
#7	ALB	Transport protein in serum	70.7	5.75	41
#8	CCT8	Chaperone	60.1	5.44	47
	HSPD1 (possible)	Chaperone	61.1	5.91	10

MW, molecular weight; pI, isoelectric point

CHAPTER SIX

FINAL CONCLUSIONS

6.1 Summary

The major goal of this project was to elucidate the role of oxidative stress and the stress-response pathways in mediating HU-induced developmental toxicity during early organogenesis. Exposure of CD1 mouse embryos to HU caused fetal fatality, growth retardation, as well as external and skeletal malformations. Depletion of GSH specifically enhanced the HU-induced malformations and elevated the region-specific production of 4-HNE protein adducts in the embryo, without affecting the incidence or extent of HU-induced fetal death and growth retardation. These findings suggest that oxidative stress plays a major role in the induction of specific malformations by HU.

HU treatment of pregnant mice dramatically enhanced AP-1 DNA binding activity in their embryos. The AP-1 DNA binding activity induced by HU was mainly attributable to c-Fos heterodimers; interestingly, despite its effects on the incidence of embryo malformations, GSH depletion did not alter the effects of HU on AP-1 DNA binding activity. Exposure to HU also triggered a dramatic but transient increase in the activation of p38 MAPK and JNKs in embryos, without activating ERK1/2. Selectively blocking p38 MAPK enhanced HU-induced fetal mortality without affecting growth retardation or the incidence of deformities among surviving fetuses. However, selectively blocking JNKs did not affect HU-induced fetal death although it doubled the incidence of hindlimb defects observed. Therefore, p38 MAPKs and JNKs play distinct roles in protecting the conceptus against insult. In the following subsections, the proposed role of oxidative stress, AP-1, and MAPK pathways in HU-induced developmental toxicity will be discussed further.

6.2 The role of oxidative stress in HU-induced developmental toxicity

In utero exposure to HU during early organogenesis induced dose-dependent developmental toxicity. Exposure to HU at 400 mg/kg caused only a reduction in live fetal weights, whereas exposure to HU at 500 mg/kg and 600 mg/kg dramatically enhanced the rate of fetal death, reduced the body weights of live fetuses, and elevated the rates of external and skeletal malformations. Interestingly, HU-induced external and skeletal malformations were primarily found in caudal tissues, including the hindlimb, lumbarsacral vertebral column, and tail.

HU exposure did not change the overall GSH content or the ratio of GSSG to GSH in maternal livers, in embryos, or in yolk sacs compared to controls; however, a dramatic region-specific increase in 4-HNE immunoreactivity was induced by HU treatment. Interestingly, even in the absence of HU exposure, an approximately 2-fold higher level of 4-HNE protein adducts was detected in the caudal area (malformation sensitive region) than in other parts of the embryo; exposure to high-dose HU further elevated the production of 4-HNE-protein adducts in this area. Furthermore, depletion of GSH by BSO specifically enhanced both the severity and the incidence of malformations located in the caudal region of the embryo, including hindlimb and lumbarsacral vertebral column defects, without altering the effects of HU on fetal mortality or body weights. Thus, an enhanced susceptibility to oxidative stress in the caudal area may be the basis for the sensitivity of this part of the embryo to HU-induced teratogenesis.

Limbs are highly susceptible to oxidative stress-induced malformations (Fantel and Person, 2002;Hansen et al., 2001). Forelimb buds initiate at the level of the 8th-12th somites during GD 8.5-GD 9; hindlimb buds initiate at the level of somites 23 to 27 during GD 9-GD 9.5 (Agarwal et al., 2003). On GD 9, the hindlimb initiation sites are localized to the presomitic mesoderm region within the caudal area of the embryo. Consistently, exposure to HU on GD 9 induced forelimb defects in only a few fetuses; however, this HU exposure caused a high frequency of hindlimb defects. The malformed hind and forelimbs displayed similar phenotypes: missing and/or truncation of the anterior and distal part of the limb elements. The malformed hindlimbs showed a high frequency of missing or truncated first digits and tibia, and a very low incidence of partial or complete absence of more than the first digit, with a sequence from anterior (first digit) to posterior. This phenotype closely mimics the loss of the anterior part of the AER and the underneath mesoderm of the limb bud (Moon and Capecchi, 2000).

The anterior and posterior parts of the limb bud are different with respect to morphogen expression as well as susceptibility to teratogen insult (Lewandoski et al., 2000;Sanders and Stephens, 1991). For instance, Fgf8 is expressed throughout the AER, whereas Fgf4 is mainly expressed in the posterior portion of the AER; deletion of Fgf8 in the AER only induced cell death in the anterior part of the AER and in the underneath mesoderm, due to compensation by Fgf4 in the posterior AER (Lewandoski et al., 2000;(Boulet et al., 2004). In addition, Shh, another morphogen important for cell proliferation and digit patterning, forms a gradient from the posterior to anterior regions of the limb bud mesoderm, with no expression in the region of the first digit (McGlinn and Tabin, 2006). Thus,

differential regulation of the expression of genes important in pattern formation may contribute to the susceptibility of the anterior part of the limb bud to oxidative stress.

A decrease in the expression of Fgf8 was detected in the caudal region of embryos after HU exposure; a trend towards a decrease in Shh expression was detected as well (data not shown). Interestingly, a significant decrease in Dkk1, an apoptosis inducer, was induced by HU in the caudal region. Further studies to determine how teratogen exposures affect morphogens in the limb bud, using RNA *in situ* hybridization, and the localization of cell death in the limb bud, with whole mount TUNEL staining, may help to elucidate the relative roles of morphogens and cell death in mediating HU-induced limb defects. Interestingly, a review of drug-induced limb defects in mammals indicates that missing and/or truncation of digits is the single most common limb defect that occurs almost twice as commonly in the hindlimb as in the forelimb; furthermore, truncation of the anterior digits is four times more common than the truncation of the posterior digits in the hindlimbs (Sanders and Stephens, 1991). If oxidative stress represents a common mechanism of limb malformations, antioxidant supplementation may provide an efficient strategy to prevent and/or ameliorate limb defects induced by different teratogens.

On GD 9, the caudal area of the embryo consists mainly of the primitive streak, presomitic mesoderm, and the caudal neural tube. The primitive streak contains a pool of pluripotent mesenchymal stem cells which aggregate to form the tail bud between GD 9.5-GD 10 (Griffith et al., 1992). During organogenesis, the embryo grows caudally. The stem cells in the primitive streak and tail bud that

are located at the caudal end of the embryo contribute to this embryo elongation (Tam and Tan, 1992). These stem cells divide rapidly to generate presomitic mesoderm and the caudal neural tube; signals in the presomitic mesoderm drive the formation of a new pair of somites segmented from the presomitic mesoderm in a head-to-tail sequence every 90-120 minutes in the mouse embryo, alongside the neural tube (Pourquie, 2001). Somites give rise to the axial skeleton, including vertebrae and the rib cage; the neural tube gives rise to the central nervous system. On GD 9, at the time of HU exposure in these experiments, about 18 pairs of somites (occipital, cervical, and upper thoracic level) have formed already. The caudal region of the embryo will produce somites at the lower thoracic (19th-25th) level from the primitive streak within about 12 h, and somites at the lumbarsacral level (26th-35th) from the tail bud between GD 9.5-GD 10 (about 12-24 h after HU exposure) (Tam and Tan, 1992).

HU consistently induced a very low incidence of axial skeleton defects, from the occipital to the upper part of the thoracic region; in contrast, HU caused a very high frequency of defects of the lumbarsacral vertebrae and the adjacent lower part of the thoracic vertebrae. GSH depletion further enhanced the lumbarsacral vertebral column defects. HU-induced oxidative stress causes the rapid death of cells, preferentially at S phase (Herken et al., 1978). Both HU treatment-induced oxidative stress and the activation of stress-response pathways were relatively transitory, peaking at 3 h and beginning to diminish by 6 h after an intraperitoneal dose. Thus, the rapidly dividing stem cells in the primitive streak may be a major target of oxidative stress. Consistent with this, a dramatical decrease in Fgf8 expression was detected in the caudal part of the

embryo; Fgf8 is produced predominantly in the tip of the tail (Dubrulle and Pourquie, 2004). Thus, we hypothesize that the loss of rapidly dividing stem cells in the primitive streak and disruption of tail bud formation may be the major cause of the lumbarsacral defects induced by HU-mediated oxidative stress. Determination of the regions of cell death in embryos exposed to HU, combined with antioxidant treatment, may provide evidence to support this hypothesis.

In addition to its essential role in the formation and segmentation of lumbarsacral somites, the tail bud produces tail somites (Griffith et al., 1992;Tam, 1984). Reduction of the tail bud, caused by a deficiency in Wnt 3a, induces lumbarsacral vertebrae defects and loss of the tail (Greco et al., 1996). Interestingly, HU induced a relatively low incidence of severe tail truncations; GSH depletion did not alter the incidence of tail truncation induced by HU. The somites for the tail are produced between GD 11-GD 13.5 by the tail bud. Thus, the low incidence of severe truncation of the tail may suggest that the period of oxidative stress attack after HU treatment is short and that cell growth recovers (Woo et al., 2003).

HU exposure induced a high incidence of curly tail defects. Surprisingly, GSH depletion did not increase further these curly tail defects. Curly tail defects are often related to a delay in closure of the caudal neural tube (Tran et al., 2002). Thus, curly tail defects represent a common model of neural tube defects (NTDs). NTDs are among the most common and complex of congenital anomalies. Two major known risk factors for NTDs are maternal diabetes and folic acid insufficiency during pregnancy. Oxidative stress is associated with both of these factors. Scavenging oxygen radicals, with the anti-oxidant N-

acetylcysteine, blocked the NTD induced by maternal diabetes (Wentzel et al., 1997). Folic acid is related to GSH synthesis (Zhao et al., 2006); folic acid supplementation diminished the NTD induced by hyperglycemia in rat embryos, both *in vitro* and *in vivo* (Wentzel et al., 2005). Normal closure of the caudal neural tube occurs between GD 9-GD 9.5. A delay in caudal neural tube closure has been related to an imbalance in the growth of the somites and the neural tube and the reduced proliferation of cells in the tail bud (Tran et al., 2002). An increased production of 4-HNE protein adducts in the caudal neural tube and related tissues was observed after exposure to HU. Why the transitory elevation of oxidative stress induced by HU does not enhance curly tail defects remains elusive. Further study, with co-administration of an antioxidant such as N-acetylcysteine, may help to elucidate the role of oxidative stress in HU-induced curly tail defects.

We have shown that the caudal region of the embryo is specifically susceptible to oxidative stress. What are the major targets of oxidative stress in this area? Proteins modified by 4-HNE in the tail region were identified. Interestingly, three of the identified proteins are involved in energy metabolism; these are glyceraldehyde-3-phosphate dehydrogenase (GAPDH), glutamate oxaloacetate transaminase 2 (GOT2), and aldolase 1, A isoform (ALDOA1). This finding indicates that oxidative stress may influence embryonic energy metabolism. Strikingly, the HU-induced increase in 4-HNE conjugation to GAPDH not only decreased the amount of GAPDH detected (to 50% of control), but also altered its electrophoretic mobility, indicating a conformational change. This is consistent with previous reports that 4-HNE can modify GAPDH, resulting in the

inhibition of glycolytic activity and triggering GAPDH degradation (Botzen and Grune, 2007;Ishii et al., 2003). GAPDH is a multifunctional protein. Its classic role is as a glycolytic enzyme. Interestingly, rapidly dividing cells rely mainly on glycolysis as a source of ATP (Newell et al., 1999). A transition from oxidative to glycolytic energy production occurs during the G1/S transition (Brand and Hermfisse, 1997). Glucose utilization and lactate formation increased 18-fold and 38-fold, respectively, during thymocyte proliferation (Greiner et al., 1994). Furthermore, growth factors may regulate cell proliferation via the induction of glycolysis (Nowak and Schnellmann, 1995;Vander Heiden et al., 2001).

In addition to its crucial role in glycolysis, GAPDH has been suggested to be an intracellular sensor of oxidative stress and may play an early and pivotal role in the cascade leading to apoptosis (Chuang et al., 2005). GAPDH was found to be a target of p53 and may serve as a downstream apoptosis mediator (Chen et al., 1999;Ishitani and Chuang, 1996). Translocation of GAPDH from the cytoplasm to the nucleus appears to be a critical step in the induction of apoptosis (Dastoor and Dreyer, 2001). An increase in the nuclear localization of 4-HNE-protein adducts was induced by exposure to higher doses of HU and further elevated by GSH depletion.

Thus, we hypothesize that GAPDH is a major target of HU-induced oxidative stress. Further study to elucidate the impact of HU on GAPDH glycolytic activity and embryonic cell death may shed light on the mechanism of oxidative stress-mediated developmental toxicity.

6.3 The role of AP-1 in HU-induced developmental toxicity

A dramatic increase in AP-1 DNA binding activity was detected, using the electrophoretic mobility shift assay (EMSA), in embryos and yolk sacs at 0.5 h and 3 h after exposure to HU (400, 500, and 600mg/kg). In contrast, the activity of another redox-sensitive transcription factor, NF-kB, was not affected by HU treatment, indicating that the effect of HU on AP-1 activation may be specific. Using ELISA with an antibody against either c-Fos or c-Jun, a significant increase in the DNA binding activity of c-Fos heterodimers was detected in embryos 3 h after exposure to HU at 400, 500, or 600mg/kg; this activity remained elevated by 6 h in the embryos treated with HU at 500 and 600mg/kg. A trend towards an increase in c-Fos DNA binding activity was also detected in yolk sacs. Interestingly, GSH depletion did not alter the effects of HU on AP-1 c-Fos DNA binding activity. The DNA binding activity of c-Jun dimers was not increased significantly by HU exposure in the embryos or yolk sacs.

A dramatic increase in c-Fos immunoreactivity was found in HU-treated embryos. The c-Fos immunopositive regions have some similarity to the 4-HNE immunopositive regions; however, the regions of c-Fos expression were more expanded and not specifically localized to the caudal regions of the embryo. Oxidative stress may regulate AP-1 DNA binding activity via posttranslational phosphorylation, mediated by MAPK pathways, or via the redox regulation of conserved cysteine residues in the DNA binding domains of the proteins. A dramatically increased activation of p38 MAPKs was detected in embryos after HU exposure following the same time course as c-Fos activation. p38 MAPKs activate c-Fos in response to UV stimulation (Tanos et al., 2005). Furthermore,

p38 MAPKs phosphorylate ELK, which regulates c-Fos transcription. Similar to p38 MAPKs, JNKs were significantly activated. JNKs do not phosphorylate c-Fos directly; however, JNKs can activate ELK and phosphorylate Jun family proteins, which can enhance the expression and transcriptional potential of c-Fos heterodimers. As an alternative to these MAPK pathways, a more reduced nuclear environment may favour AP-1 DNA binding activity by reducing the cysteine residues in the DNA binding domain of AP-1 components, enhancing AP-1 DNA binding; oxidation inhibits binding (Xanthoudakis and Curran, 1992).

The nuclear localization of 4-HNE protein adducts was enhanced by increased doses of HU. Interestingly, direct exposure of vascular smooth muscle cells to lower concentrations (1 μM-2.5 μM) of 4-HNE enhanced AP-1 activity, whereas exposure to higher concentrations (2.5 μM-10 μM) of 4-HNE decreased AP-1 DNA binding activity (Kakishita and Hattori, 2001). Thus, there is a possibility that the AP-1 DNA binding activity observed is a result of a combination of different factors during oxidative stress.

Alternatively, the activation of c-Fos heterodimers may be due mainly to the genotoxicity caused by HU-induced inhibition of DNA synthesis. HU exposure induced profound DNA synthesis inhibition in the embryo, including a dramatic DNA synthesis inhibition in the neural tube epithelium (Scott et al., 1971b). High intensive c-Fos immunoreactivity was detected in the neural tube epithelium. c-Fos/AP-1 is induced by many types of genotoxic reagents and implicated in maintaining genomic stability (Christmann et al., 2006). c-Fos deficient cells are impaired in the abolition of the DNA damage-induced DNA replication blockage (Christmann et al., 2006;Kaina et al., 1997). While fibroblast cells deficient in c-

Fos are hypersensitive to a broad spectrum of genotoxic effects induced by tumour therapeutic agents, these c-Fos knockout cells are not significantly hypersensitive to ionizing radiation (Kaina et al., 1997).

The exact roles of AP-1 in HU-induced developmental toxicity are still unclear. The most obvious remaining question is why there is no significant increase in AP-1 c-Jun dimer-dependent DNA binding activity. Dramatic increases in JNK activation and c-Jun phosphorylation were detected in the embryos at 3 h and 6 h after HU treatment. One possibility is that some repressors influenced the AP-1 c-Jun DNA binding activity. The AP-1 members JunB, JunD, Fra-1 and Fra-2 exhibit only weak transactivation potential (Hess et al., 2004); JunB even antagonizes the effect of c-Jun on the proliferation of keratinocytes (Zenz and Wagner, 2006). Furthermore, JDP-2 dimerizes with c-Jun, acting as a repressor of the gene activation mediated by c-Jun (Aronheim et al.,1997). There is also a possibility that a region-specific activation of AP-1 c-Jun occurred. Inhibition of JNK activation specifically enhanced hindlimb malformations. Despite the lack of a statistically significant effect, a trend towards an increase in c-Jun dimer DNA binding activity did occur at 0.5 h after HU treatment. Consistent with this, an increase in AP-1 DNA binding activity was found at 0.5 h after HU treatment by EMSA, at a time when c-Fos dimers did not show any increase in activity. However, this raises another issue. JNK activation was increased significantly 3 h after HU treatment; at 0.5 h, JNK activation showed only a slight tendency to increase. This might indicate a high sensitivity of AP-1 DNA binding activity to regulation by phosphorylation. However, the obvious inconsistency between the activation of JNK-c-Jun and AP-1 c-Jun DNA binding

activity may indicate that although phosphorylated c-Jun may not contribute to AP-1 DNA binding, it may have other functions. In fact, a co-localization of c-Jun with γ-H2AX foci was observed in fibroblasts upon ionizing irradiation (MacLaren et al., 2004).

AP-1 may regulate the transcription of genes associated with glutathione synthesis, cell cycle progression, and pro-apoptotic or anti-apoptotic factors (Dickinson et al., 2002;Bakiri et al., 2000;Le-Niculescu et al., 1999;Rebollo et al., 2000). During organogenesis, AP-1 members are involved in bone development. For instance, a tissue-specific knockout of c-Jun results in vertebral column malformations (Behrens et al., 2003). Deficiency in c-Fos results in a loss of osteoclasts; ectopic c-Fos expression results in the transformation of osteoblasts (Johnson et al., 1992;Grigoriadis et al., 1994). In addition, a tissue specific knockout of c-Jun causes open eye defects (Zenz and Wagner, 2006). Open eye defects were observed at a low frequency in the fetuses treated with HU. Furthermore, inhibition of MAPK pathways enhanced the developmental toxicity induced by HU. Altogether, these findings might indicate that activation of AP-1 provides a protective effect. However, MAPKs have other potential substrates, so AP-1 is only one part of the downstream MAPK pathways that are stimulated by teratogenic insults. To elucidate the precise function of AP-1 members, the following studies may be required: 1) elucidation of the causality of oxidative stress with AP-1 activation by antioxidant treatment; 2) evaluation of AP-1 activity after blocking the MAPK pathways; 3) localization of phosphorylated c-Jun in the embryo and within cells by immunofluorescence staining; 4) identification of the proteins in the AP-1 complexes, using the supershift assay and co-

immunoprecipitation; 5) inhibition of target AP-1 members by antisense techniques; 6) elucidation of the effects of HU treatment in mice with genetically modified AP-1 members.

Overall, AP-1 DNA binding activity is sensitive to the developmental toxicity induced by HU. ELISA is an efficient method to detect AP-1 DNA binding activity. Therefore, AP-1 DNA binding activity has the potential to be a marker for teratogen insults; however, many studies are still required to validate this suggestion.

6.4 The role of MAPKs in HU-induced developmental toxicity

Exposure to HU, at a dose of 400 mg/kg or 600 mg/kg, triggered a dramatic increase in the activation of p38 MAPKs and JNKs in embryos at 3 and 6 h after treatment, without activating ERK1/2. Selectively blocking JNKs with L-JNKI1 did not affect HU-induced fetal death and growth retardation, but doubled the incidence of hindlimb defects observed. In contrast, selectively blocking p38 MAPK with SB203580 enhanced HU-induced fetal mortality, without affecting growth retardation or the incidence of deformities among surviving fetuses. Thus, JNKs and p38 MAPKs play distinct roles to protect the embryo against HU-induced developmental toxicity.

Strikingly, inhibition of JNK pathways specifically enhanced the hindlimb defects induced by HU. GSH depletion further elevated the incidence of hindlimb defects. Activation of JNKs, but not p38 MAPKs or ERKs, in response to 4-HNE induced oxidative stress induces the expression of γ-GCSC and γ-GCSM, subunits of γ-GCS, the rate limiting enzyme of GSH synthesis (Dickinson et al.,

2002). The activation of JNKs is also required for the induction of GSTA4, the glutathione transferase isoform responsible for the metabolism of 4-HNE during oxidative stress (Desmots et al., 2005). Interestingly, HU exposure did not significantly decrease the mRNA concentrations of γ-GCSC, γ-GCSM, or GSTA4 in the caudal region, but did result in a reduction of these transcripts in other regions of the embryo. Furthermore, the anterior part of the limb is highly sensitive to a decrease in the levels of Fgf8. Activation of JNKs was accompanied by the upregulation of Fgf8 expression during chemical-induced ameloblast differentiation (Abe et al., 2007). Above all, a recent study found that the activation of JNKs in response to oxidative stress modulated a shift from aerobic metabolism to glycolysis via the phosphorylation of pyruvate dehydrogenase within mitochondria (Zhou et al., 2008). This is consistent with our finding that glycolysis may be a major target of oxidative stress.

The effects elicited by JNKs that are listed above are consistent with a role in protection of the embryo that is subjected to oxidative stress. However, it is not known how JNKs might mediate a region-specific protective effect on the hindlimb. Oxidative stress may stimulate JNKs mainly through activation of ASK1, a MAP3K (Matsuzawa and Ichijo, 2008). Interestingly, a dynamic and region-specific expression of ASK1 was detected in chick and mouse embryos, including the limb region but excluding the caudal end of the tail (Ferrer-Vaquer et al., 2007). Mice deficient in ASK1 develop normally, perhaps due to gene redundancy (Tobiume et al., 2001). However, exposure of these ASK1 knockout mice to HU may provide some interesting information on the embryonic defence response to teratogen insults.

Interestingly, JNKs-c-Jun have been suggested to function upstream of DKK1 to induce apoptosis in limbs during normal development and as a consequence of the stress induced by thalidomide, H_2O_2, or UV irradiation (Grotewold and Ruther, 2002b). Nevertheless, we found a dramatic decrease in Dkk1 expression in the caudal region of the embryo. There are three JNK isoforms: JNK1, JNK2 and JNK3. JNK1 and JNK2 are ubiquitously expressed, whereas expression of JNK3 may be highly restricted to the brain, heart, and testis in the fetal and postnatal mouse (Martin et al., 1996;Yang et al., 1997). In addition, these JNK isoforms differ in their ability to bind and phosphorylate various substrate proteins (Gupta et al., 1996). JNK1 and JNK2 showed different functions from JNK3 in regulating both embryo development and stress responses (Kuan et al., 1999). The activation of JNK3 has been associated with neuronal apoptosis induced by different stressors, including 4-HNE (Yang et al., 1997; Bruckner and Estus, 2002). In contrast, 4-HNE induced the expression γ-GCSC and γ-GCSM via the activation of JNK1 in HBE1 cells (Dickinson et al., 2002). Furthermore, the consequence of JNK activation may be dependent on the duration of its activation; robust and sustained activation of JNK under severe stress conditions normally results in apoptosis, whereas transient activation may be protective (Liu and Lin, 2005). Thus, further studies are required to identify the JNK isoforms activated by HU and to determine the substrates of these JNKs.

It is intriguing to consider the JNK pathways that may be involved in protecting embryos against HU-induced limb defects. Firstly, what is the impact of inhibition of JNKs on glycolysis? Secondly, what pathways are upstream and downstream of JNK activation? There are presently no specific pharmaceutical

inhibitors available for each isoform of JNK. Antisense techniques, co-immunoprecipitation, and pharmaceutical inhibitors for JNKs, MKK4, MKK7, or ASK1, and ASK1, JNK1, JNK2, or JNK3 knockout mice may help to answer these questions.

With a role that is distinct from the JNKs, the activation of p38 MAPKs may mainly protect the embryo from lethality. While it is likely that HU-induced malformations are due to region-specific oxidative stress, the cause of fetal death is elusive. The dead fetuses observed are mainly resorptions. Since no identifiable tissues remained by GD 18, we predict that these embryonic deaths occurred shortly after HU exposure. GSH depletion did not alter the incidence of fetal death induced by HU. One suggestion is that inhibition of DNA synthesis may be related to HU-induced embryonic death. p38 MAPK may play a role as well, since the activation of p38 often contributes to cell cycle arrest. Indeed, the activation of p38α and p38β in response to HU treatment prevented mitotic entry in some cell lines (Rodriguez-Bravo et al., 2007).

Four isoforms of p38 MAPKs have been identified in vertebrates, including p38α, p38β, p38γ and p38δ (Keesler et al., 1998). These isoforms have distinct functions. p38α is required for placental organogenesis; p38α-deficient mice die at GD 10.5–11.5 as a result of defective placental development (Mudgett et al., 2000;Adams et al., 2000). In contrast, a single knockout of p38β, γ, δ, or a double knockout of γ and δ, results in fertile and viable mice with no apparent phenotypes (Beardmore et al., 2005;Sabio et al., 2005). Furthermore, different isoforms of p38 show different sensitivities to stress stimulation (Conrad et al., 1999).

Thus, further studies are needed to determine the cause of fetal death. Since the fetal death appears to occur shortly after HU exposure, examination of embryo histology a short period after HU exposure (e.g., 12, 24 and 48 h), may help to provide some information on the causes of fetal death and whether all tissues or only specific vital organs are affected. Secondly, the identification of the p38 isoforms that are stimulated by HU exposure would be helpful. Although specific antibodies that recognize each phosphorylated isoform of p38 are not currently available, there are antibodies specific for non-phosphorylated p38α, p38β, p38γ, or p38δ. Detection of their location in the embryo after HU exposure may help in understanding their functions. Following this, studies using antisense techniques or knockout mice may provide more information about the functions of various forms of p38 in HU-induced developmental toxicity.

There is growing interest in the therapeutic potential of p38 and JNK inhibitors; many compounds are undergoing development (Kaminska, 2005;Duan and Wong, 2006;Kaneto, 2005;Clark et al., 2007). However, inhibition of the transient activation of JNKs or p38 MAPKs exaggerated teratogen-induced developmental toxicity. Thus, understanding the impact of exposure to MAPKs inhibitors during pregnancy is a priority.

6.5 Conclusions

1) HU exposure during early organogenesis induced fetal death, growth retardation, as well as external and skeletal malformations. The caudal tissues are specifically sensitive to HU-induced malformations. HU exposure did not change the overall GSH content or the ratio of GSSG to GSH in maternal livers,

embryos, or yolk sacs compared to controls. Interestingly, a markedly high level of 4-HNE protein adducts was observed in the malformation-sensitive caudal region of the embryos even in the absence of HU exposure; HU treatment further enhanced the formation of these adducts. GSH depletion specifically increased the incidence of malformations in caudal tissues, inducing hindlimb and lumbarsacral vertebral column defects, without altering the fetal death and growth retardation induced by HU. Thus, region-specific enhanced oxidative stress may be the basis for the susceptibility of the caudal region of the embryo to HU-induced teratogenesis.

2) HU-induced hindlimb malformations displayed loss of the distal and anterior parts of the limb, mimicking the phenotype of loss of the anterior part of the AER or mesoderm in the limb bud. The lumbarsacral vertebral column defects may indicate a disruption of the tail bud located at the caudal end of the embryo. Fgf8 is expressed in the AER and the caudal end of the embryo at the time of HU exposure and is essential for the growth of the anterior part of the limb bud and somite development, respectively. A significant decrease in Fgf8 was detected in the caudal region of the embryo after HU treatment. Furthermore, Dkk1 is important in limb and vertebral column development; a significant decrease in Dkk1 expression was detected in the caudal region of embryos after HU treatment. Further studies to localize HU-induced cell death and effects on the expression of Fgf8 and Dkk1 in the embryo are required.

3) Proteins modified by 4-HNE in the tail region were identified. Three of the identified proteins are involved in energy metabolism; these are glyceraldehyde-3-phosphate dehydrogenase (GAPDH), glutamate oxaloacetate

transaminase 2 (GOT2), and aldolase 1, A isoform (ALDOA1). The conjugation of 4-HNE to GAPDH induced by HU exposure remarkably decreased the amount of GAPDH detected and altered its electrophoretic mobility, indicating a conformational change. In addition to its crucial role in glycolysis, GAPDH induces apoptosis during oxidative stress. Glycolysis is essential for cell proliferation. HU induces cell death preferentially in S phase. Thus, GAPDH may be a major target of HU-induced oxidative stress.

4) HU specifically enhanced the AP-1 DNA binding activity in the embryos and yolk sacs, without affecting the activity of NF-κB. C-Fos heterodimers were mainly activated by HU treatment; GSH depletion did not alter the effect of HU on the activation of c-Fos heterodimers. A dramatic increase in c-Fos immunoreactivity was found in HU-treated embryos. The c-Fos immunopositive regions showed some similarity to the 4-HNE immunoreactive areas, but were more extensive. The determination of whether the enhanced c-Fos AP-1 DNA binding activity is triggered by oxidative stress or inhibition of DNA synthesis will require further experiments. In addition, whether the activation of AP-1 in response to HU exposure has a positive protective effect needs to be further elucidated.

5) Exposure to HU induced a dramatic increase in the activation of p38 MAPK and JNKs in embryos, without activating ERK1/2. Selectively blocking p38 MAPK enhanced HU-induced fetal mortality without affecting growth retardation or the incidence of deformities among surviving fetuses. In contrast, selectively blocking JNKs did not affect HU-induced fetal death but doubled the incidence of

hindlimb defects observed. Thus, p38 MAPKs and JNKs play distinct roles in protecting the conceptus against insult.

ORIGINAL CONTRIBUTIONS

1. During early organogenesis, the caudal region in the embryo is specifically susceptible to the induction of malformations by oxidative stress. Antioxidant supplement may be a promising strategy to prevent or interfere with the teratogenesis induced by different teratogens.

2. There is a specific increase in the formation of 4-HNE protein adducts in the malformation sensitive regions of embryos treated with HU. A number of the proteins conjugated with 4-HNE are involved in embryonic metabolism which suggests that oxidative stress may target metabolism. Specifically, GAPDH may represent a major target of oxidative stress in inducing malformations.

3. AP-1 DNA binding activity is specifically enhanced in the conceptus by HU treatment; this AP-1 DNA binding activity is dependent on c-Fos heterodimers. AP-1 DNA binding activity has the potential to serve as a marker for teratogen insult.

4. In the embryo, stress-responsive JNKs and p38 MAPKs are activated by HU exposure. Inhibition of p38 elevated the incidence of fetal death, whereas, inhibition of JNKs specifically enhanced the limb defects induced by HU. Thus, p38 MAPKs and JNKs protect the embryo via distinct pathways. The ability of MAPKs to protection the embryo against insult with a teratogen may be determined both by the nature of the insult and by the tissue-specific stress-response that is induced. Understanding the impact of MAPKs inhibitors therapy during pregnancy is a priority.

Abate C, Patel L, Rauscher FJ, III and Curran T (1990) Redox regulation of fos and jun DNA-binding activity in vitro. *Science* **249**:1157-1161.

Abe K, Miyoshi K, Muto T, Ruspita I, Horiguchi T, Nagata T and Noma T (2007) Establishment and characterization of rat dental epithelial derived ameloblast-lineage clones. *J Biosci Bioeng* **103**:479-485.

Adams RH, Porras A, Alonso G, Jones M, Vintersten K, Panelli S, Valladares A, Perez L, Klein R and Nebreda AR (2000) Essential role of p38alpha MAP kinase in placental but not embryonic cardiovascular development. *Mol Cell* **6**:109-116.

Adler V, Schaffer A, Kim J, Dolan L and Ronai Z (1995) UV irradiation and heat shock mediate JNK activation via alternate pathways. *J Biol Chem* **270**:26071-26077.

Agarwal P, Wylie JN, Galceran J, Arkhitko O, Li C, Deng C, Grosschedl R and Bruneau BG (2003) Tbx5 is essential for forelimb bud initiation following patterning of the limb field in the mouse embryo. *Development* **130**:623-633.

Akazawa S, Unterman T and Metzger BE (1994) Glucose metabolism in separated embryos and investing membranes during organogenesis in the rat. *Metabolism* **43**:830-835.

Aldini G, Gamberoni L, Orioli M, Beretta G, Regazzoni L, Maffei FR and Carini M (2006) Mass spectrometric characterization of covalent modification of human serum albumin by 4-hydroxy-trans-2-nonenal. *J Mass Spectrom* **41**:1149-1161.

Aldini G, Ie-Donne I, Vistoli G, Maffei FR and Carini M (2005) Covalent modification of actin by 4-hydroxy-trans-2-nonenal (HNE): LC-ESI-MS/MS evidence for Cys374 Michael adduction. *J Mass Spectrom* **40**:946-954.

Alin P, Danielson UH and Mannervik B (1985) 4-Hydroxyalk-2-enals are substrates for glutathione transferase. *FEBS Lett* **179**:267-270.

Aliverti V, Bonanomi L and Giavini E (1980) Hydroxyurea as a reference standard in teratological screening. Comparison of the embryotoxic and teratogenic effects following single intraperitoneal or repeated oral administrations to pregnant rats. *Arch Toxicol Suppl* **4**:239-247.

Almeida M, Han L, Martin-Millan M, O'Brien CA and Manolagas SC (2007) Oxidative stress antagonizes Wnt signaling in osteoblast precursors by diverting beta-catenin from T cell factor- to forkhead box O-mediated transcription. *J Biol Chem* **282**:27298-27305.

Andrews GK, Harding MA, Calvet JP and Adamson ED (1987) The heat shock response in HeLa cells is accompanied by elevated expression of the c-fos proto-oncogene. *Mol Cell Biol* **7**:3452-3458.

Angel P and Karin M (1991) The role of Jun, Fos and the AP-1 complex in cell-proliferation and transformation. *Biochim Biophys Acta* **1072**:129-157.

Aoyama K, Matsubara K and Kobayashi S (2006) Aging and oxidative stress in progressive supranuclear palsy. *Eur J Neurol* **13**:89-92.

Ariel IM (1970) Therapeutic effects of hydroxyurea. Experience with 118 patients with inoperable solid tumors. *Cancer* **25**:705-714.

Aronheim A, Zandi E, Hennemann H, Elledge SJ and Karin M (1997) Isolation of an AP-1 repressor by a novel method for detecting protein-protein interactions. *Mol Cell Biol* **17**:3094-3102.

Asano Y and Okaniwa A (1987) In utero morphological effects of hydroxyurea on the fetal development in Sprague-Dawley rats. *Jikken Dobutsu* **36**:143-149.

Aulehla A and Herrmann BG (2004) Segmentation in vertebrates: clock and gradient finally joined. *Genes Dev* **18**:2060-2067.

Aulehla A, Wehrle C, Brand-Saberi B, Kemler R, Gossler A, Kanzler B and Herrmann BG (2003) Wnt3a plays a major role in the segmentation clock controlling somitogenesis. *Dev Cell* **4**:395-406.

Awasthi YC, Ansari GA and Awasthi S (2005) Regulation of 4-hydroxynonenal mediated signaling by glutathione S-transferases. *Methods Enzymol* **401**:379-407.

Awasthi YC, Yang Y, Tiwari NK, Patrick B, Sharma A, Li J and Awasthi S (2004) Regulation of 4-hydroxynonenal-mediated signaling by glutathione S-transferases. *Free Radic Biol Med* **37**:607-619.

Bajt ML, Knight TR, Lemasters JJ and Jaeschke H (2004) Acetaminophen-induced oxidant stress and cell injury in cultured mouse hepatocytes: Protection by N-acetyl cysteine. *Toxicological Sciences* **80**:343-349.

Baker RE, Schnell S and Maini PK (2006) A clock and wavefront mechanism for somite formation. *Dev Biol* **293**:116-126.

Bakiri L, Lallemand D, Bossy-Wetzel E and Yaniv M (2000) Cell cycle-dependent variations in c-Jun and JunB phosphorylation: a role in the control of cyclin D1 expression. *EMBO J* **19**:2056-2068.

Barancik M, Htun P, Strohm C, Kilian S and Schaper W (2000) Inhibition of the cardiac p38-MAPK pathway by SB203580 delays ischemic cell death. *J Cardiovasc Pharmacol* **35**:474-483.

Barrera G, Di MC, Muraca R, Ferrero D, Cavalli G, Fazio VM, Paradisi L and Dianzani MU (1991) Induction of differentiation in human HL-60 cells by 4-hydroxynonenal, a product of lipid peroxidation. *Exp Cell Res* **197**:148-152.

Barrera G, Pizzimenti S and Dianzani MU (2004) 4-hydroxynonenal and regulation of cell cycle: effects on the pRb/E2F pathway. *Free Radic Biol Med* **37**:597-606.

Beardmore VA, Hinton HJ, Eftychi C, Apostolaki M, Armaka M, Darragh J, McIlrath J, Carr JM, Armit LJ, Clacher C, Malone L, Kollias G and Arthur JS (2005) Generation and characterization of p38beta (MAPK11) gene-targeted mice. *Mol Cell Biol* **25**:10454-10464.

Beck MJ, McLellan C, Lightle RL, Philbert MA and Harris C (2001) Spatial glutathione and cysteine distribution and chemical modulation in the early organogenesis-stage rat conceptus in utero. *Toxicol Sci* **62**:92-102.

Behrens A, Haigh J, Mechta-Grigoriou F, Nagy A, Yaniv M and Wagner EF (2003) Impaired intervertebral disc formation in the absence of Jun. *Development* **130**:103-109.

Behrens A, Sibilia M and Wagner EF (1999) Amino-terminal phosphorylation of c-Jun regulates stress-induced apoptosis and cellular proliferation. *Nat Genet* **21**:326-329.

Biron F, Lucht F, Peyramond D, Fresard A, Vallet T, Nugier F, Grange J, Malley S, Hamedi-Sangsari F and Vila J (1996) Pilot clinical trial of the combination of hydroxyurea and didanosine in HIV-1 infected individuals. *Antiviral Res* **29**:111-113.

Bobick BE and Kulyk WM (2004) The MEK-ERK signaling pathway is a negative regulator of cartilage-specific gene expression in embryonic limb mesenchyme. *J Biol Chem* **279**:4588-4595.

Bobick BE, Thornhill TM and Kulyk WM (2007) Fibroblast growth factors 2, 4, and 8 exert both negative and positive effects on limb, frontonasal, and mandibular chondrogenesis via MEK-ERK activation. *J Cell Physiol* **211**:233-243.

Bogoyevitch MA and Kobe B (2006) Uses for JNK: the many and varied substrates of the c-Jun N-terminal kinases. *Microbiol Mol Biol Rev* **70**:1061-1095.

Bonni A, Brunet A, West AE, Datta SR, Takasu MA and Greenberg ME (1999) Cell survival promoted by the Ras-MAPK signaling pathway by transcription-dependent and -independent mechanisms. *Science* **286**:1358-1362.

Botzen D and Grune T (2007) Degradation of HNE-modified proteins--possible role of ubiquitin. *Redox Rep* **12**:63-67.

Boulet AM, Moon AM, Arenkiel BR and Capecchi MR (2004) The roles of Fgf4 and Fgf8 in limb bud initiation and outgrowth. *Dev Biol* **273**:361-372.

Bradbury CM, Locke JE, Wei SJ, Rene LM, Karimpour S, Hunt C, Spitz DR and Gius D (2001) Increased activator protein 1 activity as well as resistance to heat-induced radiosensitization, hydrogen peroxide, and cisplatin are inhibited by indomethacin in oxidative stress-resistant cells. *Cancer Res* **61**:3486-3492.

Bradford MM (1976) A rapid and sensitive method for the quantitation of microgram quantities of protein utilizing the principle of protein-dye binding. *Anal Biochem* **72**:248-254.

Brand KA and Hermfisse U (1997) Aerobic glycolysis by proliferating cells: a protective strategy against reactive oxygen species. *FASEB J* **11**:388-395.

Breen AP and Murphy JA (1995) Reactions of oxyl radicals with DNA. *Free Radic Biol Med* **18**:1033-1077.

Brown JR, Nigh E, Lee RJ, Ye H, Thompson MA, Saudou F, Pestell RG and Greenberg ME (1998) Fos family members induce cell cycle entry by activating cyclin D1. *Mol Cell Biol* **18**:5609-5619.

Brown JR, Ye H, Bronson RT, Dikkes P and Greenberg ME (1996) A defect in nurturing in mice lacking the immediate early gene fosB. *Cell* **86**:297-309.

Bruckner SR and Estus S (2002) JNK3 contributes to c-jun induction and apoptosis in 4-hydroxynonenal-treated sympathetic neurons. *J Neurosci Res* **70**:665-670.

Brusselbach S, Mohle-Steinlein U, Wang ZQ, Schreiber M, Lucibello FC, Muller R and Wagner EF (1995) Cell proliferation and cell cycle progression are not impaired in fibroblasts and ES cells lacking c-Fos. *Oncogene* **10**:79-86.

Burch PM, Yuan Z, Loonen A and Heintz NH (2004) An extracellular signal-regulated kinase 1- and 2-dependent program of chromatin trafficking of c-Fos and Fra-1 is required for cyclin D1 expression during cell cycle reentry. *Mol Cell Biol* **24**:4696-4709.

Burd CG and Dreyfuss G (1994) RNA binding specificity of hnRNP A1: significance of hnRNP A1 high-affinity binding sites in pre-mRNA splicing. *EMBO J* **13**:1197-1204.

Bushdid PB, Brantley DM, Yull FE, Blaeuer GL, Hoffman LH, Niswander L and Kerr LD (1998) Inhibition of NF-kappaB activity results in disruption of the apical ectodermal ridge and aberrant limb morphogenesis. *Nature* **392**:615-618.

Butcher RE, Scott WJ, Kazmaier K and Ritter EJ (1973) Postnatal effects in rats of prenatal treatment with hydroxyurea. *Teratology* **7**:161-165.

Cadenas E and Davies KJ (2000) Mitochondrial free radical generation, oxidative stress, and aging. *Free Radic Biol Med* **29**:222-230.

Caldini R, Barletta E, Del RM, Giovannelli L and Chevanne M (2005) FGF2-mediated upregulation of urokinase-type plasminogen activator expression requires a MAP-kinase dependent activation of poly(ADP-ribose) polymerase. *J Cell Physiol* **202**:125-134.

Capdevila J and Izpisua Belmonte JC (2001) Patterning mechanisms controlling vertebrate limb development. *Annu Rev Cell Dev Biol* **17**:87-132.

Carbone DL, Doorn JA, Kiebler Z, Ickes BR and Petersen DR (2005a) Modification of heat shock protein 90 by 4-hydroxynonenal in a rat model of chronic alcoholic liver disease. *J Pharmacol Exp Ther* **315**:8-15.

Carbone DL, Doorn JA, Kiebler Z and Petersen DR (2005b) Cysteine modification by lipid peroxidation products inhibits protein disulfide isomerase. *Chem Res Toxicol* **18**:1324-1331.

Carbone DL, Doorn JA, Kiebler Z, Sampey BP and Petersen DR (2004a) Inhibition of Hsp72-mediated protein refolding by 4-hydroxy-2-nonenal. *Chem Res Toxicol* **17**:1459-1467.

Carbone DL, Doorn JA and Petersen DR (2004b) 4-Hydroxynonenal regulates 26S proteasomal degradation of alcohol dehydrogenase. *Free Radic Biol Med* **37**:1430-1439.

Cavigelli M, Dolfi F, Claret FX and Karin M (1995) Induction of c-fos expression through JNK-mediated TCF/Elk-1 phosphorylation. *EMBO J* **14**:5957-5964.

Cederberg J, Siman CM and Eriksson UJ (2001) Combined treatment with vitamin E and vitamin C decreases oxidative stress and improves fetal outcome in experimental diabetic pregnancy. *Pediatr Res* **49**:755-762.

Cenini G, Sultana R, Memo M and Butterfield DA (2007) Elevated Levels of Pro-apoptotic p53 and Its Oxidative Modification by the Lipid Peroxidation Product, HNE, in Brain from Subjects with Amnestic Mild Cognitive Impairment and Alzheimer's Disease. *J Cell Mol Med*.

Chang L and Karin M (2001) Mammalian MAP kinase signalling cascades. *Nature* **410**:37-40.

Chaube S and Murphy ML (1966) The effects of hydroxyurea and related compounds on the rat fetus. *Cancer Res* **26**:1448-1457.

Chen CS and Wells PG (2006) Enhanced tumorigenesis in p53 knockout mice exposed in utero to high-dose vitamin E. *Carcinogenesis* **27**:1358-1368.

Chen RH, Juo PC, Curran T and Blenis J (1996) Phosphorylation of c-Fos at the C-terminus enhances its transforming activity. *Oncogene* **12**:1493-1502.

Chen RW, Saunders PA, Wei H, Li Z, Seth P and Chuang DM (1999) Involvement of glyceraldehyde-3-phosphate dehydrogenase (GAPDH) and p53 in neuronal apoptosis: evidence that GAPDH is upregulated by p53. *J Neurosci* **19**:9654-9662.

Chen Y and Zhao X (1998) Shaping limbs by apoptosis. *J Exp Zool* **282**:691-702.

Chen Z and Cobb MH (2001) Regulation of stress-responsive mitogen-activated protein (MAP) kinase pathways by TAO2. *J Biol Chem* **276**:16070-16075.

Chinenov Y and Kerppola TK (2001) Close encounters of many kinds: Fos-Jun interactions that mediate transcription regulatory specificity. *Oncogene* **20**:2438-2452.

Choe H, Hansen JM and Harris C (2001) Spatial and temporal ontogenies of glutathione peroxidase and glutathione disulfide reductase during development of the prenatal rat. *J Biochem Mol Toxicol* **15**:197-206.

Christmann M, Tomicic MT, Origer J, Aasland D and Kaina B (2006) c-Fos is required for excision repair of UV-light induced DNA lesions by triggering the re-synthesis of XPF. *Nucleic Acids Res* **34**:6530-6539.

Chuang DM, Hough C and Senatorov VV (2005) Glyceraldehyde-3-phosphate dehydrogenase, apoptosis, and neurodegenerative diseases. *Annu Rev Pharmacol Toxicol* **45**:269-290.

Clark JE, Sarafraz N and Marber MS (2007) Potential of p38-MAPK inhibitors in the treatment of ischaemic heart disease. *Pharmacol Ther* **116**:192-206.

Closs EI, Murray AB, Schmidt J, Schon A, Erfle V and Strauss PG (1990) c-fos expression precedes osteogenic differentiation of cartilage cells in vitro. *J Cell Biol* **111**:1313-1323.

Coan C, Ji JY, Hideg K and Mehlhorn RJ (1992) Protein sulfhydryls are protected from irreversible oxidation by conversion to mixed disulfides. *Arch Biochem Biophys* **295**:369-378.

Conrad PW, Rust RT, Han J, Millhorn DE and Beitner-Johnson D (1999) Selective activation of p38alpha and p38gamma by hypoxia. Role in regulation of cyclin D1 by hypoxia in PC12 cells. *J Biol Chem* **274**:23570-23576.

Corson LB, Yamanaka Y, Lai KM and Rossant J (2003) Spatial and temporal patterns of ERK signaling during mouse embryogenesis. *Development* **130**:4527-4537.

Cowling VH and Cole MD (2006) Mechanism of transcriptional activation by the Myc oncoproteins. *Semin Cancer Biol* **16**:242-252.

Crews CM, Alessandrini A and Erikson RL (1992) The primary structure of MEK, a protein kinase that phosphorylates the ERK gene product. *Science* **258**:478-480.

Cruzalegui FH, Cano E and Treisman R (1999) ERK activation induces phosphorylation of Elk-1 at multiple S/T-P motifs to high stoichiometry. *Oncogene* **18**:7948-7957.

Cuenda A, Rouse J, Doza YN, Meier R, Cohen P, Gallagher TF, Young PR and Lee JC (1995) SB 203580 is a specific inhibitor of a MAP kinase homologue which is stimulated by cellular stresses and interleukin-1. *FEBS Lett* **364**:229-233.

Cuevas BD, Abell AN and Johnson GL (2007) Role of mitogen-activated protein kinase kinase kinases in signal integration. *Oncogene* **26**:3159-3171.

Dastoor Z and Dreyer JL (2001) Potential role of nuclear translocation of glyceraldehyde-3-phosphate dehydrogenase in apoptosis and oxidative stress. *J Cell Sci* **114**:1643-1653.

Davies MJ, Gilbert BC and Haywood RM (1991) Radical-induced damage to proteins: e.s.r. spin-trapping studies. *Free Radic Res Commun* **15**:111-127.

Davis RJ (2000) Signal transduction by the JNK group of MAP kinases. *Cell* **103**:239-252.

Delfini MC, Dubrulle J, Malapert P, Chal J and Pourquie O (2005) Control of the segmentation process by graded MAPK/ERK activation in the chick embryo. *Proc Natl Acad Sci U S A* **102**:11343-11348.

Deng X, Xiao L, Lang W, Gao F, Ruvolo P and May WS, Jr. (2001) Novel role for JNK as a stress-activated Bcl2 kinase. *J Biol Chem* **276**:23681-23688.

Dent P, Haser W, Haystead TA, Vincent LA, Roberts TM and Sturgill TW (1992) Activation of mitogen-activated protein kinase kinase by v-Raf in NIH 3T3 cells and in vitro. *Science* **257**:1404-1407.

Derijard B, Hibi M, Wu IH, Barrett T, Su B, Deng T, Karin M and Davis RJ (1994) JNK1: a protein kinase stimulated by UV light and Ha-Ras that binds and phosphorylates the c-Jun activation domain. *Cell* **76**:1025-1037.

DeSesso JM (1979) Cell death and free radicals: a mechanism for hydroxyurea teratogenesis. *Med Hypotheses* **5**:937-951.

DeSesso JM (1981) Amelioration of teratogenesis. I. Modification of hydroxyurea-induced teratogenesis by the antioxidant propyl gallate. *Teratology* **24**:19-35.

DeSesso JM and Goeringer GC (1990) Ethoxyquin and nordihydroguaiaretic acid reduce hydroxyurea developmental toxicity. *Reprod Toxicol* **4**:267-275.

DeSesso JM, Scialli AR and Goeringer GC (1994) D-mannitol, a specific hydroxyl free radical scavenger, reduces the developmental toxicity of hydroxyurea in rabbits. *Teratology* **49**:248-259.

Desmots F, Loyer P, Rissel M, Guillouzo A and Morel F (2005) Activation of C-Jun N-terminal kinase is required for glutathione transferase A4 induction during oxidative stress, not during cell proliferation, in mouse hepatocytes. *FEBS Lett* **579**:5691-5696.

Dhanasekaran DN, Kashef K, Lee CM, Xu H and Reddy EP (2007) Scaffold proteins of MAP-kinase modules. *Oncogene* **26**:3185-3202.

Dickinson DA and Forman HJ (2002) Glutathione in defense and signaling: lessons from a small thiol. *Ann N Y Acad Sci* **973**:488-504.

Dickinson DA, Iles KE, Watanabe N, Iwamoto T, Zhang H, Krzywanski DM and Forman HJ (2002) 4-hydroxynonenal induces glutamate cysteine ligase through JNK in HBE1 cells. *Free Radic Biol Med* **33**:974.

Dickinson DA, Moellering DR, Iles KE, Patel RP, Levonen AL, Wigley A, rley-Usmar VM and Forman HJ (2003) Cytoprotection against oxidative stress and the regulation of glutathione synthesis. *Biol Chem* **384**:527-537.

Donovan N, Becker EB, Konishi Y and Bonni A (2002) JNK phosphorylation and activation of BAD couples the stress-activated signaling pathway to the cell death machinery. *J Biol Chem* **277**:40944-40949.

Duan W and Wong WS (2006) Targeting mitogen-activated protein kinases for asthma. *Curr Drug Targets* **7**:691-698.

Dubrulle J, McGrew MJ and Pourquie O (2001) FGF signaling controls somite boundary position and regulates segmentation clock control of spatiotemporal Hox gene activation. *Cell* **106**:219-232.

Dubrulle J and Pourquie O (2004) fgf8 mRNA decay establishes a gradient that couples axial elongation to patterning in the vertebrate embryo. *Nature* **427**:419-422.

Eferl R, Sibilia M, Hilberg F, Fuchsbichler A, Kufferath I, Guertl B, Zenz R, Wagner EF and Zatloukal K (1999) Functions of c-Jun in liver and heart development. *J Cell Biol* **145**:1049-1061.

Eferl R, Zenz R, Theussl HC and Wagner EF (2007) Simultaneous generation of fra-2 conditional and fra-2 knock-out mice. *Genesis* **45**:447-451.

Elsaid AF, Delot EC and Collins MD (2007) Differential perturbation of the Fgf/Erk1/2 and Shh pathways in the C57BL/6N and SWV embryonic limb buds after mid-gestational cadmium chloride administration. *Mol Genet Metab* **92**:258-270.

Engelbrecht AM, Niesler C, Page C and Lochner A (2004) p38 and JNK have distinct regulatory functions on the development of apoptosis during simulated ischaemia and reperfusion in neonatal cardiomyocytes. *Basic Res Cardiol* **99**:338-350.

Enslen H, Raingeaud J and Davis RJ (1998) Selective activation of p38 mitogen-activated protein (MAP) kinase isoforms by the MAP kinase kinases MKK3 and MKK6. *J Biol Chem* **273**:1741-1748.

Errede B, Cade RM, Yashar BM, Kamada Y, Levin DE, Irie K and Matsumoto K (1995) Dynamics and organization of MAP kinase signal pathways. *Mol Reprod Dev* **42**:477-485.

Esterbauer H, Schaur RJ and Zollner H (1991) Chemistry and biochemistry of 4-hydroxynonenal, malonaldehyde and related aldehydes. *Free Radic Biol Med* **11**:81-128.

Estus S, Zaks WJ, Freeman RS, Gruda M, Bravo R and Johnson EM, Jr. (1994) Altered gene expression in neurons during programmed cell death: identification of c-jun as necessary for neuronal apoptosis. *J Cell Biol* **127**:1717-1727.

Fang J and Holmgren A (2006) Inhibition of thioredoxin and thioredoxin reductase by 4-hydroxy-2-nonenal in vitro and in vivo. *J Am Chem Soc* **128**:1879-1885.

Fantel AG and Person RE (2002) Involvement of mitochondria and other free radical sources in normal and abnormal fetal development. *Ann N Y Acad Sci* **959**:424-433.

FDA (2001). http://www.fda.gov/medwatch/SAFETY/2004/feb_PI/Hydrea_PI.pdf

Feng H, Xiang H, Mao YW, Wang J, Liu JP, Huang XQ, Liu Y, Liu SJ, Luo C, Zhang XJ, Liu Y and Li DW (2004) Human Bcl-2 activates ERK signaling pathway to regulate activating protein-1, lens epithelium-derived growth factor and downstream genes. *Oncogene* **23**:7310-7321.

Ferrer-Vaquer A, Maurey P, Firnberg N, Leibbrandt A and Neubuser A (2007) Expression of ASK1 during chick and early mouse development. *Gene Expr Patterns* **7**:808-816.

Flanagan SW, Moseley PL and Buettner GR (1998) Increased flux of free radicals in cells subjected to hyperthermia: detection by electron paramagnetic resonance spin trapping. *FEBS Lett* **431**:285-286.

Fleischmann A, Hafezi F, Elliott C, Reme CE, Ruther U and Wagner EF (2000) Fra-1 replaces c-Fos-dependent functions in mice. *Genes Dev* **14**:2695-2700.

Force T, Bonventre JV, Heidecker G, Rapp U, Avruch J and Kyriakis JM (1994) Enzymatic characteristics of the c-Raf-1 protein kinase. *Proc Natl Acad Sci U S A* **91**:1270-1274.

Fraser FC (1976) The multifactorial/threshold concept -- uses and misuses. *Teratology* **14**:267-280.

Freese EB, Gerson J, Taber H, Rhaese HJ and Freese E (1967) Inactivating DNA alterations induced by peroxides and peroxide-producing agents. *Mutat Res* **4**:517-531.

Fretts RC (2005) Etiology and prevention of stillbirth. *Am J Obstet Gynecol* **193**:1923-1935.

Friguet B, Szweda LI and Stadtman ER (1994) Susceptibility of glucose-6-phosphate dehydrogenase modified by 4-hydroxy-2-nonenal and metal-catalyzed oxidation to proteolysis by the multicatalytic protease. *Arch Biochem Biophys* **311**:168-173.

Futscher BW and Erickson LC (1990) Changes in c-myc and c-fos expression in a human tumor cell line following exposure to bifunctional alkylating agents. *Cancer Res* **50**:62-66.

Gallagher EP, Huisden CM and Gardner JL (2007) Transfection of HepG2 cells with hGSTA4 provides protection against 4-hydroxynonenal-mediated oxidative injury. *Toxicol In Vitro* **21**:1365-1372.

Garrido C, Gurbuxani S, Ravagnan L and Kroemer G (2001) Heat shock proteins: endogenous modulators of apoptotic cell death. *Biochem Biophys Res Commun* **286**:433-442.

Gavin AC and Nebreda AR (1999) A MAP kinase docking site is required for phosphorylation and activation of p90(rsk)/MAPKAP kinase-1. *Curr Biol* **9**:281-284.

Gerard-Monnier D and Chaudiere J (1996) [Metabolism and antioxidant function of glutathione]. *Pathol Biol (Paris)* **44**:77-85.

Gerwins P, Blank JL and Johnson GL (1997) Cloning of a novel mitogen-activated protein kinase kinase kinase, MEKK4, that selectively regulates the c-Jun amino terminal kinase pathway. *J Biol Chem* **272**:8288-8295.

Gius D, Botero A, Shah S and Curry HA (1999) Intracellular oxidation/reduction status in the regulation of transcription factors NF-kappaB and AP-1. *Toxicol Lett* **106**:93-106.

Glinka A, Wu W, Delius H, Monaghan AP, Blumenstock C and Niehrs C (1998) Dickkopf-1 is a member of a new family of secreted proteins and functions in head induction. *Nature* **391**:357-362.

Greco TL, Takada S, Newhouse MM, McMahon JA, McMahon AP and Camper SA (1996) Analysis of the vestigial tail mutation demonstrates that Wnt-3a gene dosage regulates mouse axial development. *Genes Dev* **10**:313-324.

Greiner EF, Guppy M and Brand K (1994) Glucose is essential for proliferation and the glycolytic enzyme induction that provokes a transition to glycolytic energy production. *J Biol Chem* **269**:31484-31490.

Griffith CM, Wiley MJ and Sanders EJ (1992) The vertebrate tail bud: three germ layers from one tissue. *Anat Embryol (Berl)* **185**:101-113.

Griffith OW and Mulcahy RT (1999) The enzymes of glutathione synthesis: gamma-glutamylcysteine synthetase. *Adv Enzymol Relat Areas Mol Biol* **73**:209-67, xii.

Grigoriadis AE, Schellander K, Wang ZQ and Wagner EF (1993) Osteoblasts are target cells for transformation in c-fos transgenic mice. *J Cell Biol* **122**:685-701.

Grigoriadis AE, Wang ZQ, Cecchini MG, Hofstetter W, Felix R, Fleisch HA and Wagner EF (1994) c-Fos: a key regulator of osteoclast-macrophage lineage determination and bone remodeling. *Science* **266**:443-448.

Grotewold L and Ruther U (2002b) The Wnt antagonist Dickkopf-1 is regulated by Bmp signaling and c-Jun and modulates programmed cell death. *EMBO J* **21**:966-975.

Grotewold L and Ruther U (2002a) Bmp, Fgf and Wnt signalling in programmed cell death and chondrogenesis during vertebrate limb development: the role of Dickkopf-1. *Int J Dev Biol* **46**:943-947.

Grotewold L, Theil T and Ruther U (1999) Expression pattern of Dkk-1 during mouse limb development. *Mech Dev* **89**:151-153.

Gruda MC, Kovary K, Metz R and Bravo R (1994) Regulation of Fra-1 and Fra-2 phosphorylation differs during the cell cycle of fibroblasts and phosphorylation in vitro by MAP kinase affects DNA binding activity. *Oncogene* **9**:2537-2547.

Gruda MC, van Amsterdam J, Rizzo CA, Durham SK, Lira S and Bravo R (1996) Expression of FosB during mouse development: normal development of FosB knockout mice. *Oncogene* **12**:2177-2185.

Grune T and Davies KJ (2003) The proteasomal system and HNE-modified proteins. *Mol Aspects Med* **24**:195-204.

Guan Z, Buckman SY, Pentland AP, Templeton DJ and Morrison AR (1998) Induction of cyclooxygenase-2 by the activated MEKK1 --> SEK1/MKK4 --> p38 mitogen-activated protein kinase pathway. *J Biol Chem* **273**:12901-12908.

Gupta S, Barrett T, Whitmarsh AJ, Cavanagh J, Sluss HK, Derijard B and Davis RJ (1996) Selective interaction of JNK protein kinase isoforms with transcription factors. *EMBO J* **15**:2760-2770.

Gupta S, Campbell D, Derijard B and Davis RJ (1995) Transcription factor ATF2 regulation by the JNK signal transduction pathway. *Science* **267**:389-393.

Gustin MC, Albertyn J, Alexander M and Davenport K (1998) MAP kinase pathways in the yeast Saccharomyces cerevisiae. *Microbiol Mol Biol Rev* **62**:1264-1300.

Haddad JJ, Olver RE and Land SC (2000) Antioxidant/pro-oxidant equilibrium regulates HIF-1alpha and NF-kappa B redox sensitivity. Evidence for inhibition by glutathione oxidation in alveolar epithelial cells. *J Biol Chem* **275**:21130-21139.

Hafezi F, Steinbach JP, Marti A, Munz K, Wang ZQ, Wagner EF, Aguzzi A and Reme CE (1997) The absence of c-fos prevents light-induced apoptotic cell death of photoreceptors in retinal degeneration in vivo. *Nat Med* **3**:346-349.

Hai T and Curran T (1991) Cross-family dimerization of transcription factors Fos/Jun and ATF/CREB alters DNA binding specificity. *Proc Natl Acad Sci U S A* **88**:3720-3724.

Hale KK, Trollinger D, Rihanek M and Manthey CL (1999) Differential expression and activation of p38 mitogen-activated protein kinase alpha, beta, gamma, and delta in inflammatory cell lineages. *J Immunol* **162**:4246-4252.

Hales BF and Brown H (1991) The effect of in vivo glutathione depletion with buthionine sulfoximine on rat embryo development. *Teratology* **44**:251-257.

Halliwell B and Aruoma OI (1991) DNA damage by oxygen-derived species. Its mechanism and measurement in mammalian systems. *FEBS Lett* **281**:9-19.

Ham J, Babij C, Whitfield J, Pfarr CM, Lallemand D, Yaniv M and Rubin LL (1995) A c-Jun dominant negative mutant protects sympathetic neurons against programmed cell death. *Neuron* **14**:927-939.

Hansen JM, Carney EW and Harris C (1999) Differential alteration by thalidomide of the glutathione content of rat vs. rabbit conceptuses in vitro. *Reprod Toxicol* **13**:547-554.

Hansen JM and Harris C (2004) A novel hypothesis for thalidomide-induced limb teratogenesis: redox misregulation of the NF-kappaB pathway. *Antioxid Redox Signal* **6**:1-14.

Hansen JM, Harris KK, Philbert MA and Harris C (2002) Thalidomide modulates nuclear redox status and preferentially depletes glutathione in rabbit limb versus rat limb. *J Pharmacol Exp Ther* **300**:768-776.

Hansen JM, Lee E and Harris C (2004) Spatial activities and induction of glutamate-cysteine ligase (GCL) in the postimplantation rat embryo and visceral yolk sac. *Toxicol Sci* **81**:371-378.

Harris C, Fantel AG and Juchau MR (1986) Differential glutathione depletion by L-buthionine-S,R-sulfoximine in rat embryo versus visceral yolk sac in vivo and in vitro. *Biochem Pharmacol* **35**:4437-4441.

Hartley DP, Ruth JA and Petersen DR (1995) The hepatocellular metabolism of 4-hydroxynonenal by alcohol dehydrogenase, aldehyde dehydrogenase, and glutathione S-transferase. *Arch Biochem Biophys* **316**:197-205.

Hatasaka HH (1994) Recurrent miscarriage: epidemiologic factors, definitions, and incidence. *Clin Obstet Gynecol* **37**:625-634.

Henle ES and Linn S (1997) Formation, prevention, and repair of DNA damage by iron/hydrogen peroxide. *J Biol Chem* **272**:19095-19098.

Herber B, Truss M, Beato M and Muller R (1994) Inducible regulatory elements in the human cyclin D1 promoter. *Oncogene* **9**:2105-2107.

Herken R, Merker HJ and Krowke R (1978) Investigation of the effect of hydroxyurea on the cell cycle and the development of necrosis in the embryonic CNS of mice. *Teratology* **18**:103-118.

Hess J, Angel P and Schorpp-Kistner M (2004) AP-1 subunits: quarrel and harmony among siblings. *J Cell Sci* **117**:5965-5973.

Hibi M, Lin A, Smeal T, Minden A and Karin M (1993) Identification of an oncoprotein- and UV-responsive protein kinase that binds and potentiates the c-Jun activation domain. *Genes Dev* **7**:2135-2148.

Hilberg F, Aguzzi A, Howells N and Wagner EF (1993) c-jun is essential for normal mouse development and hepatogenesis. *Nature* **365**:179-181.

Hiranruengchok R and Harris C (1995) Diamide-induced alterations of intracellular thiol status and the regulation of glucose metabolism in the developing rat conceptus in vitro. *Teratology* **52**:205-214.

Hirota K, Matsui M, Iwata S, Nishiyama A, Mori K and Yodoi J (1997) AP-1 transcriptional activity is regulated by a direct association between thioredoxin and Ref-1. *Proc Natl Acad Sci U S A* **94**:3633-3638.

Holmes LB (1997) Impact of the detection and prevention of developmental abnormalities in human studies. *Reprod Toxicol* **11**:267-269.

Horstmann S, Kahle PJ and Borasio GD (1998) Inhibitors of p38 mitogen-activated protein kinase promote neuronal survival in vitro. *J Neurosci Res* **52**:483-490.

Hoshino R, Chatani Y, Yamori T, Tsuruo T, Oka H, Yoshida O, Shimada Y, Ari-i S, Wada H, Fujimoto J and Kohno M (1999) Constitutive activation of the 41-/43-kDa mitogen-activated protein kinase signaling pathway in human tumors. *Oncogene* **18**:813-822.

Hu MC, Qiu WR and Wang YP (1997) JNK1, JNK2 and JNK3 are p53 N-terminal serine 34 kinases. *Oncogene* **15**:2277-2287.

Hubatsch I, Ridderstrom M and Mannervik B (1998) Human glutathione transferase A4-4: an alpha class enzyme with high catalytic efficiency in the conjugation of 4-hydroxynonenal and other genotoxic products of lipid peroxidation. *Biochem J* **330 (Pt 1)**:175-179.

Humphries KM and Szweda LI (1998) Selective inactivation of alpha-ketoglutarate dehydrogenase and pyruvate dehydrogenase: reaction of lipoic acid with 4-hydroxy-2-nonenal. *Biochemistry* **37**:15835-15841.

Hurle JM, Ros MA, Climent V and Garcia-Martinez V (1996) Morphology and significance of programmed cell death in the developing limb bud of the vertebrate embryo. *Microsc Res Tech* **34**:236-246.

Huser M, Luckett J, Chiloeches A, Mercer K, Iwobi M, Giblett S, Sun XM, Brown J, Marais R and Pritchard C (2001) MEK kinase activity is not necessary for Raf-1 function. *EMBO J* **20**:1940-1951.

Hutchison M, Berman KS and Cobb MH (1998) Isolation of TAO1, a protein kinase that activates MEKs in stress-activated protein kinase cascades. *J Biol Chem* **273**:28625-28632.

Hwang SG, Yu SS, Lee SW and Chun JS (2005) Wnt-3a regulates chondrocyte differentiation via c-Jun/AP-1 pathway. *FEBS Lett* **579**:4837-4842.

Ichijo H, Nishida E, Irie K, Ten DP, Saitoh M, Moriguchi T, Takagi M, Matsumoto K, Miyazono K and Gotoh Y (1997) Induction of apoptosis by ASK1, a mammalian MAPKKK that activates SAPK/JNK and p38 signaling pathways. *Science* **275**:90-94.

Ijiri K, Zerbini LF, Peng H, Correa RG, Lu B, Walsh N, Zhao Y, Taniguchi N, Huang XL, Otu H, Wang H, Wang JF, Komiya S, Ducy P, Rahman MU, Flavell RA, Gravallese EM, Oettgen P, Libermann TA and Goldring MB (2005) A novel role for GADD45beta as a mediator of MMP-13 gene expression during chondrocyte terminal differentiation. *J Biol Chem* **280**:38544-38555.

Ishii T, Tatsuda E, Kumazawa S, Nakayama T and Uchida K (2003) Molecular basis of enzyme inactivation by an endogenous electrophile 4-hydroxy-2-nonenal: identification of modification sites in glyceraldehyde-3-phosphate dehydrogenase. *Biochemistry* **42**:3474-3480.

Ishitani R and Chuang DM (1996) Glyceraldehyde-3-phosphate dehydrogenase antisense oligodeoxynucleotides protect against cytosine arabinonucleoside-induced apoptosis in cultured cerebellar neurons. *Proc Natl Acad Sci U S A* **93**:9937-9941.

Ito K, Hirao A, Arai F, Takubo K, Matsuoka S, Miyamoto K, Ohmura M, Naka K, Hosokawa K, Ikeda Y and Suda T (2006) Reactive oxygen species act through p38 MAPK to limit the lifespan of hematopoietic stem cells. *Nat Med* **12**:446-451.

Jin C, Ugai H, Song J, Murata T, Nili F, Sun K, Horikoshi M and Yokoyama KK (2001) Identification of mouse Jun dimerization protein 2 as a novel repressor of ATF-2. *FEBS Lett* **489**:34-41.

Jin EJ, Lee SY, Choi YA, Jung JC, Bang OS and Kang SS (2006) BMP-2-enhanced chondrogenesis involves p38 MAPK-mediated down-regulation of Wnt-7a pathway. *Mol Cells* **22**:353-359.

Jin P and Ringertz NR (1990) Cadmium induces transcription of proto-oncogenes c-jun and c-myc in rat L6 myoblasts. *J Biol Chem* **265**:14061-14064.

Jochum W, Passegue E and Wagner EF (2001) AP-1 in mouse development and tumorigenesis. *Oncogene* **20**:2401-2412.

Johnson RS, Spiegelman BM and Papaioannou V (1992) Pleiotropic effects of a null mutation in the c-fos proto-oncogene. *Cell* **71**:577-586.

Johnson RS, van LB, Papaioannou VE and Spiegelman BM (1993) A null mutation at the c-jun locus causes embryonic lethality and retarded cell growth in culture. *Genes Dev* **7**:1309-1317.

Junttila MR, Li SP and Westermarck J (2007) Phosphatase-mediated crosstalk between MAPK signaling pathways in the regulation of cell survival. *FASEB J.*

Kaina B, Haas S and Kappes H (1997) A general role for c-Fos in cellular protection against DNA-damaging carcinogens and cytostatic drugs. *Cancer Res* **57**:2721-2731.

Kakishita H and Hattori Y (2001) Vascular smooth muscle cell activation and growth by 4-hydroxynonenal. *Life Sci* **69**:689-697.

Kalinich JF, Ramakrishnan R, McClain DE and Ramakrishnan N (2000) 4-Hydroxynonenal, an end-product of lipid peroxidation, induces apoptosis in human leukemic T- and B-cell lines. *Free Radic Res* **33**:349-358.

Kallunki T, Deng T, Hibi M and Karin M (1996) c-Jun can recruit JNK to phosphorylate dimerization partners via specific docking interactions. *Cell* **87**:929-939.

Kallunki T, Su B, Tsigelny I, Sluss HK, Derijard B, Moore G, Davis R and Karin M (1994) JNK2 contains a specificity-determining region responsible for efficient c-Jun binding and phosphorylation. *Genes Dev* **8**:2996-3007.

Kaminska B (2005) MAPK signalling pathways as molecular targets for anti-inflammatory therapy--from molecular mechanisms to therapeutic benefits. *Biochim Biophys Acta* **1754**:253-262.

Kanegae Y, Tavares AT, Izpisua Belmonte JC and Verma IM (1998) Role of Rel/NF-kappaB transcription factors during the outgrowth of the vertebrate limb. *Nature* **392**:611-614.

Kaneto H (2005) The JNK pathway as a therapeutic target for diabetes. *Expert Opin Ther Targets* **9**:581-592.

Kapphahn RJ, Giwa BM, Berg KM, Roehrich H, Feng X, Olsen TW and Ferrington DA (2006) Retinal proteins modified by 4-hydroxynonenal: identification of molecular targets. *Exp Eye Res* **83**:165-175.

Karin M (1995) The regulation of AP-1 activity by mitogen-activated protein kinases. *J Biol Chem* **270**:16483-16486.

Karin M, Liu Z and Zandi E (1997) AP-1 function and regulation. *Curr Opin Cell Biol* **9**:240-246.

Kawakami Y, Rodriguez-Leon J, Koth CM, Buscher D, Itoh T, Raya A, Ng JK, Esteban CR, Takahashi S, Henrique D, Schwarz MF, Asahara H and Izpisua Belmonte JC (2003) MKP3 mediates the cellular response to FGF8 signalling in the vertebrate limb. *Nat Cell Biol* **5**:513-519.

Keesler GA, Bray J, Hunt J, Johnson DA, Gleason T, Yao Z, Wang SW, Parker C, Yamane H, Cole C and Lichenstein HS (1998) Purification and activation of

recombinant p38 isoforms alpha, beta, gamma, and delta. *Protein Expr Purif* **14**:221-228.

Kennedy BJ (1972) Hydroxyurea therapy in chronic myelogenous leukemia. *Cancer* **29**:1052-1056.

Kennedy JC, Memet S and Wells PG (2004) Antisense evidence for nuclear factor-kappaB-dependent embryopathies initiated by phenytoin-enhanced oxidative stress. *Mol Pharmacol* **66**:404-412.

Keppler D (1999) Export pumps for glutathione S-conjugates. *Free Radic Biol Med* **27**:985-991.

Keren A, Tamir Y and Bengal E (2006) The p38 MAPK signaling pathway: a major regulator of skeletal muscle development. *Mol Cell Endocrinol* **252**:224-230.

Kerppola TK and Curran T (1994) Maf and Nrl can bind to AP-1 sites and form heterodimers with Fos and Jun. *Oncogene* **9**:675-684.

Kharbanda S, Saxena S, Yoshida K, Pandey P, Kaneki M, Wang Q, Cheng K, Chen YN, Campbell A, Sudha T, Yuan ZM, Narula J, Weichselbaum R, Nalin C and Kufe D (2000) Translocation of SAPK/JNK to mitochondria and interaction with Bcl-x(L) in response to DNA damage. *J Biol Chem* **275**:322-327.

Kim BJ, Ryu SW and Song BJ (2006) JNK- and p38 kinase-mediated phosphorylation of Bax leads to its activation and mitochondrial translocation and to apoptosis of human hepatoma HepG2 cells. *J Biol Chem* **281**:21256-21265.

Knobloch J, Shaughnessy JD, Jr. and Ruther U (2007) Thalidomide induces limb deformities by perturbing the Bmp/Dkk1/Wnt signaling pathway. *FASEB J* **21**:1410-1421.

Kolbus A, Herr I, Schreiber M, Debatin KM, Wagner EF and Angel P (2000) c-Jun-dependent CD95-L expression is a rate-limiting step in the induction of apoptosis by alkylating agents. *Mol Cell Biol* **20**:575-582.

Korashy HM and El-Kadi AO (2008) The role of redox-sensitive transcription factors NF-kappaB and AP-1 in the modulation of the Cyp1a1 gene by mercury, lead, and copper. *Free Radic Biol Med* **44**:795-806.

Kovacic P and Somanathan R (2006) Mechanism of teratogenesis: electron transfer, reactive oxygen species, and antioxidants. *Birth Defects Res C Embryo Today* **78**:308-325.

Kovary K and Bravo R (1991b) The jun and fos protein families are both required for cell cycle progression in fibroblasts. *Mol Cell Biol* **11**:4466-4472.

Kovary K and Bravo R (1991a) Expression of different Jun and Fos proteins during the G0-to-G1 transition in mouse fibroblasts: in vitro and in vivo associations. *Mol Cell Biol* **11**:2451-2459.

Ku BM, Lee YK, Jeong JY, Mun J, Han JY, Roh GS, Kim HJ, Cho GJ, Choi WS, Yi GS and Kang SS (2007) Ethanol-induced oxidative stress is mediated by p38 MAPK pathway in mouse hippocampal cells. *Neurosci Lett* **419**:64-67.

Kuan CY, Yang DD, Samanta Roy DR, Davis RJ, Rakic P and Flavell RA (1999) The Jnk1 and Jnk2 protein kinases are required for regional specific apoptosis during early brain development. *Neuron* **22**:667-676.

Kurose A, Tanaka T, Huang X, Traganos F and Darzynkiewicz Z (2006) Synchronization in the cell cycle by inhibitors of DNA replication induces histone H2AX phosphorylation: an indication of DNA damage. *Cell Prolif* **39**:231-240.

Kutuk O and Basaga H (2007) Apoptosis signalling by 4-hydroxynonenal: a role for JNK-c-Jun/AP-1 pathway. *Redox Rep* **12**:30-34.

Kwon YW, Ueda S, Ueno M, Yodoi J and Masutani H (2002) Mechanism of p53-dependent apoptosis induced by 3-methylcholanthrene: involvement of p53 phosphorylation and p38 MAPK. *J Biol Chem* **277**:1837-1844.

Kyriakis JM, App H, Zhang XF, Banerjee P, Brautigan DL, Rapp UR and Avruch J (1992) Raf-1 activates MAP kinase-kinase. *Nature* **358**:417-421.

Kyriakis JM and Avruch J (1996) Sounding the alarm: protein kinase cascades activated by stress and inflammation. *J Biol Chem* **271**:24313-24316.

Landschulz WH, Johnson PF and McKnight SL (1988) The leucine zipper: a hypothetical structure common to a new class of DNA binding proteins. *Science* **240**:1759-1764.

Laurora S, Tamagno E, Briatore F, Bardini P, Pizzimenti S, Toaldo C, Reffo P, Costelli P, Dianzani MU, Danni O and Barrera G (2005) 4-Hydroxynonenal modulation of p53 family gene expression in the SK-N-BE neuroblastoma cell line. *Free Radic Biol Med* **38**:215-225.

Lauterburg BH, Smith CV, Hughes H and Mitchell JR (1984) Biliary-Excretion of Glutathione and Glutathione Disulfide in the Rat - Regulation and Response to Oxidative Stress. *Journal of Clinical Investigation* **73**:124-133.

Lawler S, Fleming Y, Goedert M and Cohen P (1998) Synergistic activation of SAPK1/JNK1 by two MAP kinase kinases in vitro. *Curr Biol* **8**:1387-1390.

Le-Niculescu H, Bonfoco E, Kasuya Y, Claret FX, Green DR and Karin M (1999) Withdrawal of survival factors results in activation of the JNK pathway in neuronal cells leading to Fas ligand induction and cell death. *Mol Cell Biol* **19**:751-763.

Leonard DA, Rajaram N and Kerppola TK (1997) Structural basis of DNA bending and oriented heterodimer binding by the basic leucine zipper domains of Fos and Jun. *Proc Natl Acad Sci U S A* **94**:4913-4918.

Leonarduzzi G, Robbesyn F and Poli G (2004) Signaling kinases modulated by 4-hydroxynonenal. *Free Radic Biol Med* **37**:1694-1702.

Leppa S, Saffrich R, Ansorge W and Bohmann D (1998) Differential regulation of c-Jun by ERK and JNK during PC12 cell differentiation. *EMBO J* **17**:4404-4413.

Lewandoski M, Sun X and Martin GR (2000) Fgf8 signalling from the AER is essential for normal limb development. *Nat Genet* **26**:460-463.

Lewis TS, Shapiro PS and Ahn NG (1998) Signal transduction through MAP kinase cascades. *Adv Cancer Res* **74**:49-139.

Li B, Tournier C, Davis RJ and Flavell RA (1999) Regulation of IL-4 expression by the transcription factor JunB during T helper cell differentiation. *EMBO J* **18**:420-432.

Li N and Karin M (1998) Ionizing radiation and short wavelength UV activate NF-kappaB through two distinct mechanisms. *Proc Natl Acad Sci U S A* **95**:13012-13017.

Li N and Karin M (1999) Is NF-kappaB the sensor of oxidative stress? *FASEB J* **13**:1137-1143.

Li Y, Cao Z, Zhu H and Trush MA (2005) Differential roles of 3H-1,2-dithiole-3-thione-induced glutathione, glutathione S-transferase and aldose reductase in protecting against 4-hydroxy-2-nonenal toxicity in cultured cardiomyocytes. *Arch Biochem Biophys* **439**:80-90.

Li YS, Shyy JY, Li S, Lee J, Su B, Karin M and Chien S (1996) The Ras-JNK pathway is involved in shear-induced gene expression. *Mol Cell Biol* **16**:5947-5954.

Lin AW, Barradas M, Stone JC, van AL, Serrano M and Lowe SW (1998) Premature senescence involving p53 and p16 is activated in response to constitutive MEK/MAPK mitogenic signaling. *Genes Dev* **12**:3008-3019.

Liochev SI and Fridovich I (2002) The Haber-Weiss cycle -- 70 years later: an alternative view. *Redox Rep* **7**:55-57.

Lisnock J, Griffin P, Calaycay J, Frantz B, Parsons J, O'Keefe SJ and LoGrasso P (2000) Activation of JNK3 alpha 1 requires both MKK4 and MKK7: kinetic characterization of in vitro phosphorylated JNK3 alpha 1. *Biochemistry* **39**:3141-3148.

Liu J and Lin A (2005) Role of JNK activation in apoptosis: a double-edged sword. *Cell Res* **15**:36-42.

Liu L and Wells PG (1995) DNA oxidation as a potential molecular mechanism mediating drug-induced birth defects: phenytoin and structurally related teratogens initiate the formation of 8-hydroxy-2'-deoxyguanosine in vitro and in vivo in murine maternal hepatic and embryonic tissues. *Free Radic Biol Med* **19**:639-648.

Liu W, Akhand AA, Kato M, Yokoyama I, Miyata T, Kurokawa K, Uchida K and Nakashima I (1999) 4-hydroxynonenal triggers an epidermal growth factor receptor-linked signal pathway for growth inhibition. *J Cell Sci* **112 (Pt 14)**:2409-2417.

Longo L, Vanegas OC, Patel M, Rosti V, Li H, Waka J, Merghoub T, Pandolfi PP, Notaro R, Manova K and Luzzatto L (2002) Maternally transmitted severe glucose 6-phosphate dehydrogenase deficiency is an embryonic lethal. *EMBO J* **21**:4229-4239.

Luo X, Puig O, Hyun J, Bohmann D and Jasper H (2007) Foxo and Fos regulate the decision between cell death and survival in response to UV irradiation. *EMBO J* **26**:380-390.

MacDonald BT, Adamska M and Meisler MH (2004) Hypomorphic expression of Dkk1 in the doubleridge mouse: dose dependence and compensatory interactions with Lrp6. *Development* **131**:2543-2552.

Mackler B, Person RE, Nguyen TD and Fantel AG (1998) Studies of the cellular distribution of superoxide dismutases in adult and fetal rat tissues. *Free Radic Res* **28**:125-129.

MacLaren A, Black EJ, Clark W and Gillespie DA (2004) c-Jun-deficient cells undergo premature senescence as a result of spontaneous DNA damage accumulation. *Mol Cell Biol* **24**:9006-9018.

Maekawa T, Bernier F, Sato M, Nomura S, Singh M, Inoue Y, Tokunaga T, Imai H, Yokoyama M, Reimold A, Glimcher LH and Ishii S (1999) Mouse ATF-2 null mutants display features of a severe type of meconium aspiration syndrome. *J Biol Chem* **274**:17813-17819.

Mahmood R, Bresnick J, Hornbruch A, Mahony C, Morton N, Colquhoun K, Martin P, Lumsden A, Dickson C and Mason I (1995) A role for FGF-8 in the initiation and maintenance of vertebrate limb bud outgrowth. *Curr Biol* **5**:797-806.

Malecki A, Garrido R, Mattson MP, Hennig B and Toborek M (2000) 4-Hydroxynonenal induces oxidative stress and death of cultured spinal cord neurons. *J Neurochem* **74**:2278-2287.

Malemud CJ (2007) Inhibitors of stress-activated protein/mitogen-activated protein kinase pathways. *Curr Opin Pharmacol* **7**:339-343.

Manjon C, Sanchez-Herrero E and Suzanne M (2007) Sharp boundaries of Dpp signalling trigger local cell death required for Drosophila leg morphogenesis. *Nat Cell Biol* **9**:57-63.

March of Dimes (2006) Hidden toll of dying and disabled childern. http://www.marchofdimes.com/

Marinari UM, Nitti M, Pronzato MA and Domenicotti C (2003) Role of PKC-dependent pathways in HNE-induced cell protein transport and secretion. *Mol Aspects Med* **24**:205-211.

Marshall HE, Merchant K and Stamler JS (2000) Nitrosation and oxidation in the regulation of gene expression. *FASEB J* **14**:1889-1900.

Martin G (2001) Making a vertebrate limb: new players enter from the wings. *Bioessays* **23**:865-868.

Martin JH, Mohit AA and Miller CA (1996) Developmental expression in the mouse nervous system of the p493F12 SAP kinase. *Brain Res Mol Brain Res* **35**:47-57.

Matsukawa J, Matsuzawa A, Takeda K and Ichijo H (2004) The ASK1-MAP kinase cascades in mammalian stress response. *J Biochem* **136**:261-265.

Matsuo K, Galson DL, Zhao C, Peng L, Laplace C, Wang KZ, Bachler MA, Amano H, Aburatani H, Ishikawa H and Wagner EF (2004) Nuclear factor of activated T-cells (NFAT) rescues osteoclastogenesis in precursors lacking c-Fos. *J Biol Chem* **279**:26475-26480.

Matsuzawa A and Ichijo H (2008) Redox control of cell fate by MAP kinase: physiological roles of ASK1-MAP kinase pathway in stress signaling. *Biochim Biophys Acta*.

Matsuzuka T, Sakamoto N, Ozawa M, Ushitani A, Hirabayashi M and Kanai Y (2005) Alleviation of maternal hyperthermia-induced early embryonic death by administration of melatonin to mice. *J Pineal Res* **39**:217-223.

Mayeda EA and Bard AJ (1974) Singlet oxygen. The suppression of its production in dismutation of superoxide ion by superoxide dismutase. *J Am Chem Soc* **96**:4023-4024.

McGlinn E and Tabin CJ (2006) Mechanistic insight into how Shh patterns the vertebrate limb. *Curr Opin Genet Dev* **16**:426-432.

Meister A and Tate SS (1976) Glutathione and related gamma-glutamyl compounds: biosynthesis and utilization. *Annu Rev Biochem* **45**:559-604.

Miller DM, Buettner GR and Aust SD (1990) Transition metals as catalysts of "autoxidation" reactions. *Free Radic Biol Med* **8**:95-108.

Millicovsky G and DeSesso JM (1980) Cardiovascular alterations in rabbit embryos in situ after a teratogenic dose of hydroxyurea: an in vivo microscopic study. *Teratology* **22**:115-124.

Mirkes PE, Wilson KL and Cornel LM (2000) Teratogen-induced activation of ERK, JNK, and p38 MAP kinases in early postimplantation murine embryos. *Teratology* **62**:14-25.

Mohit AA, Martin JH and Miller CA (1995) p493F12 kinase: a novel MAP kinase expressed in a subset of neurons in the human nervous system. *Neuron* **14**:67-78.

Moon AM and Capecchi MR (2000) Fgf8 is required for outgrowth and patterning of the limbs. *Nat Genet* **26**:455-459.

Morton S, Davis RJ and Cohen P (2004) Signalling pathways involved in multisite phosphorylation of the transcription factor ATF-2. *FEBS Lett* **572**:177-183.

Mudgett JS, Ding J, Guh-Siesel L, Chartrain NA, Yang L, Gopal S and Shen MM (2000) Essential role for p38alpha mitogen-activated protein kinase in placental angiogenesis. *Proc Natl Acad Sci U S A* **97**:10454-10459.

Mukhopadhyay M, Shtrom S, Rodriguez-Esteban C, Chen L, Tsukui T, Gomer L, Dorward DW, Glinka A, Grinberg A, Huang SP, Niehrs C, Belmonte JC and Westphal H (2001) Dickkopf1 is required for embryonic head induction and limb morphogenesis in the mouse. *Dev Cell* **1**:423-434.

Mulcahy RT and Gipp JJ (1995) Identification of a putative antioxidant response element in the 5'-flanking region of the human gamma-glutamylcysteine synthetase heavy subunit gene. *Biochem Biophys Res Commun* **209**:227-233.

Muller JM, Cahill MA, Rupec RA, Baeuerle PA and Nordheim A (1997) Antioxidants as well as oxidants activate c-fos via Ras-dependent activation of extracellular-signal-regulated kinase 2 and Elk-1. *Eur J Biochem* **244**:45-52.

Murakami M, Sonobe MH, Ui M, Kabuyama Y, Watanabe H, Wada T, Handa H and Iba H (1997) Phosphorylation and high level expression of Fra-2 in v-src transformed cells: a pathway of activation of endogenous AP-1. *Oncogene* **14**:2435-2444.

Musatov A, Carroll CA, Liu YC, Henderson GI, Weintraub ST and Robinson NC (2002) Identification of bovine heart cytochrome c oxidase subunits modified by the lipid peroxidation product 4-hydroxy-2-nonenal. *Biochemistry* **41**:8212-8220.

Nakashima I, Liu W, Akhand AA, Takeda K, Kawamoto Y, Kato M and Suzuki H (2003) 4-hydroxynonenal triggers multistep signal transduction cascades for suppression of cellular functions. *Mol Aspects Med* **24**:231-238.

Naya M, Mataki Y, Takahira H, Deguchi T and Yasuda M (1990) Effects of phorone and/or buthionine sulfoximine on teratogenicity of 5-fluorouracil in mice. *Teratology* **41**:275-280.

Nelson K and Holmes LB (1989) Malformations due to presumed spontaneous mutations in newborn infants. *N Engl J Med* **320**:19-23.

New DA (1978) Whole-embryo culture and the study of mammalian embryos during organogenesis. *Biol Rev Camb Philos Soc* **53**:81-122.

Newell MK, Harper ME, Fortner K, Desbarats J, Russo A and Huber SA (1999) Does the oxidative/glycolytic ratio determine proliferation or death in immune recognition? *Ann N Y Acad Sci* **887**:77-82.

Nicol CJ, Zielenski J, Tsui LC and Wells PG (2000) An embryoprotective role for glucose-6-phosphate dehydrogenase in developmental oxidative stress and chemical teratogenesis. *FASEB J* **14**:111-127.

Niehrs C (2006) Function and biological roles of the Dickkopf family of Wnt modulators. *Oncogene* **25**:7469-7481.

Noguchi K, Yamana H, Kitanaka C, Mochizuki T, Kokubu A and Kuchino Y (2000) Differential role of the JNK and p38 MAPK pathway in c-Myc- and s-Myc-mediated apoptosis. *Biochem Biophys Res Commun* **267**:221-227.

Nowak G and Schnellmann RG (1995) Integrative effects of EGF on metabolism and proliferation in renal proximal tubular cells. *Am J Physiol* **269**:C1317-C1325.

Oh CD, Chang SH, Yoon YM, Lee SJ, Lee YS, Kang SS and Chun JS (2000) Opposing role of mitogen-activated protein kinase subtypes, erk-1/2 and p38, in the regulation of chondrogenesis of mesenchymes. *J Biol Chem* **275**:5613-5619.

Ohuchi H, Nakagawa T, Yamamoto A, Araga A, Ohata T, Ishimaru Y, Yoshioka H, Kuwana T, Nohno T, Yamasaki M, Itoh N and Noji S (1997) The mesenchymal factor, FGF10, initiates and maintains the outgrowth of the chick limb bud through interaction with FGF8, an apical ectodermal factor. *Development* **124**:2235-2244.

Ornoy A (2007) Embryonic oxidative stress as a mechanism of teratogenesis with special emphasis on diabetic embryopathy. *Reprod Toxicol* **24**:31-41.

Ouwens DM, de Ruiter ND, van der Zon GC, Carter AP, Schouten J, van der BC, Kooistra K, Bos JL, Maassen JA and van DH (2002) Growth factors can activate ATF2 via a two-step mechanism: phosphorylation of Thr71 through the Ras-MEK-ERK pathway and of Thr69 through RalGDS-Src-p38. *EMBO J* **21**:3782-3793.

Ozolins TR and Hales BF (1999b) Tissue-specific regulation of glutathione homeostasis and the activator protein-1 (AP-1) response in the rat conceptus. *Biochem Pharmacol* **57**:1165-1175.

Ozolins TR and Hales BF (1999a) Post-translational regulation of AP-1 transcription factor DNA-binding activity in the rat conceptus. *Mol Pharmacol* **56**:537-544.

Ozolins TR and Hales BF (1997) Oxidative stress regulates the expression and activity of transcription factor activator protein-1 in rat conceptus. *J Pharmacol Exp Ther* **280**:1085-1093.

Ozolins TR, Harrouk W, Doerksen T, Trasler JM and Hales BF (2002) Buthionine sulfoximine embryotoxicity is associated with prolonged AP-1 activation. *Teratology* **66**:192-200.

Paliga AJ, Natale DR and Watson AJ (2005) p38 mitogen-activated protein kinase (MAPK) first regulates filamentous actin at the 8-16-cell stage during preimplantation development. *Biol Cell* **97**:629-640.

Paniagua-Castro N, Escalona-Cardoso G, Madrigal-Bujaidar E, Martinez-Galero E and Chamorro-Cevallos G (2008) Protection against cadmium-induced teratogenicity in vitro by glycine. *Toxicol In Vitro* **22**:75-79.

Parola M, Robino G, Marra F, Pinzani M, Bellomo G, Leonarduzzi G, Chiarugi P, Camandola S, Poli G, Waeg G, Gentilini P and Dianzani MU (1998) HNE interacts directly with JNK isoforms in human hepatic stellate cells. *J Clin Invest* **102**:1942-1950.

Pastor N, Weinstein H, Jamison E and Brenowitz M (2000) A detailed interpretation of OH radical footprints in a TBP-DNA complex reveals the role of dynamics in the mechanism of sequence-specific binding. *J Mol Biol* **304**:55-68.

Patel L, Abate C and Curran T (1990) Altered protein conformation on DNA binding by Fos and Jun. *Nature* **347**:572-575.

Pearson G, Robinson F, Beers GT, Xu BE, Karandikar M, Berman K and Cobb MH (2001) Mitogen-activated protein (MAP) kinase pathways: regulation and physiological functions. *Endocr Rev* **22**:153-183.

Platanias LC (2003) The p38 mitogen-activated protein kinase pathway and its role in interferon signaling. *Pharmacol Ther* **98**:129-142.

Platt OS, Orkin SH, Dover G, Beardsley GP, Miller B and Nathan DG (1984) Hydroxyurea enhances fetal hemoglobin production in sickle cell anemia. *J Clin Invest* **74**:652-656.

Poggi SH, Goodwin KM, Hill JM, Brenneman DE, Tendi E, Schninelli S and Spong CY (2003) Differential expression of c-fos in a mouse model of fetal alcohol syndrome. *Am J Obstet Gynecol* **189**:786-789.

Poli G, Schaur RJ, Siems WG and Leonarduzzi G (2007) 4-Hydroxynonenal: A membrane lipid oxidation product of medicinal interest. *Med Res Rev.*

Pourquie O (2001) Vertebrate somitogenesis. *Annu Rev Cell Dev Biol* **17**:311-350.

Pramanik R, Qi X, Borowicz S, Choubey D, Schultz RM, Han J and Chen G (2003) p38 isoforms have opposite effects on AP-1-dependent transcription through regulation of c-Jun. The determinant roles of the isoforms in the p38 MAPK signal specificity. *J Biol Chem* **278**:4831-4839.

Pugazhenthi S, Phansalkar K, Audesirk G, West A and Cabell L (2006) Differential regulation of c-jun and CREB by acrolein and 4-hydroxynonenal. *Free Radic Biol Med* **40**:21-34.

Qiang M and Ticku MK (2005) Role of AP-1 in ethanol-induced N-methyl-D-aspartate receptor 2B subunit gene up-regulation in mouse cortical neurons. *J Neurochem* **95**:1332-1341.

Ramesh GT, Manna SK, Aggarwal BB and Jadhav AL (1999) Lead activates nuclear transcription factor-kappaB, activator protein-1, and amino-terminal c-Jun kinase in pheochromocytoma cells. *Toxicol Appl Pharmacol* **155**:280-286.

Raza H and John A (2006) 4-hydroxynonenal induces mitochondrial oxidative stress, apoptosis and expression of glutathione S-transferase A4-4 and cytochrome P450 2E1 in PC12 cells. *Toxicol Appl Pharmacol* **216**:309-318.

Rebollo A, Dumoutier L, Renauld JC, Zaballos A, Ayllon V and Martinez A (2000) Bcl-3 expression promotes cell survival following interleukin-4 deprivation and is controlled by AP1 and AP1-like transcription factors. *Mol Cell Biol* **20**:3407-3416.

Ritter EJ, Scott WJ and Wilson JG (1973) Relationship of temporal patterns of cell death and development to malformations in the rat limb. Possible mechanisms of teratogenesis with inhibitors of DNA synthesis. *Teratology* **7**:219-225.

Rittner HL, Hafner V, Klimiuk PA, Szweda LI, Goronzy JJ and Weyand CM (1999) Aldose reductase functions as a detoxification system for lipid peroxidation products in vasculitis. *J Clin Invest* **103**:1007-1013.

Rodriguez-Bravo V, Guaita-Esteruelas S, Salvador N, Bachs O and Agell N (2007) Different S/M checkpoint responses of tumor and non tumor cell lines to DNA replication inhibition. *Cancer Res* **67**:11648-11656.

Ruef J, Rao GN, Li F, Bode C, Patterson C, Bhatnagar A and Runge MS (1998) Induction of rat aortic smooth muscle cell growth by the lipid peroxidation product 4-hydroxy-2-nonenal. *Circulation* **97**:1071-1078.

Sabapathy K, Jochum W, Hochedlinger K, Chang L, Karin M and Wagner EF (1999) Defective neural tube morphogenesis and altered apoptosis in the absence of both JNK1 and JNK2. *Mech Dev* **89**:115-124.

Sabio G, Arthur JS, Kuma Y, Peggie M, Carr J, Murray-Tait V, Centeno F, Goedert M, Morrice NA and Cuenda A (2005) p38gamma regulates the localisation of SAP97 in the cytoskeleton by modulating its interaction with GKAP. *EMBO J* **24**:1134-1145.

Sahambi SK and Hales BF (2006) Exposure to 5-bromo-2'-deoxyuridine induces oxidative stress and activator protein-1 DNA binding activity in the embryo. *Birth Defects Res A Clin Mol Teratol* **76**:580-591.

Sakano S, Murata Y, Iwata H, Sato K, Ito T, Kurokouchi K and Seo H (1997) Protooncogene expression in osteogenesis induced by bone morphogenetic protein. *Clin Orthop*240-246.

Salmeron A, Ahmad TB, Carlile GW, Pappin D, Narsimhan RP and Ley SC (1996) Activation of MEK-1 and SEK-1 by Tpl-2 proto-oncoprotein, a novel MAP kinase kinase kinase. *EMBO J* **15**:817-826.

Sampey BP, Carbone DL, Doorn JA, Drechsel DA and Petersen DR (2007) 4-Hydroxy-2-nonenal adduction of extracellular signal-regulated kinase (Erk) and the inhibition of hepatocyte Erk-Est-like protein-1-activating protein-1 signal transduction. *Mol Pharmacol* **71**:871-883.

Sanders DD and Stephens TD (1991) Review of drug-induced limb defects in mammals. *Teratology* **44**:335-354.

Sanyal MK and Wiebke EA (1979) Oxygen requirement for in vitro growth and differentiation of the rat conceptus during organogenesis phase of embryo development. *Biol Reprod* **20**:639-647.

Schaur RJ (2003) Basic aspects of the biochemical reactivity of 4-hydroxynonenal. *Mol Aspects Med* **24**:149-159.

Schorpp-Kistner M, Wang ZQ, Angel P and Wagner EF (1999) JunB is essential for mammalian placentation. *EMBO J* **18**:934-948.

Schreiber M, Kolbus A, Piu F, Szabowski A, Mohle-Steinlein U, Tian J, Karin M, Angel P and Wagner EF (1999) Control of cell cycle progression by c-Jun is p53 dependent. *Genes Dev* **13**:607-619.

Schreiber M, Wang ZQ, Jochum W, Fetka I, Elliott C and Wagner EF (2000) Placental vascularisation requires the AP-1 component fra1. *Development* **127**:4937-4948.

Scott WJ, Ritter EJ and Wilson JG (1971a) DNA synthesis inhibition and cell death associated with hydroxyurea teratogenesis in rat embryos. *Dev Biol* **26**:306-315.

Scott WJ, Ritter EJ and Wilson JG (1971b) DNA synthesis inhibition and cell death associated with hydroxyurea teratogenesis in rat embryos. *Dev Biol* **26**:306-315.

Sears R, Leone G, DeGregori J and Nevins JR (1999) Ras enhances Myc protein stability. *Mol Cell* **3**:169-179.

Sears RC and Nevins JR (2002) Signaling networks that link cell proliferation and cell fate. *J Biol Chem* **277**:11617-11620.

Sekine K, Ohuchi H, Fujiwara M, Yamasaki M, Yoshizawa T, Sato T, Yagishita N, Matsui D, Koga Y, Itoh N and Kato S (1999) Fgf10 is essential for limb and lung formation. *Nat Genet* **21**:138-141.

Serafini MT, Arola L and Romeu A (1991) Glutathione and Related Enzyme-Activity in the 11-Day Rat Embryo, Placenta and Perinatal Rat-Liver. *Biology of the Neonate* **60**:236-242.

Sevanian A and Hochstein P (1985) Mechanisms and consequences of lipid peroxidation in biological systems. *Annu Rev Nutr* **5**:365-390.

Sever L, Lynberg MC and Edmonds LD (1993) The impact of congenital malformations on public health. *Teratology* **48**:547-549.

Sharma R, Brown D, Awasthi S, Yang Y, Sharma A, Patrick B, Saini MK, Singh SP, Zimniak P, Singh SV and Awasthi YC (2004) Transfection with 4-hydroxynonenal-metabolizing glutathione S-transferase isozymes leads to phenotypic transformation and immortalization of adherent cells. *Eur J Biochem* **271**:1690-1701.

Shaulian E and Karin M (2002) AP-1 as a regulator of cell life and death. *Nat Cell Biol* **4**:E131-E136.

Shaulian E, Schreiber M, Piu F, Beeche M, Wagner EF and Karin M (2000) The mammalian UV response: c-Jun induction is required for exit from p53-imposed growth arrest. *Cell* **103**:897-907.

Shen Q, Uray IP, Li Y, Krisko TI, Strecker TE, Kim HT and Brown PH (2008) The AP-1 transcription factor regulates breast cancer cell growth via cyclins and E2F factors. *Oncogene* **27**:366-377.

Shepard TH, Muffley LA and Smith LT (1998) Ultrastructural study of mitochondria and their cristae in embryonic rats and primate (N. nemistrina). *Anat Rec* **252**:383-392.

Shepard TH, Tanimura T and Robkin MA (1970) Energy metabolism in early mammalian embryos. *Symp Soc Dev Biol* **29**:42-58.

Shi ZZ, Osei-Frimpong J, Kala G, Kala SV, Barrios RJ, Habib GM, Lukin DJ, Danney CM, Matzuk MM and Lieberman MW (2000) Glutathione synthesis is essential for mouse development but not for cell growth in culture. *Proc Natl Acad Sci U S A* **97**:5101-5106.

Shifley ET and Cole SE (2007) The vertebrate segmentation clock and its role in skeletal birth defects. *Birth Defects Res C Embryo Today* **81**:121-133.

Shin SY, Kim CG, Jho EH, Rho MS, Kim YS, Kim YH and Lee YH (2004) Hydrogen peroxide negatively modulates Wnt signaling through downregulation of beta-catenin. *Cancer Lett* **212**:225-231.

Siems W and Grune T (2003) Intracellular metabolism of 4-hydroxynonenal. *Mol Aspects Med* **24**:167-175.

Skinner M, Qu S, Moore C and Wisdom R (1997) Transcriptional activation and transformation by FosB protein require phosphorylation of the carboxyl-terminal activation domain. *Mol Cell Biol* **17**:2372-2380.

Slott VL and Hales BF (1987b) Protection of rat embryos in culture against the embryotoxicity of acrolein using exogenous glutathione. *Biochem Pharmacol* **36**:2187-2194.

Slott VL and Hales BF (1987a) Effect of glutathione depletion by buthionine sulfoximine on rat embryonic development in vitro. *Biochem Pharmacol* **36**:683-688.

Sluss HK and Davis RJ (2006) H2AX is a target of the JNK signaling pathway that is required for apoptotic DNA fragmentation. *Mol Cell* **23**:152-153.

Sneeden JL and Loeb LA (2004) Mutations in the R2 subunit of ribonucleotide reductase that confer resistance to hydroxyurea. *J Biol Chem* **279**:40723-40728.

Solis WA, Dalton TP, Dieter MZ, Freshwater S, Harrer JM, He L, Shertzer HG and Nebert DW (2002) Glutamate-cysteine ligase modifier subunit: mouse Gclm gene structure and regulation by agents that cause oxidative stress. *Biochem Pharmacol* **63**:1739-1754.

Soshnikova N, Zechner D, Huelsken J, Mishina Y, Behringer RR, Taketo MM, Crenshaw EB, III and Birchmeier W (2003) Genetic interaction between Wnt/beta-catenin and BMP receptor signaling during formation of the AER and the dorsal-ventral axis in the limb. *Genes Dev* **17**:1963-1968.

Srinivasan S, Hatley ME, Bolick DT, Palmer LA, Edelstein D, Brownlee M and Hedrick CC (2004) Hyperglycaemia-induced superoxide production decreases eNOS expression via AP-1 activation in aortic endothelial cells. *Diabetologia* **47**:1727-1734.

Srivastava S, Chandra A, Bhatnagar A, Srivastava SK and Ansari NH (1995) Lipid peroxidation product, 4-hydroxynonenal and its conjugate with GSH are excellent substrates of bovine lens aldose reductase. *Biochem Biophys Res Commun* **217**:741-746.

Stokoe D, Campbell DG, Nakielny S, Hidaka H, Leevers SJ, Marshall C and Cohen P (1992) MAPKAP kinase-2; a novel protein kinase activated by mitogen-activated protein kinase. *EMBO J* **11**:3985-3994.

Stubbe J (1990) Ribonucleotide reductases. *Adv Enzymol Relat Areas Mol Biol* **63**:349-419.

Suliman HB, Ali M and Piantadosi CA (2004) Superoxide dismutase-3 promotes full expression of the EPO response to hypoxia. *Blood* **104**:43-50.

Summerbell D (1974) A quantitative analysis of the effect of excision of the AER from the chick limb-bud. *J Embryol Exp Morphol* **32**:651-660.

Sunjic SB, Cipak A, Rabuzin F, Wildburger R and Zarkovic N (2005) The influence of 4-hydroxy-2-nonenal on proliferation, differentiation and apoptosis of human osteosarcoma cells. *Biofactors* **24**:141-148.

Szapacs ME, Riggins JN, Zimmerman LJ and Liebler DC (2006) Covalent adduction of human serum albumin by 4-hydroxy-2-nonenal: kinetic analysis of competing alkylation reactions. *Biochemistry* **45**:10521-10528.

Takeda K, Hatai T, Hamazaki TS, Nishitoh H, Saitoh M and Ichijo H (2000) Apoptosis signal-regulating kinase 1 (ASK1) induces neuronal differentiation and survival of PC12 cells. *J Biol Chem* **275**:9805-9813.

Takekawa M, Posas F and Saito H (1997) A human homolog of the yeast Ssk2/Ssk22 MAP kinase kinase kinases, MTK1, mediates stress-induced activation of the p38 and JNK pathways. *EMBO J* **16**:4973-4982.

Tam PP (1984) The histogenetic capacity of tissues in the caudal end of the embryonic axis of the mouse. *J Embryol Exp Morphol* **82**:253-266.

Tam PP and Tan SS (1992) The somitogenetic potential of cells in the primitive streak and the tail bud of the organogenesis-stage mouse embryo. *Development* **115**:703-715.

Tanimura T and Shepard TH (1970) Glucose metabolism by rat embryos in vitro. *Proc Soc Exp Biol Med* **135**:51-54.

Tanos T, Marinissen MJ, Leskow FC, Hochbaum D, Martinetto H, Gutkind JS and Coso OA (2005) Phosphorylation of c-Fos by members of the p38 MAPK family. Role in the AP-1 response to UV light. *J Biol Chem* **280**:18842-18852.

Thauvin-Robinet C, Maingueneau C, Robert E, Elefant E, Guy H, Caillot D, Casasnovas RO, Douvier S and Nivelon-Chevallier A (2001) Exposure to hydroxyurea during pregnancy: a case series. *Leukemia* **15**:1309-1311.

The March of Dimes global report on birth defect, the hidden toll of dying and disabled children (2006). http: // www. Marchofdimes.com/professionals/871_18587.asp port on Birth Defects.

Thelander L and Reichard P (1979) Reduction of ribonucleotides. *Annu Rev Biochem* **48**:133-158.

Thepot D, Weitzman JB, Barra J, Segretain D, Stinnakre MG, Babinet C and Yaniv M (2000) Targeted disruption of the murine junD gene results in multiple defects in male reproductive function. *Development* **127**:143-153.

Tobiume K, Matsuzawa A, Takahashi T, Nishitoh H, Morita K, Takeda K, Minowa O, Miyazono K, Noda T and Ichijo H (2001) ASK1 is required for sustained activations of JNK/p38 MAP kinases and apoptosis. *EMBO Rep* **2**:222-228.

Torres M and Forman HJ (2003) Redox signaling and the MAP kinase pathways. *Biofactors* **17**:287-296.

Tran P, Hiou-Tim F, Frosst P, Lussier-Cacan S, Bagley P, Selhub J, Bottiglieri T and Rozen R (2002) The curly-tail (ct) mouse, an animal model of neural tube defects, displays altered homocysteine metabolism without folate responsiveness or a defect in Mthfr. *Mol Genet Metab* **76**:297-304.

Troppmair J, Bruder JT, Munoz H, Lloyd PA, Kyriakis J, Banerjee P, Avruch J and Rapp UR (1994) Mitogen-activated protein kinase/extracellular signal-regulated protein kinase activation by oncogenes, serum, and 12-O-tetradecanoylphorbol-13-acetate requires Raf and is necessary for transformation. *J Biol Chem* **269**:7030-7035.

Tsuchiya Y, Okuno Y, Hishinuma K, Ezaki A, Okada G, Yamaguchi M, Chikuma T and Hojo H (2007) 4-Hydroxy-2-nonenal-modified glyceraldehyde-3-phosphate dehydrogenase is degraded by cathepsin G. *Free Radic Biol Med* **43**:1604-1615.

Tufan AC, Daumer KM, DeLise AM and Tuan RS (2002) AP-1 transcription factor complex is a target of signals from both WnT-7a and N-cadherin-dependent cell-cell adhesion complex during the regulation of limb mesenchymal chondrogenesis. *Exp Cell Res* **273**:197-203.

Turjanski AG, Vaque JP and Gutkind JS (2007) MAP kinases and the control of nuclear events. *Oncogene* **26**:3240-3253.

Turner NA, Xia F, Azhar G, Zhang X, Liu L and Wei JY (1998) Oxidative stress induces DNA fragmentation and caspase activation via the c-Jun NH2-terminal kinase pathway in H9c2 cardiac muscle cells. *J Mol Cell Cardiol* **30**:1789-1801.

Uchida K (2003) 4-Hydroxy-2-nonenal: a product and mediator of oxidative stress. *Prog Lipid Res* **42**:318-343.

Uchida K, Shiraishi M, Naito Y, Torii Y, Nakamura Y and Osawa T (1999) Activation of stress signaling pathways by the end product of lipid peroxidation. 4-hydroxy-2-nonenal is a potential inducer of intracellular peroxide production. *J Biol Chem* **274**:2234-2242.

Uchida K and Stadtman ER (1993) Covalent attachment of 4-hydroxynonenal to glyceraldehyde-3-phosphate dehydrogenase. A possible involvement of intra- and intermolecular cross-linking reaction. *J Biol Chem* **268**:6388-6393.

Ullrich A and Schlessinger J (1990) Signal transduction by receptors with tyrosine kinase activity. *Cell* **61**:203-212.

Valko M, Rhodes CJ, Moncol J, Izakovic M and Mazur M (2006) Free radicals, metals and antioxidants in oxidative stress-induced cancer. *Chem Biol Interact* **160**:1-40.

Valpuesta JM, Martin-Benito J, Gomez-Puertas P, Carrascosa JL and Willison KR (2002) Structure and function of a protein folding machine: the eukaryotic cytosolic chaperonin CCT. *FEBS Lett* **529**:11-16.

van HR, Eggermont AM and ten Hagen TL (2006) Endothelial monocyte-activating polypeptide-II and its functions in (patho)physiological processes. *Cytokine Growth Factor Rev* **17**:339-348.

Vander Heiden MG, Plas DR, Rathmell JC, Fox CJ, Harris MH and Thompson CB (2001) Growth factors can influence cell growth and survival through effects on glucose metabolism. *Mol Cell Biol* **21**:5899-5912.

Venugopal R and Jaiswal AK (1998) Nrf2 and Nrf1 in association with Jun proteins regulate antioxidant response element-mediated expression and coordinated induction of genes encoding detoxifying enzymes. *Oncogene* **17**:3145-3156.

Verma IM, Stevenson JK, Schwarz EM, Van Antwerp D and Miyamoto S (1995) Rel/NF-kappa B/I kappa B family: intimate tales of association and dissociation. *Genes Dev* **9**:2723-2735.

Vindis C, Escargueil-Blanc I, Elbaz M, Marcheix B, Grazide MH, Uchida K, Salvayre R and Negre-Salvayre A (2006) Desensitization of platelet-derived growth factor receptor-beta by oxidized lipids in vascular cells and atherosclerotic lesions: prevention by aldehyde scavengers. *Circ Res* **98**:785-792.

Vindis C, Escargueil-Blanc I, Uchida K, Elbaz M, Salvayre R and Negre-Salvayre A (2007) Lipid oxidation products and oxidized low-density lipoproteins impair platelet-derived growth factor receptor activity in smooth muscle cells: implication in atherosclerosis. *Redox Rep* **12**:96-100.

Waas WF, Lo HH and Dalby KN (2001) The kinetic mechanism of the dual phosphorylation of the ATF2 transcription factor by p38 mitogen-activated protein (MAP) kinase alpha. Implications for signal/response profiles of MAP kinase pathways. *J Biol Chem* **276**:5676-5684.

Wada T, Stepniak E, Hui L, Leibbrandt A, Katada T, Nishina H, Wagner EF and Penninger JM (2007) Antagonistic control of cell fates by JNK and p38-MAPK signaling. *Cell Death Differ*.

Wang XZ and Ron D (1996) Stress-induced phosphorylation and activation of the transcription factor CHOP (GADD153) by p38 MAP Kinase. *Science* **272**:1347-1349.

Wang ZQ, Liang J, Schellander K, Wagner EF and Grigoriadis AE (1995) c-fos-induced osteosarcoma formation in transgenic mice: cooperativity with c-jun and the role of endogenous c-fos. *Cancer Res* **55**:6244-6251.

Wang ZQ, Ovitt C, Grigoriadis AE, Mohle-Steinlein U, Ruther U and Wagner EF (1992) Bone and haematopoietic defects in mice lacking c-fos. *Nature* **360**:741-745.

Ward IM and Chen J (2001) Histone H2AX is phosphorylated in an ATR-dependent manner in response to replicational stress. *J Biol Chem* **276**:47759-47762.

Wells PG, Bhuller Y, Chen CS, Jeng W, Kasapinovic S, Kennedy JC, Kim PM, Laposa RR, McCallum GP, Nicol CJ, Parman T, Wiley MJ and Wong AW (2005) Molecular and biochemical mechanisms in teratogenesis involving reactive oxygen species. *Toxicol Appl Pharmacol* **207**:354-366.

Wells PG, Kim PM, Laposa RR, Nicol CJ, Parman T and Winn LM (1997) Oxidative damage in chemical teratogenesis. *Mutat Res* **396**:65-78.

Wentzel P, Gareskog M and Eriksson UJ (2005) Folic acid supplementation diminishes diabetes- and glucose-induced dysmorphogenesis in rat embryos in vivo and in vitro. *Diabetes* **54**:546-553.

Wentzel P, Thunberg L and Eriksson UJ (1997) Teratogenic effect of diabetic serum is prevented by supplementation of superoxide dismutase and N-acetylcysteine in rat embryo culture. *Diabetologia* **40**:7-14.

White BP, Davies MH and Schnell RC (1987) Circadian variations in hepatic glutathione content, gamma-glutamylcysteine synthetase and gamma-glutamyl transferase activities in mice. *Toxicol Lett* **35**:217-223.

Whitfield J, Neame SJ, Paquet L, Bernard O and Ham J (2001) Dominant-negative c-Jun promotes neuronal survival by reducing BIM expression and inhibiting mitochondrial cytochrome c release. *Neuron* **29**:629-643.

Widmann C, Gibson S, Jarpe MB and Johnson GL (1999) Mitogen-activated protein kinase: conservation of a three-kinase module from yeast to human. *Physiol Rev* **79**:143-180.

Wilcox AJ, Baird DD and Weinberg CR (1999) Time of implantation of the conceptus and loss of pregnancy. *N Engl J Med* **340**:1796-1799.

Wilson JG, Scott WJ, Ritter EJ and Fradkin R (1975) Comparative distribution and embryotoxicity of hydroxyurea in pregnant rats and rhesus monkeys. *Teratology* **11**:169-178.

Wisdom R (1999) AP-1: one switch for many signals. *Exp Cell Res* **253**:180-185.

Wisdom R, Johnson RS and Moore C (1999) c-Jun regulates cell cycle progression and apoptosis by distinct mechanisms. *EMBO J* **18**:188-197.

Wong M, Helston LM and Wells PG (1989) Enhancement of murine phenytoin teratogenicity by the gamma-glutamylcysteine synthetase inhibitor L-buthionine-(S,R)-sulfoximine and by the glutathione depletor diethyl maleate. *Teratology* **40**:127-141.

Woo GH, Bak EJ, Nakayama H and Doi K (2005) Hydroxyurea (HU)-induced apoptosis in the mouse fetal lung. *Exp Mol Pathol* **79**:59-67.

Woo GH, Katayama K, Jung JY, Uetsuka K, Bak EJ, Nakayama H and Doi K (2003) Hydroxyurea (HU)-induced apoptosis in the mouse fetal tissues. *Histol Histopathol* **18**:387-392.

Wu J, Harrison JK, Vincent LA, Haystead C, Haystead TA, Michel H, Hunt DF, Lynch KR and Sturgill TW (1993) Molecular structure of a protein-tyrosine/threonine kinase activating p42 mitogen-activated protein (MAP) kinase: MAP kinase kinase. *Proc Natl Acad Sci U S A* **90**:173-177.

Xanthoudakis S and Curran T (1992) Identification and characterization of Ref-1, a nuclear protein that facilitates AP-1 DNA-binding activity. *EMBO J* **11**:653-665.

Xanthoudakis S, Miao GG and Curran T (1994) The redox and DNA-repair activities of Ref-1 are encoded by nonoverlapping domains. *Proc Natl Acad Sci U S A* **91**:23-27.

Xu Q, Konta T, Nakayama K, Furusu A, Moreno-Manzano V, Lucio-Cazana J, Ishikawa Y, Fine LG, Yao J and Kitamura M (2004) Cellular defense against H2O2-induced apoptosis via MAP kinase-MKP-1 pathway. *Free Radic Biol Med* **36**:985-993.

Yamaguchi K, Shirakabe K, Shibuya H, Irie K, Oishi I, Ueno N, Taniguchi T, Nishida E and Matsumoto K (1995) Identification of a member of the MAPKKK family as a potential mediator of TGF-beta signal transduction. *Science* **270**:2008-2011.

Yamamoto K, Ichijo H and Korsmeyer SJ (1999) BCL-2 is phosphorylated and inactivated by an ASK1/Jun N-terminal protein kinase pathway normally activated at G(2)/M. *Mol Cell Biol* **19**:8469-8478.

Yan J and Hales BF (2005) Activator protein-1 (AP-1) DNA binding activity is induced by hydroxyurea in organogenesis stage mouse embryos. *Toxicol Sci* **85**:1013-1023.

Yan J and Hales BF (2006) Depletion of glutathione induces 4-hydroxynonenal protein adducts and hydroxyurea teratogenicity in the organogenesis stage mouse embryo. *J Pharmacol Exp Ther* **319**:613-621.

Yan JX, Wait R, Berkelman T, Harry RA, Westbrook JA, Wheeler CH and Dunn MJ (2000) A modified silver staining protocol for visualization of proteins compatible with matrix-assisted laser desorption/ionization and electrospray ionization-mass spectrometry. *Electrophoresis* **21**:3666-3672.

Yang DD, Kuan CY, Whitmarsh AJ, Rincon M, Zheng TS, Davis RJ, Rakic P and Flavell RA (1997) Absence of excitotoxicity-induced apoptosis in the hippocampus of mice lacking the Jnk3 gene. *Nature* **389**:865-870.

Yang SH, Whitmarsh AJ, Davis RJ and Sharrocks AD (1998) Differential targeting of MAP kinases to the ETS-domain transcription factor Elk-1. *EMBO J* **17**:1740-1749.

Yang Y, Cheng JZ, Singhal SS, Saini M, Pandya U, Awasthi S and Awasthi YC (2001) Role of glutathione S-transferases in protection against lipid peroxidation. Overexpression of hGSTA2-2 in K562 cells protects against hydrogen peroxide-induced apoptosis and inhibits JNK and caspase 3 activation. *J Biol Chem* **276**:19220-19230.

Yu C, Minemoto Y, Zhang J, Liu J, Tang F, Bui TN, Xiang J and Lin A (2004) JNK suppresses apoptosis via phosphorylation of the proapoptotic Bcl-2 family protein BAD. *Mol Cell* **13**:329-340.

Yuan Q, Zhu X and Sayre LM (2007) Chemical nature of stochastic generation of protein-based carbonyls: metal-catalyzed oxidation versus modification by products of lipid oxidation. *Chem Res Toxicol* **20**:129-139.

Zanke BW, Boudreau K, Rubie E, Winnett E, Tibbles LA, Zon L, Kyriakis J, Liu FF and Woodgett JR (1996) The stress-activated protein kinase pathway mediates cell death following injury induced by cis-platinum, UV irradiation or heat. *Curr Biol* **6**:606-613.

Zarkovic N (2003) 4-hydroxynonenal as a bioactive marker of pathophysiological processes. *Mol Aspects Med* **24**:281-291.

Zarubin T and Han J (2005) Activation and signaling of the p38 MAP kinase pathway. *Cell Res* **15**:11-18.

Zenz R and Wagner EF (2006) Jun signalling in the epidermis: From developmental defects to psoriasis and skin tumors. *Int J Biochem Cell Biol* **38**:1043-1049.

Zhang L, Wang W, Hayashi Y, Jester JV, Birk DE, Gao M, Liu CY, Kao WW, Karin M and Xia Y (2003) A role for MEK kinase 1 in TGF-beta/activin-induced epithelium movement and embryonic eyelid closure. *EMBO J* **22**:4443-4454.

Zhang S, Lin Y, Kim YS, Hande MP, Liu ZG and Shen HM (2007) c-Jun N-terminal kinase mediates hydrogen peroxide-induced cell death via sustained poly(ADP-ribose) polymerase-1 activation. *Cell Death Differ* **14**:1001-1010.

Zhao W, Mosley BS, Cleves MA, Melnyk S, James SJ and Hobbs CA (2006) Neural tube defects and maternal biomarkers of folate, homocysteine, and glutathione metabolism. *Birth Defects Res A Clin Mol Teratol* **76**:230-236.

Zhao Y, Bjorbaek C and Moller DE (1996) Regulation and interaction of pp90(rsk) isoforms with mitogen-activated protein kinases. *J Biol Chem* **271**:29773-29779.

Zhou Q, Lam PY, Han D and Cadenas E (2008) c-Jun N-terminal kinase regulates mitochondrial bioenergetics by modulating pyruvate dehydrogenase activity in primary cortical neurons. *J Neurochem* **104**:325-335.

Zinaman MJ, Clegg ED, Brown CC, O'Connor J and Selevan SG (1996) Estimates of human fertility and pregnancy loss. *Fertil Steril* **65**:503-509.

Zorn AM (2001) Wnt signalling: antagonistic Dickkopfs. *Curr Biol* **11**:R592-R595.

Zucker RM, Hunter ES, III and Rogers JM (1999) Apoptosis and morphology in mouse embryos by confocal laser scanning microscopy. *Methods* **18**:473-480.

Zuzarte-Luis V, Montero JA, Rodriguez-Leon J, Merino R, Rodriguez-Rey JC and Hurle JM (2004) A new role for BMP5 during limb development acting through the synergic activation of Smad and MAPK pathways. *Dev Biol* **272**:39-52.

APPENDIX